Nanomedicines for the Prevention/Reduction of Vaginal Transmission of HIV and Chlamydia

By

Sidi Yang

A Thesis submitted to the Faculty of Graduate Studies of The University of Manitoba in partial fulfillment of the requirements of the degree of

DOCTOR OF PHILOSOPHY

College of Pharmacy, Rady Faculty of Health Sciences, University of Manitoba
Winnipeg

Abstract

The development of vaginal microbicides could provide women an accessible alternative to protect themselves against sexually transmitted infections (STIs). We developed an intravaginal nanomedicine for the active delivery of saquinavir (SQV) to CD4+ immune cells to prevent/reduce vaginal acquisition of HIV. The nanomedicine was prepared with poly(lactic-co-glycolic acid) (PLGA) and conjugated to anti-CD4 antibody, which could achieve a more than two-fold increase in the intracellular delivery of SQV in vitro without causing any cytotoxicity. In order to better combat vaginal transmission of HIV, we developed a dual-preventive pH-sensitive RNAi-based combination nanomicrobicide for the prevention/reduction of vaginal transmission of HIV by knocking down host factor CCR5 and viral protein Nef simultaneously. The nanomicrobicide possessed a pH-dependent release profile to prevent siRNA from releasing in acidic vaginal environment and release siRNA in neutral intracellular environment. We also proved that knocking down Nef could reactivate Nef-blocked autophagy in vitro and the nanomicrobicide significantly inhibited replication of HIV in vitro. Anti-CD4 antibody conjugation to the nanomicrobicide significantly improved the vaginal distribution and tissue uptake of siRNA, and allowed the nanomicrobicide to achieve targeted gene knockdown in intravaginal CD4+ cells in mice. We further expanded the application of antibody-conjugated nanomedicine in the area of intravaginal delivery of antibody. Herein, we used the system to deliver anti-α4β7 monoclonal antibody (α4β7 Ab) intravaginally as a potential microbicide against HIV. The α4β7 Ab-conjugated nanomedicine decreased the percentage of $\alpha4\beta7^{high}$ CD4+ T cells and $\alpha4\beta7^{high}$ CD3+ T cells by half in the vaginal tract of RM 72 hr after a single administration without detectable systemic distribution. In

addition, we developed a siRNA-polyethyleneimine (PEI)-based nanomicrobicide with dual preventative activities of reducing bacterial binding and improving host autophagic degradation of bacteria as a potential strategy against vaginal infection of chlamydia trachomatis (C. trachomatis). Platelet derived growth factor-β (PDGFR-β), an irreversible bacterial binding factor on host cells, was knocked down by siRNA and autophagic degradation of C. trachomatis was improved by the introduction of PEI. By working together this dual preventative strategy resulted in 63% decrease of C. trachomatis inclusions in vitro without causing inflammation, apoptosis or reduction in cell viability.

Acknowledgements

Firstly, I would like to express my sincere gratitude to my advisor Dr. Emmanuel Ho for the continuous support of my Ph.D study and related research, for his patience, motivation, and immense knowledge. His guidance helped me in all the time of research and writing of this thesis. I could not have imagined having a better advisor and mentor for my Ph.D study.

Besides my advisor, I would like to thank the rest of my thesis committee: Dr. Xiaochen Gu, Dr. Wen Zhong and Dr. External Examiner for not only their support and encouragement through my graduate study, but also for their insightful comments and questions which incented me to deepen my research and thesis from various perspectives.

My sincere thanks also goes to Dr. Neal Davies, Dr. Yuewen Gong, Dr. Elena Martinelli, and Dr. Ruey-Chyi Su, who gave me access to the laboratory and research facilities, who generously offered their expertise and technical support on HIV, and who provided me an opportunity to be a part of their collaboration projects with Dr. Ho. Without their precious support, it would not be possible to complete the research of this thesis.

I thank my fellow lab mates and friends, Mr. Yannick Traore, Ms. Miral Fumakia, Dr. Jijin Gu and Mr. Roien Ahmadie for the stimulating discussions, for the sleepless nights we were working together, and for all the fun we have had in the last six years. Also I thank my summer students, Ms. Celine Jimenez, Ms. Alicia Dash, Mr. Kaien Gu, Ms. Juliana Nguyen and Ms. Giulia Hardouin for all their help and support on my research.

I am also very grateful to my dear husband and research mate Mr. Yufei Chen for his enduring love in life, for his great support during hard times and for his understanding and company over those late nights and working holidays. He is also my best research mate who could always offer me suggestions and solutions for research troubles and who could constantly encourage me when the tasks seemed arduous and insurmountable.

Last but not the least, I would like to thank my parents and my parents-in-law for supporting me spiritually throughout my graduate study and for giving me their endless love in life.

Table of Contents

Contributions of authors

Ms. Sidi Yang and Dr. Emmanuel A. Ho conceived all the experiments in this thesis. Sidi Yang was the principal researcher conducting all the experiments in the thesis except for anti-HIV study in Chapter 3 and in vivo RM study with gel loaded with α4β7 antibody conjugated NP in Chapter 4. She also analyzed all the results presented in this thesis. Dr. Elena Martinelli also participated in conceiving the experiments of Chapter 4 and helped revise the chapter.

Mr. Yufei Chen helped develop and validate the HPLC method for SQV, perform in vitro cell targeting study in Chapter 2. He also provided assistance in all the in vivo studies in Chapter 3.

Dr. Jijin Gu helped optimize the siRNA NP formulation in Chapter 3.

Mr. Kaien Gu and Ms. Alicia Dash helped prepare SQV-NP and analyzed release samples on HPLC.

Dr. Casey L. Sayre and Dr. Neal M. Davies offered help for the development of SQV HPLC method.

Dr. Geraldine Arrode-Bruses, Dr. Ines Frank, Dr. Brooke Grasperge, Dr. James Blanchard and Dr. Agegnehu Gettie performed the in vivo RM study and analyzed samples from RM in Chapter 4.

Ms. Celine Jimenez helped conduct the autophagy and cytotoxicity studies in Chapter 5 and she also helped write the introduction of Chapter.

Abbreviations and Terms

AIDS: acquired immunodeficiency syndrome

ACE%: antibody conjugation efficiency

ATZ: atazanavir

α4β7: Integrin α4β7

CD4: cluster of differentiation type 4

CXCR4: C-X-C chemokine receptor type 4

CCR5: C-C chemokine receptor type 5

CCR5 NP: scramble siRNA and siRNA targeting CCR5 co-encapsulated siRNA-PEI NP prepared by PLGA-PEG

$\alpha4\beta7^{high}$ CD4+ T cells: a subtype of CD4+ T cells expressing high level of α4β7

$\alpha4\beta7^{high}$ CD3+ T cells: a subtype of CD4+ T cells expressing high level of α4β7

C. trachomatis: Chlamydia trachomatis

Cy-3 scramble NP: Cy-3 labeled scramble siRNA-PEI encapsulated NP prepared by PLGA-PEG

Cy-3 scramble NP-(h)CD4: antihuman anti-CD4 antibody conjugated Cy-3 scramble NP

Cy-3 scramble NP-(h)IgG: antihuman IgG antibody conjugated Cy-3 scramble NP

Cy-3 scramble NP-(m)CD4: antimouse anti-CD4 antibody conjugated Cy-3 scramble NP

Cy-3 scramble NP-(m)IgG: antimouse IgG antibody conjugated Cy-3 scramble NP

DLS: dynamic light scattering

DMEM: Dulbecco's Modified Eagle's Medium

EE%: encapsulation efficiency

EDC: 1-Ethyl-3-(3-dimethylaminopropyl)carbodiimide

ELISA: enzyme linked immunosorbent assay

EB: elementary body

FBS: fetal bovine serum

FGT: female genital tract

GAPDH: glyceraldehyde 3-phosphate dehydrogenase

GALT: gut-associated lymphoid tissues

HIV: human immunodeficiency virus

HSV-2: herpes simplex virus type 2

HPV: human papilloma virus

HEC: hydroxyethyl cellulose

HPLC: high performancelLiquid chromatography

HEPES: 4-(2-hydroxyethyl)-1-piperazineethanesulfonic acid

LC: Langerhans cells

LC3A: microtubule-associated protein 1A/1B-light chain 3A

LC3B: microtubule-associated protein 1A/1B-light chain 3B

LGV: lymphogranuloma venereum

MHC-II: major histocompatibility complex class II

MES: 2-(N-morpholino)ethanesulfonic acid

MTS: (3-(4,5-dimethylthiazol-2-yl)-5-(3-carboxymethoxyphenyl)-2-(4-sulfophenyl)-2H-tetrazolium)

(m)siRNA CCR5 NP-(m)IgG: antimouse IgG antibody conjugated siRNA CCR5 (targeting mouse CCR5) NP

(m)siRNA CCR5 NP-(m)CD4: antimouse CD4 antibody conjugated siRNA CCR5 (targeting mouse CCR5) NP

MAdCAM-1: mucosal addressin cell adhesion molecule-1

NP: nanoparticle

NP-Ab: antibody-conjugated NP

NHS: N-hydroxysuccinimide

Nef: negative regulatory factor

Nef-ER: Sup-T1 cells stably expressing Nef

Nef NP: scramble siRNA and siRNA targeting Nef co-encapsulated siRNA-PEI NP prepared by PLGA-PEG

Nef-CCR5 NP: siRNA targeting Nef and siRNA targeting CCR5 co-encapsulated siRNA-PEI NP prepared by PLGA-PEG

NP-α4β7 Ab: anti-RM anti-α4β7 antibody conjugated NP

NP-α4β7 IgG: anti-RM IgG antibody conjugated NP

NP-α4β7 Ab Gel: 1% HEC gel loaded with anti-RM anti-α4β7 antibody conjugated NP

NP-α4β7 IgG Gel: 1% HEC gel loaded with anti- RM IgG antibody conjugated NP

PBS: phosphate buffered saline

PCL: poly(epsilon-caprolactone)

PLG: poly(lactide-co-glycolide)

PLGA: Poly(D,L-lactide-co-glycolide)

PVA: poly(vinyl alcohol)

PEI: polyethylenimine

PLGA-PEG: poly(lactic-co-glycolic acid)- polyethylene glycol

PDGFR-β: platelet derived growth factor receptor-β

PDI: polydispersity index

qRTPCR: quantitative real-time polymerase chain reaction

RNAi: RNA interference

RM: rhesus macaque

RB: reticulate body

RLDC: repeated low-dose challenges

STIs: sexually transmitted infections

SEM: Scanning electron microscopy

siRNA: small interfering RNA

SQV: saquinavir

SQV-NP: SQV-encapsulated nanoparticles

SQV-NP-CD4: Anti-CD4 antibody-conjugated SQV-NP

SD: standard deviation

scramble NP: siRNA-PEI encapsulated NP prepared by PLGA-PEG

scramble NP-(m)CD4: antimouse anti-CD4 antibody conjugated scramble NP

SIV: simian immunodeficiency virus

Tris-EDTA: tris- Ethylenediaminetetraacetic acid

TECPR-1: tectonin beta-propeller repeat-containing protein-1

UVRAG: UV radiation resistance-associated gene protein

VFS: vaginal fluid simulant

VPS34: class III phosphatidylinositide 3-kinase

4-HT: 4-hydroxytamoxifen

List of Tables

List of Figures

Chapter 1

Introduction

Sections partially taken from:
"Advancements in the field of intravaginal siRNA delivery"

Yang S, Chen Y, Ahmadie R, Ho EA
Journal of Controlled Release, 2013 Apr 10;167(1):29-39.

1.1 HIV, Global Epidemics of HIV and Vaginal Transmission of HIV

HIV is a lentivirus that attacks CD4+ cells of the immune system in humans [1], including CD4+ T lymphocytes [2], dendritic cells [3] and macrophages [4]. Viral infection of these cells causes progressive destruction of both innate and adaptive immunity [5], consequently leading to the development of AIDS [6]. A HIV virion consists of two single-stranded RNAs, enzymes (protease, integrase, and reverse transcriptase) within a protein core, and a lipid envelope surrounding the core [7]. There are also viral proteins (gp120 and gp41) inserted into the envelope as molecules for entry into targeted cells [7]. The viral RNA encodes structural proteins, various enzymes, and proteins to regulate transcription of viral genes and viral life cycle.

Currently HIV/AIDS is considered to be one of the most significant global health concerns of the 21st century. It has already killed more than 25 million people since it was discovered [8]. Despite a continuing decrease in new HIV infections (2.1 million in 2015 vs. 3.5 million in 2001), the number of HIV-positive people continues to ascend over the past three decades [9]. By the end of 2015, a total number of 36.7 million people living with HIV was estimated globally [9]. The prevalence of HIV shows a regional distribution across the world [10]. Sub-Saharan Africa is the most heavily affected region, which contributes to approximately 70% of the global cases. Many other developing regions are also significantly infected while developed regions are less infected. In Canada, HIV is a disease that has affected over 75,500 individuals by 2014, with over 2,500 new HIV infections occurring each year [11].

Current HIV incidence appears to have a disproportionate impact on women. Latest data revealed that women account for 51% of adults living with HIV globally with young women and adolescent girls (15-24 years old) at particularly high risk of HIV infection [12, 13]. In some regions, women are bearing higher HIV burden, e.g. in Sub-Saharan Africa and Caribbean, nearly 60% of the HIV-positive people are women [14]. A recent survey indicated that HIV/AIDS has become the leading cause of death for women among reproductive age [15]. An estimated 30-40% of new infections in women occur through vaginal intercourse and HIV infection via female genital tract has contributed to approximately 12.6 million of global HIV cases [16]. Women are at a greater risk of heterosexual transmission of HIV than men via unprotected sexual intercourse due to biological susceptibility to infection and social vulnerability to exposure [17]. In certain countries, due to social and cultural reasons, women are less able to negotiate the use of condoms or more likely to be exposed to non-consensual sex, thus resulting in higher susceptibility for HIV acquisition [17] [14].

HIV can infect the vaginal, ectocervical, and endocervical mucosa, but the contribution of each site to HIV transmission is uncertain [16]. Several studies indicated that HIV enters the epithelial layer through the lower female genital tract [16]. HIV invasion into the genital mucosa consists of the following sequential steps: penetration of the cervicovaginal mucus; penetration of the intravaginal epithelium; infection of sentinel immune cells; and dissemination into systemic circulation through the migration of infected immune cells to the draining lymph nodes and blood vessels [16]. Most HIV-infected donor cells are trapped in the mucus while some of the free virions can penetrate through the mucus mesh. The invading cell-free virions then migrate into the

intraepithelial layer via physical abrasions, gaps between epithelial cells and transcytosis [16]. Several surface proteins contribute to the process of transcytosis. Two cell-surface glycosphingolipids, sulphated lactosylceramide on vaginal epithelial cells [18] and galactosylceramide on ectocervical epithelial cells [19], bind to gp120 and mediate the transcytosis of virions. Other proteins such as syndecans (on genital epithelial cells) [20], scavenger receptor gp340 (on genital epithelial cells) [21] and chemokine receptors CCR5 (on both genital epithelial cells and immune cells) [19] may also play a role in fostering transcytosis. When the virus migrates into the intraepithelium, it first comes into contact with and infects the resident immune cells, primarily CD4+ T cells and LC [22]. HIV infection of CD4+ T cells depends on CD4 and CCR5 receptor-mediated fusion, while the infection of LC significantly relies on CD4 and CCR5 receptor-mediated endocytosis but a marginal C-type lectin receptor-mediated endocytosis also plays a minimal role [22]. In addition, the LC with dendritic surfaces might also migrate out of epithelium and extend near to, or into, the mucosal lumen, and become infected directly by the cell-free virions [23]. The virus can also penetrate deeper into stroma and productively infect stromal dendritic cells, macrophages and CD4+ T cells [16]. Infected CD4+ T cells and LC are also able to migrate from the epithelium into stroma and may amplify the infection locally [16]. Eventually the virus gets carried into the draining lymph nodes and blood vessels via infected cells and establishes infection systemically [16]. The abrasions within the vagina also provide an unobstructed pathway for both free virions and HIV-infected donor cells to disseminate the infection in situ and systemically [16]. Initial HIV-1 infection establishment within the vaginal epithelium requires CD4 and its co-receptor CCR5 or CXCR4. The contribution of CXCR4 is very minimal but it is extensively used during the stage of progression to AIDS [24]. The high expression of

CD4 and CCR5 on CD4+ T cells and LC could be a factor contributing to the effective viral entry into both cells [22]. CD4 is an important surface receptor expressed on CD4+T cells, dendritic cells, macrophages and monocytes. It plays a vital role in connecting innate immunity and adaptive immunity. Its main function is to interact with MHC- II on antigen presenting cells to facilitate antigen presentation and signal transduction, which are essential for T cell activation [25]. CCR5 is a chemokine receptor predominantly expressed on T cells, macrophages and dendritic cells [26]. Its role is mainly seen in inflammation for recruiting immune cells to the site of inflammation and enhancing the stimulation and cytokine release from CD4+ T cells [27].

The use of condoms remains the most effective method of preventing sexual transmission of HIV, however, in some situations, women can not always determine or control the use of condoms during a heterosexual intercourse, making themselves vulnerable to unexpected HIV infection. As a result, in the absence of an effective HIV cure/vaccine, it is important to develop a feasible alternative to condoms to protect women from heterosexual transmission of HIV.

1.2 Chlamydia and Vaginal Infection of Chlamydia

Chlamydia is the most common sexually transmitted bacterial infection in the world, which is caused by the bacterium, C. trachomatis [28]. In Canada, the infection is primarily caused by C. trachomatis serovars D to K [29], while in other developing countries, the infection is commonly attributed to LGV, a different serovar of the same bacterium [30-32]. The most recent data indicated that in 2012, 103,716 cases of chlamydia infection were reported in Canada (corresponding to a rate of 298.7 per

100,000 population) [33] and the rates of reported cases have been increasing steadily since 1997 [34]. Moreover, the infection of chlamydia is thought to be underdiagnosed because the majority of infected individuals are asymptomatic and do not seek medical evaluation [32]. The infection is most common among sexually active youth and young adults [29]. Young people aged 15-24 account for approximately two thirds of the newly infected individuals [29]. Young adults under the age of 25 and pregnant women compose the high-risk population and are recommended to be screened annually [29]. It is estimated that 1 in 20 sexually active young women aged 14-24 years has chlamydia [32].

Sexually transmitted chlamydia infection occurs through the sexual contact of the penis, vagina, mouth, or anus of an infected partner [32]. Perinatal transmission of chlamydia from an untreated mother to baby is also a transmission route, which causes the chlamydia conjunctivitis or pneumonia in some exposed neonates [32]. Consistent and correct use of condoms during sexual intercourse, long-term monogamous relationship with uninfected partner, screening of high-risk population and timely medical treatment of infection can help prevent or reduce the transmission of infection [29]. C. trachomatis is a gram negative obligate intracellular bacterium with two distinct forms during its life cycle, the infectious EB and the replicative RB during its life cycle. Pathogenesis of chlamydia infection in the female genital tract begins with initial binding of EB to nonimmune genital epithelial cells, and is followed by contiguous endocytosis through a membrane-bound compartment, inclusion. After internalization, inclusion helps EB to rapidly escape the host endo-lysosomal pathway and avoid being degraded by the host defense system. At the same time, EB accomplishes the transformation into RB and begins to initiate bacterial protein synthesis. Newly synthesized inclusion membrane

proteins assist the replication of RB by collecting and supplying nutrients from the host's golgi. As RB propagates and accumulates, the life cycle enters the late phase, in which last-phase effectors and EB effectors are being synthesized and the differentiation of new EB from RB is accomplished shortly afterwards. Eventually, newly produced EB leaves the host via extrusion (a process where a cell exports large particles or organelles through its cell membrane to the outside) or host lysis to establish future infections in host [35].

Chlamydia infection often appears asymptomatic in both men and women but some clinical manifestations can occur sometimes. Infected females may experience abnormal vaginal discharge, abdominal or pelvic pain, dyspareunia, dysuria, hematuria, urinary urgency and frequency [36], while male patients may experience urethral discharge, urethral itch, testicular pain, urethritis and dysuria [36]. Once these symptoms are developed, patients should seek medical examination to confirm the chlamydia infection. The most commonly used medical test for chlamydia infection is non-invasive urine-based nucleic acid amplification test, which uses polymerase chain reaction or transcription-mediated amplification to identify the presence of C. trachomatis [29]. This test is more sensitive and specific than cell culture, enzyme immunoassay and direct fluorescent antibody assay but sometimes may be interfered by some specific biological samples, in which cases, the other tests are more applicable [29].

Although chlamydial infection can be easily managed by macrolides or tetracyclines, the constant recurrence, the potential to develop antibiotic resistance [37], the safety of antibiotic use during pregnancy [38-40] and the common systemic side effects of antibiotics [41, 42] are always problems and concerns encountered in the healthcare setting. In an effort to control the prevalence of chlamydia, various screening programs

have been established in different countries around the world. However, new cases and recurrent cases still pose a challenge in disease control [43]. As a result, a safe non-antibiotic based therapy needs to be developed to provide alternative prevention choices for physicians and patients.

1.3 Microbicides and Advantages of Vagina as a Local Drug Administration Route

In order to address the gaps in current preventative strategies of sexually transmitted diseases (STIs), World Health Organization has recommended that microbicides can be used as a feasible alternative to condoms to prevent or reduce STIs [44]. Microbicides are products applied within the vaginal or rectal tract to prevent STIs [44]. They can be formulated as gels, tablets, creams, films, suppositories, sponge or intravaginal rings containing single or multiple pharmaceutically active compounds [45-47]. The development of microbicides provides an option that presents a promising hope in the current prevention landscape of STIs. Microbicides play a very important role in preventing STIs, especially in situations where condoms are not feasible to use due to sociocultural factors [44]. Compared to condoms, the use of microbicides is more women-controllable because it does not require consent, corporation or even knowledge of the partners.

To date, the potential candidates of microbicides can be classified into four groups: buffers, surfactants, blockers and antimicrobial agents [48]. Each of them works in a distinct way to combat STIs. Microbicides containing buffers maintain the naturally acidic pH of cervicovaginal environment, when it is substantially affected by alkaline semen during sexual intercourse or by pathogens during infections, to preserve the

physiological defensive barrier of vagina [48]. Surfactant microbicides inactivate invading pathogens by disrupting the integrity of membranes directly or altering the structures of membranes to render them more liable to disruption [48]. Blocker microbicides refer to candidates such as polyanionic sulfated or sulfonated polymers that can bind to the invading pathogens via electrostatic interaction therefore preventing them from attaching to or fusing with the host cells [48]. However, these blocker microbicides have a very limited spectrum of activity and are mainly designed to target the HIV envelope protein gp41 [48]. Currently, the candidate microbicides holding the greatest promise are those formulated with small molecules or macromolecules with active antimicrobial activities. They effectively inhibit one or more steps in the microbial life cycle to prevent the invasion or dissemination of pathogens [48].

A vaginal microbicide is designed specifically to act in the FGT to protect women against heterosexual intercourse. During the past decades, the vagina has been studied as a route for both local and systemic drug delivery of small molecules [49] , DNA/plasmids [50] , siRNAs [51] and peptides/proteins [52]. Many advantages contribute to its role in drug administration. The vagina has a rich vascular plexus that makes it an ideal site for absorbing and distributing drugs [53]. The venous drainage from the vagina is directed to the heart via passage through the internal iliac vein and inferior vena cava; therefore, drugs absorbed via the vagina enter the systemic circulation without undergoing extensive first-pass hepatic metabolism [53]. Secondly, the outer third of the vaginal wall is prominently lined with a corrugated surface, known as vaginal rugae [54]. The presence of rugae increases the surface of the vagina and provides a larger area for drug absorption, and it also permits the extension and stretching of vaginal tissues, allowing for the long-

term placement of larger drug delivery devices such as vaginal rings to achieve controlled or sustained drug delivery [54]. Thirdly, many intravaginal medications are designed to work topically in the vaginal lumen or vaginal tissues [49, 55, 56]. This site-specific drug delivery significantly reduces the risk of systemic side effects and lowers the doses of administration for expected efficacy [57]. Last but not least, the ease of self-administration and compatibility of intravaginal formulations make the vagina an appealing route for drug administration in women.

1.4 Challenges of Intravaginal Drug Delivery and Current Intravaginal Drug Delivery Systems

The vagina has a complex environment that significantly influences intravaginal drug delivery. Vaginal flora, acidic vaginal environment, cervicovaginal mucus, active vaginal enzymes and the physiological structure of intravaginal epithelium are the major factors that need to be taken into consideration for intravaginal drug delivery.

Non-pathogenic microbes colonize the vaginal mucosa forming vaginal flora, which have significant implications for female reproductive health [58]. Lactobacillus is considered to be the most dominant bacteria in vaginal flora to maintain the microenvironment in healthy women [59]. They compete with invading microbes for nutrients, prevent pathogens from attaching the mucosa and secrete defensive molecules such as hydrogen peroxides and bacteriocins to kill pathogens or inhibit their growth [60]. They also produce lactic acid to maintain the low pH of the vagina to serve as a defensive barrier for pathogens but may also be an obstacle for intravaginal drug delivery [59]. Generally, the vaginal environment of healthy women exhibits a typical pH ranging from 3.5 to 4.9 with

a production volume of 1.0-11.0 mL/day [61]. Any compounds that are labile to acidic pH are likely to be degraded. A wide range of active enzymes including α-amylase [62], aminopeptidase [63], β-glucuronidase, phosphogluconate dehydrogenase, ribonuclease [64] and various microbial enzymes (e.g. mucinase, sialidase, and protease) [65] are also found in the vagina. These enzymes have the ability to cleave pharmacologically active chemicals, saccharides, proteins/peptides and nucleotides, lowering or disabling the therapeutic activity of compounds delivered intravaginally.

Vaginal lactic acid and enzymes are actually trapped in a layer of mucus (gel-like fluid) that covers the cervicovaginal mucosa. It is composed of 95% water, 2%–5% mucin fibers and trace amount of lactic acid, lipids, salts, proteins, enzymes and cells [66]. Cervicovaginal mucus is continuously secreted, shed, degraded and recycled in the vaginal lumen. The majority of cervicovaginal mucus is derived from cervical mucus produced by glandular cells in the cervix [67, 68]. The cervical mucus flows over the vaginal lumen and mixes with vaginal transudate secreted from Skene's and Bartholin's glands on the vaginal walls, forming the so-called “cervicovaginal mucus” [68]. The thickness of the cervicovaginal mucus is expected to be at least tens of microns in humans, but the precise number has not been reported yet [69]. The typical lifetime of cervicovaginal mucus has never been experimentally measured but is estimated to be on the order of a few hours [69]. Clearance of cervicovaginal mucus is primarily achieved via the vaginal motions driven by body movements and intra-abdominal pressure [70, 71]. These forces squeeze the vaginal wall and facilitate the mucus to be expelled through the opening. The exfoliation of intravaginal epithelium also contributes to the shedding and replenishment of the cervicovaginal mucus. The resident vaginal flora can produce

enzymes to degrade mucin fibres in cervicovaginal mucus via hydrolysis [72]. The property of cervicovaginal mucus is primarily regulated by the level of hormones in females and can change dramatically by ovulation. During the non-ovulatory period, the cervicovaginal mucus is viscous and composed as mentioned above, while during ovulation, the cervicovaginal mucus becomes watery and the mucin fibres line up to allow sperm to pass through the cervicovaginal tract more easily [66].

In the cervicovaginal mucus, mucin fibres play a key role in determining the fundamental properties of mucus, which is closely related to the three-dimensional disposition of mucins in cervicovaginal mucus. Mucin fibres are large molecules formed by the linking of numerous mucin monomers, which are typically 0.3–0.5 million Dalton in size and coated with a complex array of proteoglycans [73, 74]. The mucins can be generally categorized into two types: cell-associated mucins (0.1–0.5 μm in length involving a trans-membrane domain) and secreted mucins (several microns in length, existing in the luminal mucus) [75, 76]. Secreted mucin fibres crosslink into tiny nets in which water is trapped, forming thousands of micro-scale watery channels [69, 77]. Studies have shown that the pore size of non-ovulatory cervicovaginal mucus is 50 – 1800 nm, with an average size of 340 ± 70 nm [78]. Mucin fibres are reported to be negatively charged due to the presence of carboxyl or sulfate groups on mucin proteoglycans [79]. Disulfide bond–stabilized globular regions are also present along mucin fibres, which contribute to the hydrophobicity nature of the mucins [79]. Therefore, cervicovaginal mucus is considered a barrier to impede the diffusion and absorption of certain drugs in the vaginal tract. The physical contacts between drug molecules/drug vectors and mucin fibres generate multiple adhesive interactions including physical entanglement, hydrophobic

interaction, and electrostatic attraction [80]. It is possible for small molecules to diffuse freely through mucus due to their dramatically small size but sometimes, small molecules can diffuse more slowly than other molecules of similar or larger size due to the presence of hydrophobic interactions. Studies have shown that the diffusion rate of molecules with higher nonpolar/polar partition coefficient is much smaller than those with lower nonpolar/polar partition coefficient [69]. Most of the large molecules and particles are thought to be significantly hindered by mucus due to their large size, but several globular proteins and capsid virus particles are reported to have comparable diffusion rates in mucus as in water [81]. Particles smaller than 500 nm can also enter the mucus layer but those falling in the range of 200-500 nm and modified with a hydrophilic surface layer have been reported to exhibit improved penetration ability [80]. Some compounds or systems that are positively-charged in cervicovaginal mucus can interact with negatively charged mucin fibres, therefore reducing transportation in the mucus layer [75], [76] and [79].

Physical entanglement is considered a crucial factor influencing mucus penetration ability. In order to penetrate mucus, drugs or drug vehicles must be small enough to fit into and penetrate the dense mucin fibre mesh. Diffusion and penetration of particles into mucus is largely determined by particle size and surface properties. The size regulates the ability to fit into the mesh pores generated by the cross-linked mucin fibres while the surface properties control the interaction between the particles and the mucin fibres. Thus, the combination of these two parameters collectively determines the penetration potential. In the specific case of non-adhesive drug delivery systems, it has been shown that particles as large as 500 nm can penetrate all the way down to the surface of the epithelial

layer [82]. Due to the fact that particles larger than 500 nm exhibit limited ability to diffuse freely within the mucus layer, particles with diameters less than 500 nm are assumed to be able to migrate through the mucin mesh. Experiments conducted by Hanes et al. revealed that the particle size with which particles can penetrate through the whole mucus layer can be extended to as small as 200 nm [83] however, further decrease in particle size does not improve mucus-penetrating ability but instead, increase the chance of being retained by mucus pores since smaller particles often travel further into smaller channels that are always accompanied with dead ends [80]. Therefore, sizes between 200 and 500 nm is considered to be the optimal size for mucus penetration. Hydrophobic domains are distributed along mucin fibres [78], therefore the use of hydrophobic polymers for nanoparticle fabrication can form interactions with the exposed hydrophobic domains of mucin fibres through hydrophobic binding, thus leading to complete retardation of transport [77]. Upon entrapment within the mucus layer, therapeutic NP undergo rapid mucociliary clearance especially those within the luminal mucus layer. As a result, a significant fraction of drug is eliminated resulting in reduced therapeutic drug dose. Electrostatic attraction is another parameter that can limit transport across mucus. Mucin fibers contain negatively charged moieties, which can interact with compounds or systems having a positive-charged surface, thus reducing transportation of medications [75], [76] and [79].

Besides the cervicovaginal mucus, the layers of intravaginal epithelium are also considered to be another factor influencing the drug diffusion and delivery into targeted intraepithelial cells. The female reproductive tract is mainly composed of three sections, the vagina, ectocervix and endocervix. Human vagina and ectocervix are lined with

stratified non-keratinized squamous epithelium that serves as a defense line to prevent pathogens from entering the body [84]. Continuous epithelial sloughing also helps eliminate pathogens from the vaginal lumen and maintain a healthy ecosystem [84]. Epithelial intercellular junctions help preserve the tensile strength of the vagina and regulate the molecular transportation across the intraepithelial layers [84]. Three types of intercellular junctions: tight junctions, adherens junctions and desmosomes, are reported to be present in the vagina and ectocervix with an uneven distribution along the epithelium transitional cross section [84]. In the apical layers of the vaginal and ectocervical epithelia, no junctional molecules are detected, while in the lower two thirds of the epithelium, tight junctional molecules are detected to be present, forming cell-cell adhesions [84]. Besides that, adherens junctions and desmosomes are also reported to present in human ectocervix but not the vagina [84]. With regards to human endocervix, columnar epithelial cells are the main cell type lining the apical mucosal surface and a typical tripartite junction pattern is observed in the endocervix with tight junctions present in the apical region, adherens junctions present in the middle region and desmosomes in the basal region [84]. The presence of intracellular junctions affects the permeability of macromolecules, such as IgG, which is only diffusible through superficial layers of the vaginal and ectocervical epithelium [84].

A wide range of formulations have been developed for intravaginal drug delivery and below, the table provides a summary of current intravaginal formulations with comparisons of the advantages and disadvantages of each system.

Table 1.1 Current intravaginal drug delivery systems

Intravaginal Drug Delivery Systems	Advantages	Disadvantages	Therapeutic Agents loaded in the systems	Reference
Gel	Rapid and nice vaginal distribution Lubricating Property Feasibility of loading water-sensitive and water-stable compounds (aqueous gel and non-aqueous gel)	Short-term effect Leakage User adherence disadvantage Weak abilities to protect therapeutic agents	Maraviroc Metronidazole Progesterone Tenofovir IQP-0528, a Pyrimidinedione Liposomes NPs	[55, 85-91]
Film	No applicator needed Options for water-sensitive compounds	Short-term effect Potential dis-uniform drug distribution Absorption affected by local hydration Concerns of local discomfort and difficulty in insertion Weak abilities to protect therapeutic agents	Dapivirine IQP-0528, a Pyrimidinedione EFdA and CSIC NPs Clotrimazole Fluconazole	[92-97]
	Long-term effect and improved user adherence	Potential dis-uniform drug distribution	Tenofovir Nevirapine	[98-102]

Intravaginal Ring	Feasibility of sustained/controlled drug release profile Ability of drug protection	Absorption affected by local hydration Concerns of local irritation and difficulty in insertion	Saquinavir MIV-150 Zinc acetate Carrageenan Levonorgestrel Ovarin-IgG oxybutynin Ethinyl estradiol Desogestrel	
Cream	No applicator needed Applicable option for hydrophobic drugs Good moisturizing property	Short-term effect Potential dis-uniform drug distribution Leakage Weak abilities to protect therapeutic agents	Garlic and thyme Clotrimazole Miconazole Conjugated equine estrogen/ estradiol Ciclopirox Olamine Clindamycin	[103-107]
Suppository	No applicator needed Complete dissolving ability Applicable option for hydrophobic drugs	Short-term effect Potential dis-uniform drug distribution Limited ability of delivering hydrophilic drugs	Prostaglandin E2 Povidone-iodine Hydrocortisone Butoconazole Boric acid	[108-112]

Tablets	No applicator needed Feasibility of delivering both hydrophilic and hydrophobic drugs	Short-term effect Potential dis-uniform drug distribution Concerns of incomplete dissolution	Ketoconazole Estradiol Microsphere Misoprostol Dapivirine Progesterone Hyaluronic acid	[113-119]
NPs	Versatility of delivering a wide range of drugs Ability of providing drug protection, nice vaginal distribution, mucus penetration and etc to enhance efficacy. Potential to be further formulated into a vaginal formulation (e.g. gel, film)	Short-term effect Leakage Incomplete drug release during short periods Inefficient penetration into intravaginal epithelium	PSC-RANTES Tenofovir Efavirenz Saquinavir Dapivirine Raltegravir DNA constructs Camptotecin Paclitaxel siRNAs	[120-129]

1.5 Nanoparticles as Intravaginal Drug Delivery Systems

The first application of NP for use as drug delivery carriers can be dated back to early 1950s when Dr. Jatzkewitz and his colleagues first attempted to apply polymer-drug conjugates as drug delivery systems [130]. Generally accepted NPs in pharmaceutics are

defined as “particulate dispersions or solid particles formulated by polymers with a size in the range of 10-1000 nm. The drug can be dissolved, encapsulated or attached to a NP matrix [131]. The application of NP in pharmaceutical sciences has been extensively investigated and developed in the past three decades due to its advantages in promoting drug delivery. NP offer the feasibility for encapsulating various substances including both small molecules (hydrophilic/hydrophobic) [132] and macromolecules (proteins/peptides/DNA/siRNA) [51, 133, 134]. The shell of the NP can offer protection to encapsulated therapeutic agents against various physiological environments and avoid degradation of endogenous enzymes, acids and alkalis [135]. The small size of NP allows for effective cell uptake into the majority of cell types and facilitates the intracellular delivery of highly hydrophilic/hydrophobic drugs, macromolecules or ionized drugs that cannot easily transport across cell membranes [135]. The nano size of the particles also allows effective penetration of NP through vascular endothelium, mucosal epithelium, blood brain barrier and tumor tissues and accumulate selectively at target sites [136-138]. The small size provides a higher surface area to volume ratio over other drug delivery systems and diverse functional molecules can be attached to the large surface area to provide targeted drug delivery, achieve desirable pharmacokinetics and improve mucus penetration [49, 139, 140]. The diverse composition of NP with polymers, lipids and other materials improves bioavailability, biocompatibility and achieves sustained or stimuli-responsive drug release profiles [141-144].

NPs have the potential to penetrate through vaginal tissues and deliver drugs into target cells. Study has shown that intravaginally delivered nano-size quantum dots could transport across vaginal tissues and get into adjacent lymph nodes [145]. The penetration

was evidently observed 4 hr post installation, increased over time and eventually peaked at 36 hr post treatment [145]. There was no evidence indicating that cell-mediated transport took place [145]. The exact mechanism of NP penetration through vaginal walls is still not fully understood, but according to the mechanism of NP penetration through the extracellular matrix, NP penetration through vaginal tissues may depend on diffusion and convection [146]. Further studies are needed to investigate the certain mechanism. Internalization of NPs into cells is mediated by endocytic processes including pinocytosis, phagocytosis or endocytosis depending on particle size, surface property and cell types [146]. After internalization, NPs are transported from endosomes to lysosomes. Some types of NPs could escape from lysosomes using different strategies such as proton sponge effect, ion-pair formation and membrane destabilization [146, 147]. Afterwards, NPs diffuse into cytoplasm and deliver their payloads intracellularly. Some NPs could even penetrate into nucleus if the particle size is smaller than 9 nm [146].

A wide range of NP-based platforms, such as polymeric NP, liposomes and dendrimers, have been developed for intravaginal drug delivery but among these platforms, polymeric NP is the most investigated carrier system. Polymeric NPs are composed of polymer-based materials. The preparation of polymeric NPs can be achieved by well-documented methods such as emulsion evaporation, emulsion diffusion and nanoprecipitation to encapsulate various types of drugs [148]. Polystyrene, Eudragit ® S-100, chitosan, PCL, PLG, and PLGA are all documented in the formulation of NP-based intravaginal drug delivery systems [149]. Biomaterials (e.g. chitosan, PCL, PLG, PLGA) account for a large proportion of the polymers that are used in intravaginal drug delivery due to their biocompatibility, biodegradability, well-documented safety profile and controllable

degradation rate. These materials are completely capable to coexist with living organs or tissues without causing any inflammatory or immune responses. Within living organisms, these materials can be gradually degraded through biological actions, generating degradation products that are natural, non-toxic and can be safely excreted out of body. The degradation rate of biomaterials can also be internally controlled depending on the composition, molecular weight and physicochemical properties (e.g. crystallinity, hydrophilicity) of the materials to achieve different drug release profiles, even though external factors such as pH, enzymes, ions, and physiological conditions can influence the degradation process [150].

Among all the biomaterials, PLGA is the most attractive and extensively used polymer for the development of intravaginal NP formulations. PLGA is a FDA-approved polymer that has been widely used in the preparation of NP due to its attractive properties including biodegradability, biocompatibility and versatility for encapsulating hydrophilic/hydrophobic small molecules and large molecules, capability for sustained drug release and possibility for surface modifications. PLGA naturally degrades into lactic acid and glycolytic acid through the ester bond hydrolysis in the body [151]. These two monomers can either enter the tri-carboxylic acid cycle for further breakdown into carbon dioxide and water or remain unchanged, and subsequently eliminated from the body [152, 153]. The hydrolytic rate can be altered ranging from days to months depending on the molecular weight of PLGA and the composition ratio of the two monomers [154]. A wide range of drugs (nucleotides, proteins/peptides and small molecules) is formulated into PLGA NP to achieve a controlled release profile. The PLGA polymers are manufactured with different end groups including carboxyl,

hydroxyl, amine and ester. These terminal groups, especially the carboxyl and amine groups, can be functionalized with a wide range of biomolecules such as antibodies [155], aptamers [156], peptides [157] and polymers as a strategy to enhance targeting, biodistribution and cell uptake.

Currently, many FDA-approved NP formulations have been extensively used in the clinic as anti-cancer medications, anti-fungal treatments, macular degeneration therapies, iron replacement reagents and anaesthesia reagents [158]. A liposome formulation encapsulating propofol (Diprivan) was first approved by FDA in 1989 for the induction and maintenance of anesthesia. Later, many liposome formulations encapsulating anthracyclines (e.g. Doxil/Caelyx, DaunoXome) for the treatment of cancer were approved and marketed in the 1990s and 2000s. Surface modification of PEG was also introduced to some of these formulations to improve pharmacokinetics and decrease cardiotoxicity. At the same time, iron-replacement nanoparticle therapies were widely promoted and many products such as DexFerrum/DexIron were approved for the treatment of iron deficient anemia. The applications of NP were also investigated in fungal infections and macular degeneration. Two products AmBisome and Visudyne were approved by FDA for treating invasive fungal infections and macular degeneration, respectively. However, currently there are still no FDA-approved nanomedicines for STI applications.

1.6 Gels as Intravaginal Drug Delivery Systems

Various vaginal dosage forms including gels, rings, films and suppositories are being developed for preventing STIs [159], among which gels are the most investigated dosage

form. Many preclinical and clinical reports have indicated the safety, compatibility and acceptability of gels, making it a very promising dosage form for treating and preventing STIs [160]. Compared to other vaginal dosage forms, gels have the closest physico-chemical properties to cervicovaginal mucus; therefore, it is the most feasible formulation to use intravaginally without significantly disturbing the cervicovaginal mucus, which serves as an important barrier for invading pathogens. A gel formulation can nicely adhere to the vaginal surface and immerse itself with cervicovaginal mucus, prolonging the exposure of therapeutic agents to tissues [160]. Vaginal gels are defined as "semi-solid, three-dimensional, polymeric matrices comprising small amounts of solid, dispersed in relatively large amounts of liquid." [160]. The solid materials dissolve and cross-link with each other forming a supportive matrix, in which liquid is trapped. Even though small amount of solid is dispersed in relatively large amounts of liquid, vaginal gel exhibits a more solid-like character [160]. A wide variety of drugs can be dissolved or resuspended in a gel system, making it a versatile tool for intravaginal delivery of antimicrobials [161], spermicides [162], hormones [163] and soothing or lubricating agents [164].

Typically, vaginal gels are composed of gelling agents (such as hydroxyethyl cellulose, carbopol, poloxamer), buffering/acidifying agents, humectants (such as glycerin, polyethylene glycol, propylene glycol), preservatives (a combination of methyl paraben and propyl paraben is most commonly used) and therapeutic agents or vehicles loading therapeutic agents (such as NP, liposomes) [165]. The selection of excipients for preparing vaginal gels should always consider the compliance of excipients and the compatibility among the excipients and therapeutic compounds when various excipients

are provided to vaginal drug delivery systems, since an ideal vaginal gel system should be discrete, non-irritating and safe for continuous use.

According to the nature of the formation of gelling network, gel systems can be classified into two types, chemical gel and physical gel. Chemical gels are formulated with polymers that can produce covalently bonded network through chemical reactions to form the irreversible gel network. This type of gel is not commonly seen in intravaginal drug delivery but is extensively used in implantable hydrogel delivery systems. In contrast, physical gels are formed by physical entanglement of polymers through external forces (e.g. shearing force) [89]. The formation of gels is largely dependent on external physical factors like temperature, pH, solvent composition, the presence of ions and so forth. Physical gels are reversible and can switch between gel and solid states and they compose the majority of vaginal gels that are being used and developed today. The solid phase, in most cases, polymers are dispersed in aqueous solutions, forming a semisolid aqueous gel system. Aqueous vaginal gels are extensively used as microbicides, contraceptives, labour inducers, treatments of vaginal bacterial vaginosis and intravaginal warts, and for the delivery of vesicles containing therapeutic agents such as NP and liposomes [160]. Sometimes the aqueous solutions can be replaced by other hydrophilic non-aqueous solutions such as glycerin, PEG, propylene glycol, forming a non-aqueous gel formulation. Recently, a non-aqueous vaginal gel has been developed as a microbicide for the delivery of the HIV-1 entry inhibitor maraviroc [166].

Another important type of gels is stimuli-responsive gels. These gels can change their physical characteristics dramatically as a result of exposure to temperature, light, pH, glucose level, pressure, electrolytes and so forth [167]. The development and evaluation

of thermo-sensitive and pH-sensitive gels has drawn much attention for the use of intravaginal therapies. Thermo-sensitive gels are gels that are capable of gelling in response to temperature change, generally from ambient to body temperature [160]. The main goal of thermosensitive gels is to enhance the mucoadhesiveness of gels by increasing viscosity after application within the vaginal tract. A mucoadhesive thermos-sensitive vaginal gel containing clotrimazole has been shown to prolong the antifungal effect in the treatment of vaginitis [168]. The mechanism of pH-sensitive gels is that the change of pH regulates the swelling-shrinking state of the gel network, which further controls the on-off state of drug release from the gel system. Some gels are designed to release drugs in a neutral pH environment as a semen-triggered vaginal microbicidal/spermicidal vehicle [169] and some gels are developed to release drugs in acidic environment for delivering drugs intravaginally under normal physiological conditions [170].

Gels prepared with bioadhesive polymers such as sodium carboxymethyl cellulose, HEC, carbopol-PEG and hydroxypropyl methyl cellulose adhere to tissues for prolonged time compared to nonadhesive liquid preparations and increase the exposure period of tissues to active ingredients in gels [171]. The subsequent drug/cargo release from non-stimuli gel depends on the diffusion of molecules/cargoes through the gel network [172]. Substances at the contact layer are absorbed by tissues in the first place, generating a concentration gradient and this concentration gradient promotes substances away from the contact layer to diffuse out and get absorbed by tissues [172]. Moreover, the influx of water into the gel system to dilute the gelling agent below its critical gelation concentration also contributes to drug/cargo release [172].

HEC is a FDA-approved polymer that is widely used in pharmaceutical manufacturing. HEC is a non-ionic water-soluble polymer developed from reaction of ethylene oxide with alkali-cellulose under certain conditions. HEC is supplied as fluffy, white, neutral pH dry powders; but once it swells in water, the volume can increase up to 1000 times their original volume. Depending on the degree of cross-linking and molecular weight, pharmaceutical grade HEC polymers are classified into different types to provide either pseudo-plastic or shear-thinning rheological properties for different applications. Gels made from HEC are transparent, non-irritating, pharmacologically inactive, and compatible with a wide variety of therapeutic ingredients including proteins and peptides. The product appears rich and thick in containers but can easily spread over skin or intraepithelium. The hydrophilic nature of HEC makes it readily dissolved in cold or hot water to provide a neutral gel system with different viscosities. The pH of HEC gels can be adjusted to acidic or alkaline to accommodate the solubility or compatibility of different compounds for different applications. Glycerine and PEG are the most common thickening agents and humectants used in gel and sometimes preservatives are added to prolong the shelf life. The gel systems can also accommodate other vehicles for therapeutic compounds as a secondary delivery system.

1.7 Overview of Research in the Thesis

STIs pose a threat to women's health, and microbicides can be promoted as an alternative to condoms to protect women against STIs. Therefore, my research aims at developing novel microbicides against HIV and chlamydia using cutting edge nanotechnology and biotechnology to improve efficacy and decrease side effects of current therapeutic agents. As mentioned above, the use of NPs provides good drug protection against the acidic and

enzyme-rich intravaginal environment, and proper surface modifications with functional ligands allows the system to have improved abilities in mucus penetration and targeted drug delivery. However, the NP formulation does not provide users the ease of administration and potentially does not facilitate itself with nice vaginal retention. Therefore, in order to provide ease in self-administration and increase vaginal retention of NPs, the NP formulation loaded with active compounds could be further formulated into a gel dosage form to overcome these challenges. In this thesis, four nanomedicines against HIV or chlamydia using different strategies were subsequently developed and reported. Physiochemical properties of the formulations were characterized mechanically. Biological mechanism, safety profile and therapeutic potential of these nanomedicines were evaluated in vitro and in vivo. These nanomedicines presented a potential platform for the development of novel microbicides and intravaginal drug delivery systems.

Chapter 2

Novel intravaginal nanomedicine for the targeted delivery of saquinavir to CD4+ immune cells

Sidi Yang, Yufei Chen, Kaien Gu, Alicia Dash, Casey L. Sayre, Neal M. Davies, and Emmanuel A. Ho

Int J Nanomedicine. 2013;8:2847-58. doi: 10.2147/IJN.S46958

(Introduction revised from the paper)

2.1 Abstract

The goal of this study was to develop and characterize an intravaginal nanomedicine for the active delivery of SQV to CD4+ immune cells as a potential strategy to prevent or reduce HIV infection. The nanomedicine was formulated into a vaginal gel to provide ease in self-administration and to enhance retention within the vaginal tract. SQV-NP were prepared from PLGA and conjugated to antihuman anti-CD4 antibody. SQV-NP-CD4 had an encapsulation efficiency of 65.3±2.3% and an antibody conjugation efficiency of 80.95±1.11%. NP were rapidly taken up by Sup-T1 cells with more than a two-fold increase in the intracellular levels of SQV when delivered by SQV-NP-CD4 in comparison to controls, 1 hr post-treatment. No cytotoxicity was observed when the vaginal epithelial cells were treated for 24 hr with drug-free NP-Ab (1000 μg/mL), placebo gel (200 mg/mL) or drug-free NP-CD4 loaded gel (5 mg NP/g gel). Overall, we described an intravaginal nanomedicine that is non-toxic and can specifically deliver SQV into CD4+ immune cells. This platform may demonstrate potential utility in its application as a post-exposure prophylaxis for the treatment or reduction of HIV infection, but further studies are required.

2.2 Rationale, hypothesis, objectives and scope of proposed study

HIV poses a significant threat to global health, especially women's health [173, 174]. In the absence of a vaccine, researchers have attempted to develop strategies that can prevent/reduce heterosexual transmission of HIV in women. Vaginal microbicides that are applied vaginally prior to or after sexual intercourse as a pre/post-exposure prophylactics are being developed [175-177]. Vaginal microbicides for the delivery of anti-HIV agents have been formulated as various dosage forms including gels, films, and rings. Unfortunately, these strategies do not allow the drug to attack HIV-infected immune cells specifically. The advancement of novel drug delivery systems such as NPs allows researchers to overcome the challenge of this barrier. Antibodies, peptides and other functional ligands are promptly conjugated to NP surface to facilitate targeted delivery of therapeutic compounds to organs and cells.

SQV is an FDA-approved protease inhibitor that has been widely used in prevention or treatment of HIV/AIDS. It is active against both HIV-1 and HIV-2 including strains that are resistant to reverse transcriptase inhibitors [178]. It inhibits the process of viral protein cleavage, thus preventing the assembly of newly produced virus. Currently, only oral formulations of SQV are available in the market, however, the systemic administration is potentially associated with many side effects, including nausea, vomiting, diarrhea, fatigue, hyperlipidemia, elevated hepatic enzymes or even prolongation of QT and heart block [179]. Intravaginal drug delivery can minimize the systemic exposure of therapeutic agents, therefore improving the local therapeutic effect as well as decreasing systemic side effects of drugs.

As a result, in this study, we aimed at developing a novel intravaginal formulation of SQV to actively achieve the targeted delivery of SQV to CD4+ immune cells (target cells for HIV infection [178, 180]).

Nanocarriers have been designed for the delivery of a variety of compounds for the treatment of disease [181-184]. The extensive application of NP in medicine is a result of their desirable attributes discussed in Chapter 1. To be noted, NP facilitate drug delivery to hard-to-transfect cells, such as T cells [185], macrophages[186] and dendritic cells [187], all of which are HIV-targeted cells [180]. However, to achieve efficient intravaginal delivery and to increase patient user adherence, NP need to be formulated so that it can be easily administrated and retained within the vaginal lumen. Due to the physiochemical similarities between vaginal gels and cervicovaginal mucus, vaginal gels remain to be the most preferable choice for intravaginal administration. More importantly, previous studies have established the possibility of using vaginal gels to deliver anti-HIV drug loaded NP as a prophylaxis [188]. In this project, PLGA was used to prepare NP since it is compatible with SQV can facilitate antibody conjugation and HEC was used to formulate vaginal gel for the delivery of NP-Ab.

Therefore, we hypothesized that SQV could be formulated into a NP formulation using biodegradable and biocompatible polymer PLGA and antihuman anti-CD4 antibody could be conjugated to NPs to facilitate targeted delivery of SQV to CD+ immune cells. The nanomedicine could be potentially formulated into a gel dosage form to provide ease in self-administration and enhance retention within the vaginal tract.

The objectives of this study included (1) Develop and optimize an antibody conjugated PLGA NP formulation for SQV (2) Develop and optimize a gel formulation for NPs (3) Characterize the physiochemical properties of the formulation (4) Evaluate in vitro targeting ability and cytotoxicity for the formulation

During the early stages of vaginal entry and infection, HIV substantially invades intraepithelial vaginal Langerhans cells and CD4+ T cells through trauma or epithelial transcytosis [22]. In an ex vivo model of human vagina, HIV-1 virions were detected in both Langerhans cells and CD4+ T cells 2 hr after virus challenge [22]. In another study, SIV/HIV-1 infected cells were reported to be detected in the draining lymph nodes in pig-tailed RMs 48 hr post intravaginal inoculation of SIV/HIV-1 [189]. Therefore, after intravaginal exposure of HIV, the virus appears to be retained within local vaginal tissues for a short period of time before it reaches the lymphatic system and establishes progressive infection. This retention window provides us an opportunity to inhibit/decrease local viral replication, therefore reducing the systemic dissemination of HIV to prevent/reduce vaginal acquisition of HIV. As a result, our formulation is intended to be used as a pre/post-exposure prophylactic for sexual intercourse to control and reduce HIV infection particularly in women who have limited access to condoms.

2.3 Materials and Methods

2.3.1 Materials used for NP preparation and antibody conjugation

Saquinavir mesylate (MW 766.96 g/mol) was purchased from U.S. Pharmacopeial Convention (MD, USA). Carboxylic acid terminated PLGA (lactide: glycolide ratio 50:50, MW 7-17 K), PVA (MW 31-50 K), MES, coumarin-6 were purchased from

Sigma-Aldrich (ON, Canada). EDC and NHS were obtained from G-Bioscience (MO, USA). Mouse monoclonal anti-CD4 antibody and or HRP-labeled rabbit polyclonal secondary antibody to goat IgG were purchased from Abcam (ON, Canada). TMB substrate kit was purchased from Fisher Scientific (ON, Canada). HEC (NatrosolTM, 250 HX PHARM) was a kind gift from Ashland (GA, USA). Glycerol and dipotassium phosphate were purchased from Fisher Scientific (ON, Canada). Heat-inactivated FBS was purchased from PAA (ON, Canada), RPMI-1640, penicillin–streptomycin and PBS were purchased from Lonza (SC, USA). Keratinocyte-SFM and its supplements were purchased from Invitrogen (ON, Canada). Calcium chloride was purchased from Sigma-Aldrich (ON, Canada). Ethyl acetate, methanol and acetonitrile (HPLC grade) were purchased from EMD (ON, Canada). MF-Millipore Membrane (mixed cellulose esters, hydrophilic, 5.0 μm) was purchased from Millipore (NS, Canada). CellTiter 96® AQueous One Solution Cell Proliferation Assay (MTS) was purchased from Promega (ON, Canada).

2.3.2 HPLC method for SQV quantitation

The chromatographic separation was performed on a Nova-Pak® C-18 4 μm column (150 mm × 3.9 mm I.D.) at room temperature protected by a Nova-Pak® C-18 4 μm guard column (20× 3.9 mm I.D.) on a liquid chromatography machine (LC-2010 A, Shimadzu, MD, USA). The columns were purchased from Waters (ON, Canada). The mobile phase was composed of 45% 5 mM K_2HPO_4 and 55% acetonitrile (adjusted to pH 8.0 with H_3PO_4). The chromatographic run was performed by an isocratic elution for 10 mins at a flow rate of 1 mL/min, detected at a wavelength of 242 nm, and SQV was quantitated by

area under curve (integrated with EZstart software). The standard curve of SQV was generated in the same medium and ran at the same conditions as the samples.

2.3.3 Fabrication of SQV- NP

SQV-NP was prepared by a solvent evaporation method [190]. In brief, SQV was dissolved in methanol, making a 10 mg/mL SQV stock solution. SQV (50 µL) was combined with 30 mg/mL of PLGA-carboxylic acid ethyl acetate solution (575 µL), forming the organic phase. The organic phase was emulsified with an aqueous phase solution containing 5% PVA (4.38 mL) for 2 mins on ice under continuous sonication by a microtip probe sonicator (Branson sonifier 150D, QSonica, USA). The resulting oil-in-water emulsion was then stirred for 3 hr at 4 ºC to evaporate the organic solvent. SQV-NP were collected by centrifugation (20,000g, 10 min, 25 ºC) (Sorvall RC6+, Thermo Fisher, Asheville, USA) and washed twice with autoclaved Milli-Q water to remove excess emulsifier and free drug. Courmarin 6-encapsulated NP was prepared following the same method.

2.3.4 Antibody conjugation to NP

The NP suspension in pH 5.0 of MES buffer (2 mg/mL) was incubated with 50 µL of 1.5 mg/mL EDC and 50 µL of 1.5 mg/mL NHS solutions at 4 ºC for 1 hr on a rotary shaker (Roto-Shake Genie, Scientific Industries, NY, USA) for carboxylic group activation [191]. The activated NP were incubated with 100 µL of 40 ng/mL anti-CD4 antibody or HRP-labeled rabbit polyclonal secondary antibody to goat IgG at 4 ºC for 2 hr on a rotary shaker. The SQV-NP-CD4 was washed and collected by centrifugation to remove excess

NHS, EDC and unconjugated antibodies. The resulting NP conjugated with antibody were resuspended in PBS and used immediately.

2.3.5 Preparation and characterization of 1 % (w/w) HEC gel

Approximately 1 g of HEC (2%) was added to 40 mL of PBS (pH 5.0) and stirred at 4 ºC for 2 hr until dissolved. To adjust the viscosity of the gel to be similar to gels used for microbicide evaluation, 5 g of glycerol (10%) was added and stirred until it was uniformly dispersed. The pH of the gel was adjusted to 5.0±0.2 (physiological vaginal pH) and the total weight was adjusted to 50 g using PBS (pH 5.0). As for loading NP into HEC gel, SQV-NP-CD4 was resuspended in PBS (pH 5.0) to make a concentration of 10 mg/mL. The NP suspension was combined with the HEC gel and stirred at 4 ºC for 2 hr resulting in a preparation containing 1% HEC gel loaded with 0.5% NP. Homogeneity of NP in the gel was confirmed by randomly sampling different parts of the gel containing coumarin 6-encapsulated NP and comparing the fluorescence readings of each sample.

The viscosity of the gel was determined using an AR550 Rheometer (TA Instruments, New Castle, USA) with a 20 mm 2º steel cone at 37 ºC.

2.3.6 Characterization of NP

2.3.6.1 Particle size

SQV-NP and SQV-NP-CD4 were resuspended in autoclaved Milli-Q water. Particle size (25 µg/mL of NP suspension) was determined by dynamic light scattering (DLS) using ZetaPALS (Brookhaven Instruments). Samples were tested in triplicate for 3 runs of 2 mins each.

2.3.6.2 Zeta potential

SQV-NP and SQV-NP-CD4 were resuspended in autoclaved Milli-Q water. Zeta potential (100 µg/mL of NP suspension; smulchovski mode) was determined by dynamic light scattering (DLS) using ZetaPALS (Brookhaven Instruments). Samples were tested in triplicate for 3 runs of 2 mins each.

2.3.6.3 Surface morphology

SEM was used to visualize the surface morphology and size of NP. SEM images were taken on a Field Emission Auger Electron Microprobe JEOL JAMP 9500F equipped with a floating type micro ion etching device (FMIED) for charge neutralization on non-conducting NP samples (5-10 mg/mL). The images were taken and analysed using the EOS 9500 image acquisition software at a voltage of 5.0 kV.

2.3.6.4 Encapsulation efficiency of NP

To determine the EE%), the amount of unencapsulated SQV in the wash solutions was quantified by HPLC. Encapsulation efficiency was determined by the following equation:

$$\text{EE } \% = \frac{\text{amount of total drug in µg} - \text{amount of unentrapped drug in µg}}{\text{amount of total drug in µg}} \times 100\%$$

2.3.6.5 Antibody conjugation efficiency of anti-CD4 antibody to NP

To determine the ACE% of anti-CD4, HRP-conjugated rabbit polyclonal secondary antibody to goat IgG was used as a surrogate for anti-CD4 antibody conjugation following the method described in section 2.4. Various concentrations of anti-CD4 antibody were evaluated to optimize the ACE%. Unconjugated antibody recovered in the

supernatant was quantified using a TMB substrate kit. TMB is a chromogenic substrate that can be oxidized by HRP. Upon reaction with HRP, the TMB yields a blue color, which further changes to yellow (with maximum absorbance at 450 nm) upon addition of a sulfuric acid stop solution. The absorbance at 450 nm is proportional to the amount of HRP, which reflects the amount antibody. Therefore, by generating a standard of HRP-conjugated antibody, the amount of HRP-conjugated antibody was quantified. ACE% was determined by the following equation:

$$\text{ACE } \% = \frac{\text{amount of total antibody in } \mu g - \text{amount of unconjugated antibody in } \mu g}{\text{amount of total antibody in } \mu g} \times 100\%$$

2.3.6.6 In vitro release studies

To determine SQV release from NP, 1 mg SQV-NP were resuspended in 1 mL PBS (pH 4.2) as release medium and maintained at 37 ºC on a rotary shaker at a speed of 100 rpm. At different time points, samples were centrifuged and 200 µL of release medium was removed and replenished with equal amount of fresh release medium [128]. Samples were filtered through a 0.2 µm GHP filter (Pall, ON, Canada) and the amount of SQV released was quantified by HPLC using the method mentioned above.

To determine SQV release from the gel, 100 µL of gel was immersed into 1 mL of PBS (pH 4.2) and incubated at 37 ºC on a rotary shaker. At various time points, samples were centrifuged and 200 µL of release medium was removed, filtered through 0.2 µm GHP filter (ON, Canada) and analyzed by HPLC. Release media was replenished with equal volume of medium. To further investigate the release profile of NP-loaded gel, 200 µL of gel was placed into the donor chamber of a Franz cell with 5 mL of PBS added into the

receptor chamber [55]. Between the donor and receptor chambers, a 5 μm semi-permeable membrane was sandwiched to mimic the mucus mesh in the vaginal cavity. The Franz cells were incubated in a circulating water bath at 37 ºC. At various time points (1-24 hr), 0.5 mL of release medium was removed and replenished with equal amount of fresh release medium. Samples were centrifuged and filtered through a 0.2 μm GHP filter (ON, Canada) and the amount of SQV released was quantified by HPLC.

2.3.6.7 In vitro cell targeting studies

Since intravaginal epithelial cells co-exist with immune cells (CD4+ T cells, dendritic cells and macrophages) in the vagina, a typical CD4+ cell line (Sup-T1) and a CD4- vaginal epithelial cell line (VK2/E6E7) were selected for the in vitro cell targeting studies [192]. Sup-T1 cells (CD4+) were obtained from the National Institutes of Health AIDS Reagent Program and maintained at 37°C and 5% CO_2 with RPMI-1640 culture media supplemented with 10% heat-inactivated FBS and penicillin (100 U/mL)-streptomycin (100 μg/mL). 1×10^6 Sup-T1 cells were seeded in 6-well tissue culture treated plates (Corning, NY, USA) in 5 mL culture medium on the day of the experiments.

Vaginal epithelial cells (VK2/E6E7) (CD4-) were obtained from ATCC and maintained at 37°C and 5% CO_2 with culture media supplemented with 0.1 ng/mL human recombinant EGF, 0.05 mg/mL bovine pituitary extract, and additional calcium chloride 44.1 mg/L and penicillin (100 U/mL)-streptomycin (100 μg/mL). 5 x 10^5 VK2/E6E7 cells were seeded in 6-well tissue culture treated plates (Corning, NY, USA) in 2.5 mL culture medium one day prior to the experiments.

Prior to the initiation of cell targeting studies, the impact of drug-loaded NP (SQV-NP-CD4) on Sup-T1 cell viability was determined. In brief, 1 x 10^5 cells were seeded in a 96-well plate and subjected to various concentrations of SQV-NP-CD4 (200-1000 μg/mL) for 2 and 24 hr respectively. Negative control was blank cell media and positive control was 1 M acrylamide in cell media. At the end of the treatment period, 20 μL of MTS solution was added into each well and incubated for 1 hr. Interference generated by NP was deducted by running parallel samples with NP alone in the same media. The plate was read using a microplate reader (BioTek Instruments, VT, US) at wavelength of 490 nm.

SQV-NP-CD4 or SQV-NP were resuspended in PBS and subjected to Sup-T1 or VK2/E6E7 cells at a final concentration of 600 μg/mL in each well. All treatment groups were maintained at 37 ºC, 5% CO_2 and treated for 0.5, 1, 2 and 6 hr respectively. Targeted delivery of SQV into Sup-T1 cells was evaluated by quantifying intracellular uptake of SQV. In brief, at various time points, cells were collected by centrifugation at 100xg for 5 mins, washed twice with PBS, and lysed with 200 μL of 90% DMSO in PBS at room temperature for 10 mins. The lysate was then centrifuged at 20,000 g, at 4 ºC for 20 mins, filtered through a GHP filter and analyzed by HPLC. Delivery of SQV into CD4- cells (VK2/E6E7) was included as a control to determine the specificity of SQV-NP-CD4 targeted delivery. In brief, at various time points, medium containing NP were removed and cells were washed twice with PBS, and lysed with 200 μL of 90% DMSO in PBS at room temperature for 10 mins. The lysate was collected and centrifuged at 20,000xg, at 4 ºC for 20 mins, filtered through a GHP filter and analyzed by HPLC using the method mentioned above.

2.3.6.8 In vitro cellular cytotoxicity study

Cellular cytotoxicity was determined using the MTS assay. VK2/E6E7 cells were plated at 10^5 cells/well on 96-well tissue culture treated plates (BD Biosciences, ON, Canada) in 100 µL culture medium. Varying concentrations of drug free NP-Ab (200-1000 µg/mL), 1% HEC placebo gel (40-200 µg/mL), and 1% HEC gel loaded with drug free NP-Ab (5 mg NP/ g gel) (40-200 µg/mL) were pre-mixed with culture media, added to cells, and incubated for 2 hr and 24 hr. Negative control was blank cell media and positive control was 1 M acrylamide in cell media. At the end of the treatment period, cells were washed, replaced with fresh medium containing 20 µL of MTS solution, and incubated for 1 hr. The plate was analyzed on a microplate reader (BioTek Instruments, VT, US) at 490 nm.

2.3.7 Statistical Analysis

Student's t-test (unpaired, two-sample, unequal variance with two-tailed distribution) was performed on all results with $p<0.05$ considered significant. Data shown are expressed as mean +/- SD.

2.4 Results

2.4.1 Characterizations of NP

Nanoparticle size, zeta potential and EE% of drug-free NP, SQV-NP, and SQV-NP-CD4 are listed in Table 2.1. Average particle sizes for SQV-NP and SQV-NP-CD4 were found to be in the range of 200 - 300 nm. Zeta potentials for SQV-NP and SQV-NP-CD4 were determined to be around -18.8±2.9 mV and -9.7±3.1 mV, respectively. EE% of SQV-NP formulated in this study was 74.4±3.7%. ACE% of SQV-NP is shown in Table 2.2.

ACE% of SQV-NP was determined using antibodies of varying concentrations (10, 20 and 40 ng/mL) resulting in an ACE% of 80.95±1.1%, 79.91±0.55%, and 74.29±2.67% respectively. The ACE% decreased as the concentration of antibody increased. In terms of the amount of antibody conjugated to 1 mg of NP, there was a proportionate increase in the amount of antibody conjugated with increasing concentration of antibody added. The SEM images of SQV-NP and SQV-NP-CD4 are shown in Figure 2.1. SQV-NP and SQV-NP-CD4 both appeared to be spherical in shape with a smooth surface. Furthermore, there does not appear to be any nanoparticle aggregation and the size distribution observed from SEM images further supported the results obtained with dynamic light scattering (Table 2.1).

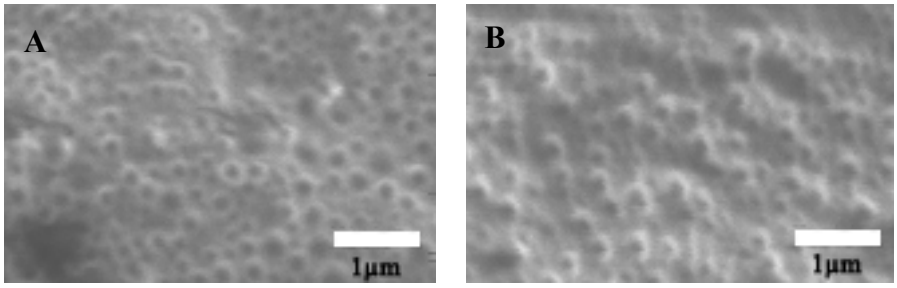

Figure 2.1: SEM images of SQV-NP and SQV-NP-CD4. Images were taken under a magnification of 3000X. (A) SQV-NP (B) SQV-NP-CD4

Table 2.1: Particle size, zeta potential and EE% of Blank (drug-free) NP, SQV-NP and SQV-NP-CD4.

	Blank NP	SQV-NP	SQV-NP-CD4
Size (nm)	177±1.4	245.7±8.4	280.2±11.9
Zeta Potential (mV)	-21.4±4.7	-18.8±2.9	-9.7±3.1
EE%	—	74.4±3.7	65.3±2.3
SQV loading (μg/mg NP)	—	31±1.5	27.2±0.9

Table 2.2: ACE% and antibody loading of SQV-NP

Concentration of antibody (ng/mL)	10	20	40
ACE (%)	80.95±1.10	79.91±0.55	74.29±2.67
Antibody loading (ng/mg NP)	9.71±0.13	19.17±0.13	35.66±1.28

2.4.2 In vitro release study of SQV from NP and SQV from 1% HEC gel loaded with SQV-NP-CD4

As shown in Figure 2.2, the release of SQV from NP was sustained throughout the entire study period. More than 50% of SQV was released after 3 days. There was a burst release of approximately 35% (10.1 μg/mL) of total loading within the first 3 hours, and 43% (12.6 μg/mL) of total loaded SQV was released after 24 hr at pH 4.2. Subsequently, the SQV-NP demonstrated a sustained linear release profile with approximately 2-3% of total loaded SQV released per day.

In vitro release studies performed in microcentrifuge tubes containing 1% HEC gel loaded with SQV-NP (5 mg NP/g gel) in PBS (pH 4.2), suggested a nearly linear release profile of SQV with approximately 3% of total loaded SQV released within 24 hr (Figure 2.3A). Figure 2.4B shows the in vitro release profile of SQV from 1% HEC gel loaded with SQV-NP-CD4 (5 mg NP/ g gel) for the same period in PBS (pH 4.2) conducted in Franz cells. The release of SQV from NP when loaded in a gel dosage form also exhibits a near-linear release profile after the first 24 hr with 0.18±0.04 % of total loaded SQV released.

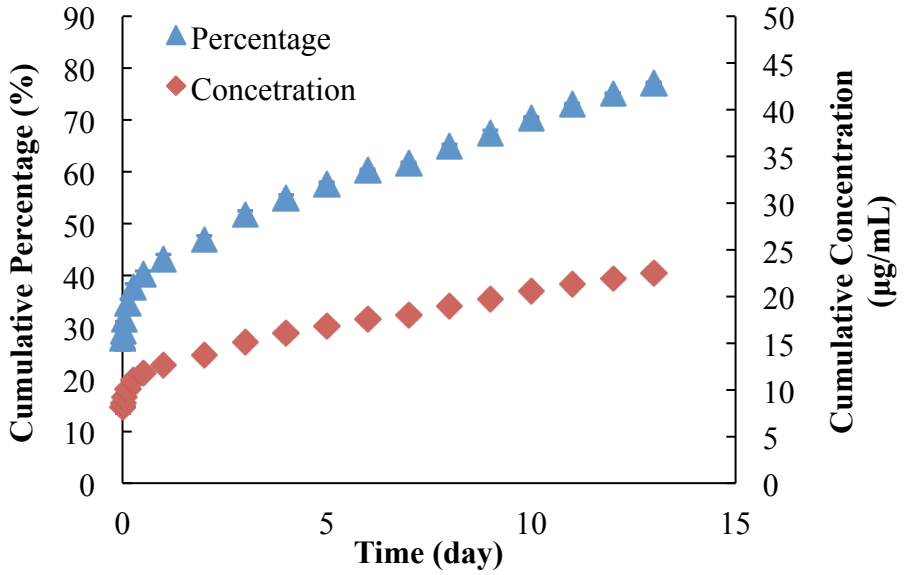

Figure 2.2: In vitro cumulative release of SQV from SQV-NP at 37 °C in PBS (pH 4.2). Values represent the mean±SD, n=5.

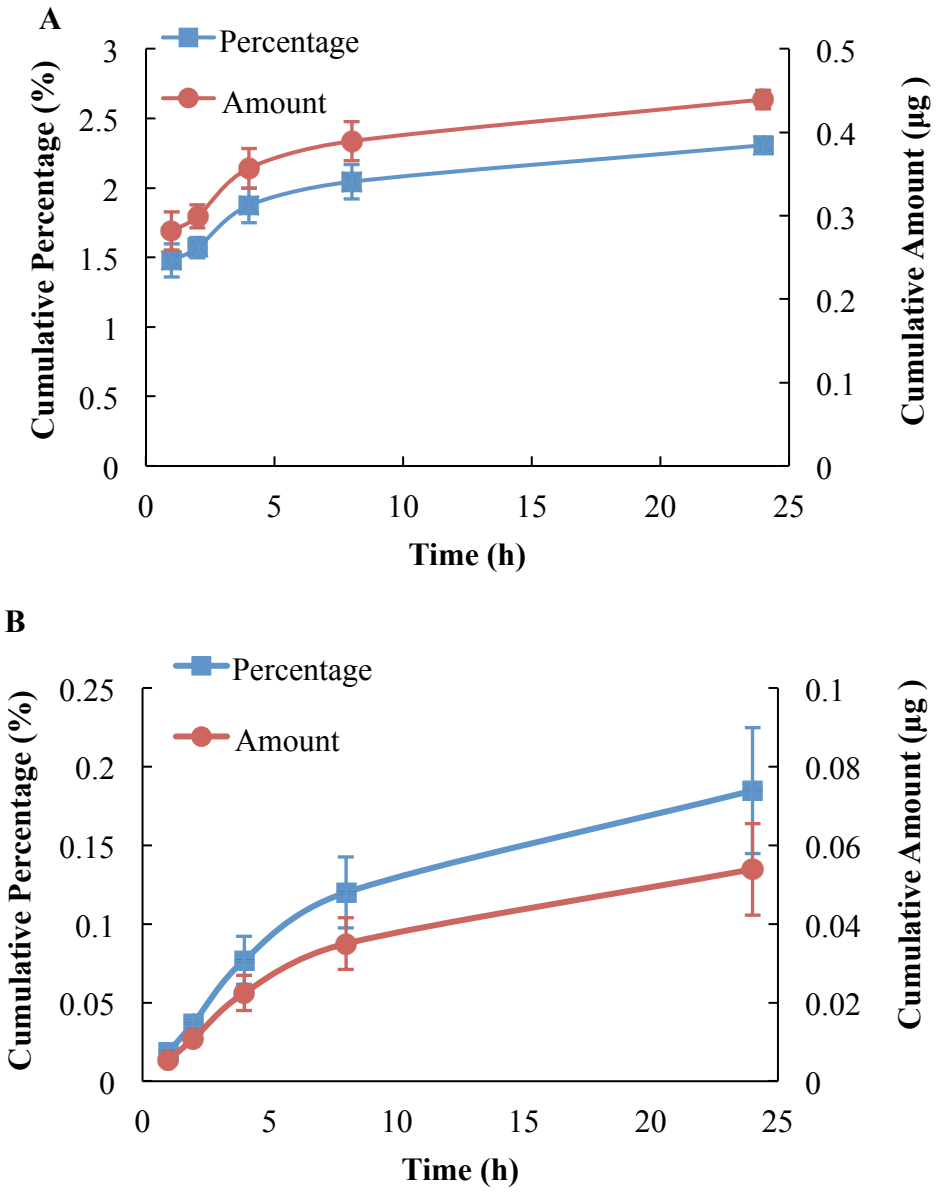

Figure 2.3: In vitro cumulative release of SQV from 1% HEC gel loaded with SQV-NP-CD4 at 37°C in PBS (pH 4.2). (A) Release study conducted in microcentrifuge tubes (B) release study conducted in Franz cells. Values represent the mean±SD n=3.

2.4.3 Characterization of 1% HEC gel loaded with SQV-NP

The fluorescence reading of 1% HEC gel loaded with coumarin 6-encapsulated NP coming from three different parts of the gel was 8095, 8321 and 7945 respectively, indicating the NP were homogenously dispersed. As shown in Figure 2.4, the flow curves for both 1% HEC placebo gel and 1% SQV-NP-CD4 loaded HEC gel (5 mg NP/g gel) displayed non-Newtonian shear-thinning behavior. The viscosity of the 1% SQV-NP-CD4 loaded HEC gel was determined to be around 2.800 Pa.s at a shear rate of 60 s^{-1}. At the same shear rate, it has been reported that over-the-counter lubricant products such as KY Jelly and Astroglide gel have viscosities of 2.765 Pa.s and 2.071 Pa.s respectively [193]. Moreover, it was reported that a 1% tenofovir intravaginal gel used in a Phase 2 clinical trial also had a similar viscosity of 2.736 Pa.s [194]. As a result, the 1% HEC gel is an appropriate choice for our study.

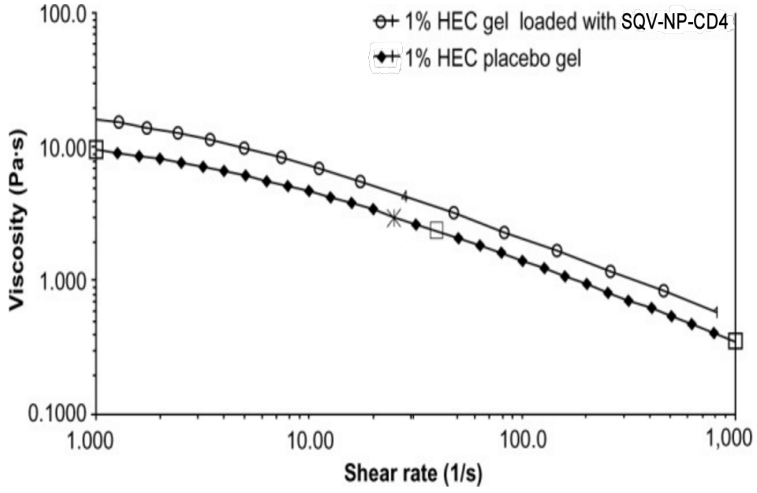

Figure 2.4: Steady-state flow curves of 1% HEC placebo gel and 1% HEC gel loaded SQV-NP-CD4 (5 mg NP/g gel) at a measurement temperature of 37 ºC. Viscosity profiles were shown as single measurements.

2.4.4 In vitro cell targeting studies

Prior to evaluating the targeting ability of NP-Ab into CD4+ cells, Sup-T1 cells were treated with SQV-NP-CD4 to determine a drug concentration that was non-cytotoxic. Based on our studies, no significant effects on cell viability were observed when cells were treated with concentrations <800 μg/mL of SQV-NP-CD4. As a result, a medium concentration (600 μg/mL) was chosen for our cell targeting studies. The active targeting ability of SQV-NP-CD4 was evaluated in a human CD4+ T-cell line, Sup-T1, and in a human CD4- cell line, VK2/E6E7. Figure 2.5A shows the impact of drug-loaded NP (SQV-NP-CD4) on Sup-T1 cell viability. No significant cytotoxicity was observed at concentrations up to 800 μg/mL while concentrations above that (1000 μg/mL) significantly induced cell death. Figure 2.5B compared the ability of SQV-NP and SQV-NP-CD4 to deliver SQV intracellularly into Sup-T1 cells at various time intervals. Our data showed that SQV-NP and SQV-NP-CD4 could achieve fast intracellular delivery of SQV into CD4+ T-cells. Significant differences ($p<0.05$) in the intracellular accumulation of SQV were observed in the SQV-NP-CD4 group when compared to the SQV-NP group at all the time points. The intracellular concentrations of SQV delivered by SQV-NP-CD4 was 1.7 fold, 2.2 fold, 1.4 fold, and 1.8 fold higher than unconjugated SQV-NP at 0.5 h, 1 h, 2 h and 6 h time points, respectively, suggesting that SQV-NP-CD4 could actively target the delivery of SQV into Sup-T1 cells. In contrast, no significant differences were observed in the cellular uptake of SQV by the CD4- cell line, VK2/E6E7 when delivered by SQV-NP or SQV-NP-CD4 at any time points (Figure 2.5B). Although there was an increase in the accumulation of SQV with time, the results suggested non-specific delivery of SQV into VK2/E6E7 (Figure 2.5C). More importantly, the in vitro IC_{50} of

SQV against HIV-1 is reported to be 0.031± 0.022 µM (0.02013±0.01476 µg/mL) [195]. The highest non-toxic concentration of SQV-NP (1000 µg/mL) contains 31 µg/mL SQV, which is much higher than the IC_{50} of SQV, hence, our formulation is safe and potentially effective against HIV-1.

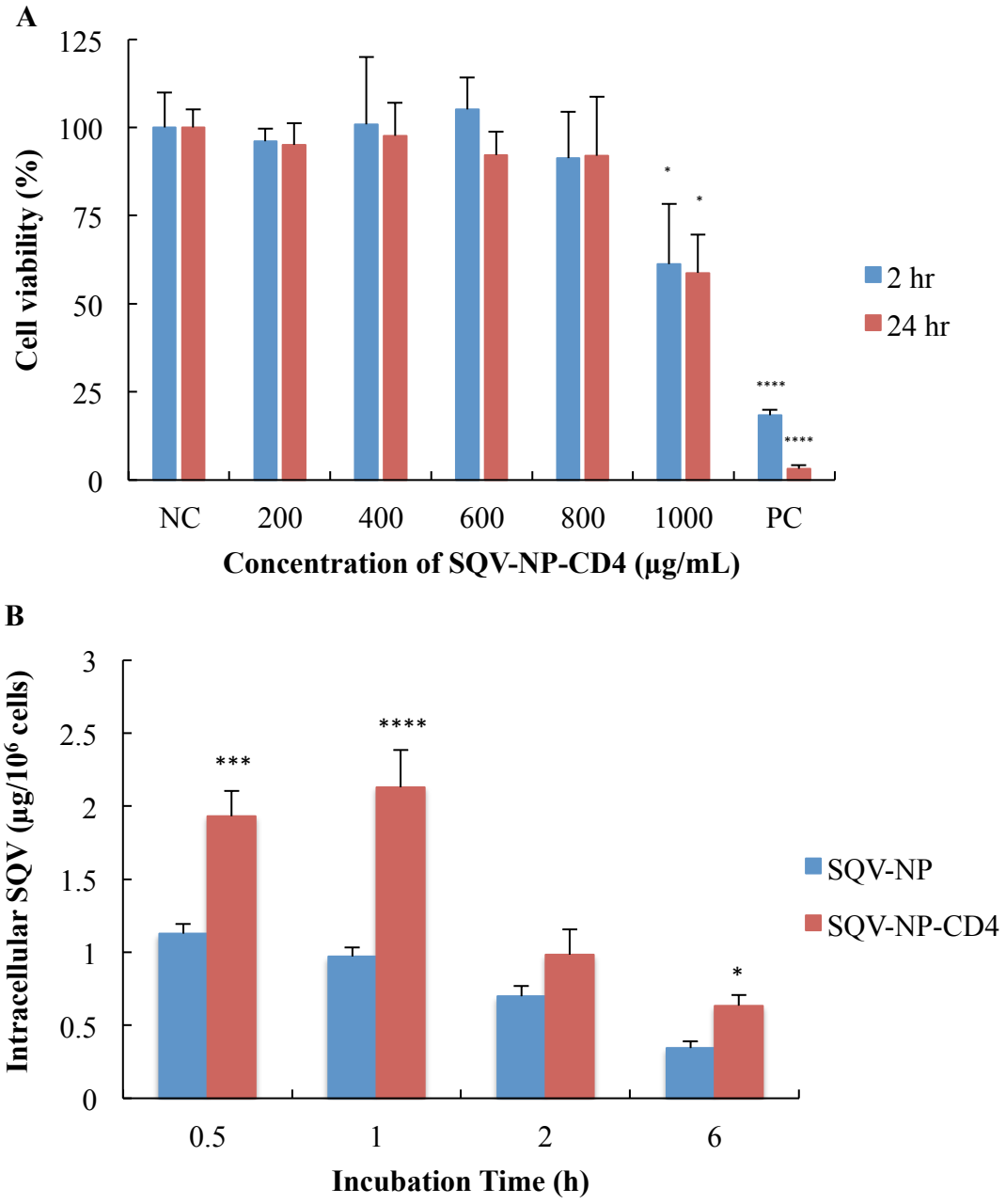

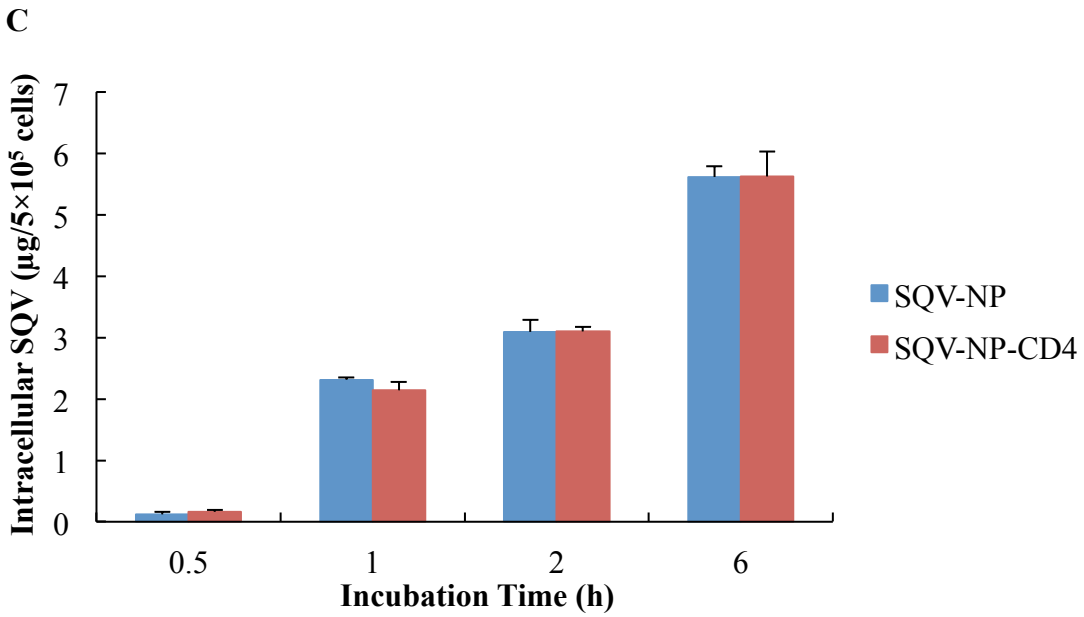

Figure 2.5: (A) MTS assay of SQV-NP-CD4 in Sup-T1 cells. The data shown represent the mean±S.D, N=4. (B) Intracellular accumulation of SQV in Sup-T1 cells and (C) Intracellular accumulation of SQV in VK2/E6E7 cells, *p<0.05, ***p<0.001, ****p<0.0001 vs SQV-NP. Values represent the mean±SD, n=5.

2.4.5 In vitro cytotoxicity study

The in vitro cytotoxicity study was measured using the method mentioned above to evaluate the in vitro safety profile of the formulation. According to Figure 2.6, drug-free NP-CD4, 1% HEC placebo gel, and 1% HEC gel loaded with drug-free NP-CD4 (5mg NP-Ab/g gel) appeared to have no significant impact on the cell viability of VK2/E6E7 up to concentrations of 1000 µg/mL, 200 mg/mL and 200 mg/mL respectively after exposure for 2 and 24 hr. Cell culture media was used as negative control and 1% polyacrylamide solution was used as positive control.

A

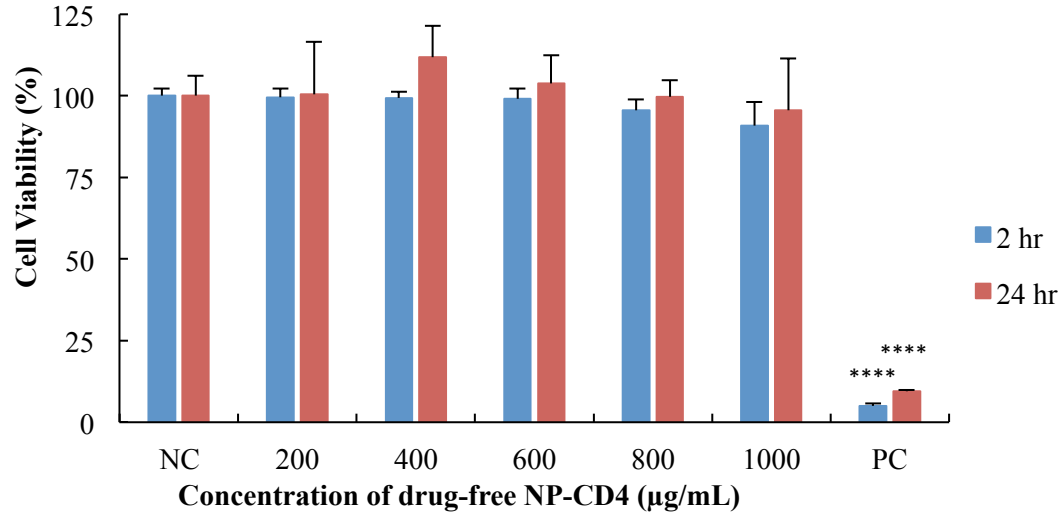
125
100
75
50
25
0
Cell Viability (%)
****
****
2 hr
24 hr
NC
200
400
600
800
1000
PC
Concentration of drug-free NP-CD4 (µg/mL)

B

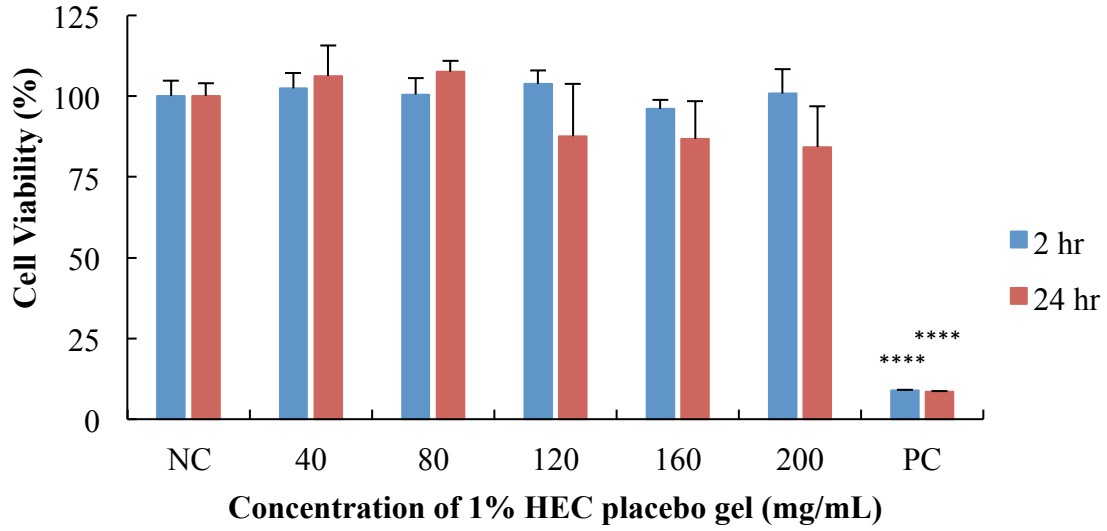
125
100
75
50
25
0
Cell Viability (%)
****
****
2 hr
24 hr
NC
40
80
120
160
200
PC
Concentration of 1% HEC placebo gel (mg/mL)

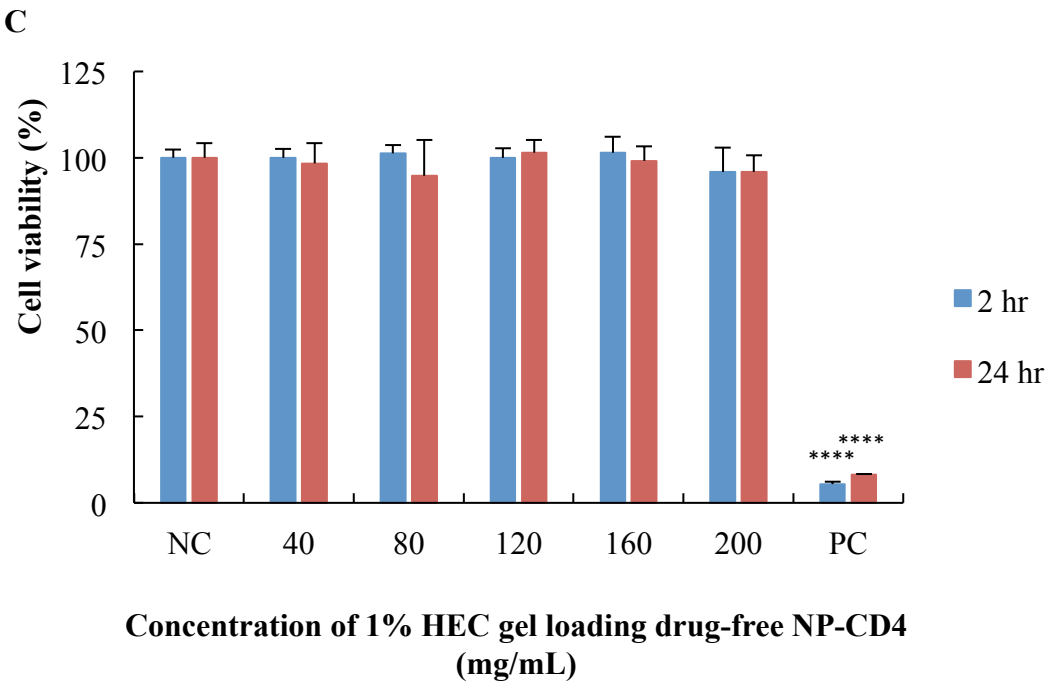

Figure 2.6: MTS assay of various formulations in VK2/E6E7 cells (A) drug-free NP-CD4 (B) 1% HEC placebo gel (C) 1% HEC gel loaded with drug-free NP-CD4 (5 mg NP/g gel).

2.5 Discussion

Nanoparticle-based therapy is a promising modality for the prevention and treatment of HIV/AIDS [196]. Previous studies have established effective and safe intracellular delivery of antiretroviral drugs into human peripheral blood mononuclear cells or human monocyte/macrophage by NP [197, 198]. Further studies have also demonstrated favorable antiretroviral efficacy against HIV-1 when the drug is delivered into human monocyte-derived macrophages [199]. Since unprotected heterosexual vaginal intercourse has become one of the major modes of transmission, there is an increasing interest in developing intravaginal microbicides against HIV infection. For example, Zhang et al.

developed a pH-responsive nanoparticle formulation that can achieve increased sustained release of tenofovir in acidic environments as a potential intravaginal microbicide [200]. Das Neves et al. also compared different types of polymeric NP for delivering dapivirine as a microbicide, in terms of efficacy and cytotoxicity in various HIV-related cells [201]. Woodrow et al. developed an intravaginal delivery system that can effectively silence herpes simplex virus genes with small interfering RNA[128]. Antibody-conjugated NP has been long investigated for the treatment of numerous diseases including cancer [202-206]. Our team is interested in extending the application of NP-Ab for intravaginal delivery. Previous studies have developed non-targeting SQV-NP using poly(ethylene oxide)-modified poly(epsilon-caprolactone) for the delivery into a human monocyte/macrophage (Mo/Mac) cell line [198] and CD4-targeted lipid NP have been shown to enhance the antiretroviral activity of indinavir [207]. However, our study is the first to demonstrate active targeted delivery of SQV into CD4+ cells via antibody-conjugated biodegradable NP.

In our study, the size distribution of NP (drug-free NP, SQV-NP and SQV-NP-CD4) was unimodal with a mean diameter of 177-280 nm as detected by dynamic light scattering. Particle size increased slightly as drug was loaded and antibody was conjugated to NP. The particle size of SQV-NP-CD4 could be controlled within the range of 200-500 nm (mean size 280 nm), which was previously reported to be the optimal size range for intravaginal drug delivery [208]. Therefore, it is rational to speculate that SQV-NP-CD4 developed in this study has potential abilities to achieve intravaginal delivery but further in vivo studies are required. The zeta potentials of drug-free NP, SQV-NP and SQV-NP-CD4 were determined to be negative because of the presence of terminal carboxylic

groups in PLGA. Encapsulation of SQV into NP increased the zeta potential, which may be a result of SQV adsorbed onto the surface of NP to mask the charges generated by the carboxylic groups. The zeta potential was further increased as antibody is conjugated to NP because of the direct interaction between the antibody and the carboxylic groups on the surface [209]. Our formulation demonstrated a SQV EE% of approximately 75%, which is higher in comparison to other SQV delivery systems (<60%) [198, 210]. This could be due to the fact that the salt form of SQV, SQV mesylate, has a relatively high hydrophobicity (log P (o/w)= 4.1) [211], allowing it to enter the organic phase rather than the aqueous phase during NP preparation, hence, resulting in favorable EE%. Therefore, it can be expected that the formulation established in this study can be applied to similar lipophilic drugs.

Covalent NP-Ab conjugates were achieved under the catalysis of EDC/NHS to form amide bonds through the amino groups from antibody and terminal carboxyl groups from PLGA [212]. ACE% results displayed a concentration-dependent trend. Highest ACE% was achieved when the lowest concentration of antibody was used, while the greatest amount of antibody conjugated to NP was achieved when the greatest amount of antibody was added. Since NP present a certain surface area that can accommodate limited amount of antibody, the amount of antibody that can be conjugated to NP will reach a saturation limit. When the amount of antibody added is far below the saturation limit, ideally, all the antibody could potentially be able to conjugate to NP and reach a close-to-100% ACE%. However, because some carboxyl groups on the surface remain inactivated, the highest ACE% that could be achieved is always below 100%. In our study, addition of 10 or 20 ng/mL of antibody achieved around 80% conjugation efficiency. In contrast, addition of

40 ng/mL of antibody resulted in a significant reduction in ACE% (74%) and further increase in the antibody concentration will lead to a further decreased ACE%.

The normal human vaginal environment is slightly acidic (pH 3.8 – 4.5) due to the production of lactic acid by lactobacilli [213, 214]. As a result, our in vitro release studies were conducted in slightly acidic buffer to mimic the pH environment of the human vaginal tract. In general, the release data showed that SQV-NP showed a sustained release of SQV in acidic environment, indicating that the SQV continuously leaked out of NP in vaginal lumen before it was delivered intracellularly. However, after antibody conjugation, when the SQV-NP-CD4 was formulated into a gel dosage form, the release of SQV was significantly reduced in acidic environment, which was favorable for retaining SQV in the formulation and improving the amount of SQV that could be delivered intracellularly. We thought this is probably due to significantly decreased interaction between SQV-NP-CD4 and large amount of release medium, leading to retarded diffusion of SQV from NP within short period of contact with acidic environment. Previous studies have shown that the release of encapsulated therapeutic agents from a matrix is mainly attributed to the diffusion of therapeutic agents during the early stage, while the later stage of release is attributed to both drug diffusion and polymer degradation [215].

According to the results, Sup-T1 cells treated with SQV-NP-CD4 exhibited higher amounts of SQV intracellularly than cells treated with SQV-NP, indicating specific active targeting by SQV-NP-CD4. The targeted delivery of SQV could be achieved rapidly in Sup-T1 cells, with peak intracellular concentrations of SQV within the first hour of treatment. Interestingly, the intracellular accumulation of SQV appeared to decrease with

time and is independent of the type of treatment. Previous studies have shown that SQV can be transported out of the cell by the multidrug resistant transporter P-glycoprotein (PGP). PGP is an ATP-driven drug efflux pump, which is found to be highly expressed in the mucosa of the gastrointestinal tract and brain capillary endothelial cells [216-219], but weakly expressed or unexpressed in human uterus and cervix [220]. As a result, it has been shown to be the main barrier that limits the oral availability and tissue penetration of SQV [221, 222]. More importantly, PGP is also found to be expressed on CD4+ T-lymphocytes, the major target for HIV-1 infection [223, 224]. Therefore, the decreased intracellular concentration in Sup-T1 cells may be attributed to the efflux of SQV by PGP. When developing future formulations for SQV, it may be beneficial to co-encapsulate a PGP inhibitor along with SQV. To further confirm the specific targeting ability of SQV-NP-CD4, a CD4- vaginal epithelial cell line, VK2/E6E7 was also treated with both SQV-NP and SQV-NP-CD4. As expected, non-specific uptake of SQV-NP and SQV-NP-CD4 was observed with no significant differences detected between the two treatment groups. In addition, the intracellular accumulation of SQV increased with time in VK2/E6E7 cells, suggesting that SQV is stable in the formulation for intracellular uptake and further supporting the observation that decreased cellular accumulation of SQV in Sup-T1 cells may largely be due to the efflux of SQV.

Studies have shown that SQV can be metabolized by the cytochrome P450 (CYP 450) enzyme system, primarily CYP3A4 [225]. Currently, there appears to be a lack of studies demonstrating CYP 450 expression in human T-cells. As mentioned earlier, we did not detect any SQV degradants/metabolites using our HPLC method. It is possible that CYP

450 plays a role in metabolizing SQV and contributes to the decreased levels of SQV in cells, but further studies are required to confirm this.

Cytotoxicity is another important aspect when evaluating an intravaginal microbicide formulation. HEC was chosen as the main polymer for our intravaginal gel formulation because several studies have shown that it is non-cytotoxic in the presence of epithelial cell lines and peripheral blood mononuclear cells [193]. Clinical studies using HEC-containing gels have also demonstrated a high safety profile (94.3%) [226]. Although previous studies have investigated the individual safety profiles of PLGA NP and HEC gel, we decided to evaluate the maximum concentration of each individual component as well as in combination (PLGA-NP, placebo 1% HEC gel, and PLGA-NP-loaded 1% HEC gel) that can be tolerated by vaginal epithelial cells. The VK2/E6E7 cell line was able to tolerate up to 1000 μg/mL of PLGA-NP alone, 200 mg/mL of 1% HEC placebo gel, and 5 mg of PLGA-NP per gram of 1% HEC gel before cytotoxicity was observed. As a result, our formulation appears to be safe for vaginal applications.

Chapter 3

pH-sensitive RNAi-based combination nanomicrobicide for the prevention/reduction of vaginal transmission of HIV

Sidi Yang, Yufei Chen, Jijin Gu, Angelia Harris, Ruey-Chyi Su, Emmanuel A. Ho.

3.1 Abstract

Women are more susceptible to HIV transmission through unprotected heterosexual intercourse due to biological and social vulnerabilities. Intravaginal delivery of siRNAs targeting viral genes, host genes, or in combination has shown promising outcomes against HSV, HPV and HIV. Therefore, in this study, we designed, developed and evaluated a pH-sensitive RNAi-based combination nanomicrobide for the prevention/reduction of vaginal transmission of HIV. The nanomicrobide was composed of siRNA-PEI encapsulated PLGA-PEG NP loaded in a HEC gel dosage form, and siRNA targeting host gene CCR5 and siRNA targeting viral gene Nef were co-encapsulated into NP as a dual preventive strategy. Knocking down CCR5 could prevent HIV from attaching to and entering host cells in the first place and knocking down Nef could reactivate autophagy that was inhibited by Nef to improve the elimination of intracellular virus that escaped the first line of defense through autophagy. The siRNA NP showed a desirable particle size and zeta potential for intravaginal delivery and a pH-dependent release profile that could preserve siRNA under acidic vaginal conditions (VFS, pH 4.2) but release siRNA under neutral intracellular conditions (PBS, pH 7.4). The CCR5-Nef NP could efficiently knock down CCR5 and Nef, reactivate Nef-blocked autophagy and inhibit the replication of HIV in vitro. After being formulated into a gel dosage form, siRNA NP could be readily released from the gel, penetrated the vaginal epithelial layer, and got taken up into target cells and knockdown Nef and CCR5 without causing cytotoxicity in a vaginal mucosal co-culture model. Further anti-CD4 antibody conjugation to the siRNA NP could improve the vaginal distribution and uptake of siRNA in a mouse model when it was subjected to 4-dose treatments of 0.5% HEC gel loaded

with siRNA NP-CD4 and the distribution of siRNA was restricted to reproductive tract without causing any unwanted systemic distribution. CCR5 was used as a model gene to evaluate the gene knockdown efficacy of 0.5% HEC gel loaded with siRNA NP-(m)CD4 in mouse vagina and the results indicated that 0.5% HEC gel loaded with siRNA NP-(m)CD4 could significantly downregulate approximately 40% of CCR5 protein in lower vagina and 36% of CCR5 protein in upper vagina and cervix, while 0.5% HEC gel loaded with siRNA NP-IgG could not cause any significant gene knockdown in either location.

3.2 Rationale, hypothesis, objectives and scope of this study

RNAi refers to a sequence-specific post-transcriptional gene silencing process in the cytoplasm achieved by siRNAs that contains complementary sequence to the target gene [227]. A vaginal microbicide containing siRNAs holds great promise in preventing infections such as HIV, HSV-2, and HPV. The application of therapeutic siRNAs targeting single or multiple viral factors can suppress the viral life cycle resulting in the prevention of viral replication and the establishment of productive infection [228-230], and those targeting host genes can inhibit the viral entry into target cells and prevent the infection in the first place [231, 232]. Therapeutic siRNAs targeting both viral genes and host genes can also be used in combination for enhanced antiviral activity [233, 234]. A vaginal microbicide is designed to specifically elicit its effects at the site of initial infection and reduce systemic adverse effects. However, naked siRNAs have difficulties in achieving efficient mucosal uptake if administered directly into the vagina due to its rapid degradation, poor cellular uptake, and low endosomal escape efficiency [235]. Developing drug delivery systems that are capable of transporting siRNA through extracellular and intracellular barriers to specific sites is the priority of developing siRNA-based therapy. To date, a few studies have successfully use NP as a delivery system for intravaginal delivery of siRNA and achieved inhibition of HIV, HSV and HPV in vitro and in vivo [49, 228, 232].

HIV uses CD4 and the co-receptor CCR5 or CXCR4 to gain entry into the host cells [22]. CCR5 is predominantly used in the establishment of initial HIV infection while CXCR4 is extensively used at later stage of the disease [24, 236]. Both in vivo and ex vivo studies also indicated that human cervicovaginal tissues preferentially support the productive

infection of R5 HIV-1 rather than that of X4 HIV-1 [237]. Therefore, CCR5 is the dominant co-receptor involved in the vaginal infection of HIV and can be considered as the target for preventing viral entry into target cells. And this proposal is further supported by the fact that people with homozygous CCR5 delta32 gene (a mutant CCR5 gene with a 32 base pair deletion in the sequence) are naturally resistant to HIV-1 infection but pose no significant immune deficiency [238].

The HIV accessory protein, negative regulatory factor (Nef), has also been shown to be an important mediator in HIV production. Studies have revealed that patients infected with Nef-defective HIV-1 strains do not progress to AIDS or develop AIDS much more slowly than those infected with standard strains [239, 240]. This outcome may be related to the biological functions of Nef, which includes preventing infected cells from being recognized by cytotoxic T cells, inducing apoptosis in bystander T cells, and inhibiting autophagy in macrophages [241-249]. Autophagy is a self-degradative process for providing energy under stressed conditions, degrading and recycling long-lived proteins and damaged organelles as well as playing an important role in eliminating intracellular pathogens (i.e. viruses and bacteria) [250]. Nef primarily inhibits the degradation stage of autophagy, thus preventing the host elimination of intracellular virus through autophagy [249]. However, when Nef was removed from viral genome, the host elimination of HIV via autophagy was resumed [249].

Therefore, targeting CCR5 and Nef by siRNAs simultaneously can be used as a dual preventive strategy against the vaginal transmission of HIV. Downregulation of CCR5 inhibits viral entry into host cells, serving as a first line of defense against HIV, and knocking down Nef decreases viral pathogenicity and reactivate Nef-blocked autophagy

to eliminate the invading virus that escape the first line of defense, serving as the second line to further protect cells from HIV infection.

Autophagy has been divided into three types: macroautophagy, microautophagy and chaperone-mediated autophagy. Among the three types, macroautophagy appears to play an important role in protecting cells against microbial infection [251]. Macroautophagy is composed of two subsequent stages, the initiation stage and the degradation stage [251]. During the initiation stage, a membrane called phagophore is invaginated from cell membrane and elongated to sequester components targeted for degradation, forming an enclosed double-membrane vesicle called autophagosome. This stage is subsequently followed by the degradation stage, during which the autophagosomes will then fuse with the acidic, enzyme-enriched lysosome, forming the degradative vesicle, autolysosome. During the fusion, only the outer layer of the double membrane of autophagosome fuses with lysosome while the inner layer becomes degraded, resulting in a single-membrane autolysosome. After that, the components inside of the autolysosomes are degraded into amino acids, fatty acids, nucleic acid and so forth for recycle and reuse [250]. Detecting and identifying the bacterial components that are attached to or inside of the cytoplasm of mammalian cells is a key process for initiating macroautophagy. Recognition of bacterial lipopolysaccharide by toll-like receptor 4 [252], detection of bacterial peptidoglycan by NOD-like receptors [253] as well as the identification of intracellular bacteria by sequestosome-1-like receptors [254] are identified pathways for the initiation of autophagy in the defense against bacterial infection. Various regulatory proteins (e.g. Beclin-1 and VPS 34) [255, 256] are synthesized and recruited to initiate the nucleation of the phagophore, and as the phagophore elongates and grows into a complete

autophagosome, a protein called LC3B starts to be synthesized from its precursor LC3A and becomes localized on autophagosomes [255]. As autophagy proceeds, autophagosomes begin to fuse with lysosomes and mature into degradative autolysosomes with LC3B internalized. At the same time, other regulatory proteins (e.g. TECPR-1 and UVRAG) [256, 257] are synthesized and recruited to promote the maturation of autolysosomes. Eventually, the pathogens as well as LC3B are degraded in autolysosomes by the enzymes and substances delivered from lysosomes.

PLGA is the most widely used polymer for constructing vehicles to deliver siRNA intravaginally. Woodrow et al. have shown that PLGA NP with a size of about 200-300 nm could penetrate into the mouse vaginal epithelium and reach a layer as deep as approximately 70 μm. Efficient gene knockdown was successfully achieved when siRNA was densely loaded into PLGA NP [128]. Moreover, Hanes et al. have found that NP modified with a dense coating of low molecular weight PEG could significantly improve mucus penetration ability [49]. Besides that, the addition of PEG to the system also decreases the aggregation of NP and reduces interaction of NP with proteins and small molecules in complex physiological environment [258]. PEG is a FDA-approved polymer and its application has been seen in many of the FDA-approved medications including intravenous injections.

siRNAs are difficult to be encapsulated into PLGA NP with high efficiency and loading using the classical double emulsion evaporation preparation method [259]. Due to the relatively low molecular weight of siRNA, it can easily leak from the inner water phase into the outer water phase during the preparation process [259]. Also, the hydrophilic nature and the electrostatic repulsion between negatively charged phosphate groups of

siRNA backbone and anionic acid groups of PLGA hinder its close contact with PLGA polymer [259]. However, the utility of PEI, a polycation, effectively solves this problem by complexing siRNA. PEI condenses low molecular weight siRNA into high molecular weight complexes through electrostatic attraction between the amine groups of PEI and the phosphate groups of siRNA, thus facilitating higher incorporation of siRNA into NP [260]. Studies have shown that with the complexation of PEI, the encapsulation efficiency of siRNA can be greatly improved from 43% to 86% within PLGA NP [260].

Therefore, in this study, we hypothesized that therapeutic siRNAs against CCR5 and Nef could be condensed by PEI and encapsulated into PLGA-PEG NP, an the PLGA-PEG NP could be further formulated into a gel dosage form to provide ease in self administration and improve vaginal retention of NP. This RNAi-based nanomedicine could effectively knock down CCR5 and Nef simultaneously and reactivate the Nef-blocked autophagy in host cells in vitro. By working together, this combination RNAi-based nanomedicine could efficiently inhibit HIV replication in vitro. Improved in vivo delivery of siRNA and gene knockdown in vaginal CD4+ cells could be achieved by conjugating anti-CD4 antibody to nanomedicine to improve efficacy and side effects.

The objectives of this study includes: (1) Develop and optimize an antibody conjugated PLGA-PEG NP formulation for siRNA (2) Develop and optimize a gel formulation for NPs (3) Characterize the physiochemical properties of the formulation (4) Evaluate in vitro gene knockdown, reactivation of Nef-blocked autophagy, inhibition of HIV and cytotoxicity in vitro (5) Evaluate in vivo biodistribution and gene knockdown in vaginal CD4+ and CD4- cells.

3.3 Materials and Methods

3.3.1 Materials

Scramble siRNA and Cy-3 scramble siRNA were purchased from Thermo Fisher (ON, Canada). PCR primers and siRNA targeting CCR5, and Nef were purchased from Dharmacon (ON, Canada) and Thermo Fisher (ON, Canada). Sequences are listed below.

Table 3.1: siRNA and primer sequences

Name	Sequence
siRNA Nef	Sense: 5'-UGUGCUUCUAGCCAGGCACdTdT-3' Antisense: 3'-dTdTACACGAAGAUCGGUCCGUG-5'
Anti-human siRNA CCR5	Sense: 5'-GUUCAGAAACUACCUCUUAdTdT-3' Antisense: 3'-dTdTCAAGUVUUUGAUGGAGAAU-5’
Anti-mouse siRNA CCR5	Sense: 5'-CAGUAGUUCUAAUAGACUAdTdT-3' Antisense: 3'-dAdCGUCAUCAAGAUUAUCUGAU-5’
Nef primer	Forward: 5’-AGAGGAGGAAGAGGTGGGTTTT-3’ Reverse: 5’GGGAGTGAATTAGCCCTTCCA-3’
Human CCR5 primer	Forward: 5’-TTCATCATCCTCCTGACAATCG-3’ Reverse: 5’-GCCACCACCCAAGTGATCAC-3’
Human GAPDH primer	Forward: 5’-AAGAAGGTGGTGAAGCAGGCG-3’ Reverse: 5’-AGACAACCTGGTCCTCAGTGTAGC-3’
Mouse CCR5 primer	Forward: 5’-TGTCCTCCTCCTGACCACCTT-3’ Reverse: 5’-ACTCCGGAACTTCTCTCCAACA-3’
Mouse GAPDH primer	Forward: 5’-GATGCCCCCATGTTTGTGAT-3’ Reverse: 5’-GGTCATGAGCCCTTCCACAAT-3’

Branched PEI (25 KDa), polyvinyl alcohol (PVA) (31~50 KDa) and coumarin-6 were purchased from Sigma-Aldrich (ON, Canada). Carboxylic acid terminated PLGA (50/50)(10 KDa)-PEG(2 KDa), was synthesized by Advanced Polymer Materials (QC, Canada). HEC (Natrosol^{TM}, 250 HX PHARM) was a kind gift from Ashland (GA, USA). Glycerol and dipotassium phosphate were purchased from Fisher Scientific (ON, Canada). Ethyl acetate and chloroform were purchased from EMD (ON, Canada). MF-Millipore Membrane (mixed cellulose esters, hydrophilic, 5.0 μm) was purchased from Millipore (NS, Canada). CellTiter 96® AQueous One Solution Cell Proliferation Assay (MTS) was purchased from Promega (ON, Canada). E.Z.N.A.® RNA isolation kit was purchased from Omega Bio-Tek (ON, Canada). CYTO-ID® Autophagy detection kit was purchased from Enzo Life Sciences (NY, USA). Pierce™ BCA Protein Assay Kit, Pierce™ protein-free blocking buffer, biotin-conjugated anti-ER antibody [MA5-13062] and 96-well flat bottom immune plate, 96-well qRT-PCR plates and plate sealing membrane were purchased from Thermo Fisher (ON, Canada). TNF-α, IL1-β, IL-6, IL-8 ELISA kits, streptavidin-HRP [DY998], ELISA coating buffer (pH 7.4) [DY006], reagent diluent concentrate [DY995], wash buffer [WA126], substrate solution [DY999] and stop-solution [DY994] were purchased from R&D Systems (MN, USA). Anti-human anti-LC3B antibody [5H12], Donkey anti-mouse IgG H&L [Alexa Fluor 488], mouse IgG1 [CT6] isotype control, Anti-HIV1 Nef antibody [3D12], were purchased from Abcam (ON, Canada). BD staining buffer, human BD Fc Block and anti-human anti-CCR5 antibody-PE Cy-7 were purchased from BD Biosciences (ON, Canada). qScript™ cDNA and PerfeCTa SYBR Green SuperMix were purchased from Quanta (ON, Canada).

3.3.2 Cell culture

Sup-T1 cells and Sup-T1 cells stably expressing Nef (Nef-ER) were obtained from the National Institutes of Health (NIH) Reagent Program (MD, USA). VK2/E6E7 cells were purchased from ATCC (VA, USA). Heat-inactivated FBS was purchased from PAA (ON, Canada), RPMI-1640, penicillin–streptomycin and PBS were purchased from Lonza (ON, Canada). Keratinocyte-SFM and its supplements were purchased from Invitrogen (ON, Canada). Calcium chloride was purchased from Sigma-Aldrich (ON, Canada). Sup-T1 cells were maintained at 37°C and 5% CO_2 with RPMI-1640 culture media supplemented with 10% heat-inactivated FBS and penicillin-streptomycin (100 μg/mL-100 U/mL). Nef-ER cells were maintained at 37°C and 5% CO2 with RPMI-1640 culture media supplemented with 10% heat-inactivated FBS, 100 μg/mL penicillin-streptomycin (100 U/mL), 1.5 μg/mL puromycin and 20 μM of 2-mercaptoethanol. VK2/E6E7 cells were maintained at 37°C and 5% CO_2 with Keratinocyte-SFM medium supplemented with 0.1 ng/mL human recombinant EGF, 0.05 mg/ml bovine pituitary extract, 44.1 mg/L calcium chloride and penicillin-streptomycin (100 μg/mL-100 U/mL).

3.3.3 NP preparation

siRNA was first condensed by PEI and then encapsulated into NP by a double-emulsion evaporation method using the biodegradable di-block copolymer, PLGA-PEG [128]. In brief, equal volume of siRNA (25-100 μg) and PEI (dissolved in TE buffer, pH 7.5) were combined together at various N/P ratios and incubated at room temperature for 15 min. The siRNA-PEI complex was then run on a 15% polyacrylamide gel at 90 V, 400 mA for 130 min to determine the proper N/P ratio for complete condensation of siRNA

(PEGylated poly (ethylene imine) copolymer-delivered siRNA inhibits HIV replication in vitro). The siRNA-PEI complex was then continuously emulsified with 600 μL of PLGA-PEG (10 mg/mL) dissolved in methylene chloride for 15 s. The primary emulsion was further emulsified with 4.3 mL of 2% PVA for 3 min, forming a w/o/w emulsions. The resulting emulsion was stirred overnight at 4 ºC to evaporate the organic solvent to harden the NP. NP was then collected by centrifuge (20,000 g for 15 min at 4 ºC) and washed twice with water to eliminate excess PVA and unencapsulated drug. Coumarin 6 and siRNA encapsulated (1.25 %) NP (coumarin 6-siRNA NP) was prepared by the same method by dissolving Coumarin 6 in methylene chloride along with PLGA-PEG.

3.3.4 Preparation of intravaginal gel loaded with NP

Approximately 1 g of HEC (2%, stock HEC gel) was dissolved in 40 mL of NaH_2PO_4 (pH 5.0 for human use and pH 7.0 for mouse use) by a propeller at 4 ºC. Viscosity of the gel was adjusted by adding 5 g of glycerol (10%) and mixed until it was uniformly dispersed. The pH of the gel was adjusted to 5.0±0.2 or 7.0±0.2 (physiological vaginal pH) and the total weight was brought to 50 g using NaH_2PO_4 (pH 5.0/pH 7.0). Then NP was resuspended in NaH_2PO_4 (pH 5.0/pH 7.0) and combined with the stock HEC gel prepared earlier at proper ratios and stirred at 4 ºC for 2 hr resulting in a 1% or 0.5% HEC gel loaded with NP.

3.3.5 Characterization of NP

3.3.6.4 Particle size and zeta potential

For determining nanoparticle size, NP was resuspended in PBS (pH 7.4), or VFS (pH 4.2) [61] at a concentration of 25 μg/mL and measured using ZetaPALS (Brookhaven

Instruments). For zeta potential measurements, the particles were resuspended in the same buffers but at a concentration of 50 µg/mL and analyzed using ZetaPALS under smulchovski mode.

3.3.5.2 Encapsulation efficiency of NP

To determine the EE%, Cy-3 scramble siRNA were encapsulated into the NP using the same method described above. EE% was calculated using the equation below. Cy-3 scramble siRNA dissolved in blank NP suspension was used as a standard curve.

$$\text{EE \%} = \frac{\text{amount of total siRNA in µg} - \text{amount of unencapsulated siRNA in µg}}{\text{amount of total siRNA in µg}} \times 100\%$$

3.3.5.3 Release profile of siRNA from NP

To determine the release profile of NP, about 0.7 mg of NP encapsulating Cy-3 scramble siRNA were resuspended in 1 mL of PBS (pH 7.4) or VFS (pH 4.2) and incubated at 37 °C on a rotary shaker. At different time points, samples were centrifuged at 20,000g for 15 min at 4 ºC and 200 µL of supernatant was removed and replenished with fresh medium. Free siRNA was resuspended in the same release medium and samples were taken along with release samples to exclude the influence of degradation of siRNA. The siRNA was quantified using a plate reader (Synergy HT, BioTek) at an excitation wavelength of 530±25 nm and emission wavelength of 590±35 nm.

3.3.5.4 In vitro cell uptake of NP

Sup-T1 cells were seeded in 24-well tissue culture treated plates (Corning, New York, USA) in 0.5 mL culture medium on the day of the experiments. Cy-3 scramble NP were

resuspended in PBS and subjected to Sup-T1 at a final concentration of 600 µg/mL, siRNA-free NP was used as control. All treatment groups were maintained at 37 ºC, 5% CO2 and treated for different time points. At the end of each treatment, cells were collected by centrifugation at 100 g for 5 mins, washed twice with PBS, and analyzed by flow cytometry (Canto II, BD).

3.3.5.5 CCR5 and Nef gene knockdown in Nef-ER cells

Equal amount of siRNA CCR5 and siRNA Nef (50 µg of each) were co-encapsulated in NP using the method mentioned above. For in vitro gene knockdown studies, a previously established cell model, Nef-ER was used [261]. Nef-ER cells (0.8×10^5) were seeded in 24-well plate in 450 µL of culture medium and treated with 50 µL of NP of varying concentrations. 4-HT was added to cells at a final concentration of 5 µM simultaneously when NP was added to induce the expression of activated Nef. The cells were incubated at 37 ºC, 5% CO_2 for different time intervals. To determine mRNA knockdown efficiency, cells were centrifuged at 200 g for 5 min at room temperature and lysed with E.Z.N.A.® RNA Isolation Kit 48 hr post treatment. The extracted RNA was converted to cDNA by qScript™ cDNA SuperMix using a SimpliAmp™ Thermal Cycler (Thermo Fisher, ON, Canada) and quantitated using real-time PCR with PerfeCTa SYBR Green SuperMix on a QuantStudio™ 6 Flex Real-Time PCR System (Thermo Fisher, ON, Canada). To determine changes in protein expression, cells were collected by centrifugation at 200 g for 5 min at room temperature 72 hr post treatment. CCR5 protein levels were measured by flow cytometry, while Nef protein level were measured by ELISA. For measuring CCR5, cells were first fixed in 2% paraformaldehyde for 20 min on ice, and then washed and blocked with Human BD Fc Block at room temperature for

10 min. After that, cells were stained with anti-human anti-CCR5 antibody for 30 min on ice. Eventually, cells were collected, washed and analyzed by flow cytometry. For measuring Nef, cells were first lysed following a previously described method to extract total protein [261]. Total protein was then quantified using the Pierce™ BCA Protein Assay Kit and diluted to a final concentration of 100 μg/mL with the ELISA reagent diluent (for ELISA, all reagents were diluted in ELISA reagent diluent unless specified). One day before the experiment, anti-Nef antibody was diluted in ELISA plate-coating buffer at a final concentration of 2μg/mL and each well of the plate was immediately coated with 100μL antibody and incubated at 4◦C overnight. On the day of the experiments, the plate was washed three times with ELISA wash buffer (300 μL/well) and blocked with Pierce™ protein-free blocking buffer (300 μL/well). Samples (100 μL) were then loaded into each well and incubated at room temperature for 2 hrs. After that, the wells were washed and 100 μL of 1.3 μg/mL biotin-conjugated anti-ER antibody was added and incubated at room temperature for 2 hr. Streptavidin-HRP (diluted to 1:200) was added into each well and incubated at room temperature for 20 mins. After that, 100 μL of substrate solution was added and incubated at room temperature for 10-20 mins to develop the color. Eventually, stop solution was added and the plate was read at 450 nm.

3.3.5.6 In vitro re-activation of autophagy

Sup-T1 and Nef-ER cells were seeded at a density of 0.8×10^5 cells/well in 24-well plates with 450 μL culture medium respectively. 50 μL of NP suspension in PBS was treated to cells at a final concentration of 1.334 mg/mL. 4-HT was treated to the cells simultaneously at a final concentration of 5 μM to induce the expression of activated Nef. The cells were incubated at 37 ºC and 5% CO_2 for 48hr. The medium was replenished

with 1 mL of fresh medium containing the same concentration of 4-HT and cells were incubated for another 18 hr before analysis. For the detection of autophagic flux, the cells were subjected to Cyto-ID® Autophagy Detection Kit following the manufacturer's instruction. For the detection of LC3B levels, the cells were first fixed in 2% paraformaldehyde for 20 min on ice, washed once and permeabilized with 0.1% saponin/PBS solution for 15 min at room temperature. Next, Human BD Fc Block was added to each sample incubated with cells for 10 min at room temperature. After that, Human BD Fc Block was removed and cells were resuspended in 0.1% saponin/PBS solution again and stained with primary antibody, anti-human anti-LC3B antibody or its isotype control antibody for 30 min on ice; followed by stained with a secondary antibody, anti-mouse IgG H&L (Alexa Fluor® 488) for another 30 min on ice; washing was conducted in between. Eventually, cells were collected, washed and analyzed by flow cytometry.

3.3.5.7 In vitro HIV infection

Sup-T1 cells were seeded at a density of 0.8×10^5 cells/well in 24-well plates with 450 µL of culture medium. 50 µL of NP suspension in PBS was treated to cells at a final concentration of 1.3 mg/mL (Day 1) and cells were incubated at 37 ºC, 5% CO_2 for 48 hr. Then cells were passaged at a density of 0.8×10^5 cells/well in 24-well plates with fresh medium, treated with 4 µg/mL of polybrene in 100 mM HEPES, pH 8.0 and infected with HIV-1 Bal (Cat#510, Lot# 130361, National Institutes of Health, MD, USA) at a p24 concentration of 70 pg/mL (Day 3). Cells were incubated for another 7 days and passaged every 2 days with treatment (1.334 mg/mL) reapplied at the time of passage. Supernatant was collected on Day 5, 7 and 9 for the analysis of p24.

3.3.6 Characterization of intravaginal gel loaded with NP

3.3.6.1 Rheological profile

The rheology of the various gel formulations was determined using an AR550 Rheometer (TA Instruments, New Castle, USA) with a 20 mm 2º steel cone at 37 ºC.

3.3.6.2 Release of NP from intravaginal gel

To evaluate the NP release from the intravaginal gel, Coumarin 6-siRNA NP were loaded into 0.5% or 1% HEC gel. 50 µL of 1% and 0.5% HEC gel loaded with NP were loaded onto Transwell® permeable supports with 3µm-pore-size polyester membrane (Corning, NY, USA) and the transwells were inserted into 24-well plates. 1 mL of VFS was loaded into each well as release medium. The samples were incubated at 37◦C on an incubating orbital shaker (VWR, ON, Canada). At different time points, 200 µL of release medium was removed from wells and replenished with fresh medium. The released NP was quantified using a plate reader (Synergy HT, BioTek).

3.3.6.3 Penetration of NP from intravaginal gel through vaginal epithelial layer in vaginal mucosal co-culture model

The vaginal mucosal co-culture model was used to evaluate penetration of NP as described previously with slight modification [262]. In brief, VK2/E6E7 cells were seeded onto the upper face of collagen I- and fibronectin-coated 6.5-mm-diameter, 3-µm-pore-size polycarbonate membrane transwells (Corning, New York, USA) at a density of 10^5 cells/well and were cultured for about one week until the resistance exceeded 600 Ω/cm^2 to achieve an intact monolayer. On the day of the experiment, 0.8×10^5 of Nef-ER

cells were seeded into each well of a 24-well plate with 500 μL culture medium an then the transwell with VK2/E6E7 cells were inserted. After that, 0.5% HEC gel loaded with NP was treated to VK2/E6E7 cells and at various time points, cells were taken and analyzed by flow cytometry and the medium containing intravaginal gel with NP was analyzed by a plate reader.

3.3.6.4 CCR5 and Nef gene knockdown in vaginal mucosal co-culture model

On the day of experiment, 0.8×10^5 of Nef-ER cells were seeded into each well of a 24-well plate with 450 μL culture medium an then the transwell with VK2/E6E7 cells were inserted. After that, 0.5% HEC gel loaded with NP was treated to VK2/E6E7 cells and 4-HT was treated to Nef-ER cells at a concentration of 5 μM. The cells were incubated for 72 hr for gene knockdown analysis at RNA level and protein level by the methods mentioned above.

3.3.7 In vitro cytotoxicity study

Cellular cytotoxicity was determined using the CellTiter 96® AQueous One Solution Cell Proliferation Assay (MTS assay). Sup-T1 cells were plated at 3×10^4 cells/well and VK2/E6E7 cells were plated at 5×10^4 cells/well on 96-well tissue culture treated plates (BD, ON, Canada) in 80 μL of culture medium separately. Varying concentrations of NP and 0.5% HEC gel loaded with NP were pre-mixed with culture media, added to cells, and incubated for 24 hr and 72 hr. Cell culture media was used as negative control and 1 M acrylamide in cell media was used as positive control. At the end of the treatment period, VK2/E6E7 cells were washed to remove the formulations, replaced with fresh medium, treated with 20 μL of MTS solution, and incubated for 1 hr. The plate was

analyzed on a microplate reader, (BioTek Instruments, VT, US) at 490 nm. While for the Sup-T1 cells, 20 μL of MTS solution was added directly, and incubated for 1 hr. Formulations incubated without cells and treated the same way were used as control to subtract background from experimental groups. To evaluate the cytokine production, the supernatant from each treatment groups were collected and centrifuged at 20,000 g at 4°C for 15 min to remove the formulations, and then subjected to ELISA following the manufacturer's instructions.

3.3.8 Antibody conjugation to NPs and in vitro targeted delivery of siRNA to CD4+ cells

Approximately 4 mg NP were then resuspended in 1700 μL of 0.1 M MES (Sigma-Aldrich, ON, Canada) buffer (pH 6.0). 200 μL of 275 mg/mL sulfo-NHS (G-Biosciences, MO, USA) and 100 μL of 200 mg/mL EDC (G-Biosciences, MO, USA) were added into the NP suspension. The mixer was stirred at room temperature at a speed of 700 rpm for 30 min to activate the carboxyl group. Then the NP was centrifuged at 10,000 g for 5 min followed by 20,000 g for another 5 min at room temperature to remove excess sulfo-NHS and EDC. The NP was then resuspended in 180 μL of 0.1 M NaH_2PO_4 buffer (pH 7.4) and 200 μg of antibody in a volume of 400 μL was added and stirred at a speed of 1400 rpm for 4 hr at room temperature to allow the antibody to be conjugated (Mouse monoclonal anti-human CD4 antibody (RPA-T4) and mouse IgG1 κ isotype control were purchased from Abcam (ON, Canada). Rat monoclonal anti-mouse CD4 antibody (RM4-5) and rat IgG2a κ isotype control were purchased from BD Biosciences (ON, Canada)). In the end, the resulting NP were collected, washed and loaded into 1% HEC gel.

Sup-T1 cells were seeded at a density of 2×10^5 cells/well in 24-well plates with 450 μL of culture medium. 50 μL of Cy-3 scramble NP-(h)CD4 or Cy-3 scramble NP-(h)IgG1 suspension in PBS was treated to cells at a final concentration of 1.3 mg/mL. The cells were then incubated at 37 ºC, 5% CO_2 for 2 hr, 4 hr and 8 hr respectively. At the end of each treatment, cells were washed with PBS and analyzed on flow cytometry (Canto II, BD, ON, Canada) immediately.

3.3.9 In vivo delivery of siRNA into CD4+ cells and gene knockdown

Animal protocol was approved by Animal Care Committee at University of Manitoba. Female mice (CD1, 5-8 weeks) were purchased from German Mouse Clinic and housed under a 12:12-hour light/dark cycle with ad libitum access to food and water. Female mice were subcutaneously injected with 2 mg Depo-Provera (Pfizer) 5-7 days before treatment. On the day of treatment, female mice were anesthetized and the reproductive tract was washed with 100 μL of PBS for three times and swabbed with a mini calcium alginate tipped applicator (Puritan, ME, USA). 30 μL of PBS or 1% HEC gel loaded with NP conjugated to antibody was administered intravaginally in the morning and evening with 8 hr duration in between for 2 concessive days. Animals were kept for another 20 min under anesthesia after administration. Biodistribution study was conducted with formulation encapsulating Cy-3 scramble siRNA and female mice were treated as mentioned above. 24 hr after the last treatment, the reproductive tract was washed three times with 100 μL of PBS to remove any residual formulation and blood was collected from heart. Animals were then euthanized and organs including heart, liver, kidney, lung, spleen and the whole reproductive tract were collected. Distribution of Cy-3 scramble siRNA in various organs was visualized using Perkin Elmer IVIS Spectrum. Images were

taken with Living Image software. CCR5 was used as a model gene for in vivo gene knockdown and a commercial available anti-mouse CCR5 siRNA (Cat# 4390816-s64112, Thermo Fisher, ON, Canada) was encapsulated into formulation. Animals were treated as mentioned above and 48 hr after the last treatment, animals were anesthetized and the whole reproductive tract was washed three times with 100 μL of PBS and removed after animals were euthanized. Tissues were immersed in RNAlater® stabilization solution (Thermo Fisher, ON, Canada) at 4 °C overnight and kept in liquid nitrogen until analysis.

3.4 Results

3.4.1 N/P ratio, particle size, zeta potential and release profile of siRNA NP

To optimize the formulation of siRNA NP, the proper N/P ratio (the molar ratio of nitrogen from PEI to phosphate from siRNA) that can completely condense siRNA was first determined on a 15% polyacrylamide gel. We evaluated the N/P ratios from 0:1 to 6:1 and as shown in Figure 3.1, all the siRNA could be completely condensed at or above the N/P ratio of 5:1, so 5:1 was selected as the optimal N/P ratio. Further data also supported that when PEI was introduced at N/P ratio of 5:1, the EE% was improved from approximately 58% to 87% with an initial siRNA input of 25 μg. Next the formulation was further optimized based on polymer concentration, water phase to oil phase ratio, sonication time and so forth in order to get a formulation with stable particle size, optimal EE%, dense siRNA loading, and sustained release profile. Eventually, the formulation prepared by the parameters mentioned in the method was determined to be optimal. And the formulation was characterized in PBS (pH 7.4) and VFS (pH 4.2) respectively since different environment has to be taken into consideration for the development of microbicides. Table 3.2 compares the particle size, PDI and zeta potential of scramble NP

in two different buffers mentioned above. We found that the particle size of scramble NP remained within the range of 260-270 nm in PBS, pH 7.4 and VFS, pH 4.2 with a PDI of about 0.2, which indicated the uniformity of the size distribution. Zeta potential of the scramble NP was measured to be around -15 mV and it significantly increased from negative to close to neutral (around -8.0 mV) when the environment was switched from PBS (pH 7.4) to VFS (pH 4.2). The amount of initial siRNA input was titrated in order to determine the optimal EE% and loading capacity. EE% showed an increasing trend as the initial input of siRNA increased, but the actual siRNA loaded into NP showed an opposite trend. Even though the EE% dropped from 86% to 76%, the total loading of siRNA into NP was almost doubled when the initial siRNA input was increased from 50 μg to 100 μg (Table 3.3). Therefore, NP formulated with 100 μg of initial siRNA input was determined to be the optimal formulation, since further increase in siRNA input caused significantly enlarged particle size (>400 nm) and an even lower EE%, which would affect the stability of NP and cause a loss of siRNA.

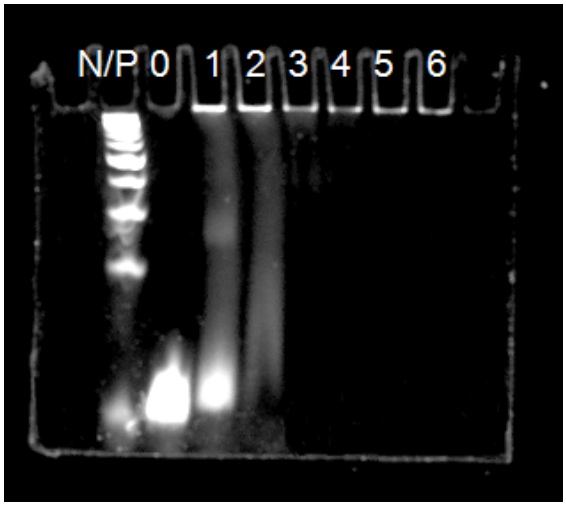

Figure 3.1: Condensation of siRNA by PEI at different N/P ratios (molar ratio of nitrogen from PEI to phosphorus from siRNA) (values above each lane).

Table 3.2: Particle size, PDI and zeta potential of scramble NP in different media. Values represent the mean±SD, n=3.

	PBS, pH 7.4			VFS, pH 4.2		
	Size (nm)	PDI	Zeta Potential (mV)	Size (nm)	PDI	Zeta Potential (mV)
scramble NP	256.0±7.2	0.178	-15.26±1.64	271.6±1.8	0.224	-8.66±2.43

Table 3.3: EE% and siRNA loading into NP. Values represent the mean±SD, n=3.

Initial siRNA input (μg)	EE%	siRNA loading into NP (siRNA/NP, μg/mg)
50	86.7±0.2	21.7±0.5
75	81.2±1.4	30.5±0.5
100	75.6±0.9	37.8±0.5

When we evaluated the release profile of the formulation in different buffers, we accidentally found a pH-dependent release profile of siRNA. As shown in Figure 3.2, NP had a sustained release profile in PBS buffer (pH 7.4) with a cumulative release of about 24% over 15 days. A burst release (about 8%) was observed within the first 4 hr (Figure 3.2A). However, when the study was conducted in VFS, pH 4.2, the release rate was detected to be fairly low and a cumulative release of less than 6% was observed over the course of 15 days with less than 2% during the first 2 days (Figure 3.2B). Based on these

findings, we next incubated the siRNA NP in VFS for 2 days first and then completely replaced the release medium with PBS, pH 7.4 to evaluate the release profile. This mimicked the change of real physiological conditions, which is the switch from intravaginal environment to intracellular environment, in clinical use. The release rate of siRNA remained at a low level (<2%) when NP was incubated in VFS, pH 4.2 but it spiked (15% burst release) within a few hours after the release medium was replaced by PBS, pH 7.4 and the release was sustained over the period of 15 days resulting in a total release of approximately 37.5% at the end of study. This indicated that the switch from VFS, pH 4.2 to PBS, pH 7.4 triggered the release of siRNA (Figure 3.2C) and resulted in a significant increase in total siRNA release.

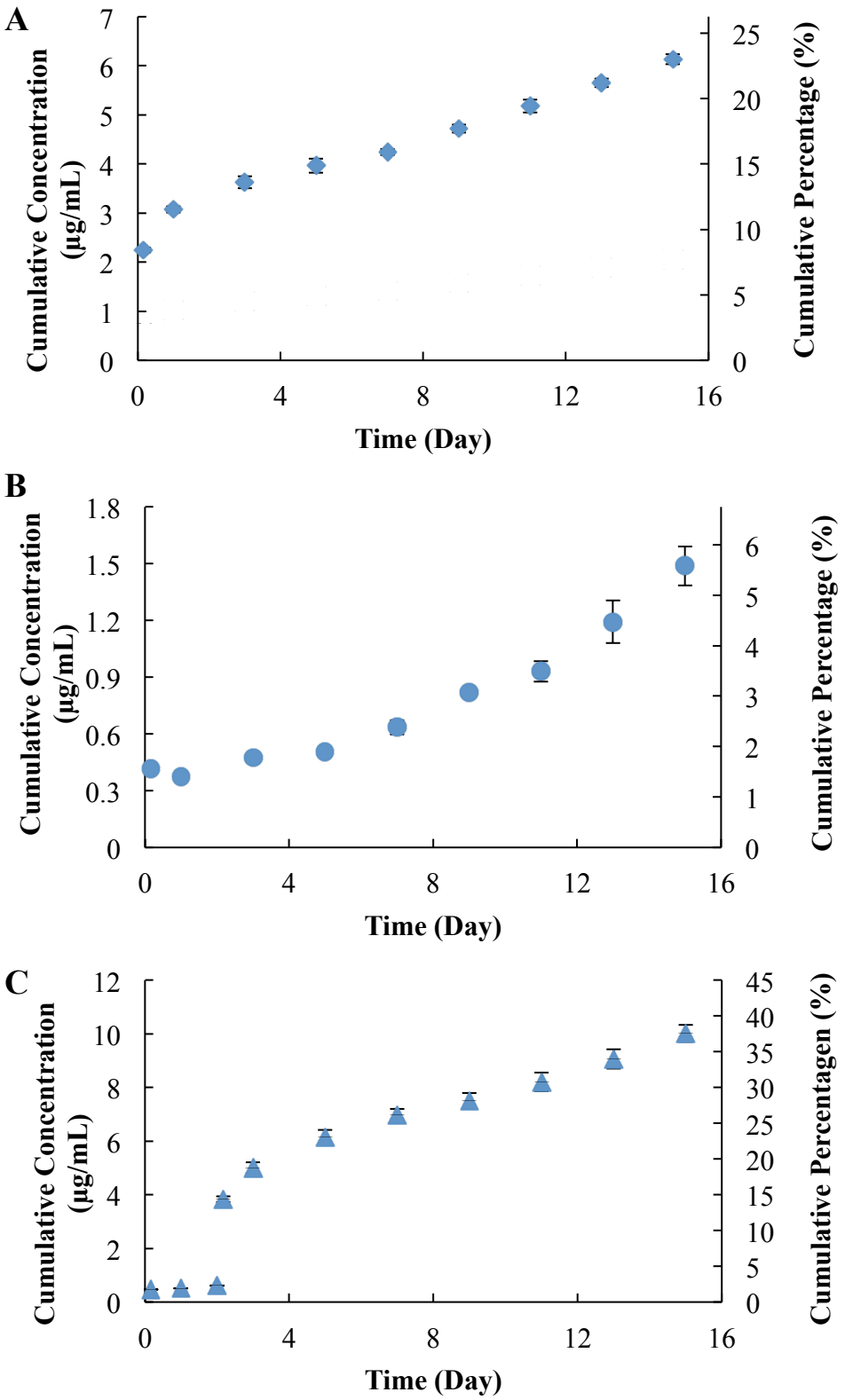

Figure 3.2: In vitro cumulative release of siRNA from Cy-3 scramble NP in various media at 37 °C. (A) PBS, pH 7.4, (B) VFS, pH 4.2, (C) Day 0-2 in VFS, pH 4.2 and Day 2-14 in PBS, pH 7.4. Values represent the mean±SD, n=3.

3.4.2 In vitro cell uptake, cytotoxicity and gene knockdown efficiency of siRNA NP

Next, we evaluated the in vitro cell uptake of siRNA. Sup-T1 cells, which express high level of CD4 were used. The cells were treated with 1.334 mg/mL of Cy-3 scramble NP and incubated for different time intervals. As shown in Figure 3.3, intracellular amount of siRNA exerted a time-dependent trend with increased amount of siRNA accumulated intracellularly over time.

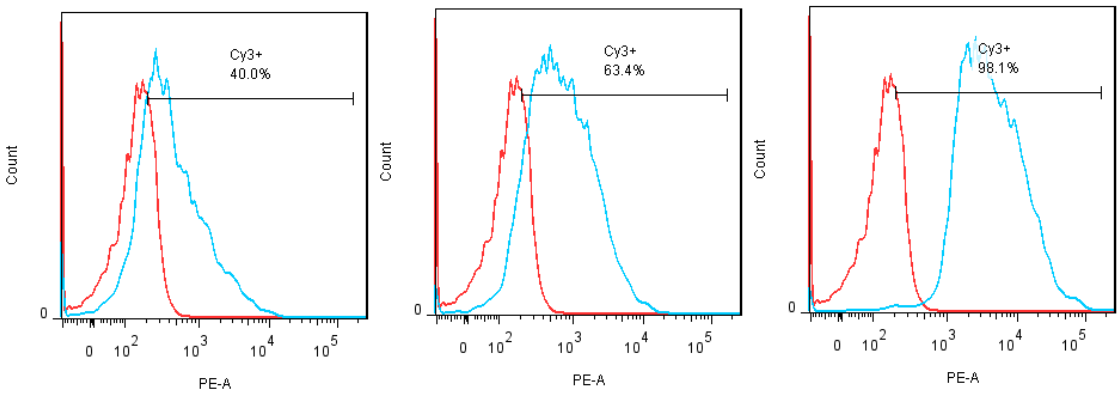

Figure 3.3: In vitro uptake of Cy-3 scramble siRNA by Sup-T1 cells treated with 1.334 mg/mL of Cy-3 scramble NP. MFI: mean fluorescence intensity. A representative histogram of flow cytometry was shown from n=3.

With the knowledge of size, zeta potential, release profile and cell uptake, we then co-encapsulated siRNA targeting CCR5 and siRNA targeting Nef into NP to evaluate the gene knockdown efficiency of the combination formulation. We first looked at the knockdown efficiency of both Nef and CCR5 at mRNA level with different treatment concentrations. In this project, all the gene knockdown studies involving Nef was performed with an in vitro cell model (Nef-ER) that could readily express Nef in Sup-T1 cells upon the induction of 4-HT. To evaluate the knockdown efficiency, Nef-ER cells were treated with 5 μM 4-HT and three different concentrations of Nef-CCR5 NP (0.34

mg/mL, 0.67 mg/mL and 1.33 mg/mL) simultaneously. The three different concentrations were all within the range of tolerable concentration of NP evaluated earlier (Figure 3.4A).

The gene knockdown at mRNA was first investigated. As shown in Figure 3.4B and C, the knockdown efficiencies showed a concentration-dependent trend. When cells were treated with 0.34 mg/mL of Nef-CCR5 NP, neither Nef nor CCR5 was significantly downregulated compared to the group treated with 4-HT + PBS or scramble NP + 4-HT. As the concentration was increased to 0.67 mg/mL, approximately 29% knockdown of Nef was observed, but it was only significantly different from the group treated with 4-HT+PBS, not the group treated with scramble NP+4-HT, indicating insufficient knockdown. As for CCR5, approximately 31% gene knockdown was achieved with significant difference at this concentration, compared to the groups treated with PBS+4-HT and scramble NP+4-HT. When the concentration was further increased to 1.33 mg/mL, a significant Nef knockdown of about 35% and a significant CCR5 knockdown of about 63% were observed, compared to the group treated with PBS+4-HT and scramble NP+4-HT. The concentration of 1.33 mg/mL achieved the highest mRNA knockdown efficiency within three treatment concentrations, therefore, it was selected as the optimal concentrations for further study.

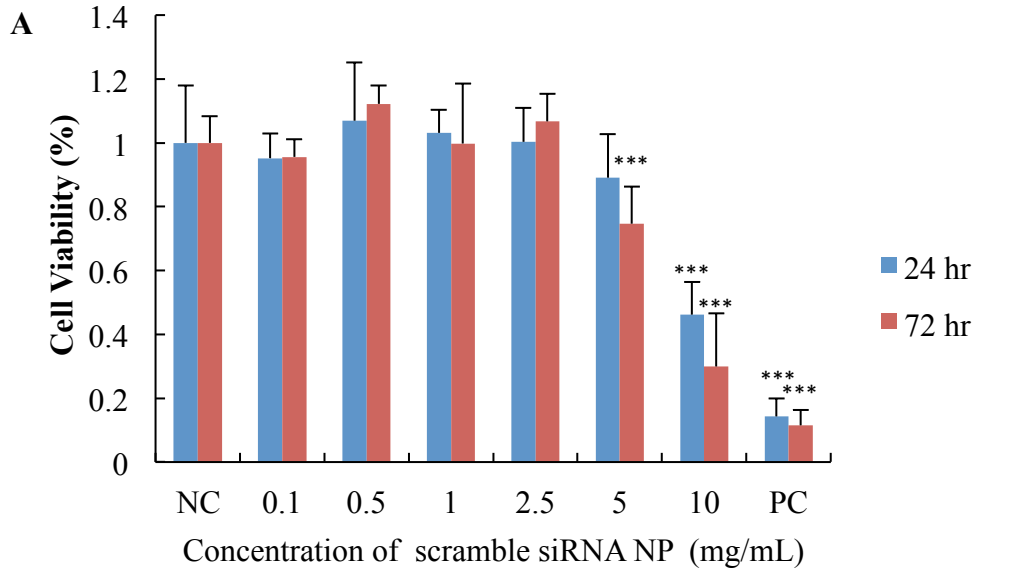
A
Cell Viability (%)
1.4
1.2
1
0.8
0.6
0.4
0.2
0
***
***
***
***
***
NC
0.1
0.5
1
2.5
5
10
PC
Concentration of scramble siRNA NP (mg/mL)
24 hr
72 hr

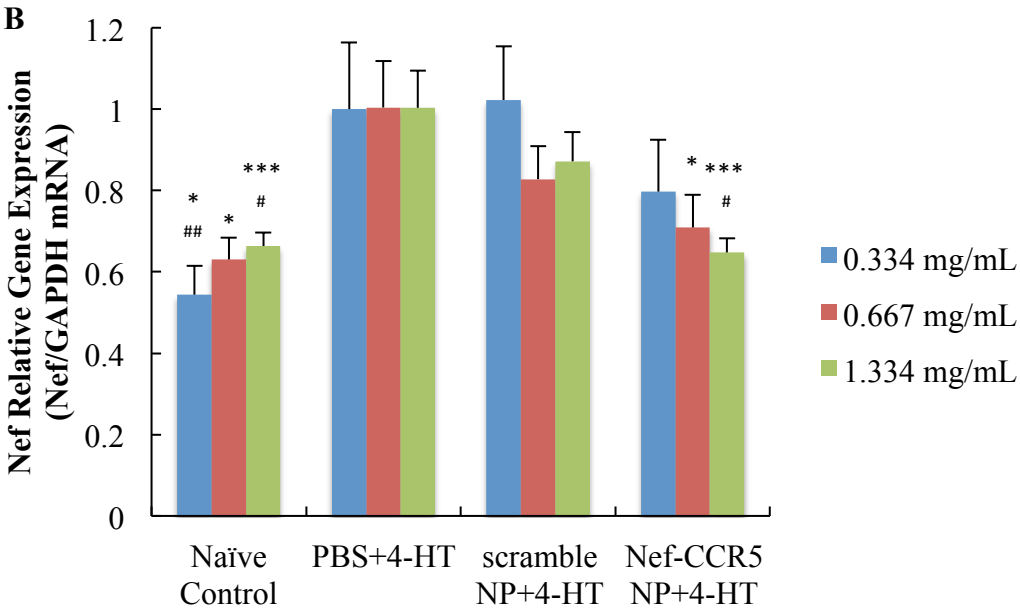
B
Nef Relative Gene Expression
(Nef/GAPDH mRNA)
1.2
1
0.8
0.6
0.4
0.2
0
*
##
*
***
#
*
***
#
Naïve Control
PBS+4-HT
scramble NP+4-HT
Nef-CCR5 NP+4-HT
0.334 mg/mL
0.667 mg/mL
1.334 mg/mL

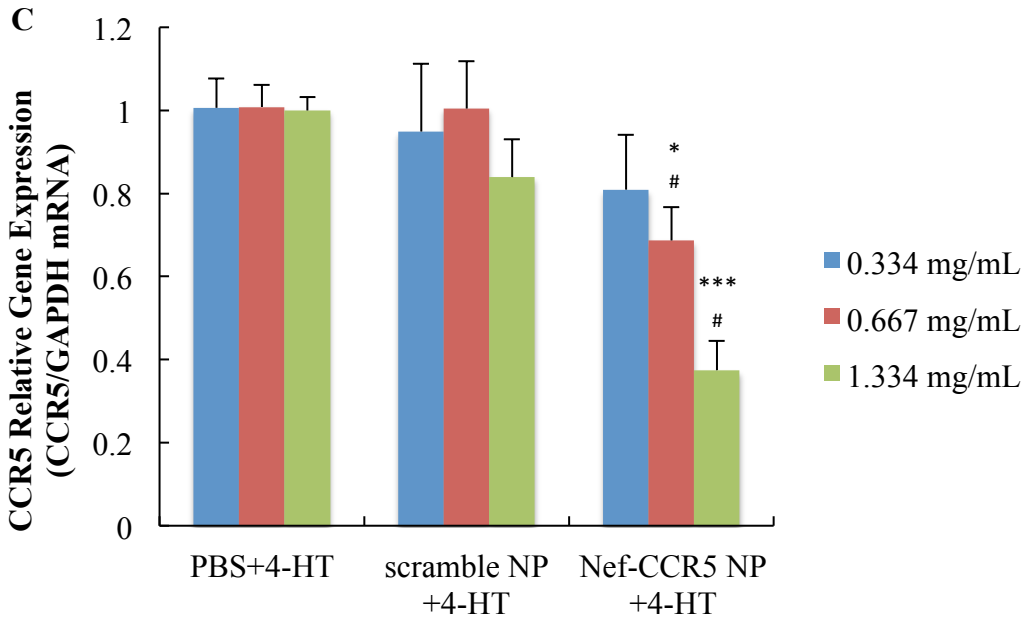

Figure 3.4: In vitro MTS assay of scramble NP and gene knockdown efficiency of Nef-CCR5 NP at mRNA level in Nef-ER cells at various treatment concentrations. (A) MTS assay of scramble NP, NC: negative control, PC: positive control. ***p<0.001 compared to negative control, Values represent the mean±SD, n=4. (B) Nef mRNA downregulation quantified by qRT-PCR, Values represent the mean±SD, n=3, *p<0.05, ***p<0.001 compared to PBS+4-HT. #p<0.05, ##p<0.01 compared to scramble NP+4-HT. (C) CCR5 mRNA downregulation quantified by qRT-PCR, Values represent the mean±SD, n=3. GAPDH was used as endogenous control. *p<0.05, ***p<0.001 compared to PBS+4-HT. #p<0.05, ##p<0.01 compared to scramble NP+4-HT.

Then we wanted to confirm the knockdown efficiency of Nef and CCR5 at the protein level with the optimal concentration. As shown in Figure 3.5, the protein level of Nef was significantly decreased by about 37% with all induced Nef reduced; and the protein level of CCR5 was significantly decreased by about 57% with CCR5+ population attenuated from 64% to 44%. Therefore, 1.33 mg/mL was selected as the optimal concentration for further study.

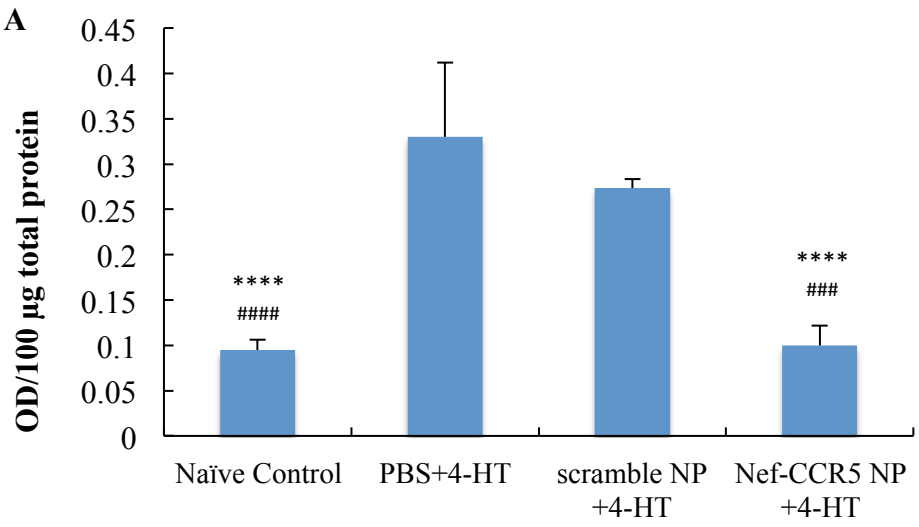
A
OD/100 µg total protein
0.45
0.4
0.35
0.3
0.25
0.2
0.15
0.1
0.05
0
****
####
****
###
Naïve Control
PBS+4-HT
scramble NP +4-HT
Nef-CCR5 NP +4-HT

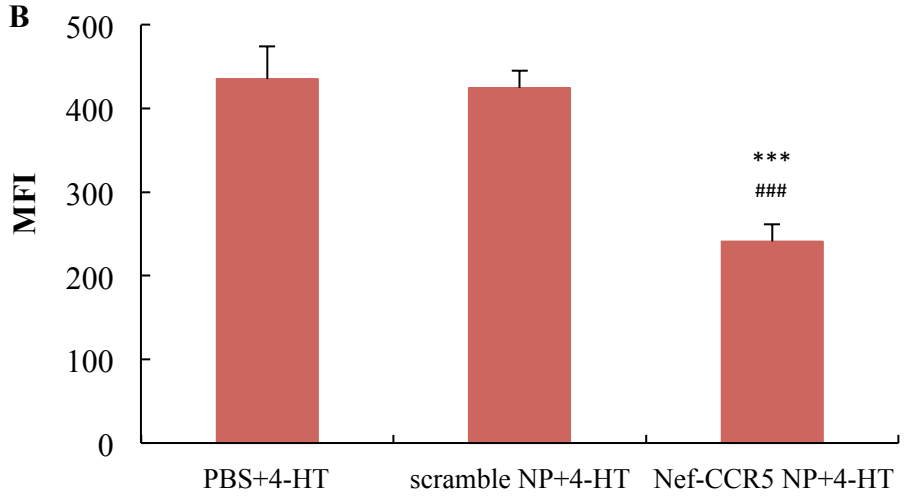
B
MFI
500
400
300
200
100
0
***
###
PBS+4-HT
scramble NP+4-HT
Nef-CCR5 NP+4-HT

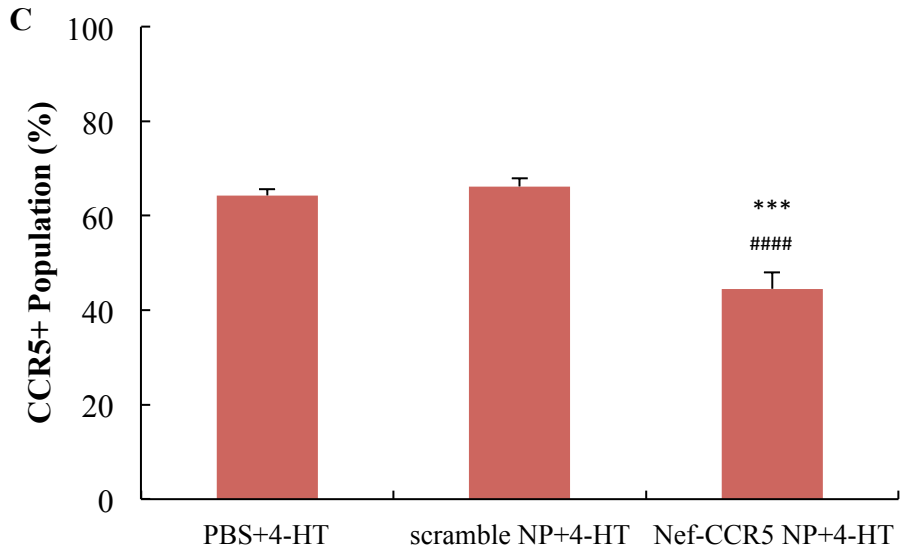
C
CCR5+ Population (%)
100
80
60
40
20
0
***
####
PBS+4-HT
scramble NP+4-HT
Nef-CCR5 NP+4-HT

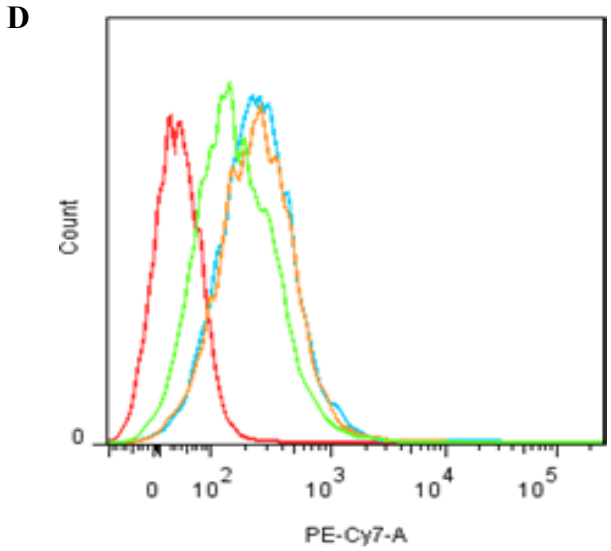

Figure 3.5: In vitro gene knockdown efficiency of Nef-CCR5 NP at protein level in Nef-ER cells. (A) Nef protein downregulation quantified by ELISA. (B-D) CCR5 protein downregulation quantified by flow cytometry. Green: Nef-CCR5 NP, orange: PBS, blue: scramble NP, red: isotype control. ***p<0.001 compared to PBS+4-HT. ####p<0.0001 compared to scramble NP+4-HT. Values represent the mean±SD, n=3.

We also collected the cell media from each treatment group for the analysis of pro-inflammatory cytokines (TNF- α, IL-6, IL1-β and IL-8) to further evaluate the cytotoxicity profile of our formulation at the concentration of 1.334 mg/mL. As shown in Figure 3.6, IL1-β and TNF-α were below the lowest detection level of the commercially available ELISA kit, therefore were shown as 0 in the figure. A decreased level of IL-6 was observed in the group treated with scramble NP and an even further decreased level was observed in the group treated with Nef-CCR5 NP, which dropped below the lowest detection level. For the other cytokine, IL-8, we did not detect any changes among the all

groups. As a result, the concentration of 1.334 mg/mL was well tolerated by cells without triggering an immune response.

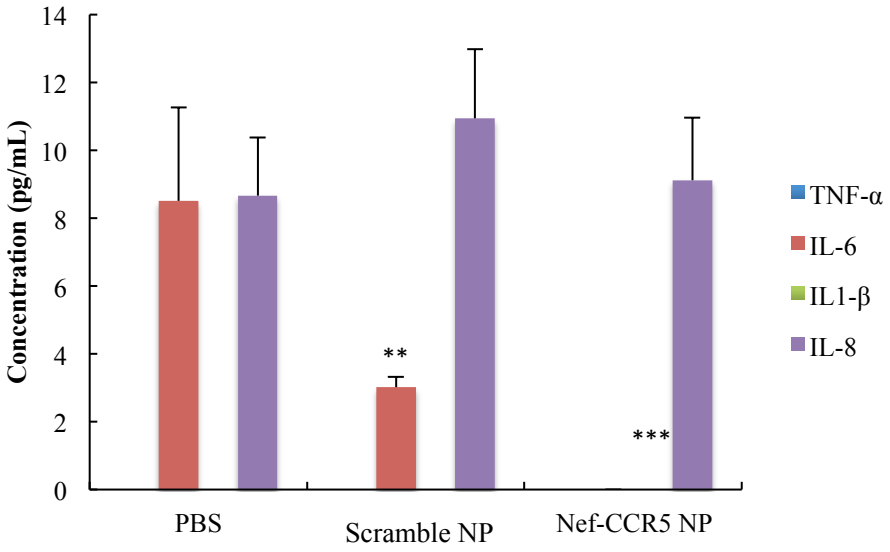

Figure 3.6: In vitro pro-inflammatory cytokine production in Nef-ER cells when cells were treated with 1.334 mg/mL of NP formulation. **p<0.01, ***p<0.001 compared to PBS. Values represent the mean±SD, n=3.

3.4.3 In vitro reactivation of autophagy by knocking down Nef

Our next aim was to investigate the relationship between Nef and autophagy inhibition in T cells since previous studies have shown that the expression of Nef can inhibit autophagy in macrophages [263]. We would like to investigate whether this inhibition would occur in T cells and whether the knockdown of Nef would counteract the inhibition. As autophagy is a dynamic process, three different methods were used to evaluate the level of autophagy. First, a commercially available kit for determining in vitro autophagic degradation activity (autophagic flux) was used. As shown in Figure 3.7 A, when Nef is induced by 4-HT in T cells, the total autophagic flux level was decreased

to approximately 80% compared to Sup-T1 cells treated with 4-HT. When the cells were treated with Nef-CCR5 NP (1.334 mg/mL), in which case the induced Nef was completely knocked down, the autophagic flux was augmented to a level that was even higher than naïve cells (Sup-T1 cells). And when the cells were treated with CCR5 NP, the autophagic flux was also slightly increased. Then the same treatment groups were further evaluated by measuring the level of LC3B, a marker protein for autophagosomes. As shown in Figure 3.7 B, when Nef was induced in T cells, the level of autophagosome increased by 4 folds. When the cells were treated with Nef-CCR5 NP, the level dropped back down to its original level; however, when treated with scramble siRNA & siRNA CCR5 NP, the autophagosome level was detected unchanged. Figure 3.7 C shows the changes in the gene expression of four autophagy-regulatory genes (Beclin-1, VPS34, TECPR1, UVRAG). When Nef was induced, only Beclin-1 was upregulated by 40% and this level remained unchanged whenever CCR5 was knocked down or Nef and CCR5 were both knocked down. However, knocking down CCR5 and Nef simultaneously could significantly upregulated VPS34 (~80%), TECPR1 (~40%) and UVRAG (~80%), and the expression levels of these three genes were even higher than their original levels in Sup-T1+scramble NP+4-HT group. Knocking down CCR5 alone could not cause the gene expression up-regulation of Beclin-1, VPS34, TECPR and UVRAG compared to the group treated with scramble NP and 4-HT.

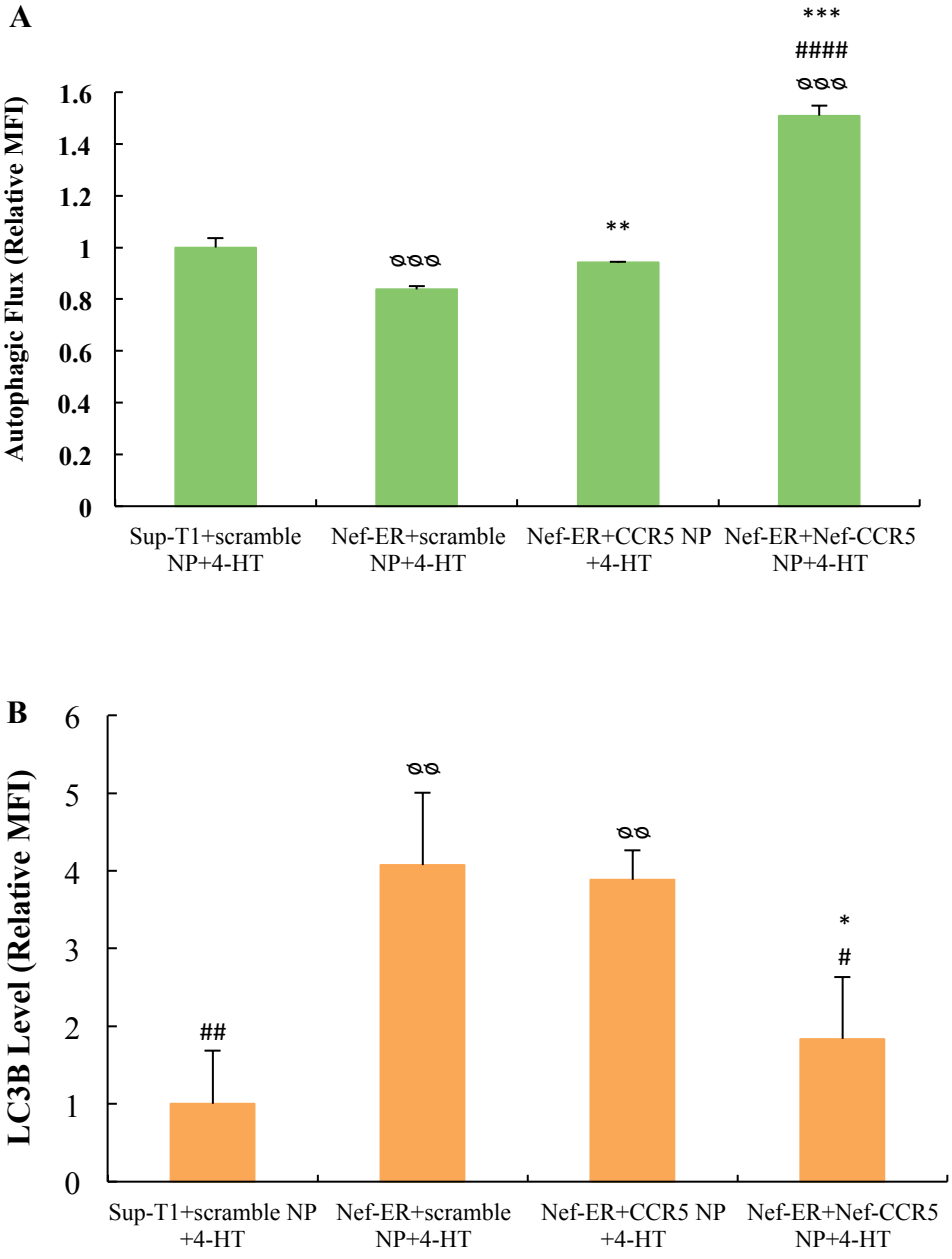
A
Autophagic Flux (Relative MFI)
1.6
1.4
1.2
1
0.8
0.6
0.4
0.2
0
***
####
ϞϞϞ
ϞϞϞ
**
Sup-T1+scramble NP+4-HT
Nef-ER+scramble NP+4-HT
Nef-ER+CCR5 NP +4-HT
Nef-ER+Nef-CCR5 NP+4-HT
B
LC3B Level (Relative MFI)
6
5
4
3
2
1
0
##
ϞϞ
ϞϞ
*
#
Sup-T1+scramble NP +4-HT
Nef-ER+scramble NP+4-HT
Nef-ER+CCR5 NP +4-HT
Nef-ER+Nef-CCR5 NP+4-HT

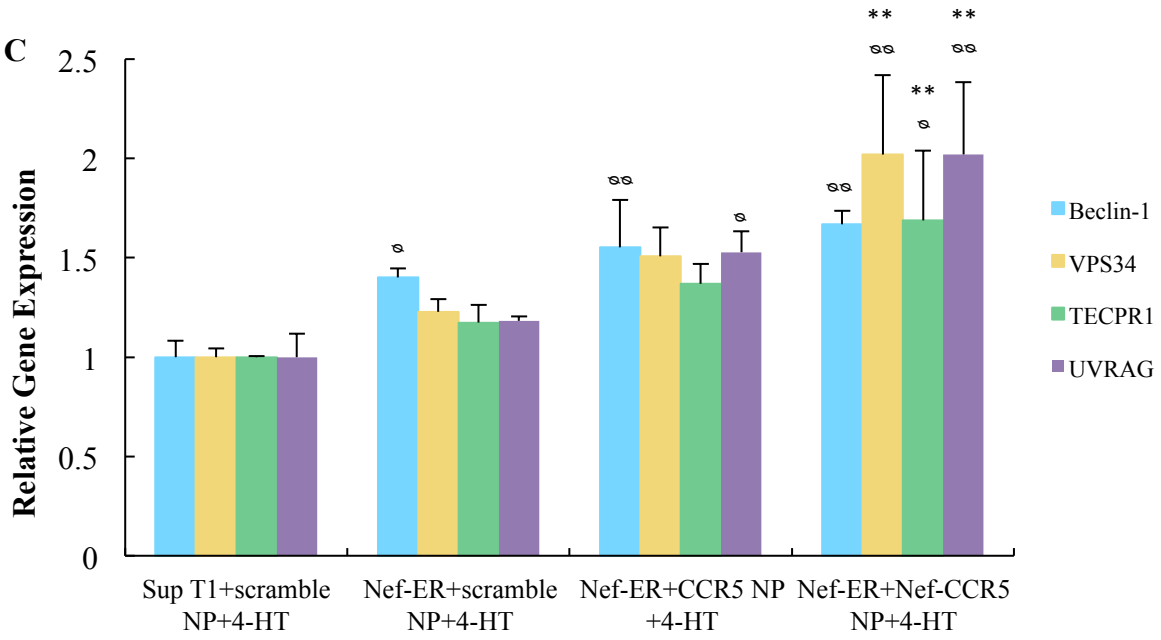

Figure 3.7: In vitro reactivation of autophagy by knocking down Nef with Nef-CCR5 NP. (A) Relative level of autophagic flux quantified with CYTO-ID® Autophagy detection kit by flow cytometry. The mean fluorescence intensity (MFI) from each group was normalized to the group of Sup-T1 treated with scramble NP and 4-HT, the basal level in naive cells was subtracted from each group as well. (B) Relative level of LC3B quantified by flow cytometry. The mean fluorescence intensity (MFI) from each group was normalized to the group of Sup-T1 treated with scramble NP and 4-HT, the basal level in naive cells was subtracted from each group as well. (C) Relative gene expressions of autophagy regulatory genes quantified by qRT-PCR. GAPDH was used as endogenous control. ϕp<0.05, ϕ ϕp<0.01, ϕ ϕ ϕp<0.001 compared to Sup-T1+scramble NP+4-HT. *p<0.05, **p<0.01, ***p<0.001, ****p<0.0001 compared to Nef-ER+scramble NP+4-HT. #p<0.05, ##p<0.01, ###p<0.001, ####p<0.0001 compared to Nef-ER+CCR5 NP+4-HT. Values represent the mean±SD, n=3.

3.4.4 In vitro inhibition of HIV by siRNA NP

Finally, we performed the in vitro anti-HIV study with our combination siRNA NP formulation. Sup-T1 cells were treated with the optimal concentration of NP (1.334 mg/mL) over a course of 9 days as cells were passaged every two days. Cells were pretreated with NP formulations/drug two days before viral challenge of HIV Bal (Day 3). Figure 3.8A showed the concentration of p24 produced during each two-day interval. The combinational siRNA NP formulation demonstrated highest inhibition effect among all the treatments, which could decrease the concentration of p24 by approximately 47%, 63% and 71.8% during each two-day interval, compared to PBS. The NP formulation containing a single type of therapeutic siRNA (siRNA Nef or siRNA CCR5) and scramble siRNA showed a similar inhibition effect as the protease inhibitor atazanavir and all three treatments showed a 30%-50% reduction (compared to PBS) over the period. Scramble NP formulation decreased the p24 concentration by about 41% during the first two days (Day 3-5) compared to PBS but afterwards it exerted a similar p24 production level as PBS. The cumulative p24 production was indicated in Figure 3.8B. Overall, combinational siRNA NP formulation demonstrated the highest cumulative p24 reduction (approximately 60%), followed by NP formulation containing a single type of therapeutic siRNA (siRNA CCR5 or siRNA Nef+ scramble siRNA) and atazanavir (about 37% for all three treatments) by the end of the study.

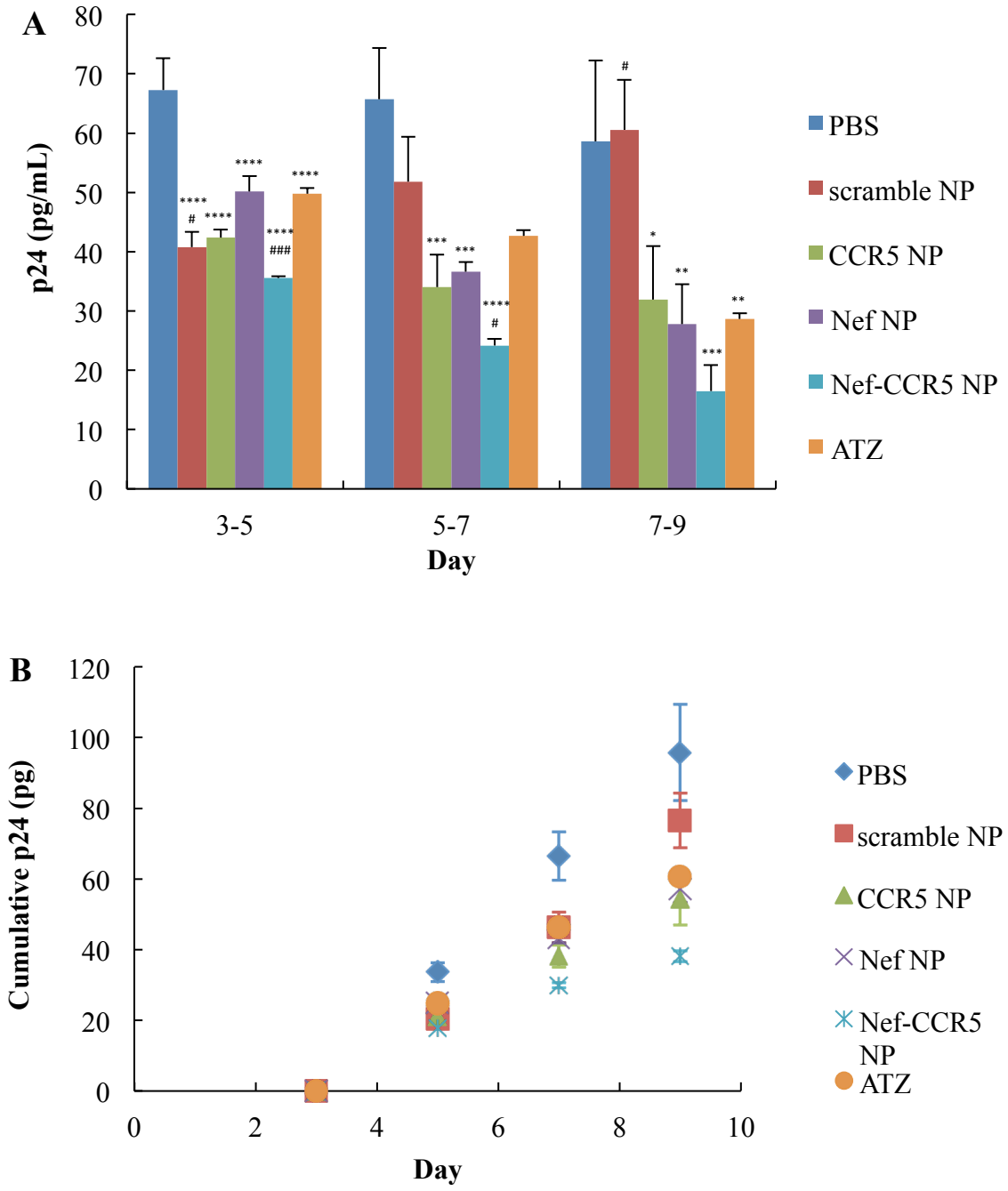

Figure 3.8: In vitro inhibition of HIV in Sup-T1 cells with repetitive treatments of NP formulations/drug. (A) Concentration of newly produced p24 during each two-day interval. (B) Cumulative production of p24. ATZ: atazanavir. *p<0.05, **p<0.01, ***p<0.001, ****p<0.0001 compared to PBS. #p<0.05, ###p<0.001 compared to ATZ. Values represent the mean±SD, n=3.

3.4.5 In vitro release of NP from vaginal gel and rheological properties of vaginal gel loaded with siRNA NP

After the optimization and characterization of NP, we went on to formulate the NP into a gel dosage form (1 mg NP/30 mg gel). First, we wanted to know whether the loaded NP could be released from the gel so the NP release study was conducted with coumarin 6-siRNA NP. Figure 3.9A compares the in vitro release profile of NP from 0.5% and 1% HEC gel loaded with NP. The data indicated that 0.5% HEC gel had higher release rate compared to 1%, with more than 17% of NP released over 48 hr. Next, the rheological profile of two concentrations of placebo gel and gel loaded with NP were measured as well. As shown in Figure 3.9B, the flow curves for 0.5% and 1% HEC placebo gel and gel loaded with NP all displayed non-Newtonian shear-thinning behavior and the loading of NP into the gel improved the viscosity. With higher release rate of NP from 0.5% HEC gel, we moved on our study with this formulation.

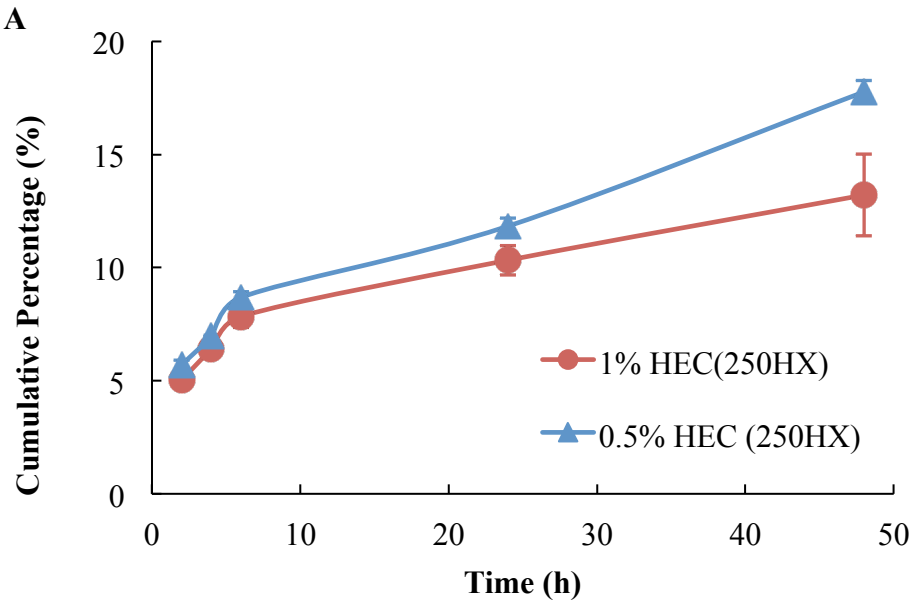

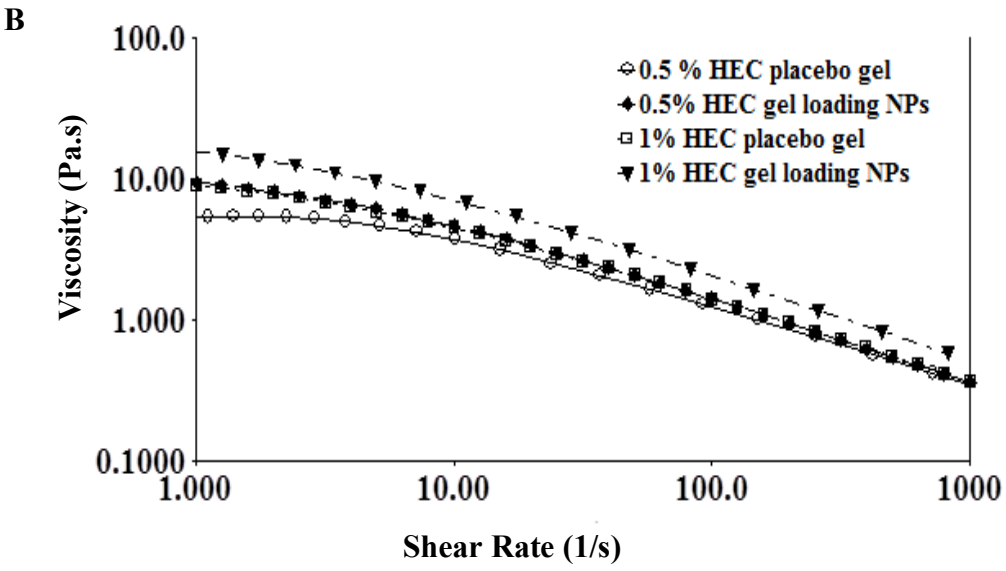

Figure 3.9: (A) In vitro release of coumarin 6-siRNA NP from 1% and 0.5% HEC gel in VFS, pH 4.2. Values represent the mean±SD, n=3. (B) Steady-state flow curves of HEC placebo gel and HEC gel loaded with siRNA NP at 37 °C. Image shows a representative measurement from n=3, the NP loading into gel was 1 mg NP/30 mg gel.

3.4.6 In vitro NP penetration through vaginal epithelial layer in vaginal mucosal co-cultural model

In order to mimic the in vivo physiological cell composition of vagina, we evaluated our formulation of 0.5% HEC gel loaded with NP (1 mg NP/30 mg gel) with a vaginal mucosal co-culture model that was established before [262] and the schematic illustration was shown in Figure 3.10. First, we evaluated the penetration of NP and cell uptake of NP from 0.5% HEC gel with this model. 0.125 g/mL of 0.5% HEC gel loaded with NP was treated to VK2/E6E7 cells in the upper chamber since this was the highest concentration that did not cause significant decrease in cell viability for a 24-hr treatment according to our MTS assay (Figure 3.11). As shown in Figure 3.12 A, the percentage of NP penetrating through VK2/E6E7 monolayer increased with time and at the end of 48

hr, more than 12% of total NP from the gel penetrated through vaginal epithelial layer. We also noticed that when the formulation was given to the co-culture model, the NP from 0.5% HEC gel were rapidly taken up by VK2/E6E7 cells and the uptake reached a saturation phase at 4 hr which lasts for 24 hr. As the incubation prolonged to 48 hr, no further increase was observed. This indicated that, during a certain period of time, the NP would first saturate the vaginal epithelial layer and then penetrate through. The NP reaching lower chamber could be rapidly taken up by Sup-T1 cells as the mean fluorescence intensity (MFI) in Sup-T1 increased with NP monolayer penetration over time (Figure 3.12 B).

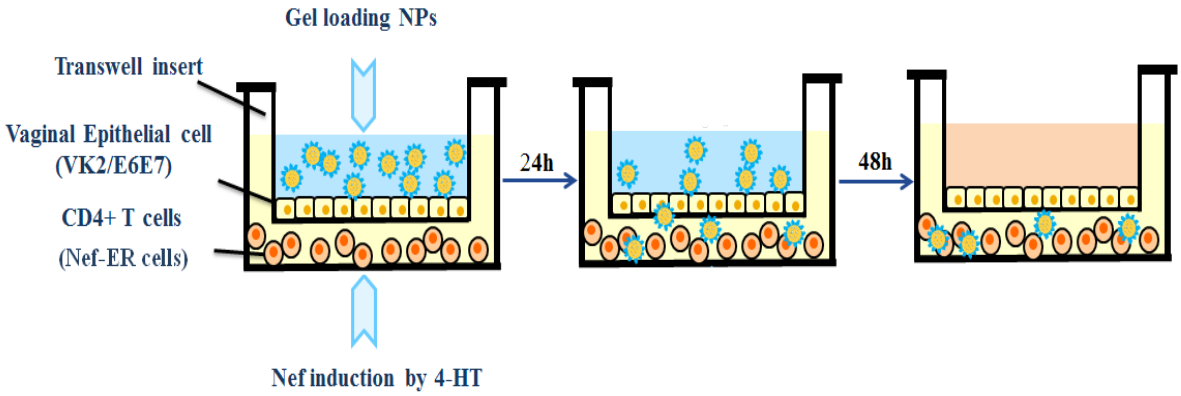

Figure 3.10: Schematic illustration of the in vitro vaginal mucosal co-culture model. Nef-ER cells: Sup-T1 cells stably expressing Nef upon addition of 4-HT. VK2/E6E7: vaginal epithelial cells, Nef: negative regulatory factor (HIV protein), 4-HT: 4-hydroxytamoxifen. NPs: nanoparticles.

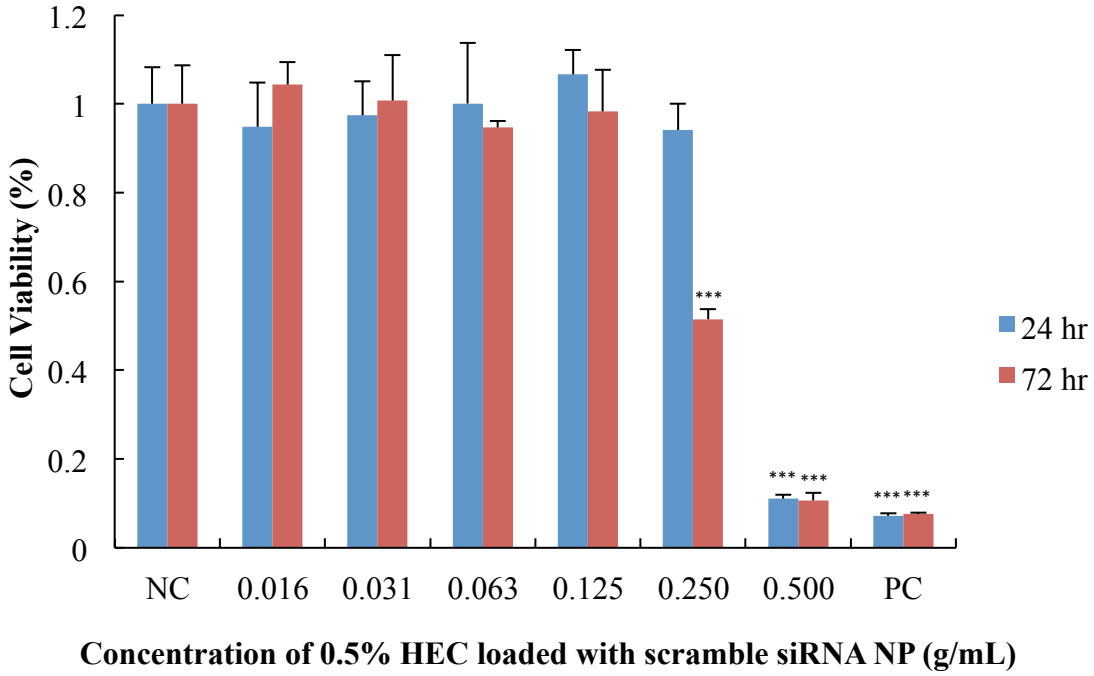

Figure 3.11: In vitro MTS assay of 0.5% HEC gel loaded with scramble NP (1 mg NP/30mg gel) in VK2/E6E7 cells. NC (negative control): cell culture medium, PC (positive control): 1% acrylamide, *** $p<0.001$ compared to NC. Values represent the mean±SD, n=3.

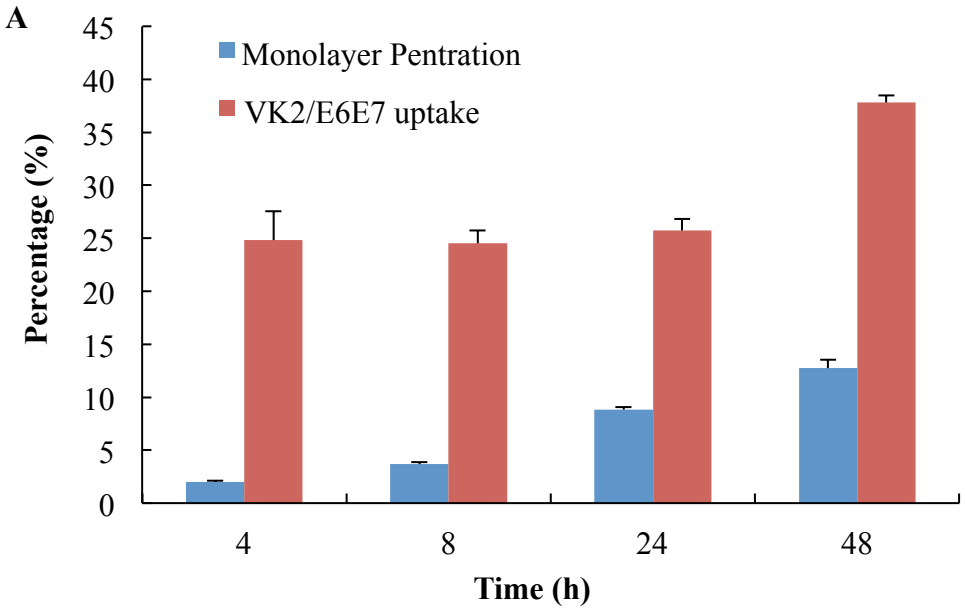

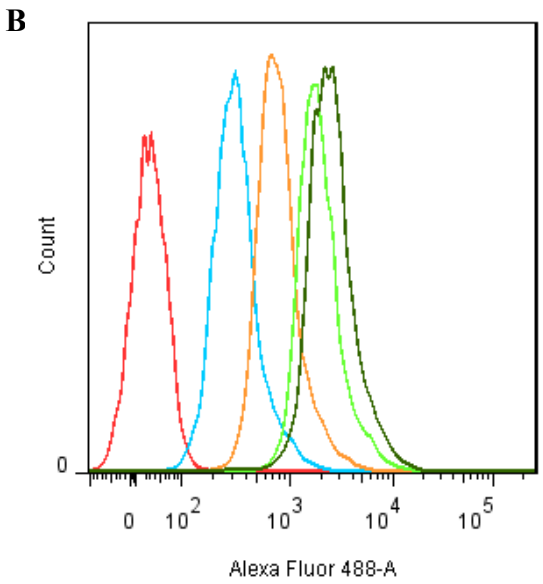

Figure 3.12: In vitro penetration of coumarin 6-siRNA NP delivered by 0.5% HEC gel across vaginal epithelial monolayer in a vaginal mucosal co-culture model. (A) The percentage of NP penetrating across vaginal epithelial monolayer V.S. taken up by vaginal epithelium. Values represent the mean±SD, n=3. (B) A representative histogram showing the uptake of NP by Sup-T1 cells in the lower chamber over time. Red: Blank NP, blue: 4 hr, orange: 8 hr, light green: 24 hr, dark green: 48 hr.

3.4.7 In vitro cytotoxicity and gene knockdown efficiency of vaginal gel loaded with siRNA NP

After confirming that the NP can be released from the gel dosage form and that NPs can penetrate across the vaginal mucosal co-culture model, we next investigated gene knockdown efficiency. Figure 15 shows the gene knockdown of Nef and CCR5 by 0.5% HEC gel loaded with Nef-CCR5 NP (1 mg NP/30 mg gel) in a vaginal mucosal co-culture model. The co-culture model was treated with 0.5% HEC gel loaded with NP (0.125g/mL) and 4-HT (5 μM) simultaneously and the formulation was maintained in the upper chamber for 72 hr; after that the cells were lysed for the analysis of Nef and CCR5 (as previously shown in Figure 3.10). By the end of the study, the resistance of the

VK2/E6E7 monolayer was re-assessed and the resistance was measured to be the same before and after treatment (Figure 3.13 A), indicating the integrity of the monolayer. The mRNA of Nef in Nef-ER cells was decreased to 66%, which is as same as that in Nef-ER cells treated without 4-HT. This indicated that all induced Nef mRNA was knocked down by the formulation. With regard to CCR5, the mRNA was decreased to 51% in Nef-ER cells at the same time. The gene knockdown of Nef and CCR5 were also confirmed by measuring the protein level. Both of the protein levels of Nef and CCR5 were significantly decreased to approximately 70%, even though the induced Nef was not totally knocked down at protein level. In addition, the CCR5+ population was also decreased from 67% to 55%. As a result, 0.5% HEC gel loaded with Nef-CCR5 NP could cause significant gene knockdown of both Nef and CCR5 in vaginal mucosal co-culture model but for future in vivo study, one single treatment may not be sufficient for considerate gene knockdown due to the limitation in the rate of epithelial transportation of NP, multiple-treatment regimen may be needed.

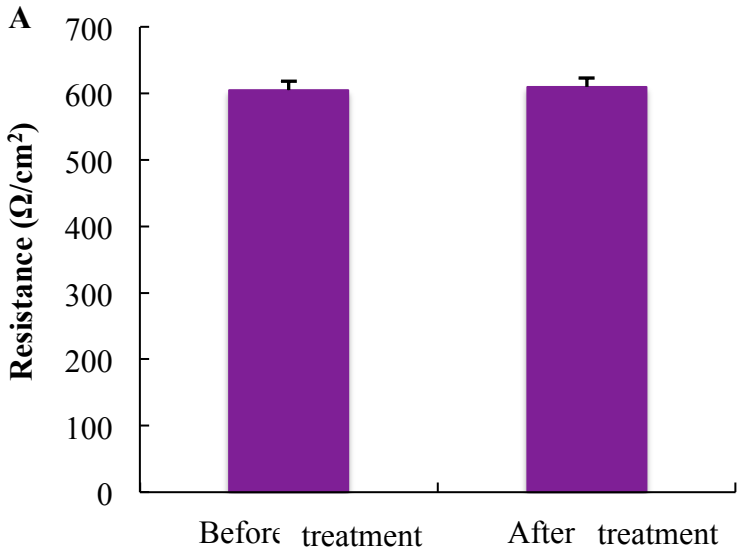

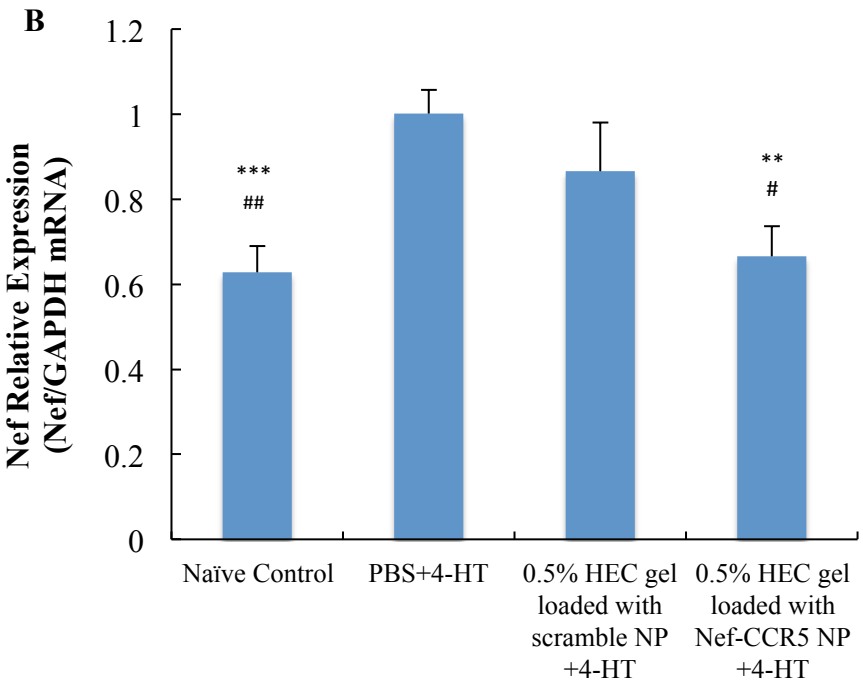
B
Nef Relative Expression (Nef/GAPDH mRNA)
1.2
1
0.8
0.6
0.4
0.2
0
***
##
**
#
Naïve Control
PBS+4-HT
0.5% HEC gel loaded with scramble NP +4-HT
0.5% HEC gel loaded with Nef-CCR5 NP +4-HT

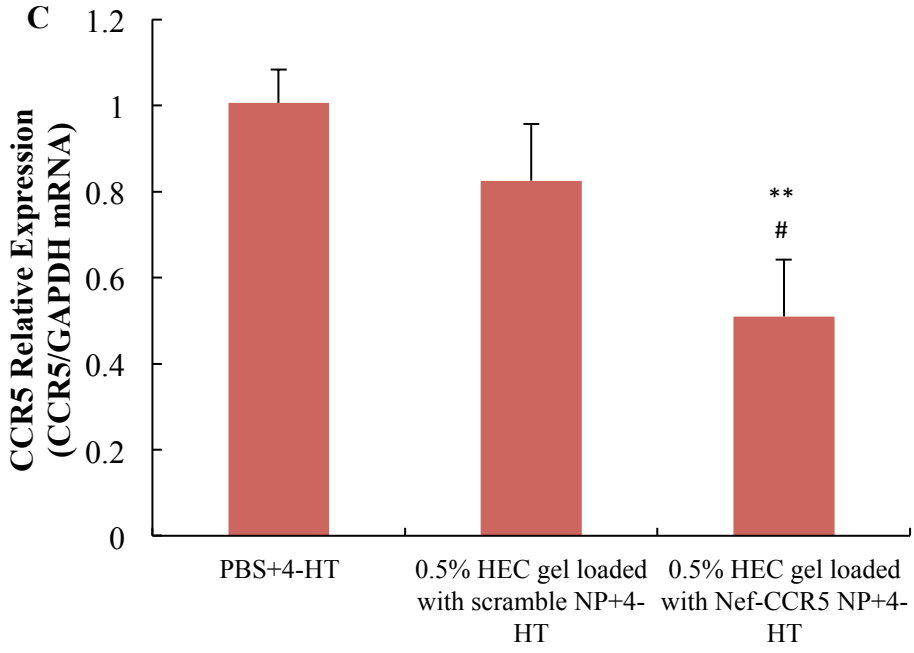
C
CCR5 Relative Expression (CCR5/GAPDH mRNA)
1.2
1
0.8
0.6
0.4
0.2
0
**
#
PBS+4-HT
0.5% HEC gel loaded with scramble NP+4-HT
0.5% HEC gel loaded with Nef-CCR5 NP+4-HT

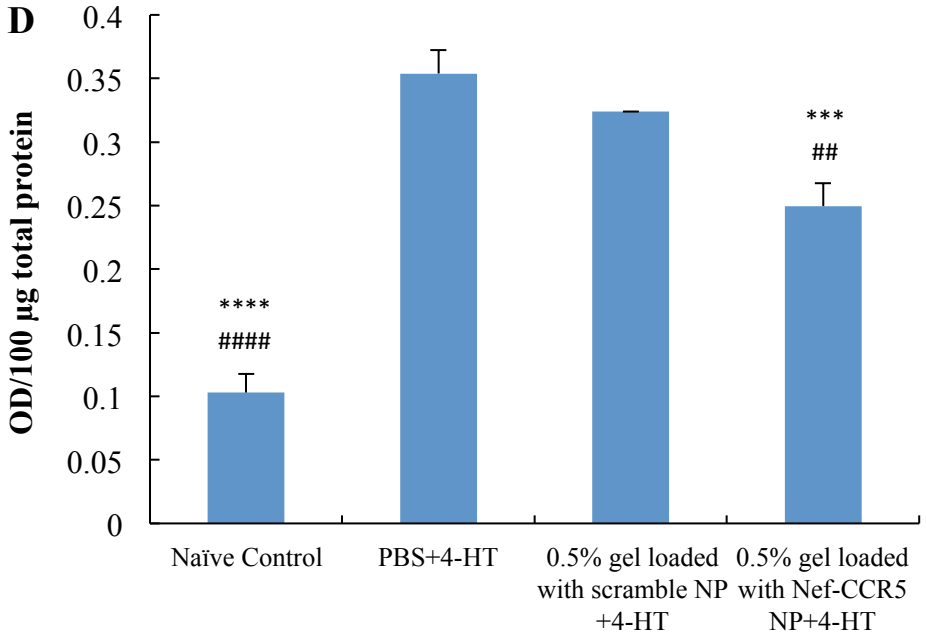
D
OD/100 µg total protein
0.4
0.35
0.3
0.25
0.2
0.15
0.1
0.05
0
****
####
***
##
Naïve Control
PBS+4-HT
0.5% gel loaded with scramble NP +4-HT
0.5% gel loaded with Nef-CCR5 NP+4-HT

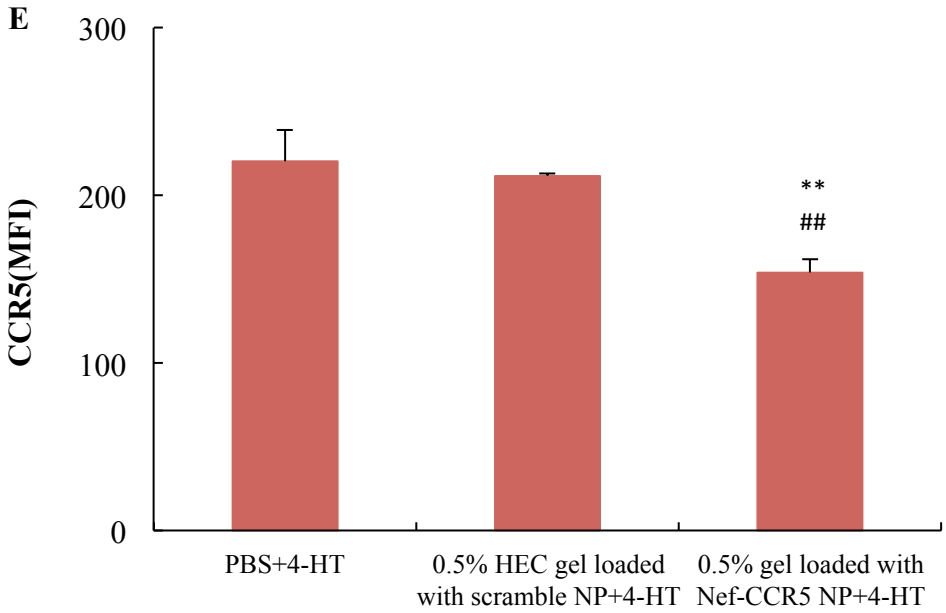
E
CCR5(MFI)
300
200
100
0
**
##
PBS+4-HT
0.5% HEC gel loaded with scramble NP+4-HT
0.5% gel loaded with Nef-CCR5 NP+4-HT

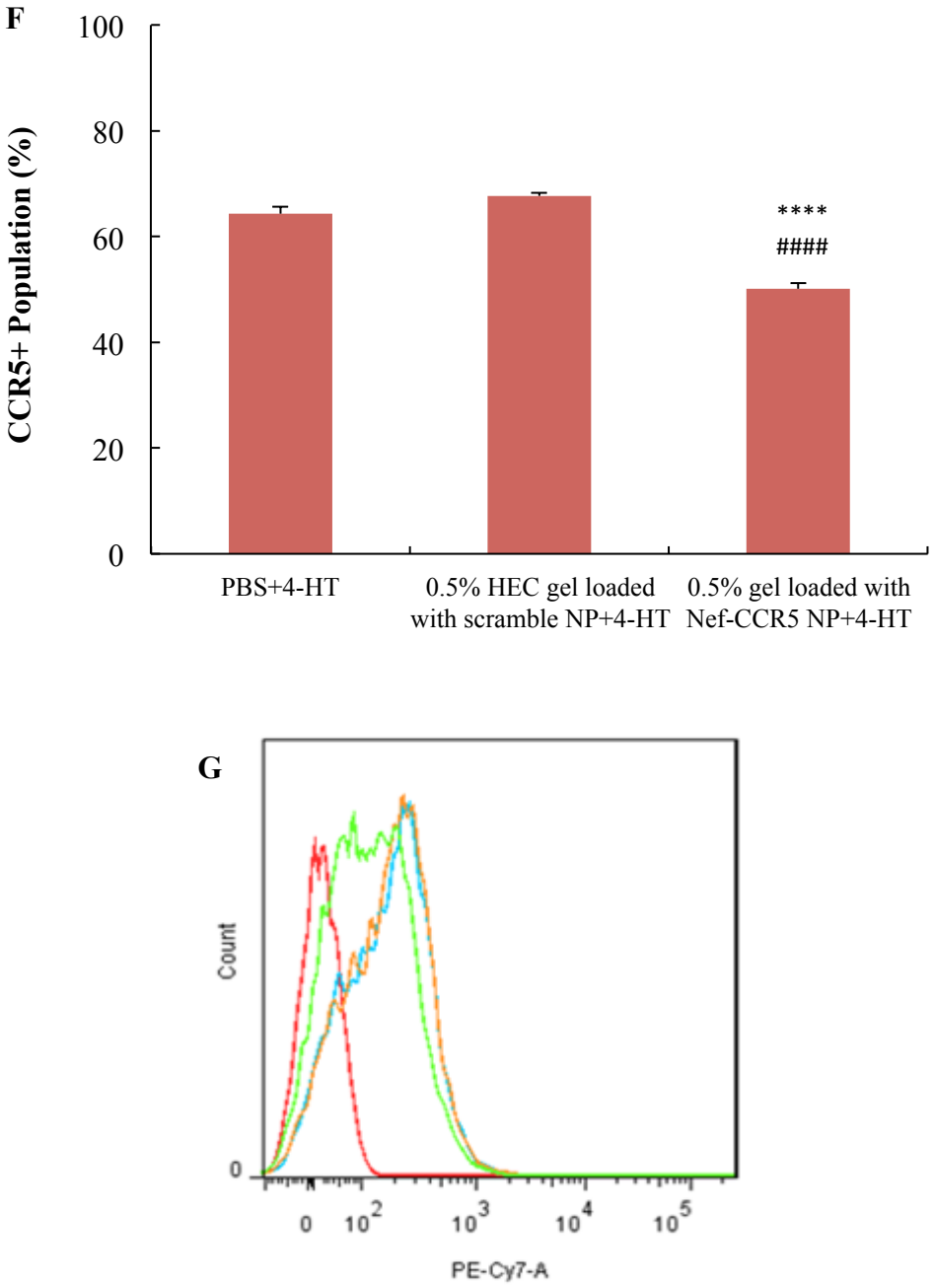

Figure 3.13: In vitro gene knockdown efficiency of 0.5% HEC gel loaded with Nef-CCR5 NP in a vaginal mucosal co-culture model. (A) Resistance of VK2/E6E7 cell monolayer before and after treatment of 0.5% HEC gel loaded with Nef-CCR5 NP. (B) Nef mRNA downregulation quantified by qRT-PCR. (C) CCR5 mRNA downregulation quantified by qRT-PCR. (D) Nef protein downregulation quantified by ELISA. (E-G) CCR5 protein downregulation quantified by flow cytometry. Red: isotype control, blue 0.5% HEC gel loaded with scramble NP, orange: PBS, green: 0.5% HEC gel loaded with Nef-CCR5 NP. GAPDH was used as an endogenous control for qRT-PCR. Values represented as mean ± SD; n = 3.

Inflammatory cytokine levels were also measured in this vaginal mucosal co-culture model to confirm the cytotoxicity profile (Figure 3.14). TNF-α, IL-6 and IL-8 remained unchanged in both VK2/E6E7 cells and Nef-ER cells when PBS or formulations were treated to cells in the vaginal mucosa co-culture model. The level of IL1-β in VK2/E6E7 dropped by approximately 40% when 0.5% HEC gel loaded with scramble NP or 0.5% HEC gel loaded with Nef-CCR5 NP was treated to VK2/E6E7 cells. IL-8 was also significantly increased in Nef-ER cells (lower chamber) by about 50% when 4-HT was treated to Nef-ER cells in the lower chamber. Therefore, the treatment of either 0.5% HEC gel loaded with scramble NP or 0.5% HEC gel loaded with Nef-CCR5 NP did not induce any pro-inflammatory cytokine production in either VK2/E6E7 cells or Nef-ER cells in the vaginal mucosal co-culture model.

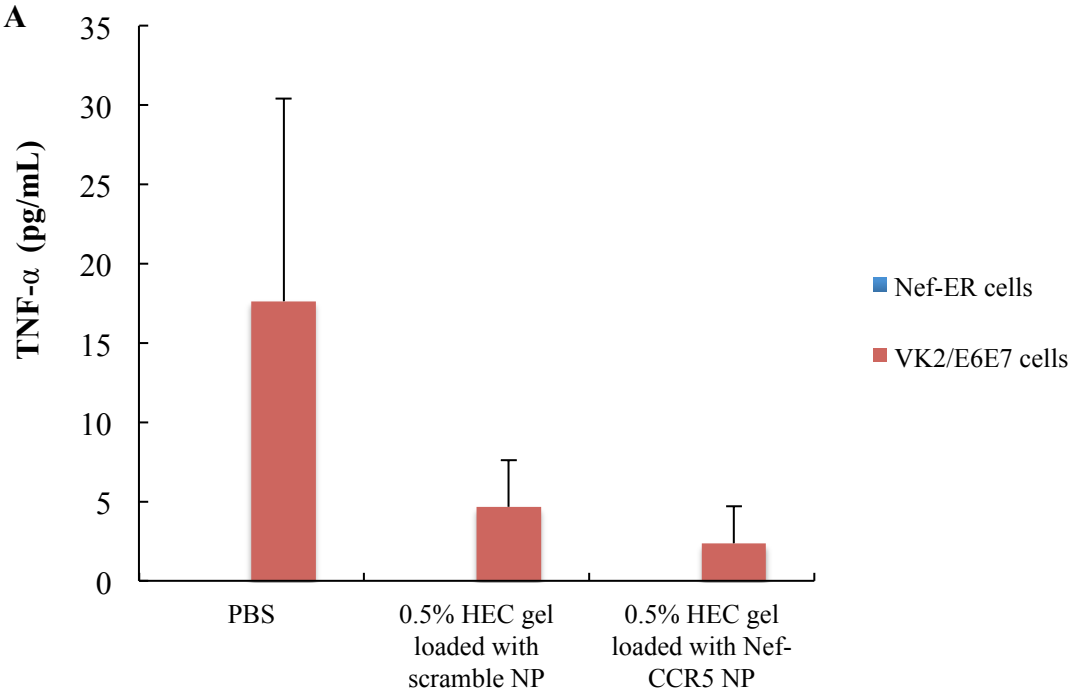

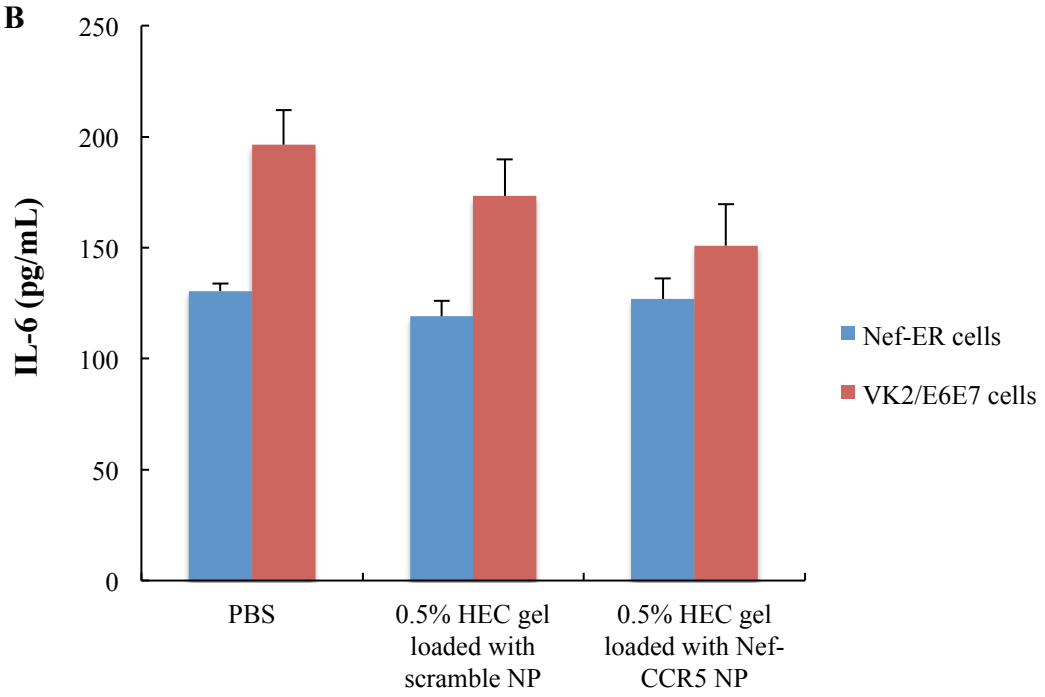
B
IL-6 (pg/mL)
250
200
150
100
50
0
PBS
0.5% HEC gel loaded with scramble NP
0.5% HEC gel loaded with Nef-CCR5 NP
Nef-ER cells
VK2/E6E7 cells

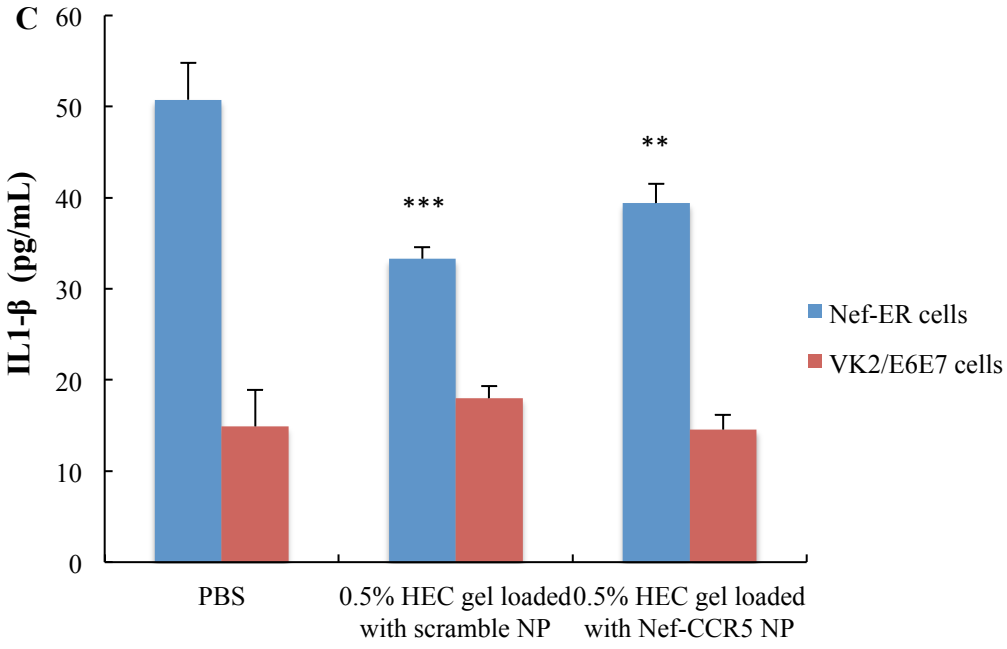
C
IL1-β (pg/mL)
60
50
40
30
20
10
0
***
**
PBS
0.5% HEC gel loaded with scramble NP
0.5% HEC gel loaded with Nef-CCR5 NP
Nef-ER cells
VK2/E6E7 cells

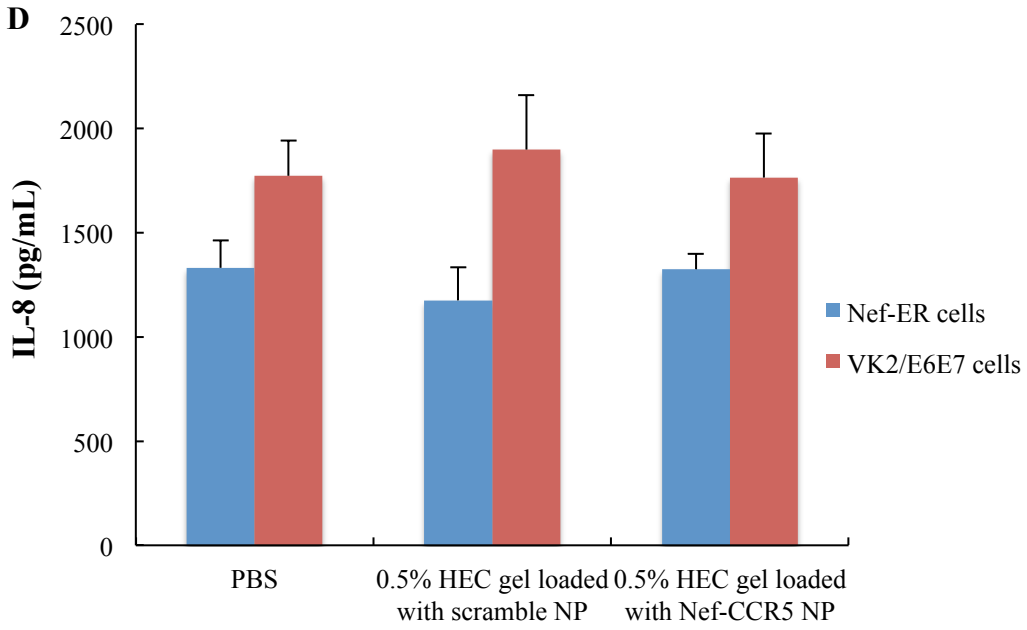

Figure 3.14: In vitro pro-inflammatory cytokine production in a vaginal mucosal co-culture model when 0.125 g/mL of 0.5% HEC gel loaded with NP formulations was added to the upper chamber. (A) TNF-α, (B) IL-6, (C) IL1-β, (D) IL-8. **p<0.01, ***p<0.001 compared to PBS. Values represented as mean ± SD; n = 3.

Eventually, we tested our formulation in a mouse model. However, when we first evaluated the uptake of siRNA in mouse vaginal tissues with 0.5% HEC gel loaded with Cy-3 scramble NP (1 mg siRNA NP/30 mg gel), we found the total uptake was low and tissues from some region of the vaginal tract received minimal or undetectable amount of siRNA (data no shown). In order to improve the intravaginal delivery of therapeutic siRNA into its target cells, we decided to conjugate anti-CD4 antibody to NP to enhance the delivery into CD4+ cells. The siRNA NP conjugated to antibody showed a particle size of 295.6±9.2 nm (PDI 0.258) and a zeta potential of -9.51±0.30 mV in PBS, pH 7.4 and a particle size of 307.2±5.2 nm (PDI 0.278) and a zeta potential of -3.54±0.63 mV in

VFS, pH 4.2. Then Sup-T1 cells (expressing high level of CD4) were treated with Cy-3 scramble NP conjugated with anti-human anti-CD4 monoclonal antibody (Cy-3 scramble NP-(h)CD4) for different time intervals to compare the intracellular uptake of siRNA, the same NP conjugated with IgG monoclonal antibody (isotype control) (Cy-3 scramble NP-(h)IgG) was used as control. According to Figure 3.15, CD4 antibody conjugation could improve the intracellular uptake of siRNA by approximately 66%, 100%, and 62% within 2 hr, 4hr and 6hr respectively. With the positive in vitro targeting data, the antibody conjugated NP was loaded into 0.5% HEC gel and the final formulation was evaluated in a mouse model for its ability in improving the intravaginal siRNA delivery. Mice were dosed with PBS, 0.5% HEC gel loaded with Cy-3 scramble NP-(m)IgG and 0.5% HEC gel loaded with Cy-3 scramble NP-(m)CD4 twice a day for two concessive days. In order to exclude the fluorescent siRNA signals coming from formulations that were trapped in the cervicovaginal mucus, vaginal lavage with 100 μL of PBS was performed three times on each animal before euthanasia and tissue collection. Figure 3.16 indicated that 0.5% HEC gel loaded with Cy-3 scramble NP-(m)CD4 could significantly increase the total uptake of siRNA into vaginal tissues and the distribution of siRNA was continuous and uniform along the whole vaginal tract. In contrast, siRNA delivered by 0.5% HEC gel loaded with Cy-3 scramble NP-(m)IgG was mainly detected from the opening of vagina and a small region of lower and upper vagina. Moreover, fluorescent siRNA was only detected in vaginal tissues and other organs of the body (such as heart, blood, liver, spleen, kidney and lung) received undetectable siRNA (Figure 3.17). In order to evaluate whether the improved siRNA uptake could result in an improved gene knockdown effect in CD4+ cells, the CCR5 was used as a model gene. siRNA targeting mouse CCR5 was encapsulated in NP and formulated into 0.5% HEC gel. Mice were dosed the same way as

mentioned above. We measured the CCR5 knockdown at protein level from CD4+ cells and CD4- cells in lower vagina or upper vagina-cervix respectively using flow cytometry to compare the gene knockdown effects. Our results showed that significant gene knockdown was only observed in CD4+ cells of vagina and cervix, indicating that anti-CD4 antibody conjugation allowed RNAi-based nanomedicine to achieve targeted gene knockdown in CD4+ cells without disrupting the gene expression in CD4- cells in the vagina. 0.5% HEC gel loaded with siRNA CCR5 NP-(m)CD4 significantly knocked down approximately 40% and 36% of CCR5 in CD4+ cells of the lower vagina and upper vagina-cervix respectively, while the 0.5% HEC gel loaded with siRNA CCR5 NP-(m)IgG achieved no CCR5 knockdown in CD4+ cells of the lower vagina and upper vagina-cervix (Figure 3.18).

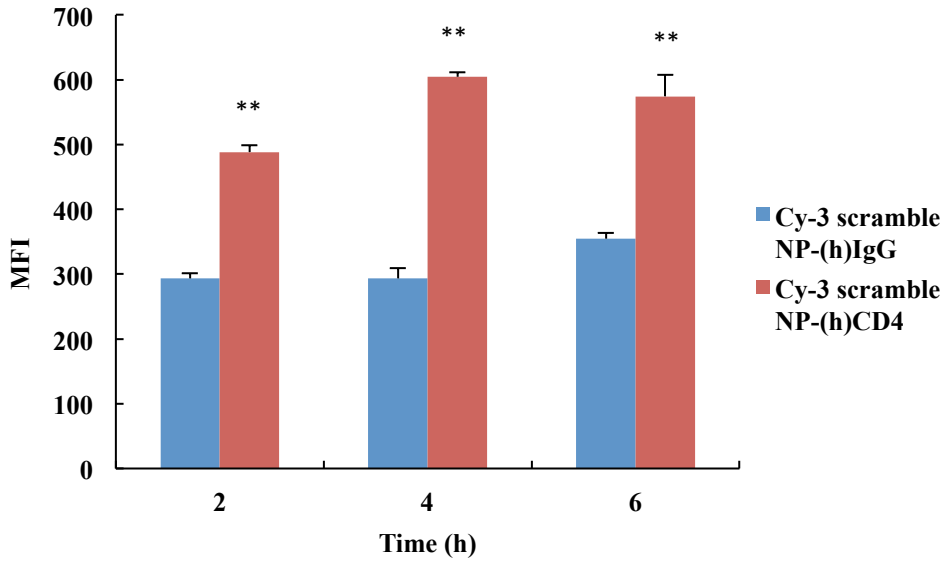

Figure 3.15: In vitro uptake of siRNA by Sup-T1 cells when cells were treated with Cy-3 scramble NP-(h)IgG or Cy-3 scramble NP-(h)CD4. **p<0.01 compared to Cy-3 scramble NP-IgG. Values represent Mean±SD, n=3.

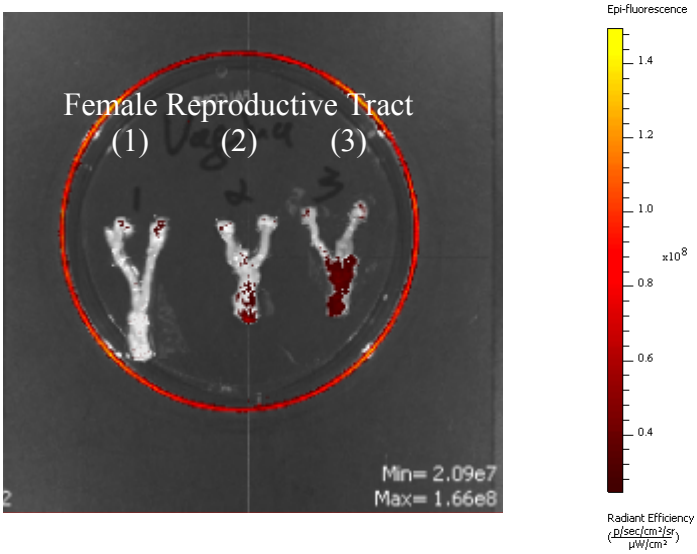

Figure 3.16: In vivo uptake of siRNA into vaginal tissues. (1) PBS treatment, (2) 0.5% HEC gel loaded with Cy-3 scramble NP-(m)IgG, (3) 0.5% HEC gel loaded with Cy-3 scramble NP-(m)CD4. A representative image from n=3 was shown.

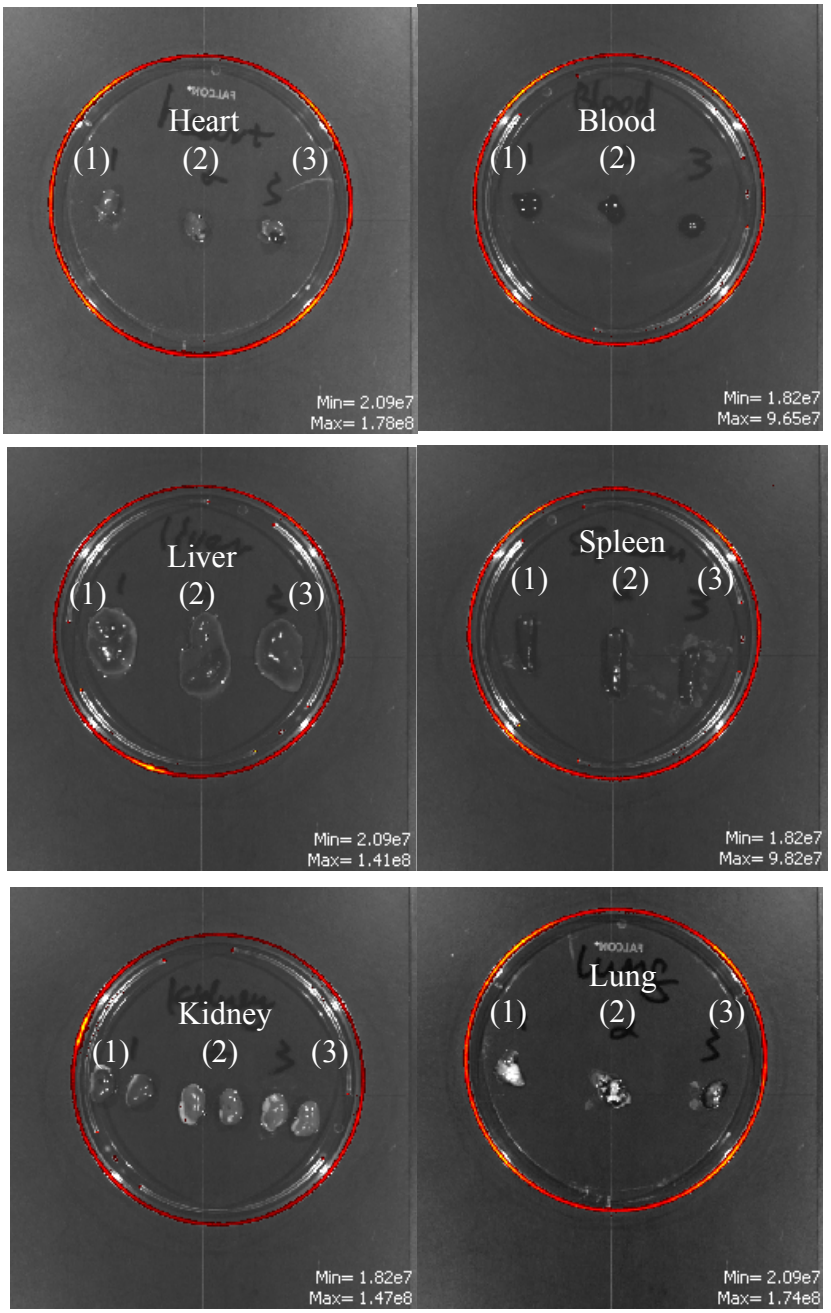

Figure 3.17: In vivo distribution of siRNA in major organs. (1) PBS treatment, (2) 0.5% HEC gel loaded with Cy-3 scramble NP-(m)IgG, (3) 0.5% HEC gel loaded with Cy-3 scramble siRNA-(m)CD4. Representative images from one group of experiment (n=1) were shown out of n=3.

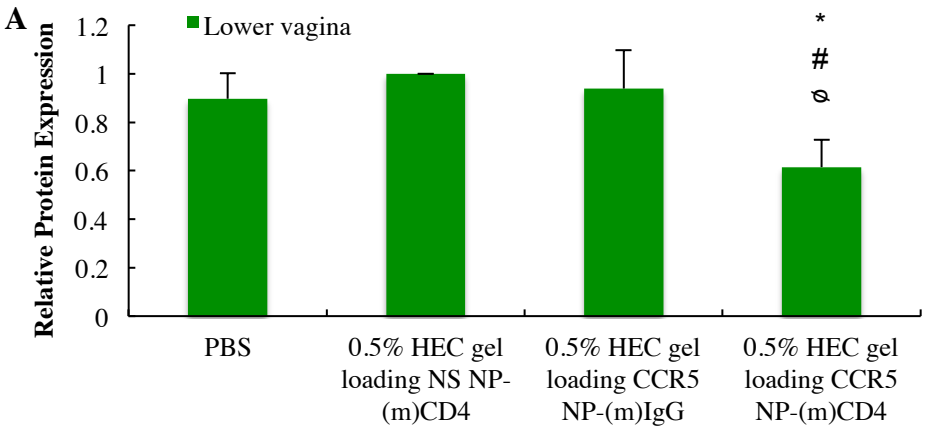
A
Lower vagina
Relative Protein Expression
1.2
1
0.8
0.6
0.4
0.2
0
*
#
ø
PBS
0.5% HEC gel loading NS NP-(m)CD4
0.5% HEC gel loading CCR5 NP-(m)IgG
0.5% HEC gel loading CCR5 NP-(m)CD4

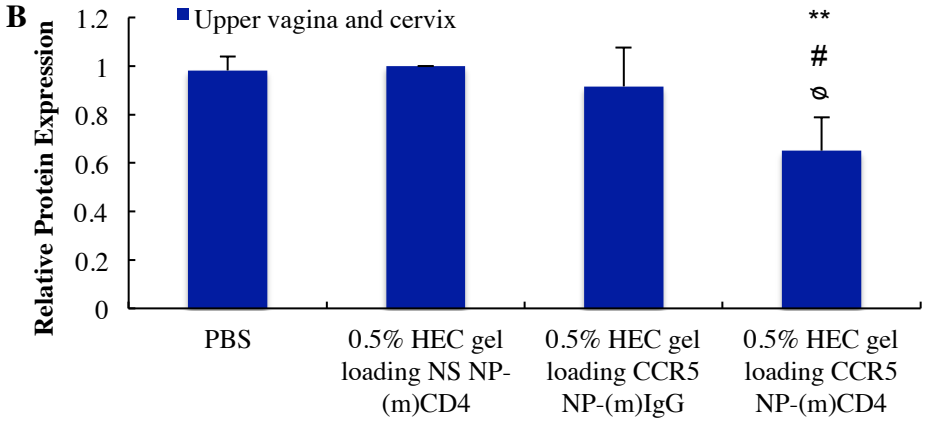
B
Upper vagina and cervix
Relative Protein Expression
1.2
1
0.8
0.6
0.4
0.2
0
**
#
ø
PBS
0.5% HEC gel loading NS NP-(m)CD4
0.5% HEC gel loading CCR5 NP-(m)IgG
0.5% HEC gel loading CCR5 NP-(m)CD4

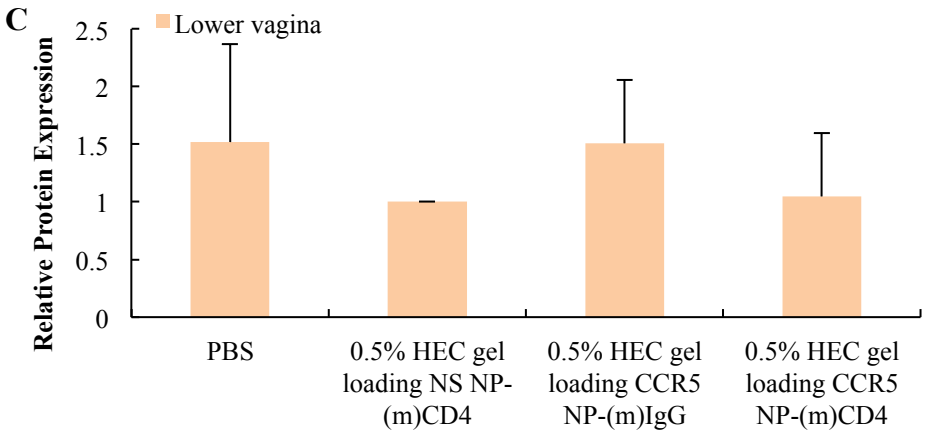
C
Lower vagina
Relative Protein Expression
2.5
2
1.5
1
0.5
0
PBS
0.5% HEC gel loading NS NP-(m)CD4
0.5% HEC gel loading CCR5 NP-(m)IgG
0.5% HEC gel loading CCR5 NP-(m)CD4

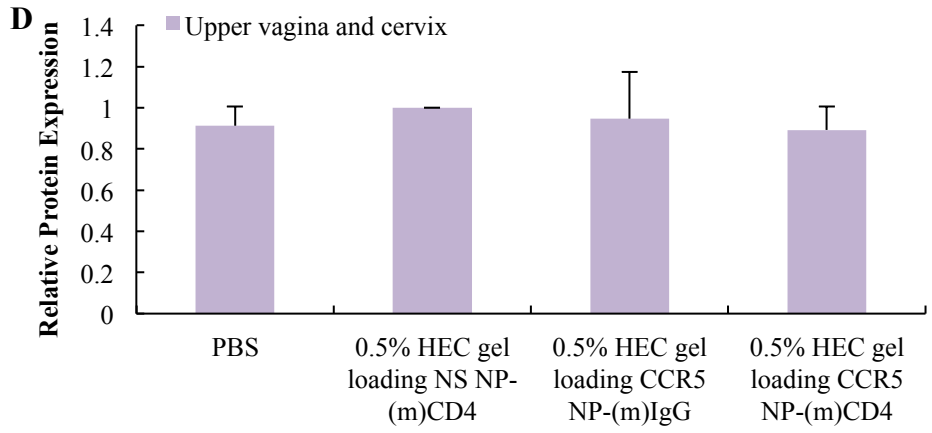

Figure 3.18: In vivo gene knockdown of CCR5 in CD4+ cells and CD4- cells of mouse vagina and cervix. (A) Relative protein expression of CCR5 in CD4+ cells of lower vagina. (B) Relative protein expression of CCR5 in CD4+ cells of upper vagina and cervix. (C) Relative protein expression of CCR5 in CD4- cells of lower vagina (D) Relative protein expression of CCR5 in CD4- cells of upper vagina and cervix. Values represent Mean±SD, n=3. *$p<0.05$, **$p<0.01$ compared to PBS, #$p<0.05$ compared to 0.5% gel loading NS NP-(m)CD4 and ∞$p<0.05$ compared to 0.5% HEC gel loading CCR5 NP-(m)IgG. Values represent Mean±SD, n=3.

3.5 Discussions

The N/P ratio reflects the ratio of siRNA (negatively charged) to PEI (positively charged). The siRNA was condensed by PEI via electrostatic interaction forming siRNA-PEI complexes. N/P ratio of 5 was selected over higher ratios as the optimum since higher N/P ratio would condense siRNA into firmer complexes via stronger electrostatic interaction, which might inhibit the release of siRNA from NP. Previous literature indicated the optimal size range of non-mucoadhesive nanosystems was 200-500 nm and the desirable zeta potential was -10 mV to 10 mV (close to neutral) [208, 264]. And the particle size (271.6±1.8 nm) and zeta potential (-8.66±2.43 mV) of siRNA NP measured

in VFS, pH 4.2 were both located within these ranges, therefore, it is likely that the siRNA NP have a potential to achieve enhanced mucus penetration. But further experiments are still required to evaluate its mucus penetration ability. Further increase in initial siRNA input over 100 μg enlarged particle size to be above 300 nm just after sonication during NP preparation. This size still seemed to be an acceptable particle size, but we had to consider the fact that particles had the potential to aggregate during the downstream phases, especially the three-time centrifugations. And our results indicated that the particle size jumped to 400-500 nm, which made it a less desirable formulation than our optimal one. And in the meanwhile, the encapsulation efficiency also dropped below 70%.

The mechanism of the pH-responsive release profile of siRNA NP was not documented previously and still remained unrevealed today. We thought it might be related to varied disassociation rate of siRNA from siRNA-PEI complexes or varied degradation rates of the PLGA-PEG to release siRNA in different buffers with different pH conditions. To investigate the first hypothesis, we performed release study of unencapsulated siRNA-PEI complexes under the same condition as shown in Figure 3.2 C and we found that the complexes themselves could only provide a burst release of about 2.3% upon switching the release medium from VFS, pH 4.2 to PBS, pH 7.4. This was 7 times lower than what was observed from siRNA NP. Therefore, it is unlikely that the pH-responsive release profile could be completely attributed to varied disassociation rate of siRNA from siRNA-PEI complexes. Subsequently, we looked into literatures to see if anyone measured the rate of PLGA-PEG degradation previously. He et al. compared the degradation rate of PLGA (80:20)-PEG-methyl ester under different pH conditions of

PBS (pH 5.0, pH 7.4 and pH 9.1) [265]. Based on their research, PLGA (80:20)-PEG-methyl ester showed a higher degradation rate in pH 7.4 than pH 5.0 and an even higher rate in pH 9.1 over the course of 8 weeks. The most dramatic difference was observed within the first two weeks [265]. This finding partly supported what was observed in our study even though the composition of PLGA-PEG we used was different from theirs (PLGA (50:50)-PEG-COOH V.S. PLGA (80:20)-PEG-methyl ester) and the release media were not entirely the same. We could rationally hypothesize that the acidic pH of VFS plays an important role in significantly slowing down the degradation rate of PLGA-PEG. Therefore, in the future, the degradation rate of the PLGA-PEG used in our study should be fully evaluated in PBS, pH 7.4 and VFS, pH 4.2 to reveal the exact mechanism of this pH-responsive release profile of siRNA. The pre-incubation of NP in VFS, pH 4.2 augmented the release profile of siRNA in PBS, pH 7.4. We thought this was probably due to the effect of higher water penetration/diffusion into NP when it was pre-incubated in aqueous VFS. The degradation of PLGA-PEG depends on the hydrolysis of ester and amide bonds in the presence of water. The acidic pH significantly inhibited the hydrolysis process when NP was in VFS, but the hydrolysis process was resumed immediately when the release medium was changed into PBS, pH7.4, and in the meanwhile, more water content in the NP could potentially accelerate the hydrolysis and degradation process, causing more siRNA to be released.

Full-length viral protein Nef from HIV strain NL4-3 was co-expressed as a fused protein with estrogen receptor hormone-binding domain, therefore kept at an inactive state due to steric hindrance. The addition of 4-HT that bound to estrogen receptor hormone-binding domain would counteract the hindrance and induce the activation of functional Nef in

cells. Therefore, Nef-ER cells routinely produced a detectable level of inactive Nef mRNA and protein without the addition of 4-HT [261]. The addition of 4-HT could boost the mRNA expression of Nef by approximately 40%, but the protein expression of Nef could be elevated by 2 folds. This different gene expression at mRNA and protein levels is probably due to the detection methods we use. qRT-PCR could not differentiate the inactive and active Nef, but Nef ELISA could do that, since the antibody binding site could be hidden when Nef is inactive. The addition of 4-HT could not only activate Nef but also boost its gene expression and the 2-fold increase in Nef protein is a result of both Nef gene upregulation (~40%) and Nef protein activation. At the optimal concentration of 1.334 mg/mL, both Nef mRNA and protein could be knocked down to its original level seen in Nef-ER without 4-HT treatment.

With respect to cytokine production, IL-6 was significantly reduced in the groups treated with scramble NP+4-HT and Nef-CCR5 NP+4-HT. We believe the results may be related to the lowest limit of quantification of the IL-6 ELISA kit, which was 3 pg/mL. T cells produced IL-6 at a very low level (around or below 10 pg/mL), therefore, when the concentration was approaching to the lowest limit of quantification, more errors might be introduced, which might explain why we saw a significant reduced IL-6 level in the scramble NP+4-HT group. As for the group treated with siRNA Nef&siRNA CCR5+4-HT, CCR5 was significantly downregulated and this is probably main reason. In previous literature, Tang et al. reported that CCR5 promotes the IL-6 production in human synovial fibroblasts [266], therefore, knocking down CCR5 could potentially decrease IL-6 production. This phenomenon was not observed in the vaginal mucosal co-cultural model probably the CCR5 downregulation was not as high as that achieved in Nef-ER

model when therapeutic NP was treated directly to cells. In the vaginal mucosal co-culture model, the treatment of our formulation did not induce any pro-inflammatory cytokine production. We were not sure why the treatment of 0.5% HEC gel loaded with either scramble NP or Nef-CCR5 NP decreased IL1-β in VK2/E6E7 cells from the vaginal mucosal co-culture model and this might be investigated in the future.

In the autophagic flux study measuring autophagic degradation activity, knocking down all the induced Nef caused an even higher level of autophagic flux compared to the original level of autophagy in control (as measured by Sup-T1 treated with scramble NP+4-HT). Theoretically, when Nef was induced in T cells, it could potentially trigger an increase in autophagic flux since it is considered a foreign protein, but this increase was not seen in the group treated with Nef-ER+scramble NP+4-HT because Nef inhibited the autophagy as well as the house-keeping autophagy in viable cells, instead, a level lower than house-keeping level of autophagic flux was observed in the that group. Therefore, the high autophagic flux seen in the group of Nef-ER+Nef-CCR5 NP+4-HT was probably around the level of the hidden autophagic flux level triggered by Nef.

The level of LC3B correlates with the amount of autophagosomes [267]. The increase in the autophagosomes was either due to improved formation or reduced degradation. Previous literature indicated that Nef primarily inhibited the degradation stage of autophagy and prevented new HIV from being degraded [263]. During the degradation stage, autophagosomes were degraded the same way as other components, therefore, in our case, the change in LC3B should be closely related to altered degradation stage. The increased level of LC3B in Nef-ER+scramble NP+4-HT group was probably due to decreased degradation of autophagosomes since Nef blocked the degradation stage of

autophagy. Knocking down the induced Nef decreased the level of LC3B, thereby reactivating the blocked degradation stage and this finding was similar to what was published before that Nef-defective HIV decreased the level of LC3B compared to standard HIV [263]. The induction of Nef contributed to an upregulation in the gene expression of Beclin-1. Previous paper revealed that Nef interacted with LC3B to inhibit the degradation stage of autophagy [263] but we were not sure whether Beclin-1 and LC3B were inherently related. Knocking down Nef reactivated blocked autophagy and promoted the gene expression of VPS 34, TECPR1 and UVRAG but further studies are also required to elaborate the specific interactions between Nef and these autophagy-regulatory proteins for revealing their roles in promoting Nef-blocked autophagy under the circumstance when Nef is knocked down. Knocking down CCR5 somehow contributed to an increased level of autophagic flux but no change was detected in the level of LC3B and the expressions of autophagy regulatory genes. We did not want to jump to the conclusion that CCR5 played a role in autophagy based on current experimental settings because Nef-ER was an in vitro cell model specifically for studying Nef not CCR5. Proper experiments should be dedicated to investigate whether CCR5 played a role in autophagy in the future.

The inhibitory effect on HIV increased over time as cells were repetitively treated with Nef-CCR5 NP probably because higher knockdown efficiencies were achieved. A protease inhibitor atazanavir was used as a control drug to compare the anti-HIV efficiency as previously published [268] and the same concentration was used as well. The combination siRNA NP formulation exerted better anti-HIV effect than atazanavir, possibly because inhibition at two different phases or sites works better than at one single

phase/site, just like the clinical application of highly active antiretroviral therapy that at least three drugs from the same or different categories should be combined together to improve efficacy and reduce drug resistance.

Fluorescence-labeled (e.g. Cy-3) siRNA was readily released from NP at a considerable level in aqueous solutions, thus fluorescent siRNA encapsulated NP should not be used as a model to represent the amount of NP. Therefore, another fluorescence marker coumarin 6 was co-encapsulated with non-labeled siRNA into NP to evaluate the NP release from gel and NP penetration through vaginal epithelium in a vaginal mucosal co-culture model. The use of coumarin 6 in NP as a model system to detect the intracellular amounts of NPs is well documented [269-271]. Coumarin 6 was released from NP at a negligible level in buffers or cell culture media without the addition of surfactant. Therefore, in our case, we believed the fluorescence signal detected could well represent the amount of NP released/penetrated or taken up by cells. The penetration of NP across vaginal epithelial layer seemed to be a rate-limiting step for the intracellular uptake of NP in Sup-T1 cells. In the vaginal mucosal co-culture model, the majority of coumarin 6 NP was taken up by vaginal epithelial cells, which was expected, since epithelial cells encountered NP in the first place and maintained a sufficient interaction with NP. As the NP readily penetrated the epithelial layer, the intracellular uptake of NP started to improve. It took almost two days for Sup-T1 cells to achieve a saturated intracellular accumulation of NP in the lower chamber. Therefore, the vaginal epithelium is not only a barrier for invading pathogens but also a barrier for NP delivery. Currently, there are still no reported techniques to achieve highly efficient NP penetration into vaginal epithelium without disrupting its integrity, thus making it an interesting but challenging field to investigate in the future.

The pH of mouse vagina is known to be neutral due to the lack of lactobacilli [272]. siRNA NP showed a negatively surface charge (about -15 mV) in neutral environment. The surface charge of cells are also negative, therefore, the delivered siRNA NP could be repelled by cells due to electrostatic effects leading to a low level of cell uptake by intravaginal cells. The conjugation of antibody increased the surface charge of the NP close to neutral, thus decreasing the repelling effect. And the strong interaction between antibody and surface receptor helped facilitate improved uptake into intravaginal cells. The exact mechanism of NP penetration through vaginal epithelium is unrevealed but could be potentially attributed to two pathways: paracellular pathway and transcellular pathway. Study has shown that the apical layers of vaginal epithelium do not contain any types of intercellular junctions [273], thus making it possible to allow some particles to transport through the intercellular spaces. However, in the middle and basal layers of epithelium, tight junctions were reported to be present, therefore, making it difficult for NP to use the paracellular pathway. Previous studies have reported that nanocapsules with a size smaller than 300 nm could penetrate the intestinal epithelium via transportation directly through epithelial cells [274]. A study also observed NP transport from mouse vagina to adjacent lymph nodes but whether the transportation is due to transcytosis (a type of transcellular pathway) of epithelial cells or migration of immune cells after NP uptake on the mucosal surface is uncertain [275]. Therefore, it may be possible that NPs could exploit a transcellular pathway, e.g. transcytosis in vagina to achieve deeper penetration through vaginal epithelium.

Chapter 4

Anti-α4β7 monoclonal antibody-conjugated nanoparticles block integrin α4β7 on intravaginal T cells in rhesus macaques as a prophylaxis strategy for the prevention of vaginal transmission of SIV/HIV

Sidi Yang, Geraldine Arrode-Bruses, Ines Frank, Brooke Grasperge, James Blanchard, Agegnehu Gettie, Elena Martinelli, Emmanuel A. Ho

4.1 Abstract

Studies have shown that intravenous administration of anti-α4β7 monoclonal antibody in rhesus macaques (RMs) may prevent the vaginal transmission of simian immunodeficiency virus (SIV) and protect gut associated lymphoid tissues from SIV. Due to potential side effects of systemic administration, development of a vaginal prophylactic strategy against HIV based on the therapeutic potential of anti-a4b7 antibody was investigated. We designed, developed and evaluated a novel dosage form, anti-α4β7 monoclonal antibody-conjugated NP loaded in 1% HEC gel, for the intravaginal delivery of anti-α4β7 monoclonal antibody. The particle size and zeta potential of antibody-conjugated NP were 250.9±3.0 nm and -0.01±0.03 mV in NaH_2PO_4, pH 7.0 and 262.5±4.0 nm and 1.68±0.20 mV in VFS, pH 4.2. A maximum antibody loading of 43.40±0.67μg antibody/mg NP was achieved with an antibody conjugation efficiency of 32.55±0.47%. The vaginal gel formulation blocked more than 75% of total α4β7 in ex vivo vaginal explants within 1 hr of incubation. When intravaginally administered as a single dose in a RM model, the formulation preferentially bound to $\alpha4\beta7^{high}$ CD4+ T cells and $\alpha4\beta7^{high}$ CD3+ T cells in vagina and decreased the percentage of each cell population by approximately 50% respectively without causing any detectable systemic distribution. Multi-dosing regimen should be considered in the future to improve the blocking effect on all T cell population. Overall, we have described a formulation that can be delivered as a potential microbicide for the prevention of HIV transmission.

4.2 Rationale, hypothesis, objectives and scope of this study

Integrins are a group of transmembrane cell adhesion receptors that facilitate cell attachment to extracellular ligands and trigger intracellular signaling pathways [276]. The integrin family consists of 24 heterodimeric proteins and each protein contains α and β subunits that are non-covalently bonded together [276]. Integrin α4β7 is a gut mucosal homing receptor that is responsible for peripheral T cell homing into GALT through the interaction with MAdCAM-1, which is mainly expressed on GALT and intestinal lamina propria [277-279]. α4β7 has been proposed to play an important role in contributing to the pathogenesis of HIV by interacting with gp120 to assist in the attachment of HIV to CD4+ T cells and promote the formation of synapses between virus and cells [280]. Notably, a subset of CD4+ T cells expressing high level of $\alpha4\beta7^{high}$ ($\alpha4\beta7^{high}$ CD4+ T cells) is highly susceptible to HIV-1 infection [281] and the administration of an anti-α4β7 monoclonal antibody (α4β7 Ab) at a dose of 50 mg/kg just before and during RLDC in RMs prevented or delayed vaginal SIV infection and protected the GALT [282]. These findings suggest that α4β7 could be targeted in the female genital mucosa to develop new strategies for the prevention of HIV vaginal transmission.

Notably, a humanized monoclonal antibody with the same antigen-binding region of the anti-α4β7 antibody with protective anti-SIV activity, Entyvio® (Vedolizumab), is a commercially available drug approved by the FDA for the treatment of ulcerative colitis and Crohn's disease [283]. Currently, a clinical trial (NCT02788175) is being conducted to investigate the safety and effectiveness of Vedolizumab in HIV+ patients [284]. As a monoclonal antibody, this medication has to be administered intravenously and closely monitored during infusion. It has been reported that adverse effects may occur including

the common flu-like symptoms (headache, sore throat, nasal congestion, sneezing, chills, fever, body pain, tiredness), skin rash and gastrointestinal upset and some other rare effects like anaphylaxis and elevation of hepatic enzymes [285]. The user-unfriendly administration route and the potential for systemic adverse effects make Vedolizumab an unideal candidate for HIV prophylaxis, prompting our group to develop new formulations for vaginal delivery of the anti-α4β7 monoclonal antibody.

In the previous chapter (Chapter 3), we have developed an antibody-conjugated NP formulation to improve the siRNA delivery to intravaginal tissues. We believe we can expand the application of this formulation to deliver antibodies intravaginally. Ensign et al. have shown that fluorescein delivered via a polystyrene-PEG NP formulation showed better vaginal distribution and retention in estrus mouse than that delivered directly from a gel dosage form [49]. Therefore, delivering anti-α4β7 antibodies conjugated to PLGA-PEG NP can potentially improve therapeutic efficacy compared to antibodies delivered directly from a gel dosage form.

Therefore, in this study, we hypothesized that vaginal gel loading anti-α4β7 antibodies-conjugated-PLGA-PEG NP would be a feasible system to deliver anti-α4β7 antibodies intravaginally and block α4β7 ligands on vaginal cells, as a potential strategy to protect women against vaginal transmission of HIV.

The objective of this study includes (1) Develop and optimize an antibody conjugated PLGA-PEG NP formulation for anti-α4β7 antibodies, (2) Formulate the NP formulation in a vaginal gel dosage form, (3) Evaluate in vitro and in vivo blockage effect of α4β7 by the formulation.

4.3 Materials and Methods

4.3.1 Preparation of vaginal gel loaded with anti-α4β7 monoclonal antibody-conjugated NP

NPs were fabricated with PEI (branched, MW 25 KDa) (Sigma-Aldrich, ON, Canada) and PLGA-PEG (10 KDa-2 KDa) (Advanced Polymeric Materials, Quebec, Canada) by a double emulsion evaporation method reported before [51]. In brief, 150 µL of tris-EDTA buffer was mixed with equal volume of 0.372 mg/mL PEI followed by the addition of 600 µL of 10 mg/mL PLGA-PEG-COOH (dissolved in methylene chloride, HPLC grade, Thermo Fisher, ON, Canada). The mixer was emulsified by sonication for 15 s. After that the primary emulsion was combined with 4.3 mL of 2% PVA and sonicated for another 2 mins. The resulting emulsion was stirred at 4 °C for more than 3 hr to evaporate the organic solvents and harden the particles. And then the NP were collected by centrifugation and washed with double distilled water to remove excess PVA. Approximate 6 mg NP were resuspended in 1.7 mL of 0.1 M MES (Sigma-Aldrich, ON, Canada) buffer (pH 6.0) and the suspension was sonicated on ice for 10-20 s to break down any aggregated chunk. Then 200 µL of 200 mg/mL EDC (G-Biosciences, MO, US) and 100 µL of 275 mg/mL sulfo-NHS (G-Biosciences, MO, US) were added into the suspension. The mixer was stirred at room temperature for 1 hr to activate the carboxyl group, and then the activated NP was collected by centrifugation to remove excess EDC and NHS. After that the NP were resuspended in 0.1 M NaH_2PO_4 buffer (pH 7.4) and anti-α4β7 monoclonal antibody (α4β7 Ab, MassBiologics, MA, USA) was added into the suspension resulting in a final volume of 290 µL. The mixer was stirred at room temperature for 4 hr to facilitate antibody conjugation. Antibody conjugation efficiency

was measured by directly quantifying the antibody on NP using BCA kit (Thermo Fisher, ON, Canada). Finally the NP were collected by centrifugation and loaded into 1% hydroxyethylcellulose (HEC, 250 HX PHARM, Ashland, Kentucky, US) gel, which was prepared by dissolving HEC in 0.1 M NaH_2PO_4 buffer (pH7.4).

4.3.2 Characterization of anti-α4β7 monoclonal antibody-conjugated NP

For measuring the particle size, NP were resuspended in NaH_2PO_4 (pH 7.0), or VFS (pH 4.2) at a concentration of 5 μg/mL. Particle size was determined by DLS using ZetaPALS (Brookhaven Instruments, New York, US) with triplicate tests for 3 runs of 2 mins each. For measuring the zeta potential, NP were resuspended in NaH_2PO_4 (pH 7.0), or VFS (pH 4.2) at a concentration of 12.5 μg/mL. Zeta potential was determined by DLS using ZetaPALS under smulchovski mode. Samples were tested in triplicate for 3 runs of 2 mins each.

4.3.3 Cell culture and in vitro α4β7 antibody-cell binding study of PE-labeled anti-α4β7 monoclonal antibody-conjugated NP loaded in 1% HEC gel

A human lymphoblastoid cell line, RPMI 8866 was purchased from Sigma-Aldrich, (ON, Canada) and maintained in RPMI 1640 containing 2 mM Glutamine (Corning, ON, Canada) + 10% Fetal Bovine Serum (Thermo Fisher, ON, Canada). PE-labeled anti-α4β7 monoclonal antibody was conjugated to NP in order to be detected on cells. On the day of experiment, approximately 3×10^5 cells were seeded onto 24-well plates in 500 μL of culture medium. Cells were then incubated with two different concentrations of 1% HEC gel loaded with anti-α4β7 monoclonal antibody-conjugated NP for 2 hr and 24 hr, respectively. The final concentrations of antibody in each group were approximately

1.15µg/mL and 1.81µg/mL respectively. At the end of incubation, cells were collected and washed with cold PBS and analyzed on flow cytometry (CantoII, BD, ON, Canada) immediately to quantify the percentage of PE+ cells.

4.3.4 Ethics statement

Ten female Indian-origin RMs (Macaca mulatta, RM; mean age: 8.3 years range: 5.8–17 years; mean weight: 8.4 kg range: 5.4–10.65 kg) were used in compliance with the regulations under the Animal Welfare Act, the Guide for the Care and Use of Laboratory Animals, at Tulane National Primate Research Center (TNPRC; LA, US). Animals were socially housed indoors in climate controlled conditions with a 12/12-light/dark cycle.

All the animals in this study were monitored twice daily to ensure their welfare. Any abnormalities, including those of appetite, stool, behavior, were recorded and reported to a veterinarian. The animals were fed with commercially prepared monkey chow twice daily. Supplemental foods were provided in the form of fruit, vegetables, and foraging treats as part of the TNPRC environmental enrichment program. Water was available at all times through an automatic watering system. The TNPRC environmental enrichment program is reviewed and approved by the IACUC semiannually. Veterinarians at the TNPRC Division of Veterinary Medicine have established procedures to minimize pain and distress through several means. RMs were anesthetized with ketamine-HCl (10 mg/kg) or tiletamine/zolazepam (6 mg/kg) prior to all procedures. Preemptive and post procedural analgesia (buprenorphine 0.01 mg/kg) was required for procedures that would likely cause more than momentary pain or distress in humans undergoing the same procedures. The above listed anesthetics and analgesics were used to minimize pain or

distress associated with this study in accordance with the recommendations of the Weatherall Report. All studies were approved by the Animal Care and Use Committee of the TNPRC (OLAW assurance #A4499-01) and in compliance with animal care procedures. TNPRC was accredited by the Association for Assessment and Accreditation of Laboratory Animal Care (AAALAC#000594).

4.3.5 Ex vivo assay on vaginal explants

RM vaginal biopsies were collected and equalized in size using 5 mm skin biopsy punches (Fisher Scientific, MA, US). RM biopsies (5 mm×5 mm; 2 pieces) are transported on ice in L15 medium containing 10% FBS, 100 U/mL penicillin, 100 μg/mL streptomycin. Tissues were extensively washed with PBS and placed into a hole in a 24-well 3 mm pore size and 6.5 mm diameter trans-well insert (Corning, NY, US), with the mucosa facing the upper chamber. The epithelium was surrounded with 3% agarose and the basolateral chamber was filled with DMEM 10% FBS containing 100 Unit/mL penicillin, 100 μg/mL streptomycin and nonessential amino acids. A 1:2 or 1:10 gel dilution (200 μL) was added on top of the tissue in duplicates. Tissues were cultured at 37°C under 5% CO_2 in a humidified incubator for 1 hr. Then tissues were removed from the insert and extensively washed with PBS. For digestion, the washed tissues were cut into small pieces in a petri dish and transferred to a tube containing Collagenase IV HBSS buffer and incubate 40 mins at 37^{o}C on shaking platform. Digested tissues were then passed through a 40-micron cell strainer. Cell suspensions were stained with the viability dye LIVE/DEAD Aqua dye (Molecular probes) before being incubated with a combination of anti-: CD4-APC-H7, CD3-V450 (all BD Bioscience) and α4β7-PE.

Cells were incubated with the antibodies for 20 mins at 4°C, washed and fixed in 2% PFA. Samples were acquired on a BD LSRII Flow Cytometer.

4.3.6 RM treatment

Six RMs were used to test intravaginal administration of NP-α4β7 Ab gel or NP-IgG Ab gel: 3 animals received 3 mL of the A4β7 gel at 1.5 mg/mL (concentration of antibody) and 3 RMs received 3 mL of IgG control at 1.5 mg/mL (concentration of antibody) applied within the vaginal cavity. Samples were collected at baseline (BL, Day-7 before treatment), 4 hr, 24 hr and 72 hr after treatment as indicated in the sampling schematic (Figure 4.1). No depot medroxyprogesterone acetate treatment was used and the menstrual cycle of these RMs were not monitored. Blood and various tissues, including lymph nodes (inguinal) and mucosal tissues (rectal, vaginal and ectocervix) were collected.

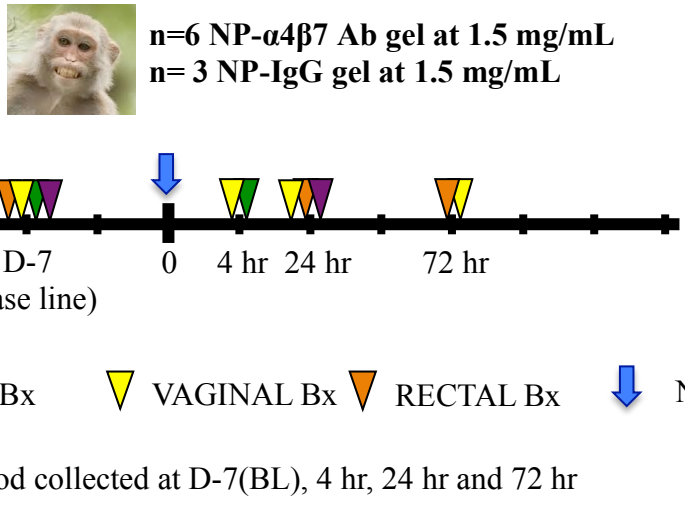

Figure 4.1: Schematic illustrations of the treatment schedule and sampling schedule of RMs. D: Day, Bx: Biopsy

4.3.7 Cell isolation and flow cytometry from in vivo samples

Mucosal tissues were cut into small pieces. Pieces were washed in HBSS with Ca^{2+}/Mg^{2+} and digested 45 mins in HBSS with 1 mg/mL Collagenase IV (Worthington Biochemical) and 1mg/mL of human serum albumin on a shaking platform at 37 °C. Then cell suspension was passed through a 40 μm nylon cell strainer. LNs were cut in small pieces and passed directly through a 40 μm cell strainer. PBMCs were isolated using Ficoll-Hypaque density gradient centrifugation [286].

Cell suspensions were stained with the viability dye LIVE/DEAD Aqua dye (Molecular probes) before being incubated with a combination of anti-CD4-BUV395, anti-CD3-V450, anti-CD95-Percp-Fluor 710 (all BD Bioscience), anti-CD49d (integrin Alpha 4, Novusbio) and anti-α4β7-PE (A4β7 Ab, non-human primate repository, Beth Israel Medical Center, Boston, MA). Cells were incubated with the antibodies for 20 mins at 4°C, washed and fixed in 2% PFA. More than 200,000 events were acquired in the lymphocyte live cell gate using the BD LSRII Flow Cytometer. Data were analyzed with FlowJo 9.9.4.

4.3.8 Statistical analysis

Mann-Whitney test (unpaired, nonparametric, two-sided distribution) was used to compare the statistical significance between NP-IgG gel and NP-α4β7 Ab gel with a confidence level of 95%.

4.4 Results

4.4.1 Particle size and zeta potential

The average particle size for NP-α4β7 Ab was found to be within the range of 200-300 nm and antibody conjugation did not significantly increase the particle size compared to NP (Table 4.1 and 4.2). Previous studies have reported that the vaginal pH in RMs was approximately 6–7, due to the lack of lactobacilli in the vaginal flora, while the vaginal pH of human females was reported to be around 3.5-4.7 due to the massive presence of lactobacilli [287]. Therefore, the NP was characterized in two different types of medium, which mimic the vaginal environment of RMs and human, respectively. Particle size was measured in NaH_2PO_4, pH 7.0 or VFS, pH 4.2 respectively, which mimics the vaginal environment of RM and human, since there is no published recipe for preparing RM vaginal fluid simulant, a simple solution of neutral pH was used instead. Zeta potential was augmented from negative to neutral after antibody conjugation.

Table 4.1: Particle size and zeta potential in different media, Values represent mean ± SD, n=3.

	NaH_2PO_4, pH 7.0			VFS, pH 4.2		
	Size (nm)	PDI	Zeta Potential (mV)	Size (nm)	PDI	Zeta Potential (mV)
NP	231.6±15.0	0.254	-7.29±1.87	232.8±6.8	0.247	1.22±1.14
NP-α4β7 Ab	250.9±3.0	0.328	-0.01±0.03	262.5±4.0	0.167	1.68±0.20

4.4.2 Antibody conjugation efficiency and antibody loading

Antibody conjugation efficiency (ACE) and antibody loading of NP are shown in Table 4.2. The antibody conjugation efficiency decreased as the input concentrations of α4β7 antibody increased, resulting in an antibody conjugation efficiency of 45.73±1.08%, 32.55±0.47% and 12.33±0.22%, respectively. However, the antibody loading (μg Ab/mg NP) increased as the as the input concentrations of α4β7 antibody increased with a maximum loading capacity of 43.40±0.67μg/mg NP within the experimental range. In order to achieve a high density of antibody conjugation on the surface of NPs, 1.4 mg/mL was used for downstream studies.

Table 4.2: ACE% and antibody loading, Values represent mean ± SD, n=3.

Concentration of α4β7 Ab (mg/mL)	ACE (%)	Ab loading (μg Ab/mg NP)
0.7	45.73±1.08	30.49±0.72
1.4	32.55±0.47	43.40±0.67
3.4	12.33±0.22	41.08±0.72

4.4.3 In vitro α4β7 antibody-cell binding study of 1% HEC gel loaded with PE-labeled anti-α4β7 monoclonal antibody-conjugated NP

Next, we evaluated whether conjugating antibody to NP and loading the NP-α4β7 into a vaginal gel would affect the binding affinity of antibody. An in vitro study comparing the antibody binding efficiency of free antibody and anti-α4β7 monoclonal antibody-conjugated NP loaded in 1% HEC gel using a cell line

expressing high level of α4β7 was conducted. In order to detect the amount of antibody bound onto the surface of cells, PE-labeled anti-α4β7 monoclonal antibody was conjugated to NP during preparation. Formulations with two different antibody concentrations of conjugation (low and high) were used to treat cells at the same NP concentration. The final concentrations of antibody conjugated to NPs were 1.15 mg/mL and 1.81 mg/mL, respectively. Cells were incubated with formulations for 2 hr and 24 hr and analyzed immediately for the amount of antibody bound onto the surface. Results showed that after 2 hr of incubation, more than 85% of cells were detected to be PE+ in the group treated with low antibody loading formulation while this value was augmented to more than 90% after 24 hr of incubation and the PE+ population at this point was as high as that in the group incubated with the same concentration of free antibody (Figure 4.2). Similar results also appeared in the group treated with high antibody loading formulation and maximum binding could be achieved within as short as 2 hr and this effect was also maintained until the 24 hr time point (Figure 4.2).

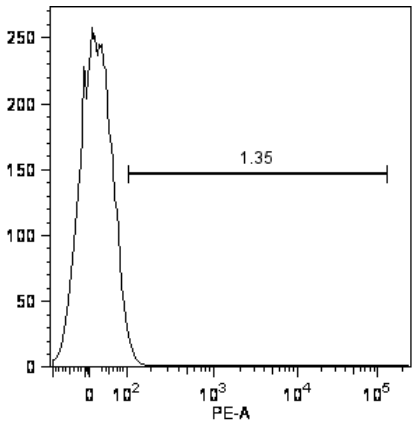

Unstained Control

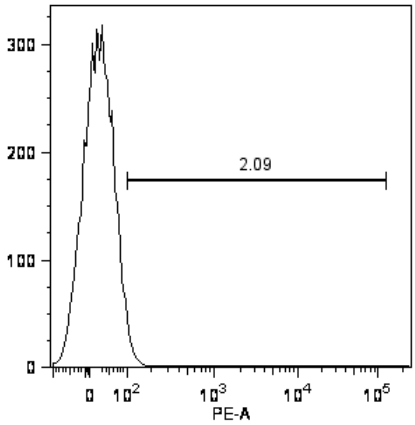

NPs-IgG Gel

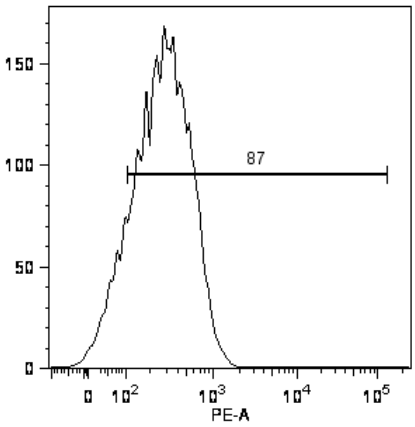

NPs-α4β7 Ab Gel_2 hr
(C_{Ab}=1.15 μg/mL)

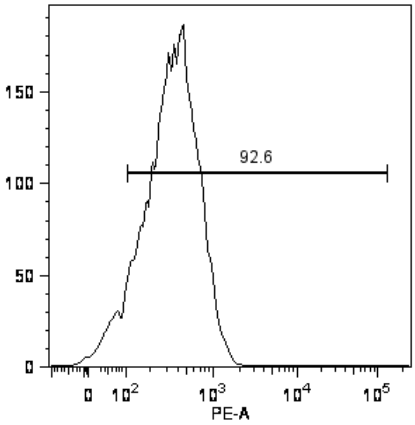

NPs-α4β7 Ab Gel_2 hr
(C_{Ab}=1.81 μg/mL)

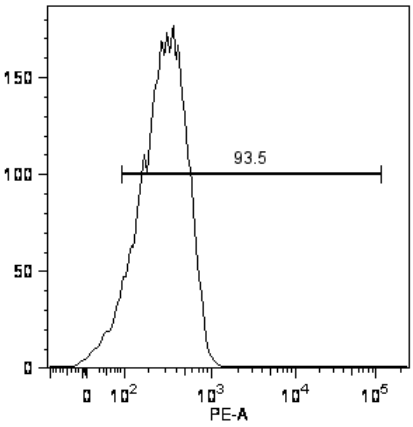

NPs-α4β7 Ab Gel_24 hr
(C_{Ab}=1.15 μg/mL)

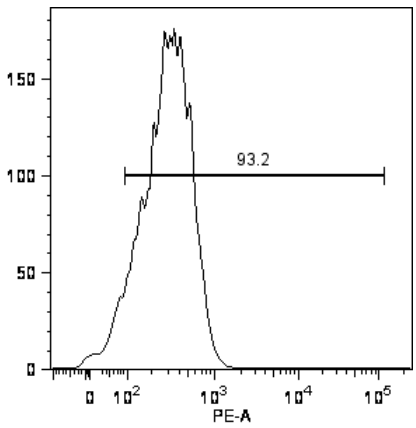

NPs-α4β7 Ab Gel_24 hr
(C_{Ab}=1.81 μg/mL)

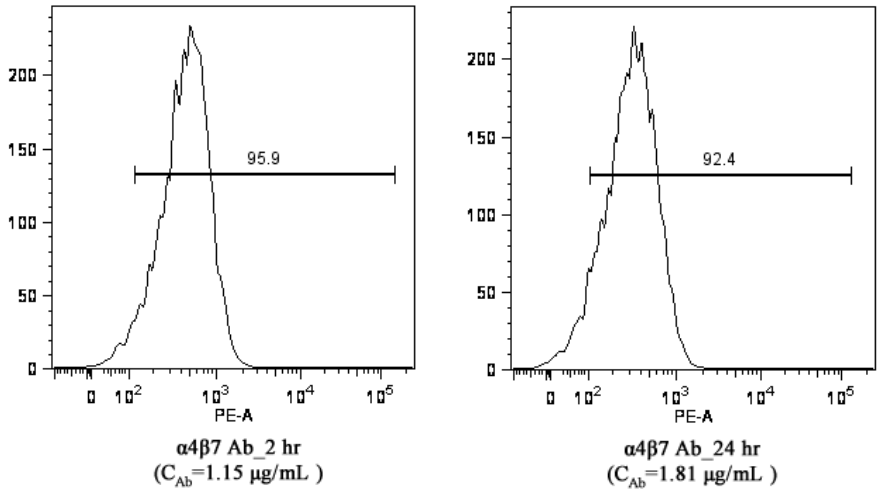

Figure 4.2: In vitro α4β7 antibody-cell binding study of 1% HEC gel loaded with PE-labeled anti-α4β7 monoclonal antibody-conjugated NPs. Data shows representative histograms from a measurement of n=3.

4.4.4 Ex vivo blockage of α4β7 on cells of vaginal explants by 1% HEC gel loaded with anti-α4β7 monoclonal antibody-conjugated NP

After confirming the binding affinity of the anti-α4β7 monoclonal antibody conjugated to NP and formulated into a gel dosage form, we evaluated the formulation in an ex vivo RM vaginal explant model. Formulations with the same antibody loading (mention again the loading) were used to treat ex vivo vaginal explant tissues at two different dilutions (1: 2 and 1: 10, corresponding to 1.5 mg/mL and 0.3 mg/mL of NP-conjugated antibody) to compare the blockage of α4β7 from the vaginal explant. After 1 hr incubation, the explant was removed and digested into single cell suspension. The cell suspension was stained with PE-labeled anti-α4β7 monoclonal antibody to identify extracellular α4β7 that was not blocked by the formulation. Compared to NP-IgG gel, NP-α4β7 gel could block more than 75% of α4β7 in the tissue at a dilution of 1:2 after only 1 hr incubation while the blockage efficacy at a

dilution of 1:10 was slightly lower, but it could still block more than 65% of α4β7 (Figure 4.3).

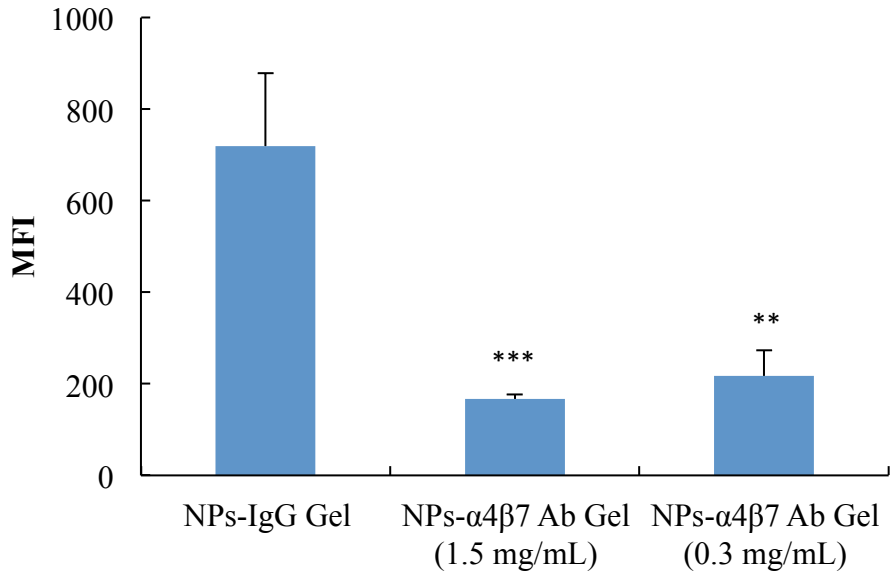

Figure 4.3: Ex vivo blockage of α4β7 on cells of vaginal explants by 1% HEC gel loaded with NP-α4β7 at two different antibody concentrations (1.5 mg/mL and 0.3 mg/mL). 1% HEC gel loaded with NP-IgG was used as control. MFI: mean fluorescence intensity. Values represent mean ± SD, n=3. ***$p<0.001$ and **$p<0.01$ compared to NP-IgG Gel.

4.4.5 In vivo blockage of α4β7 in RM by 1% HEC gel loaded with anti-α4β7 monoclonal antibody-conjugated NP

Finally, we used a RM model to evaluate the in vivo blockage ability of anti-α4β7 monoclonal antibody-conjugated NP loaded in 1% HEC gel upon a single intravaginal administration. We primarily focused on the blockage of α4β7 in vaginal tissues but other sites including peripheral blood mononuclear cells (PBMC), rectum, inguinal lymph nodes and ectocervix were also analyzed in order to evaluate if the antibody had spread

systemically. Our results indicated that the vagina was the only site where decreased level of α4β7 was detected. Basically, the treatment of NP- α4β7 Ab gel decreased the percentage of $\alpha_4\beta_7^{high}$ CD4+ T cells by half 72 hr after intravaginal application (Figure 4.4A) but the percentage of α4β7+ CD4+ T cells remained unchanged at all time points (Figure 4.4B). Similarly, the percentage of $\alpha4\beta7^{high}$ CD3+ T cells was also reduced by approximately 50% 72 hr post treatment (Figure 4.4C), while the percentage of $\alpha_4\beta_7$+ CD3+ T cells (Figure 4.4D) was not significantly decreased. The α4β7 blocking effect of was only restricted to the vagina because no decrease in the percentage of $\alpha_4\beta_7^{high}$ CD4+ T cells or $\alpha_4\beta_7$+ CD4+ T cells was detected in PBMC (Figure 4.4 E-F), rectum (Figure 4.4 G-H) or inguinal lymph nodes (Figure I-J) over the period of 72 hr after intravaginal administration. Furthermore, the blocking effect of a single dose treatment did not cover the ectocervix either since the percentage of $\alpha_4\beta_7^{high}$ CD4+ T cells, $\alpha_4\beta_7$+ CD4+ T cells, $\alpha4\beta7^{high}$ CD3+ T cells or $\alpha_4\beta_7$+ CD3+ T cells was not significantly reduced (Figure 4.4 G-N).

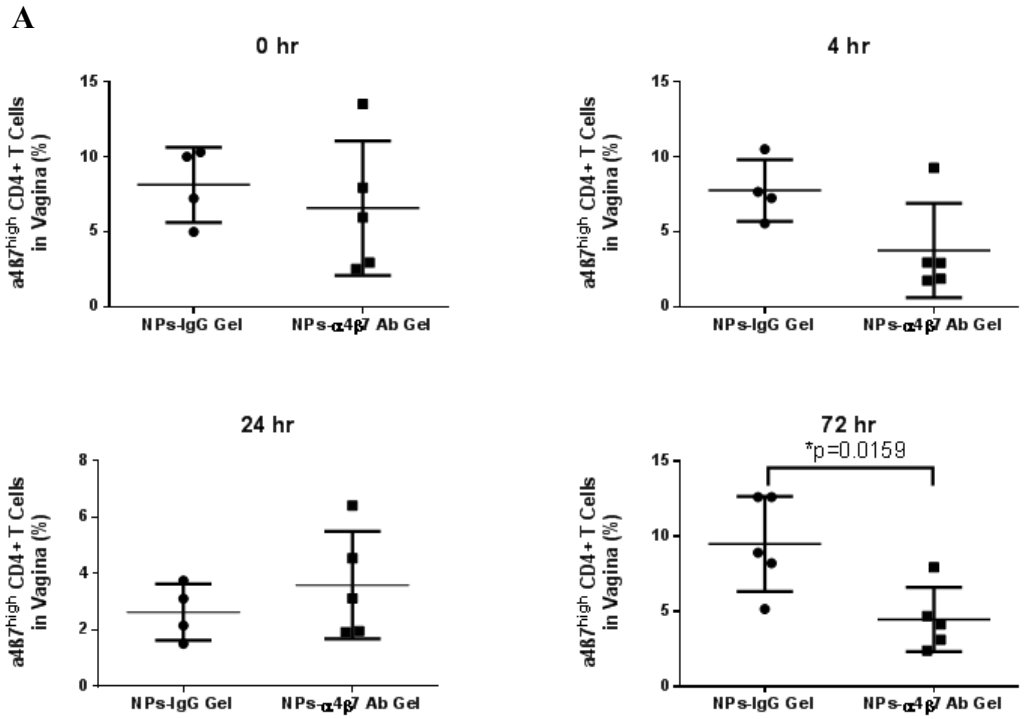
A
0 hr
4 hr
24 hr
72 hr
*p=0.0159
α4β7high CD4+ T Cells in Vagina (%)
NPs-IgG Gel
NPs-α4β7 Ab Gel

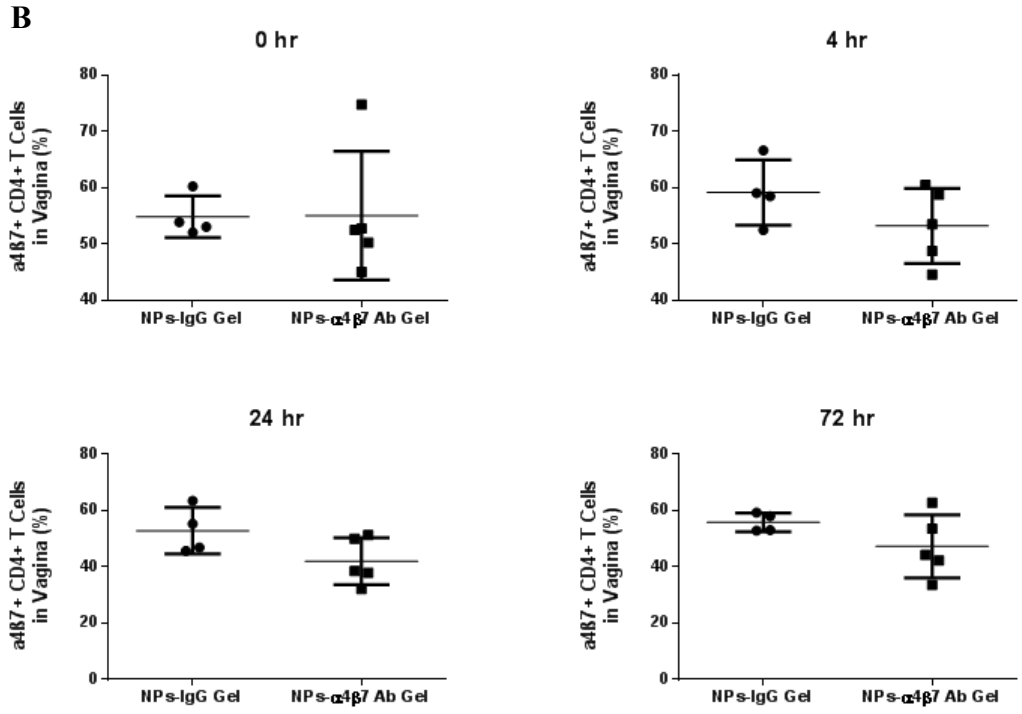
B
0 hr
4 hr
24 hr
72 hr
α4β7+ CD4+ T Cells in Vagina (%)
NPs-IgG Gel
NPs-α4β7 Ab Gel

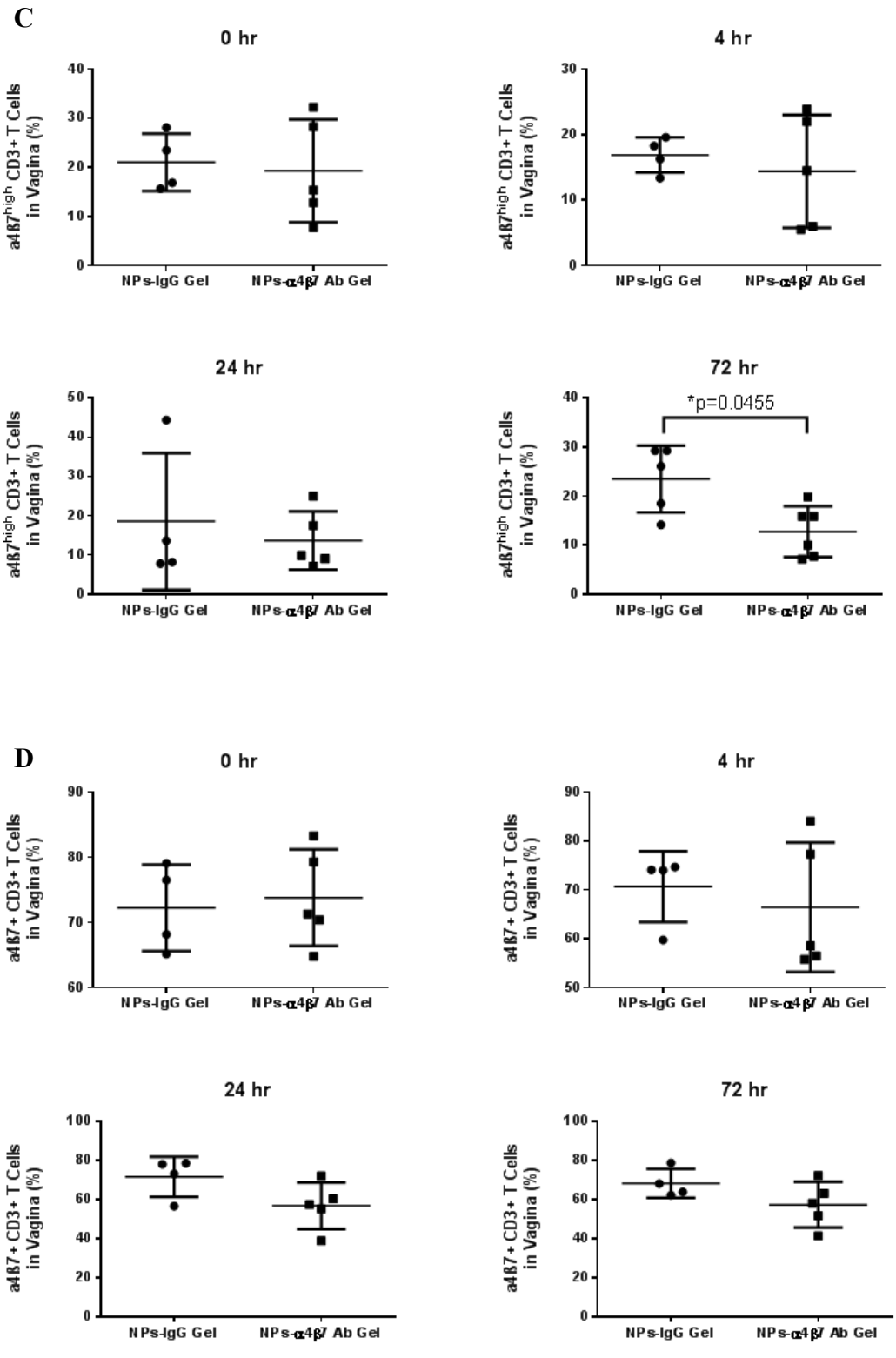
C
0 hr
4 hr
24 hr
72 hr
*p=0.0455
a4β7high CD3+ T Cells in Vagina (%)
NPs-IgG Gel
NPs-α4β7 Ab Gel
D
0 hr
4 hr
24 hr
72 hr
a4β7+ CD3+ T Cells in Vagina (%)
NPs-IgG Gel
NPs-α4β7 Ab Gel

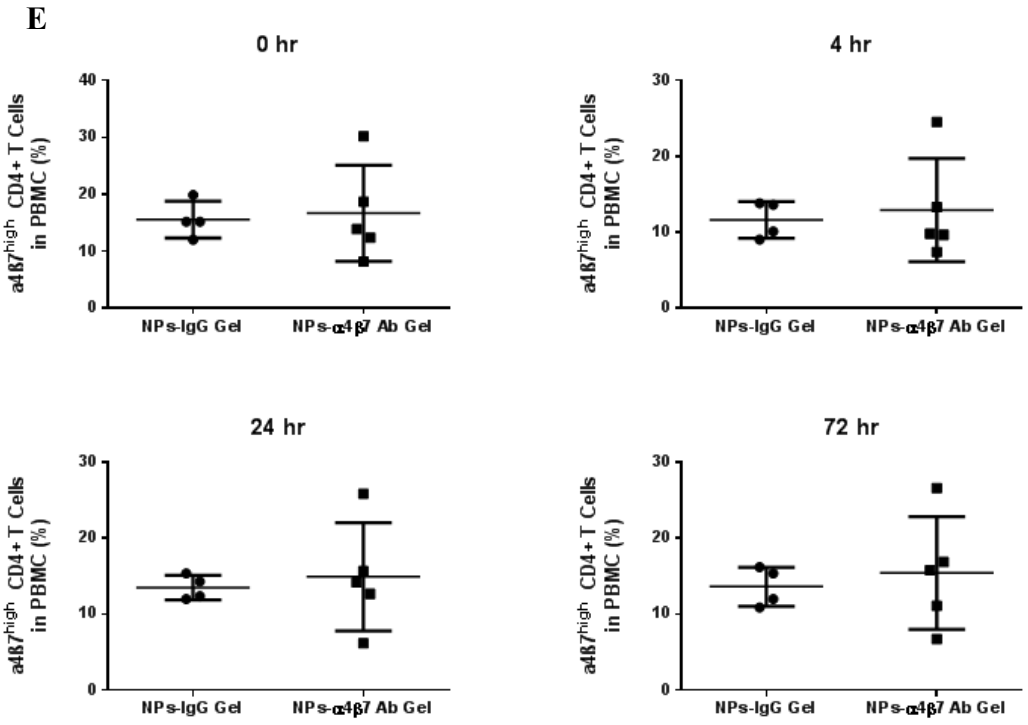
E
0 hr
4 hr
24 hr
72 hr
α4β7high CD4+ T Cells in PBMC (%)
NPs-IgG Gel
NPs-α4β7 Ab Gel

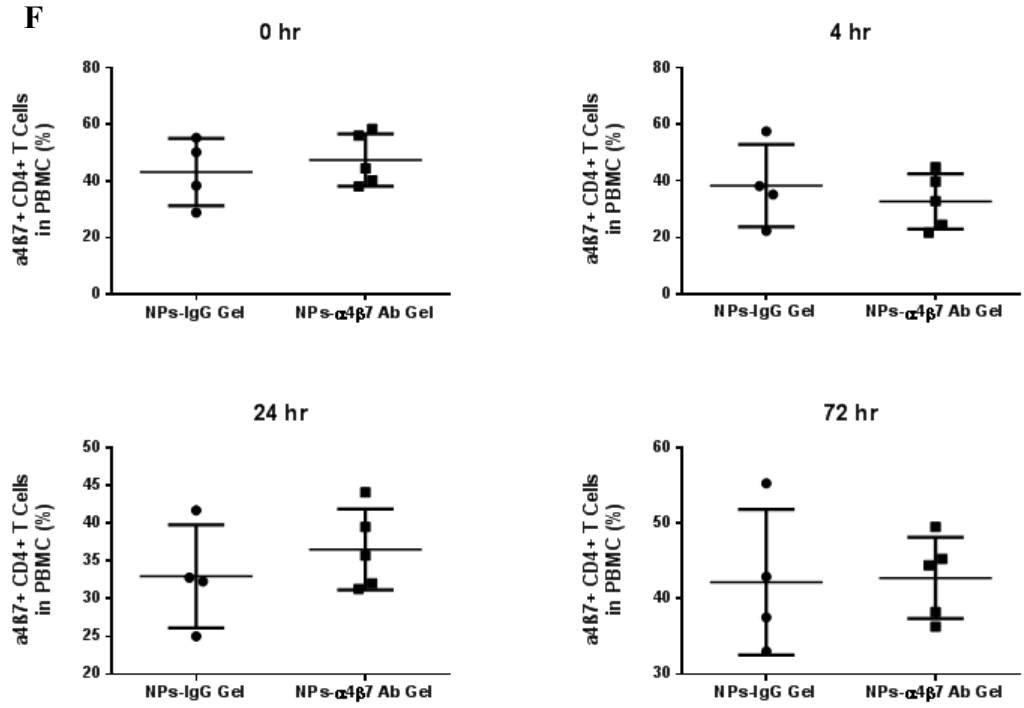
F
0 hr
4 hr
24 hr
72 hr
α4β7+ CD4+ T Cells in PBMC (%)
NPs-IgG Gel
NPs-α4β7 Ab Gel

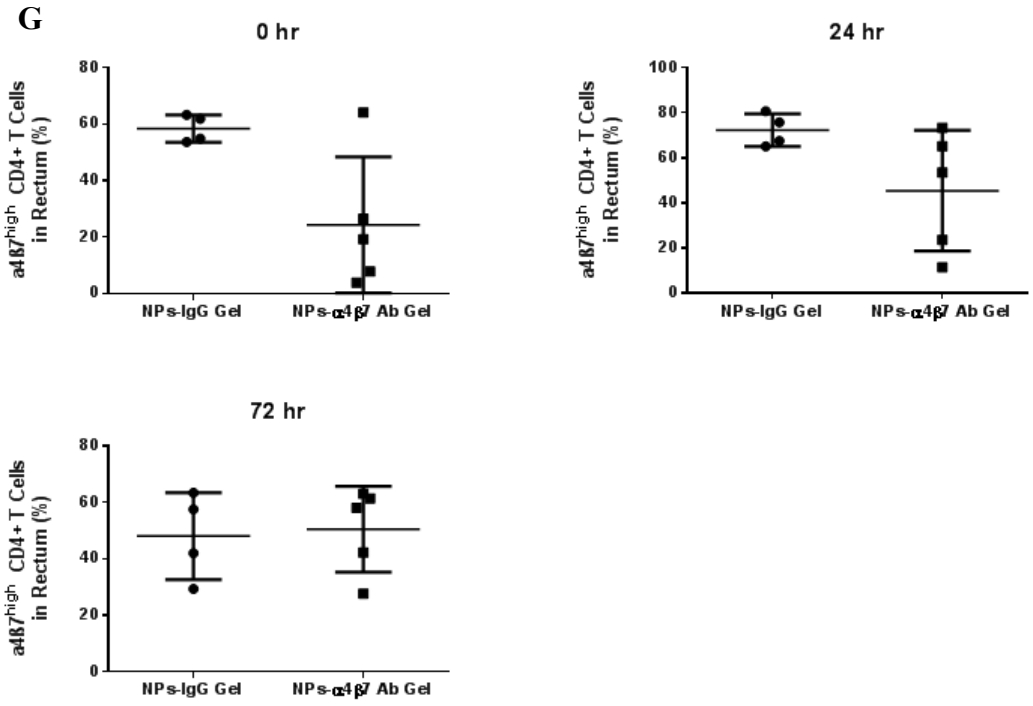
G
0 hr
24 hr
72 hr
α4β7high CD4+ T Cells in Rectum (%)
NPs-IgG Gel
NPs-α4β7 Ab Gel

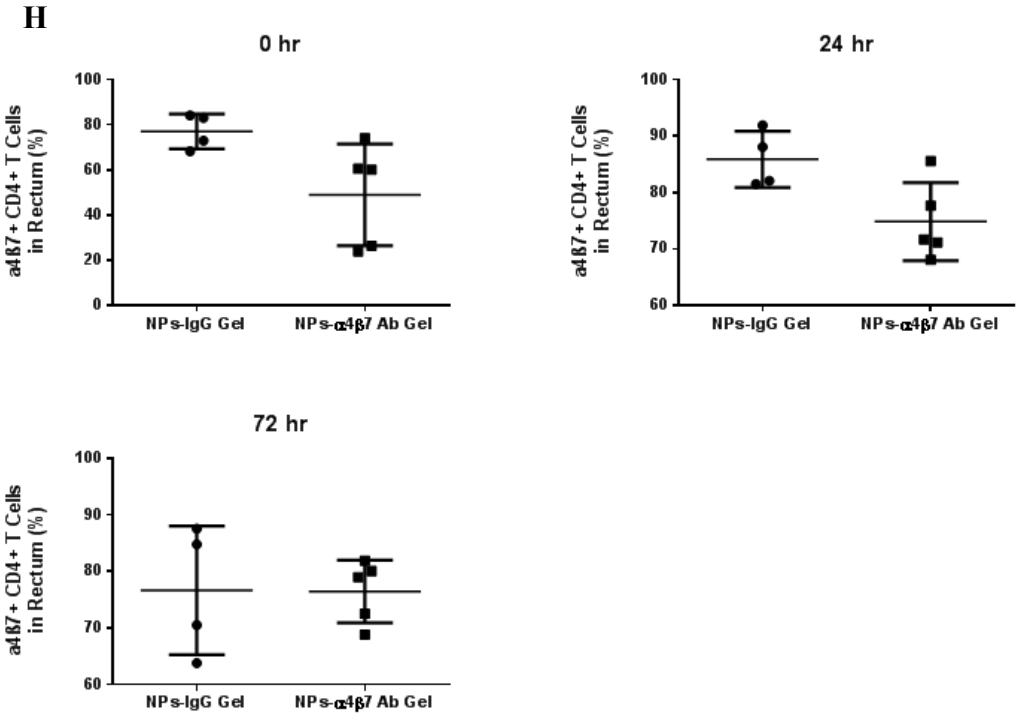
H
0 hr
24 hr
72 hr
α4β7+ CD4+ T Cells in Rectum (%)
NPs-IgG Gel
NPs-α4β7 Ab Gel

I

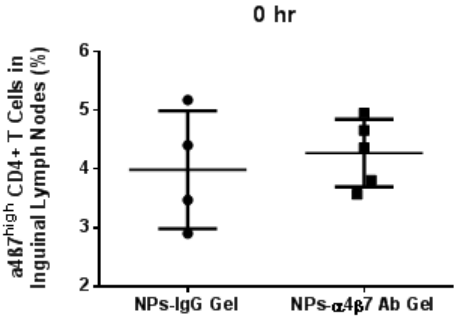
0 hr
α4β7high CD4+ T Cells in Inguinal Lymph Nodes (%)
6
5
4
3
2
NPs-IgG Gel
NPs-α4β7 Ab Gel

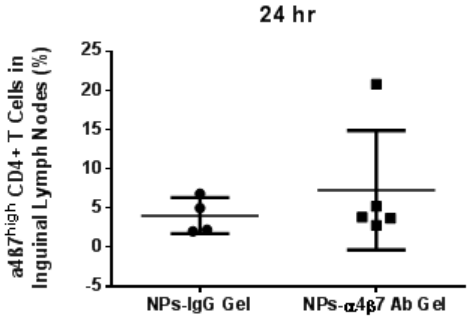
24 hr
α4β7high CD4+ T Cells in Inguinal Lymph Nodes (%)
25
20
15
10
5
0
-5
NPs-IgG Gel
NPs-α4β7 Ab Gel

J

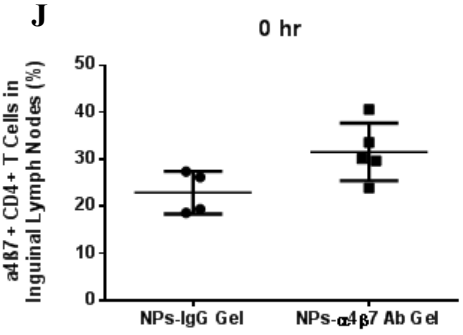
0 hr
α4β7+ CD4+ T Cells in Inguinal Lymph Nodes (%)
50
40
30
20
10
0
NPs-IgG Gel
NPs-α4β7 Ab Gel

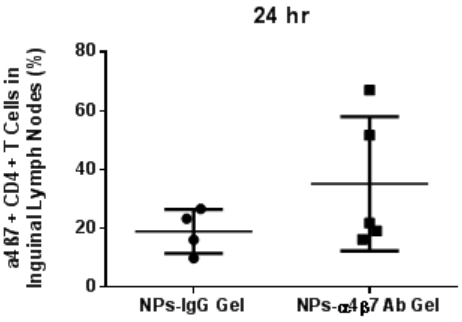
24 hr
α4β7+ CD4+ T Cells in Inguinal Lymph Nodes (%)
80
60
40
20
0
NPs-IgG Gel
NPs-α4β7 Ab Gel

K

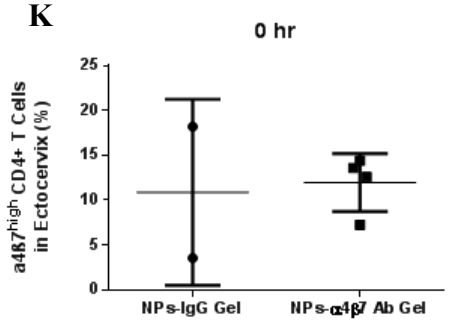
0 hr
α4β7high CD4+ T Cells in Ectocervix (%)
25
20
15
10
5
0
NPs-IgG Gel
NPs-α4β7 Ab Gel

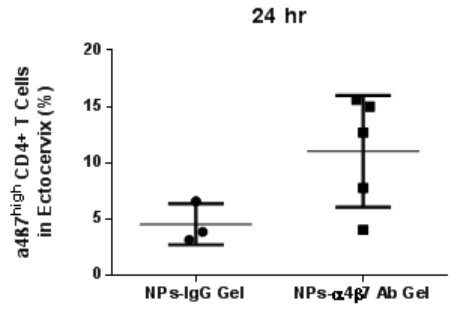
24 hr
α4β7high CD4+ T Cells in Ectocervix (%)
20
15
10
5
0
NPs-IgG Gel
NPs-α4β7 Ab Gel

L

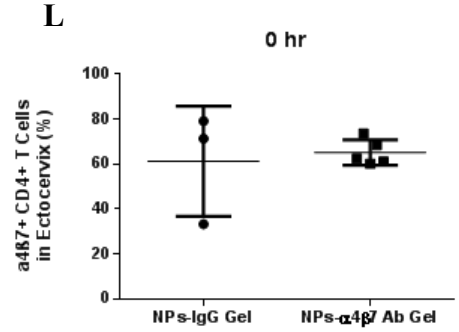
0 hr
α4β7+ CD4+ T Cells in Ectocervix (%)
100
80
60
40
20
0
NPs-IgG Gel
NPs-α4β7 Ab Gel

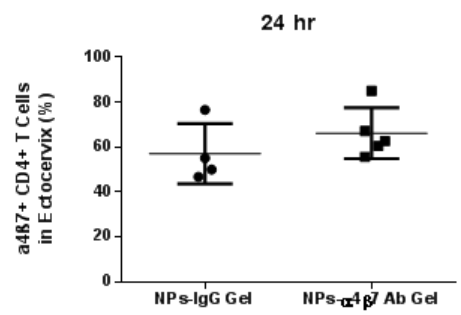
24 hr
α4β7+ CD4+ T Cells in Ectocervix (%)
100
80
60
40
20
0
NPs-IgG Gel
NPs-α4β7 Ab Gel

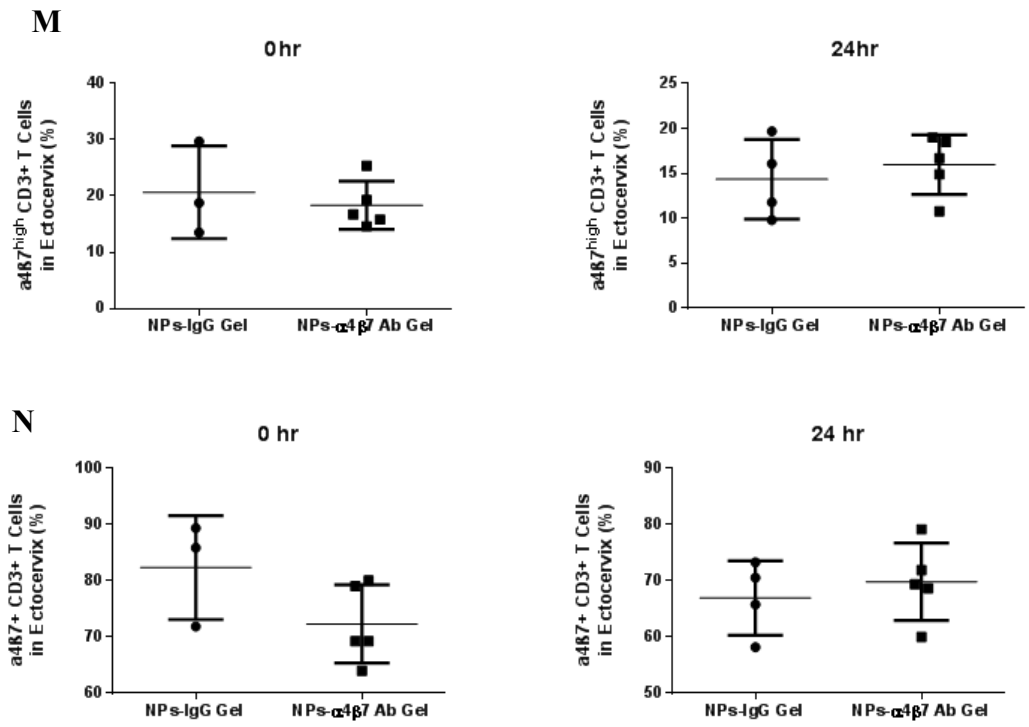

Figure 4.4: In vivo blockage of α4β7 on tissues (A-D: vaginal tissues, E-F: PBMC, G-H: rectal tissues, I-J: inguinal lymph nodes, K-N: ectocervix) from RMs by 1% HEC gel loaded with anti-α4β7 monoclonal antibody-conjugated NP in a RM model. Values represent mean ± SD, n=3 or 6. *$p<0.05$ compared to NPs-IgG gel.

4.5 Discussion

FGT is a complex environment that can influence intravaginal drug delivery [288]. The vaginal tract is covered by a thin layer of mucus that serves as a barrier to prevent the vaginal tract from external invading pathogens, while also limiting drug penetration [288]. Even though the mesh pore size of mucin network is 50-1800 nm, the optimal size of nonadhesive particles that can penetrate mucus is 200-500 nm [80]. Larger particles (>1000 nm) are trapped in the superficial layer of cervicovaginal mucus and smaller particles (~100 nm) present higher hindrance than larger ones due to the heterogeneous

structure of mucus. Those smaller particles always penetrate into smaller tortuous channels that are accompanied with dead-ends and never come out [80]. The modification of polymer with low molecular weight of PEG (~2 KDa) is the most widely accepted method for fabricating non-adhesive particles [69]. Therefore, in our study we employed PLGA-PEG (10 KDa-2 KDa) to prepare NPs for enhanced mucus penetration ability. Moreover, a close-to-neutral zeta potential (-10 mV to 10 mV) also helps improve mucus penetration [49]. The particle size after antibody conjugation is still located in the optimal range for mucus penetration and the surface charge is enhanced to neutral (around 0 mV), indicating the potential enhanced mucus penetration ability of antibody-conjugated NPs.

Increased concentration of antibody enhanced the interaction between activated NP and antibody, resulting in improved amount of antibody conjugated onto the surface of NP. However, as the concentration of antibody increased, the surface of NP that could react with antibody started to approach to saturation, causing decreased conjugation efficiency. Here we have shown that the conjugation of anti-α4β7 antibody to NP and formulation into a gel dosage form does not alter its binding affinity to α4β7. PE-labeled anti-α4β7 monoclonal antibody-conjugated NP loaded in 1% HEC gel showed the same binding efficiency as free antibody in vitro using RPMI 8866 expressing high level of α4β7. The percentage of PE+ cells did not reach 100% in either case probably because a small percentage of the antibody was continuously taken up into the cells. In the ex vivo vaginal explant model, more than 75% of α4β7 in vaginal tissues could be blocked by the anti-α4β7 monoclonal antibody-conjugated NP loaded in 1% HEC gel within 1 hr, indicating a rapid and good blocking ability of the conjugated antibody. The percentage of α4β7 blocked on cells from vaginal explant tissue did not reach 100% possibly because 1) the

formulation could not completely penetrate into the basal layer of intraepithelium due to the tight junction of the intravaginal epithelium, or 2) the formulation has limited ability in blocking cells from explant which express low level of α4β7.

With regards to the in vivo evaluation of the formulation, the anti-α4β7 monoclonal antibody-conjugated NP loaded in 1% HEC gel preferentially bound to $\alpha_4\beta_7^{high}$ CD4+ T cells (the cell population highly susceptible to HIV infection) or $\alpha4\beta7^{high}$ CD3+ T cell in the vagina with a significant blocking effect 72 hr post treatment. The blocking effect was much delayed compared to ex vivo study probably because live tissues in vivo could maintain a higher level of tissue integrity than ex vivo explant therefore it took more time for the antibody-conjugated NPs to penetrate the intraepithelium and the time for penetrating the mucus in vivo had also to be taken into account. We observed a lower blocking efficiency of α4β7 in vivo compared to ex vivo, probably due to the continuous clearance effect on the formulation by cervicovaginal mucus. Lower amount of antibody conjugated NPs reached the RM intraepithelium, thus lower blocking efficiency was observed. And the cervix did not present a significant blockage of α4β7, which could also be attributed to the clearance effect of cervicovaginal mucus. Even though the cell population that is highly susceptible to HIV infection ($\alpha_4\beta_7^{high}$ CD4+ T cells) can be significantly and preferentially decreased, other T cells expressing low level of $\alpha_4\beta_7$ are still under the risk for infection. Therefore, we believe a single dose was not enough to block α4β7 entirely especially presenting an insufficient blockage of $\alpha_4\beta_7^{low}$ T cells and cervix so a multi-dosing regimen should be considered in the future in order to achieve optimal blocking effect. Moreover, the effects of the formulation were only restricted to

the vaginal tract where the transmission of HIV is taking place and systemic side effects are expected to be reduced.

Chapter 5

Autophagy induction and PDGFR-β knockdown by siRNA-PEI encapsulated nanoparticles reduce chlamydia trachomatis infection

Sidi Yang, Celine Jimenez, and Emmanuel A. Ho

5.1 Abstract

C. trachomatis is the most common sexually transmitted bacterial infection in the world. Although the infection can be easily controlled by the use of antibiotics, several reports of clinical isolates that are resistant to antibiotics have prompted us to search for alternative strategies to manage this disease. In this paper, we developed a nanoparticle formulation (PDGFR-β siRNA-PEI-PLGA-PEG NP) that can simultaneously induce autophagy in human cells and knock down PDGFR-β gene expression, an important surface binding protein for C. trachomatis, as a strategy to reduce vaginal infection of C. trachomatis. PDGFR-β siRNA-PEI-PLGA-PEG NP significantly induced autophagy in human vaginal epithelial cells (VK2/E6E7) 48 hr post treatment by improving autophagic degradation activity without causing inflammation, apoptosis or any decrease in cell viability. Beclin-1, VPS34 (markers for initiation stage of autophagy), UVRAG, TECPR-1 (markers for degradation stage of autophagy) were found to be significantly upregulated after treatment with PDGFR-β siRNA-PEI-PLGA-PEG NP. Furthermore, PDGFR-β siRNA-PEI-PLGA-PEG NP decreased PDGFR-β mRNA expression by 50% and protein expression by 43% in VK2/E6E7 cells 48 hr post treatment. Treatment of cells with PDGFR-β siRNA-PEI-PLGA-PEG NP significantly decreased the intracellular C. trachomatis by approximately 63% in vitro by augmenting autophagic degradation pathway and reducing bacterial binding simultaneously.

5.2 Rationale, hypothesis, objectives and scope of the study

C. trachomatis is a gram-negative bacterium that preferentially infects epithelial cells of the genital tract and causes the most common sexually transmitted bacterial infection in the world [28]. Unfortunately, about 80% of chlamydial infections in women are asymptomatic or with minimal symptoms, but if left untreated, the infection can lead to pelvic inflammatory disease, tubal infertility, ectopic pregnancy, premature delivery, and increased risk of developing cervical carcinoma. Furthermore, chlamydia infection can be passed to exposed newborns during birth resulting in conjunctivitis and possibly interstitial pneumonia [43]. The infection can also affect men, but it usually appears symptomatic and manifests as urethritis, and if left untreated, the infection can lead to epididymitis and proctitis [28].

C. trachomatis is an obligate intracellular bacterium with two distinct forms, the infectious EB and the replicative RB during its life cycle. Pathogenesis of chlamydia infection in the female genital tract begins with initial binding of EB to genital epithelial cells, and is followed by contiguous endocytosis through a membrane-bound compartment, inclusion [35]. After internalization, inclusion helps EB to rapidly escape the host endo-lysosomal pathway to avoid being degraded by the host defense system. At the same time, EB accomplishes the transformation into RB and begins to initiate bacterial protein synthesis. Newly synthesized inclusion membrane proteins assist the replication of RB by collecting and supplying nutrients from the host's golgi [35]. As RB propagates and accumulates, the life cycle enters the late phase, in which last-phase effectors and EB effectors are being synthesized and the differentiation of new EB from RB is accomplished shortly afterwards. Eventually, newly produced EB leaves the host

cells via extrusion (a process where a cell exports large particles or organelles through its cell membrane to the outside) or lysis to establish future infections [35].

C. trachomatis is found to be able to infect various cell types in vitro and uses several receptors for binding to the host cells [289]. Initial binding of chlamydia starts with a primary reversible electrostatic interaction between EB and the host cell's heparan sulfate receptor, followed by an irreversible secondary binding to other possible receptors such as the PDGFR-β [290]. Elwell et al. has shown that PDGFR-β knockdown with RNA interference decreased cell-associated bacteria by 50%. PDGFR plays an important role in vascular development and a mouse model has indicated that deletion of PDGFR-α or PDGFR-β causes no vascular defects but deletion of both disrupted the vascular development in yolk sac [291]. Further studies reported that an FDA-approved PDGFR inhibitor, imatinib, for the treatment of Philadelphia chromosome-positive chronic myelogenous leukemia and gastrointestinal stromal tumors demonstrated minor adverse effects [292]. Therefore, knocking down PDGFR-β alone as a local therapy is expected to have negligible side effects. As a result, PDGFR-β can be potentially utilized as a therapeutic target to prevent and minimize chlamydia infection of host cells [290].

Autophagy is a self-degradative process for providing energy under stressed conditions, degrading and recycling long-lived proteins and damaged organelles as well as playing an important role in eliminating intracellular pathogens (i.e. viruses and bacteria) [250]. Autophagy has been divided into three types: macroautophagy, microautophagy and chaperone-mediated autophagy. Among the three types, macroautophagy appears to play an important role in protecting cells against microbial infection [251]. Macroautophagy is composed of two subsequent stages, the initiation stage and the degradation stage [251].

During the initiation stage, a membrane called phagophore is invaginated from cell membranes and elongated to sequester components targeted for degradation, forming an enclosed double-membrane vesicle called autophagosome. This stage is subsequently followed by the degradation stage, during which the autophagosomes will then fuse with the acidic, enzyme-enriched lysosome, forming the degradative vesicle, autolysosome. During the fusion, only the outer layer of the double membrane of autophagosome fuses with lysosome while the inner layer becomes degraded, resulting in a single-membrane autolysosome. After that, the components inside of the autolysosomes are degraded into amino acids, fatty acids, nucleic acids and so forth for recycle and reuse [250]. Detecting and identifying the bacterial components that are attached to or inside of the cytoplasm of mammalian cells is a key process for initiating macroautophagy. Recognition of bacterial lipopolysaccharide by toll-like receptor 4 [252], detection of bacterial peptidoglycan by NOD-like receptors [253] as well as the identification of intracellular bacteria by sequestosome-1-like receptors [254] are identified pathways for the initiation of autophagy in the defense against bacterial infection. Various regulatory proteins (e.g. Beclin-1 and VPS 34) [255, 256] are synthesized and recruited to initiate the nucleation of the phagophore, and as the phagophore elongates and grows into a complete autophagosome, a protein called LC3B starts to be synthesized from its precursor LC3A and becomes localized on autophagosomes [255]. As autophagy proceeds, autophagosomes begin to fuse with lysosomes and mature into degradative autolysosomes with LC3B internalized. At the same time, other regulatory proteins (e.g. TECPR-1 and UVRAG) [256, 257] are synthesized and recruited to promote the maturation of autolysosomes. Eventually, the pathogens as well as LC3B are degraded in autolysosomes by the enzymes and substances delivered from lysosomes. As a result,

autophagy can be considered as an innate immune response against bacterial infection and studies have shown that autophagy can restrict intracellular growth of many bacteria such as streptococcus A [293], mycobacterium tuberculosis [294], listeria monocytogenes [295] , and C. trachomatis [296].

Although chlamydial infection can be easily managed by macrolides or tetracyclines, the constant recurrence, the potential to develop antibiotic resistance [37], the safety of antibiotic use during pregnancy [38-40] and the common systemic side effects of antibiotics [41, 42] are always problems and concerns encountered in the healthcare setting. In an effort to control the prevalence of chlamydia, various screening programs have been established in different countries around the world. However, new cases and recurrent cases still pose a challenge in disease control [43]. Therefore, a safe non-antibiotic based therapy needs to be developed to provide alternative treatment choices for physicians and patients. C. trachomatis primarily targets epithelial cells as the first step to establish genital infection and forms inclusions to escape the endo-lysosomal degradation pathway. These two conditions predispose the genital epithelial cells with higher vulnerability to C. trachomatis compared to other immune cells in the genital tract. As a result, a therapy that can reduce bacterial binding to epithelial cells and induce autophagy in infected epithelial cells for the elimination of intracellular bacteria would be beneficial for combating the infection.

The use of siRNA as a gene therapy to combat sexually transmitted infections has gained a lot of success during the past decade [288, 297-299]. As a result, we proposed a novel combination therapy involving the application of a siRNA-PEI-encapsulated NP fabricated with PLGA-PEG (siRNA-PEI-PLGA-PEG NP) for the knock down of

PDGFR-β expression and the simultaneous induction of autophagy as a strategy to prevent/reduce sexually transmitted chlamydia infection in women. This therapy can help prevent/reduce the acquisition and recurrence of chlamydia infection when used topically in the vagina prior to sexual intercourse. Knocking down PDGFR-β will prevent/reduce chlamydia entry into target host cells and inducing autophagy by encapsulating a cationic polymer PEI will help degrade the intracellular pathogens that have already invaded as mentioned above. This topical siRNA-based therapy will work locally to minimize the systemic side effects such as those caused by oral administration of antibiotics and the use of siRNA is associated with little to no development of resistance in bacterial cells.

Therefore, in this study, we hypothesized that this nanomedicine could knockdown PDGFR-β and promote autophagy in host vaginal cells simultaneously to decrease the C. trachomatis entry and improve intracellular elimination of C. trachomatis without causing any apoptosis or cytotoxicity.

The objectives of this study includes (1) Evaluate the in vitro promotion of autophagy by siRNA-PEI PLGA-PEG NP (2) Evaluate the in vitro gene knockdown of PDGFR-β (3) Evaluate the in vitro cytotoxicity of the formulation (4) Evaluate the in vitro anti-C. trachomatis effect.

5.3 Materials and Methods

5.3.1 Cell culture and C. trachomatis propagation

Vaginal epithelial cells (VK2/E6E7), C. trachomatis strain K, and McCoy cells were purchased from ATCC (VA, USA). Keratinocyte-SFM and its supplements were purchased from Thermo Fisher (ON, Canada). Calcium chloride was purchased from

Sigma-Aldrich (ON, Canada). VK2/E6E7 cells were maintained at 37°C and 5% CO_2 with Keratinocyte-SFM medium supplemented with 0.1 ng/mL human recombinant epidermal growth factor (EGF), 0.05 mg/mL bovine pituitary extract, 44.1 mg/L calcium chloride and 100 µg/mL penicillin-streptomycin (Thermo Fisher, ON, Canada) (100 U/mL). McCoy cells were maintained at 37°C and 5% CO_2 with Eagle's Minimum Essential Medium (Lonza, SC, USA) supplemented with 10% FBS (PAA, ON, Canada). C. trachomatis strain K was propagated in McCoy cells according to manufacturer's instructions and C. trachomatis EBs were harvested from infected cells by sonication in PBS (Lonza, SC, USA) for 20s and the mixer was centrifuged at 500xg, 4°C for 15 min. The pellet was resuspended in PBS and sonicated for another 20s, followed by centrifugation at 30,000xg, 4°C for 60 min [300].

5.3.2 Preparation of NP

Nonsilencing siRNA and siRNA targeting PDGFR-β were synthesized by Dharmacon, (ON, Canada). Cy3-labeled nonsilencing siRNA was purchased from Thermo Fisher, (ON, Canada). Sequences are listed in supplementary information. Briefly, siRNA was first condensed by PEI and then encapsulated into NP made from the biodegradable di-block copolymer, PLGA-PEG (50/50)(10 kDa)-(2 kDa), (COOH-terminated, Advanced Polymer Materials, QC, Canada) using the double-emulsion evaporation method [297, 301]. Equal volumes of siRNA (100 µg) and PEI (Branched PEI 25 kDa, Sigma-Aldrich, ON, Canada) dissolved in TE buffer, pH 7.5 were combined together at N/P ratio = 5:1. siRNA-PEI complex was then continuously emulsified with 600 µL of PLGA-PEG (20 mg/mL) dissolved in methylene chloride (Thermo Fisher, ON, Canada) for 15 s. The primary emulsion was further emulsified with 4.3 mL of 2% polyvinyl alcohol (PVA,

31~50 kDa, Sigma-Aldrich, ON, Canada) for 2-3 min, forming a w/o/w secondary emulsion. The secondary emulsion was stirred at 4 ºC for more than 3 hr to evaporate the organic solvent and harden the NP. were then collected by centrifugation (20,000xg for 15 min at 4 °C) and washed twice with water to eliminate excess PVA and unencapsulated siRNA. Nonsilencing siRNA NP (containing no PEI), nonsilencing siRNA-PEI-PLGA-PEG NP, cy3-labeled siRNA-PEI-PLGA-PEG NP and PDGFR-β siRNA–PEI NP were prepared using this method.

5.3.3 In vitro studies of autophagy induction

LC3B level was determined by immunofluorescence. Briefly, 0.7 $\times 10^5$ VK2/E6E7 cells were seeded onto 24-well plate with 500 µL growth medium and maintained overnight. On the day of the experiment, nonsilencing siRNA NP (containing no PEI), nonsilencing siRNA-PEI-PLGA-PEG NP and PDGFR-β siRNA–PEI PLGA-PEG NP were used to treat cells at a concentration of 1.334 mg/mL. Cells treated with culture medium were used as naïve control. All groups were incubated at 37°C and 5% CO_2 for 48 hr. At the end of incubation, cells were trypsinized, washed and fixed with 2% paraformaldehyde (BD Biosciences, ON, Canada). Cells were permeabilized with 0.1% saponin/PBS and fixed with Fc blocker (BD Biosciences, ON, Canada). After that, the cells were stained with mouse anti-human anti-LC3B antibody [5H12] (Abcam, ON, Canada) (1:200 dilution) and donkey anti-mouse IgG H&L (Alexa Fluor® 488) (Abcam, ON, Canada) (1:2000) for 30 min each on ice. Mouse monoclonal IgG1 (Abcam, ON, Canada) was used as isotype control. The samples were then analyzed by flow cytometry (BD FACSCanto™ II system).

Autophagic flux was determined using the CYTO-ID® Autophagy detection kit (Enzo Life Sciences, NY, USA) with the same dosing regimen mentioned above. Cells were treated and stained according to manufacturer's instructions and the level of autophagic flux was determined by flow cytometry.

Beclin-1, VPS 34, TECPR-1 and UVRAG gene expression were evaluated in cells treated with the same treatment regimen mentioned above. Total RNA was extracted using E.Z.N.A.® Total RNA Kit I (Omega Biotek, ON, Canada). cDNA synthesis was performed with qScript™ cDNA SuperMix (Quanta Biosciences, ON, Canada) according to the manual. qRT-PCR was performed with PerfeCTa SYBR Green SuperMix from (Quanta Biosciences, ON, Canada) on QuantStudio™ 6 Flex Real-Time PCR System (Thermo Fisher, ON, Canada). The thermal cycle was conducted by incubating at 95 °C for 3 min, followed by PCR amplification of 50 cycles at 95 °C for 15s, 59 °C for 45s. melt curve was run at 95 °C for 15s followed by 60°C for 1 min. GAPDH was used as an endogenous control. All primer sequences (Dharmacon, ON, Canada) and siRNA sequences are listed in Table 5.1.

Beclin-1, VPS 34, TECPR-1 and UVRAG gene expression were evaluated in cells treated with the same treatment regimen mentioned above. Total RNA was extracted using E.Z.N.A.® Total RNA Kit I (Omega Biotek, ON, Canada). cDNA synthesis was performed with qScript™ cDNA SuperMix (Quanta Biosciences, ON, Canada) according to the manual. qRT-PCR was performed with PerfeCTa SYBR Green SuperMix from (Quanta Biosciences, ON, Canada) on QuantStudio™ 6 Flex Real-Time PCR System (Thermo Fisher, ON, Canada). The thermal cycle was conducted by incubating at 95 °C for 3 min, followed by PCR amplification of 50 cycles at 95 °C for 15s, 59 °C for 45s.

melt curve was run at 95 °C for 15s followed by 60°C for 1 min. GAPDH was used as an endogenous control. Primer sequences (Dharmacon, ON, Canada) are listed in Table 5.1.

Table 5.1: Sequences of primers and siRNAs

Name	Sequence
PDGFR-β primer	forward: 5'-ACCATTCCATGCCGAGTAACA-3' reverse: 5'-CTGTCCCCAATGGTGGTTTT-3'
GAPDH primer	forward: 5'-AAGAAGGTGGTGAAGCAGGCG-3' reverse: 5'-AGACAACCTGGTCCTCAGTGTAGC-3'
Beclin-1 primer	forward: 5'-ACCGCAAGATAGTGGCAGAAA-3' reverse: 5'-GGGCATAACGCATCTGGTTT-3'
UVRAG primer	forward: 5'-GGCAAACCCTTCCCAACCT-3' reverse: 5'-TCTGCACCCCCAAATATGGA-3'
TECPR-1 primer	forward: 5'-CCCGCCACCTACACGAAA-3' reverse: 5'-CCCCTACAGAGAGGTCGTTGAA-3'
VPS-34 primer	forward: 5'-GGAAAAGCAGTGCCTGTAGGA-3' reverse: 5'-GGCAAGACGGCTCATCTGAT-3'
PDGFR-β siRNA	sense 5'-GAAAGGAGACGUCAAAUAUdTdT-3' antisense 3'-dTdTCUUUCCUCUGCAGUUUAUA-5'

5.3.4 Cell uptake of Cy3-labeled siRNA-PEI-PLGA-PEG NP

0.7×10^5 VK2/E6E7 cells were seeded in 24-well plates with 500 μL growth medium and maintained overnight. On the day of the experiment, cells were treated with cy3-labeled siRNA-(1.334 mg/mL) at 37°C, 5% CO_2 for different time intervals. At the end of incubation, cells were washed three times with PBS and analyzed using flow cytometry.

5.3.5 In vitro cytotoxicity study

VK2/E6E7 cells (2.5×10^4) were seeded onto 96-well plates and treated with different concentrations of nonsilencing siRNA-PEI-PLGA-PEG NP the next day. Cells were incubated at 37°C, 5% CO_2 for 48 hr. Treatments with growth medium and 1M acrylamide were used as negative control and positive control, respectively. Cell viability was measured using the CellTiter 96® Aqueous One Solution Cell Proliferation Assay (Promega, ON, Canada).

0.7×10^5 VK2/E6E7 cells were seeded onto 24-well plates. The next day, cells were treated with nonsilencing siRNA-PEI-PLGA-PEG NP or PDGFR-β siRNA–PEI PLGA-PEG NP at a concentration of 1.334 mg/mL and incubated at 37°C, 5% CO_2 for 48 hr. Cells were then centrifuged at 20,000xg, 4°C for 15 min to remove NP. The supernatant was analyzed by ELISA to quantitate the concentration of pro-inflammatory cytokines (IL-1β, IL-6, IL-8 and TNF-α ELISA kits were purchased from R&D systems, Minneapolis, USA). Cells were then trypsinized, stained with FITC Annexin V/Dead Cell Apoptosis Kit (Thermo Fisher, Ontario, Canada) and analyzed for apoptosis using flow cytometry.

5.3.6 In vitro PDGFR-β downregulation study

0.7×10^5 VK2/E6E7 cells were seeded onto 24-well plates and incubated overnight. Cells were treated with either growth medium, nonsilencing siRNA-PEI-PLGA-PEG NP, or PDGFR-β siRNA-PEI-PLGA-PEG NP and incubated at 37°C, 5% CO_2 for 48 hr. At the end of incubation, cells were washed three times with growth medium and RNA was extracted using E.Z.N.A.® Total RNA Kit I. cDNA synthesis was performed using

qScript™ cDNA SuperMix and qRT-PCR was performed using PerfecTa SYBR Green SuperMix as mentioned above. The thermal cycle consisted of 95 °C for 3 min, followed by PCR amplification of 50 cycles at 95 °C for 15s, and 59 °C for 45s. Melt curves were run at 95 °C for 15s followed by 60°C for 1 min. GAPDH was used as an endogenous control.

The protein level of PDGFR-β was measured by flow cytometry. 2.8 $\times 10^5$ VK2/E6E7 cells were seeded onto 6-well plates, treated with formulations mentioned above and incubated at 37°C, 5% CO_2 for 48 hr. At the end of the study, cells were washed three times with PBS and trypsinized. Cells were fixed with 2% paraformaldehyde, blocked with 10% FBS and stained with FITC-rabbit anti-PDGFR-β antibody (958) (Santa Cruz Biotechnology, ON, Canada). The resulting samples were analyzed by flow cytometry.

5.3.7 Chlamydia infection study

VK2/E6E7 cells (0.7 $\times 10^5$) were seeded onto 24-well plates and allowed to incubate overnight. Cells were treated with growth medium, nonsilencing siRNA-PEI-PLGA-PEG NP (1.334 mg/mL) or siRNA PDGFR-β-PEI PLGA-PEG NP (1.334 mg/mL) and incubated at 37°C, 5% CO_2 for 48 hr. The cells were then washed three times (centrifugation at 800xg) with antibiotic-free growth medium and challenged with 200 µL C. trachomatis strain K (100 µg) for 60 mins. Afterwards, medium containing excess bacteria was replaced with antibiotic-free growth medium and infected cells were incubated at 37°C, 5% CO_2 for 24 hr. At the end of incubation, cells were washed with HBSS, fixed with 100% methanol (Thermo Fisher, ON, Canada) for 10 min and blocked with 3% BSA (Thermo Fisher, ON, Canada) for 60 min at room temperature. Staining

was conducted with 200 μL FITC-anti-chlamydia lipopolysaccharide antibody (B410F) (1:5 dilution) (Thermo Fisher, ON, Canada) overnight at 4°C. Images were taken using fluorescence microscopy (Nikon, ECLIPSE Ti). Fluorescence intensity of the images were quantified by Image J.

5.3.8 Statistical analysis

Data are presented as mean +/- SD. Unless specified, non-parametric One-way ANOVA (Tukey test) was used for multiple comparisons with $p<0.05$ considered to be significant.

5.4 Results

5.4.1 Autophagy induction by siRNA-PEI-PLGA-PEG NP

The PDGFR-β-siRNA-PEI-PLGA-PEG NP showed a particle size of 260.3±6.43 nm and a zeta potential of -17.8±5.2 mV in PBS, pH 7.4. Vaginal epithelial cells, VK2/E6E7, were capable of tolerating up to 5 mg/mL of nonsilencing siRNA-PEI-PLGA-PEG NP with an incubation time of 48 hr before any decline in cell viability was observed (Fig 5.1A). Cellular uptake of siRNA was rapid and efficient and the increase in intracellular siRNA followed a time-dependent manner (Fig 5.1B-C).

The number of autophagosome is a widely used marker for studying autophagy and it correlates well with the amount of LC3B, therefore, the intracellular level of LC3B was first quantified to identify changes in the dynamic pathway of autophagy. Our results indicated that compared to naïve control, nonsilencing siRNA PLGA-PEG NP significantly increased the intracellular level of LC3B by 43.1±11.9%, while nonsilencing siRNA-PEI-PLGA-PEG NP and PDGFR-β siRNA-PEI-PLGA-PEG NP did not increase

the intracellular level of LC3B at all. However, this does not mean that nonsilencing siRNA-PEI-PLGA-PEG NP and PDGFR-β siRNA-PEI-PLGA-PEG NP did not exert an effect on the formation and conversion of autophagosomes, because when we compared the LC3B levels in these two groups to that in nonsilencing siRNA PLGA-PEG NP-treated group, we found that the intracellular levels of LC3B were significantly decreased by 23.8±4.5% and 38.7±5.5% respectively, and no significant change in LC3B was detected between nonsilencing siRNA-PEI-PLGA-PEG NP-treated group and PDGFR-β siRNA-PEI-PLGA-PEG NP-treated group (Fig 5.1D).

Autophagosome is an intermediate structure in the autophagic flow when it is consistently formed and converted to autolysosome, but its number detected at any specific time does not represent the autophagic degradation activity in cells [302]. Therefore, in order to investigate whether PEI encapsulation into NP would promote autophagic degradation activity in VK2/E6E7 cells, a widely accepted autophagy detection kit (CYTO-ID® Autophagy detection kit) was used subsequently to quantify the level of autophagic flux (defined as a measure of autophagic degradation activity) in cells. The results revealed that NP without the encapsulation of PEI only increased the intracellular autophagic flux by about 3 folds compared to naïve control (Fig 5.1E). In contrast, PEI-encapsulated NP significantly enhanced the autophagic flux in cells by about 9 folds compared to naïve control, regardless if it was nonsilencing siRNA or PDGFR-β siRNA encapsulated in the NP (Fig 5.1E). Therefore, the NP formulation containing PEI could enhance the autophagic degradation activity in VK2/E6E7 cells a lot more than that without PEI, even though all three NP formulations could promote autophagic degradation activity.

To further investigate how the autophagic stages are influenced, we looked at changes in the gene expression of four common autophagy regulatory genes, Beclin-1, VPS34, UVRAG and TECPR-1. Beclin-1 and VPS34 take part in the vacuolar sorting and autophagosome biosynthesis [255, 256], thus are markers of the initiation stage of autophagy while UVRAG and TECPR-1 are required in autophagosome-lysosome fusion [256, 257], which are markers of the degradation stage. Our results showed that nonsilencing siRNA PLGA-PEG NP only caused a significant increase in the expression of VPS34 compared to naïve control. In contrast, both nonsilencing siRNA-PEI-PLGA-PEG NP and PDGFR-β siRNA-PEI-PLGA-PEG NP significantly increased the expression of all four genes. Knocking down PDGFR-β also significantly further enhanced the expression of Beclin-1 compared to nonsilencing siRNA-PEI-PLGA-PEG NP (Figure5.1F).

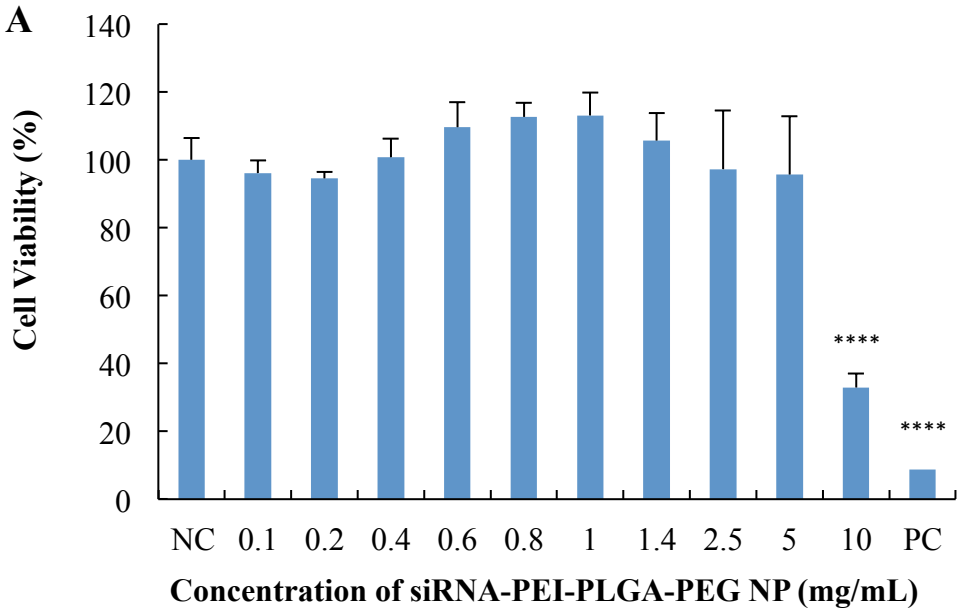

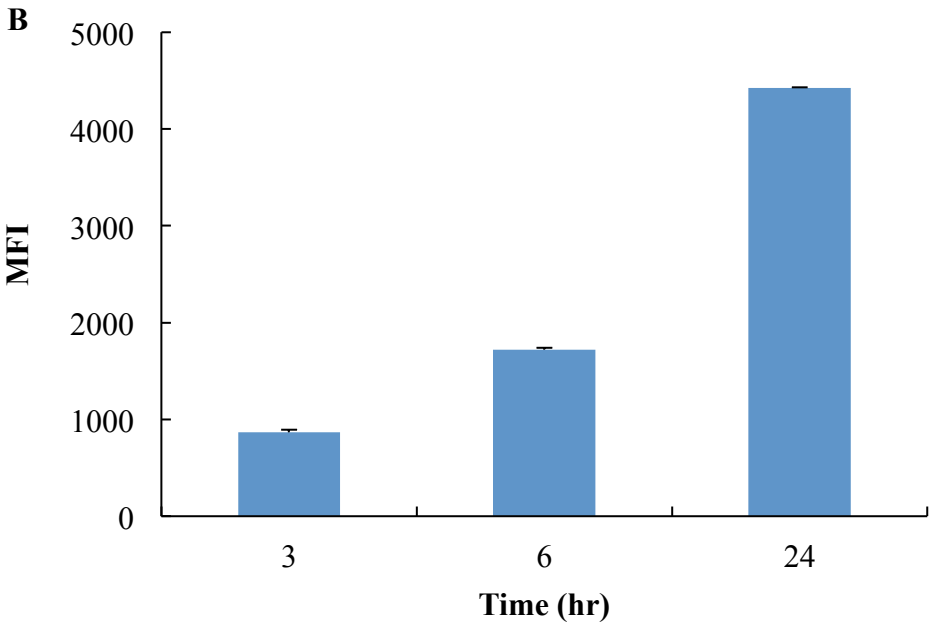
B
5000
4000
3000
2000
1000
0
MFI
3
6
24
Time (hr)

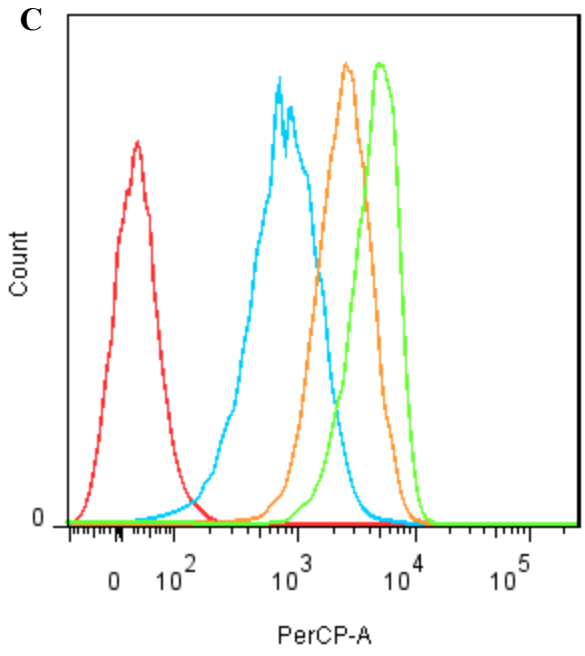
C
Count
0
0
10^2
10^3
10^4
10^5
PerCP-A

D

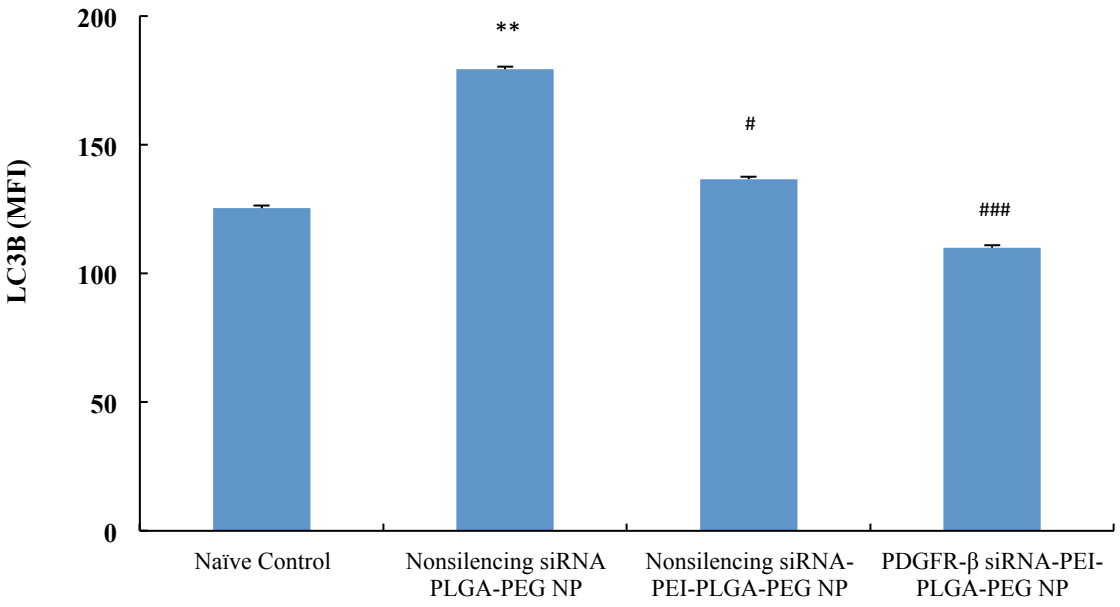
LC3B (MFI)
200
150
100
50
0
**
#
###
Naïve Control
Nonsilencing siRNA PLGA-PEG NP
Nonsilencing siRNA-PEI-PLGA-PEG NP
PDGFR-β siRNA-PEI-PLGA-PEG NP

E

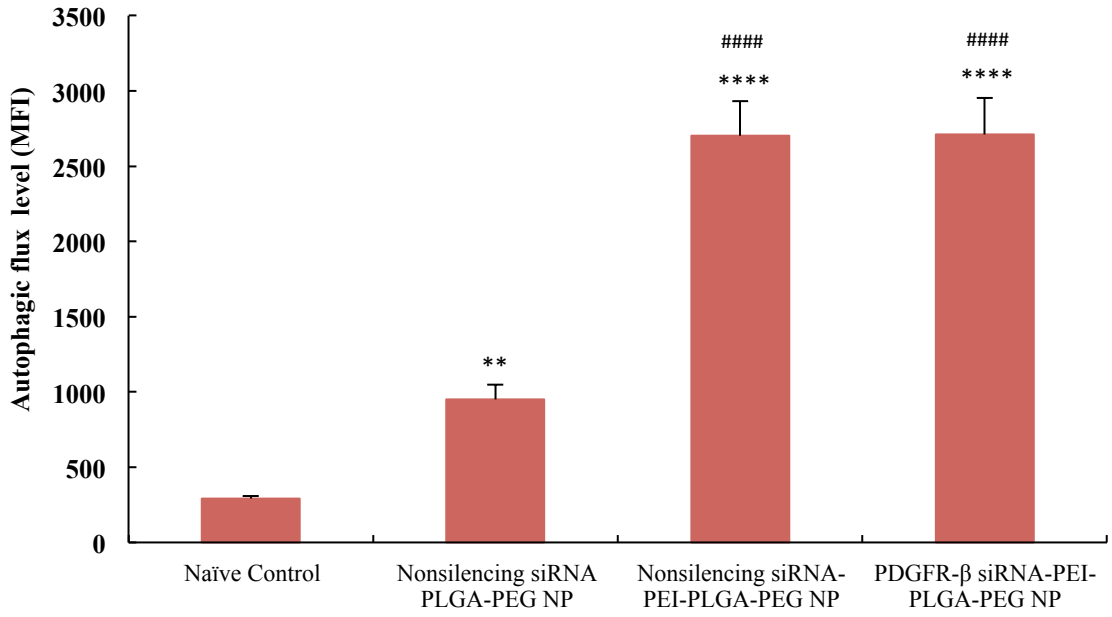
Autophagic flux level (MFI)
3500
3000
2500
2000
1500
1000
500
0
**
####
****
####
****
Naïve Control
Nonsilencing siRNA PLGA-PEG NP
Nonsilencing siRNA-PEI-PLGA-PEG NP
PDGFR-β siRNA-PEI-PLGA-PEG NP

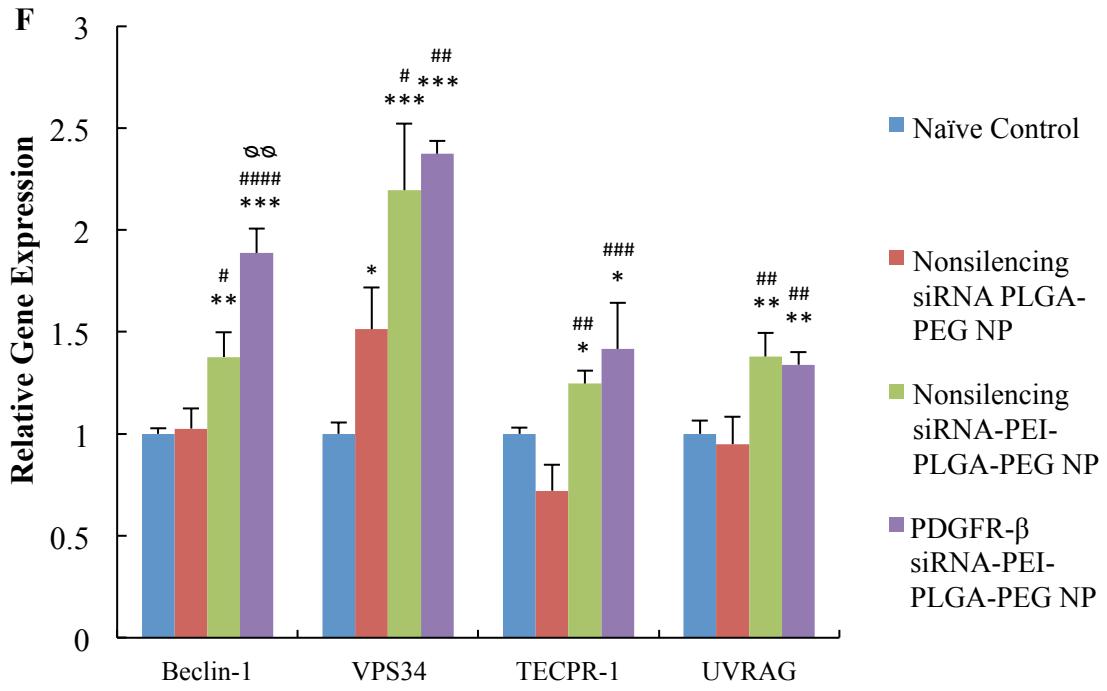

Figure 5.1: In vitro induction of autophagy in VK2/E6E7 cells by various NP formulations at a concentration of 1.334 mg/mL with an incubation period of 48 hr. (A) In vitro cytotoxicity of non-silencing siRNA-PEI-PLGA-PEG NP in VK2/E6E7 cells after 48 hr incubation. Results were measured by MTS assay. NC: negative control, PC: positive control, **** $p<0.0001$, compared to NC. Values represent the mean±SD, n=3. (B-C) In vitro cell uptake of Cy3-labeled siRNA-PEI-PLGA-PEG NP at a concentration of 1.334 mg/mL over a period of 24 hr. (B) Cumulative uptake of Cy3-labeled siRNA-PEI-PLGA-PEG NP by VK2/E6E7 cells quantified by MFI (mean fluorescence intensity) over time. (C) A representative histogram of uptake of Cy3-labeled siRNA-PEI-PLGA-PEG NP from n=3. Results were quantified by flow cytometry. Red: Non-labeled siRNA-PEI-PLGA-PEG NP, blue: 3 hr, orange: 6 hr, green: 24 hr. Values represent the mean±SD, n=3. (D) Intracellular level of LC3B quantified by flow cytometry (E) Intracellular level of autophagic flux quantified by CYTO-ID® Autophagy detection kit with flow cytometry. (F) Relative gene expression of autophagy-regulatory genes quantified by qRT-PCR with GAPDH as endogenous control. Values in (D)-(F) represent the mean±SD, n=3. MFI: mean fluorescence intensity. *: compared to naïve control, *$p<0.05$, **$p<0.01$, ***$p<0.001$, ****$p<0.0001$. #: compared to nonsilencing siRNA PLGA-PEG NP, #$p<0.05$, ##$p<0.01$, ###$p<0.001$, ####$p<0.0001$. ∞∞$p<0.01$ compared to nonsilencing siRNA-PEI-PLGA-PEG NP.

5.4.2 Autophagy induction study by free PEI

Based on the results, siRNA-PEI-PLGA-PEG NP containing PEI appeared to play an important role in increasing the autophagic degradation activity in VK2/E6E7 cells and promoting both the initiation and degradation stages of autophagy. To better understand the mechanism of action, we next examined whether free PEI could enhance autophagic degradation activity as the PEI-containing formulations did. We found that only VK2/E6E7 cells treated with 1 μg/mL showed healthy morphology while cells treated with other concentrations (> 1 μg/mL) showed significant cell lysis compared to naïve control (data not shown) under microscope, rendering them ineligible for downstream studies. As a result, only cells treated with 1 μg/mL or naïve control were processed for Cyto-ID staining. At the same time, in order to confirm the results seen under the microscope, MTS cell viability assay was conducted using two selected concentrations: 1 μg/mL and 37.4 μg/mL. The concentration of 37.4 μg/mL of PEI was equivalent to the concentration of PEI in siRNA-PEI-PLGA-PEG NP when treated at a concentration of 1.334 mg/mL, and the results for MTS matched what was observed under the microscope: 1 μg/mL was non-cytotoxic while 37.4 μg/mL caused massive cell death (Fig 5.2A). When we looked at the autophagic degradation activity, we found that 1 μg/mL of free PEI did not increase autophagic degradation activity in VK2/E6E7 cells at all compared to naïve control (Fig 5.2B). As a result, free PEI could not induce autophagy within its noncytotoxic concentration range and the encapsulation of PEI into PLGA-PEG NP helped reduce its cytotoxicity, thereby making it possible to exert its role in inducing autophagy.

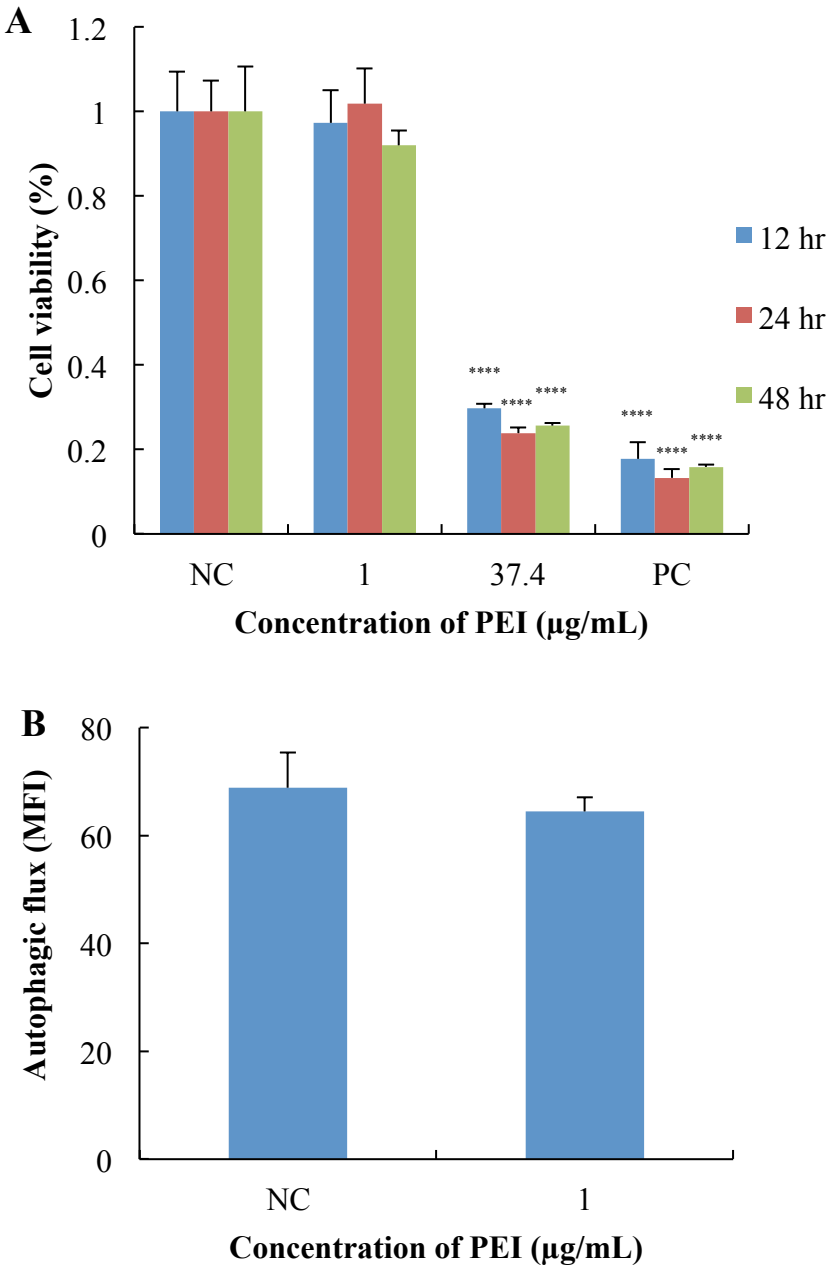

Figure 5.2: (A) In vitro cytotoxicity of free PEI in VK2/E6E7 cells after 12, 24 and 48 hr incubation. Results were measured by MTS assay. NC: negative control, PC: positive control, **** $p<0.0001$, compared to NC. (B) The level of autophagic flux quantified by CYTO-ID® Autophagy detection kit with flow cytometry. MFI: mean fluorescence intensity. Values represent the mean±SD, n=3.

5.4.3 Downregulation of PDGFR-β in VK2/E6E7 cells

In order to achieve gene knockdown of PDGFR-β, the sequence of PDGFR-β siRNA, which has been widely used in previous published literatures [290, 303] was selected and evaluated on VK2/E6E7 cells. First, we did a concentration-dependent study to evaluate the downregulation of PDGFR-β mRNA in VK2/E6E7 cells. Our results showed that PDGFR-β siRNA-PEI-PLGA-PEG NP (1.334 mg/mL) can significantly reduce PDGFR-β mRNA in VK2/E6E7 cells by 50% compared to nonsilencing siRNA-PEI-PLGA-PEG NP. Doubling the siRNA concentration to 2.668 mg/mL did not further decrease gene knockdown (Fig 5.3A), indicating that the maximum knockdown efficiency of this siRNA sequence was 50%. We also compared our mRNA downregulation results with the papers (mentioned above) that used this sequence as well (since only mRNA downregulation data was reported in these papers), and they also reported a maximum knockdown of about 50% [290, 303]. As a result, the concentration of 1.334 mg/mL was selected for the evaluation of protein downregulation. At the concentration of 1.334 mg/mL, PDGFR-β siRNA-PEI-PLGA-PEG NP can significantly reduce PDGFR-β protein expression by 43% ($p= 0.0003$ with two-sided, unpaired T test) (Fig 5.3B-C).

It was also confirmed that at this concentration, neither nonsilencing siRNA-PEI-PLGA-PEG NP or PDGFR-β siRNA-PEI-PLGA-PEG NP had a significant impact on pro-inflammatory cytokine production (IL-1β, IL-6, IL-8 and TNF-α) (Fig 5.4A) or induction of apoptosis (Fig 5.4B) in VK2/E6E7 cells compared to naïve control treated with growth medium. The concentration of 1.334 mg/mL would be the optimal concentration for conducting downstream studies

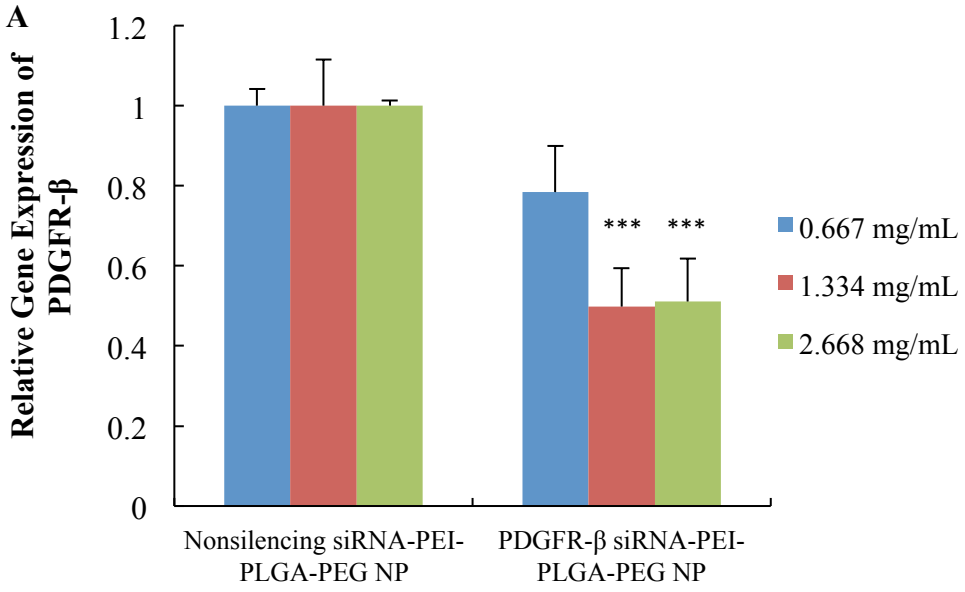
A
Relative Gene Expression of PDGFR-β
1.2
1
0.8
0.6
0.4
0.2
0
***
***
0.667 mg/mL
1.334 mg/mL
2.668 mg/mL
Nonsilencing siRNA-PEI-PLGA-PEG NP
PDGFR-β siRNA-PEI-PLGA-PEG NP

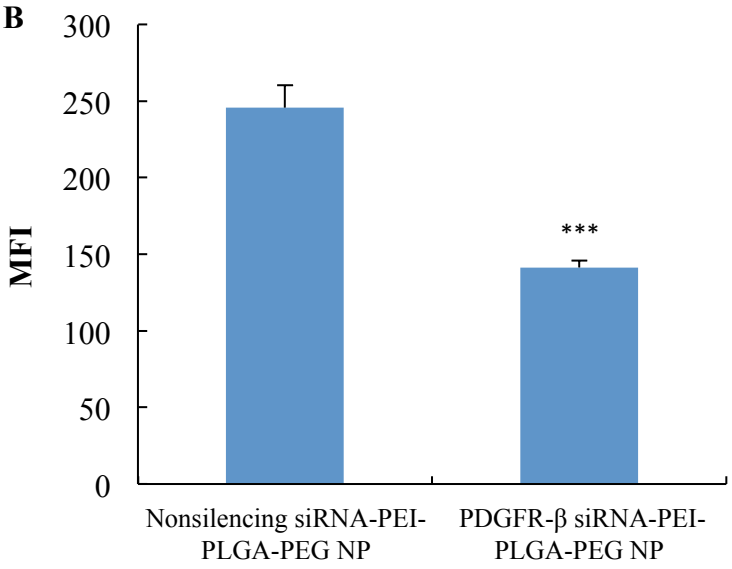
B
MFI
300
250
200
150
100
50
0
***
Nonsilencing siRNA-PEI-PLGA-PEG NP
PDGFR-β siRNA-PEI-PLGA-PEG NP

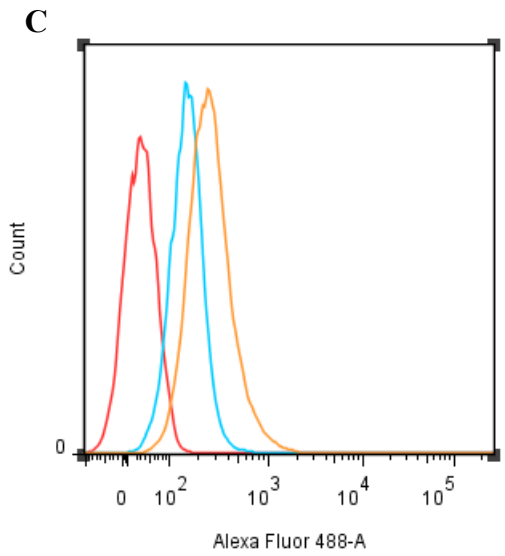

Figure 5.3: (A) In vitro mRNA downregulation of PDGFR-β in VK2/E6E7 cells by PDGFR-β siRNA-PEI-PLGA-PEG NP at different concentrations after 48 hr incubation. Results were measured by qRT-PCR. GAPDH was used as endogenous control. *** $p<0.001$ compared to nonsilencing siRNA-PEI-PLGA-PEG NP. Values represent the mean±SD, n=3. (B-C) In vitro protein downregulation of PDGFR-β in VK2/E6E7 cells by PDGFR-β siRNA-PEI-PLGA-PEG NP at a concentration of 1.334 mg/mL after 48 hr incubation. Results were measured by flow cytometry. (B) PDGFR-β protein downregulation quantified by MFI (mean fluorescence intensity). Values represent the mean±SD, n=3. *** $p<0.001$ compared to nonsilencing siRNA-PEI-PLGA-PEG NP. (C) A representative histogram from n=3. Red: isotype control, blue: PDGFR-β siRNA-PEI-PLGA-PEG NP, orange: nonsilencing siRNA-PEI-PLGA-PEG NP.

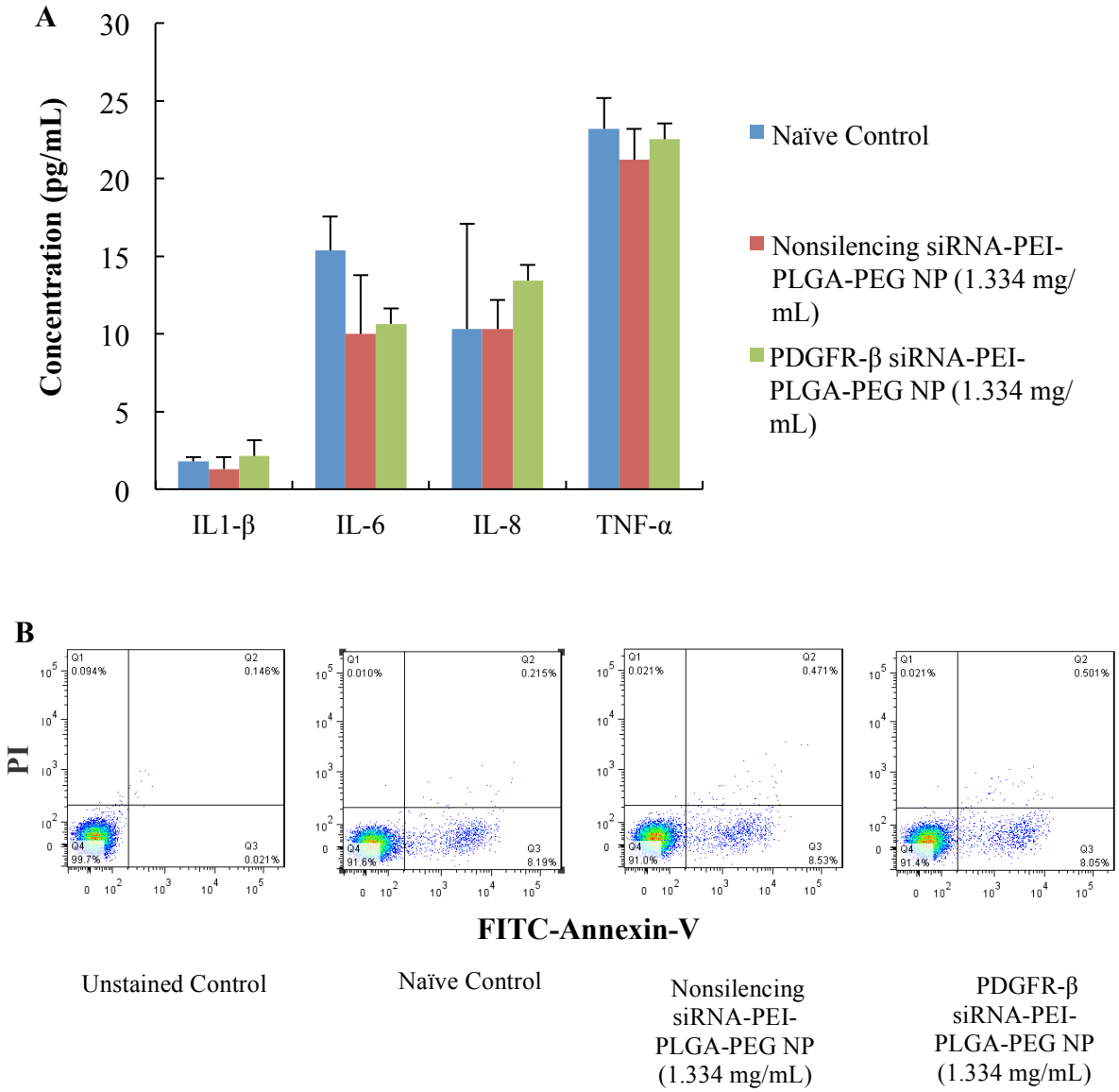

Figure 5.4: (A) In vitro proinflammatory cytokine production in VK2/E6E7 cells when cells were treated with PBS (naïve control), nonsilencing siRNA-PEI-PLGA-PEG NP (1.334 mg/mL) or PDGFR-β siRNA-PEI-PLGA-PEG NP (1.334 mg/mL) for 48 hr. Values represent the mean±SD, n=3. (B) Representative flow cytometry plots of apoptosis measured by FITC Annexin V/Dead Cell Apoptosis Kit. PI: Propidium iodide. Data was collected when VK2/E6E7 cells were treated with PBS (naïve control), nonsilencing siRNA-PEI-PLGA-PEG NP (1.334 mg/mL) or PDGFR-β siRNA-PEI-PLGA-PEG NP (1.334 mg/mL) for 48 hr. Experiments were conducted in triplicate.

5.4.4 Intracellular production of C. trachomatis RB in VK2/E6E7 cells

24-hr after infection of C. trachomatis EBs, nonsilencing siRNA-PEI-PLGA-PEG NP treatment that could promote the autophagic degradation pathway significantly decreased the intracellular RBs by approximately 25% ($p=0.0436$) and PDGFR-β siRNA-PEI-PLGA-PEG NP that could enhance the autophagic degradation pathway and inhibit bacterial binding simultaneously significantly decreased intracellular RBs by about 63% ($p= 0.0005$) compared to PBS treatment (Fig 5). Overall, knocking down PDGFR-β in combination with augmenting autophagy activity worked simultaneously to reduce the C. trachomatis infection in VK2/E6E7.

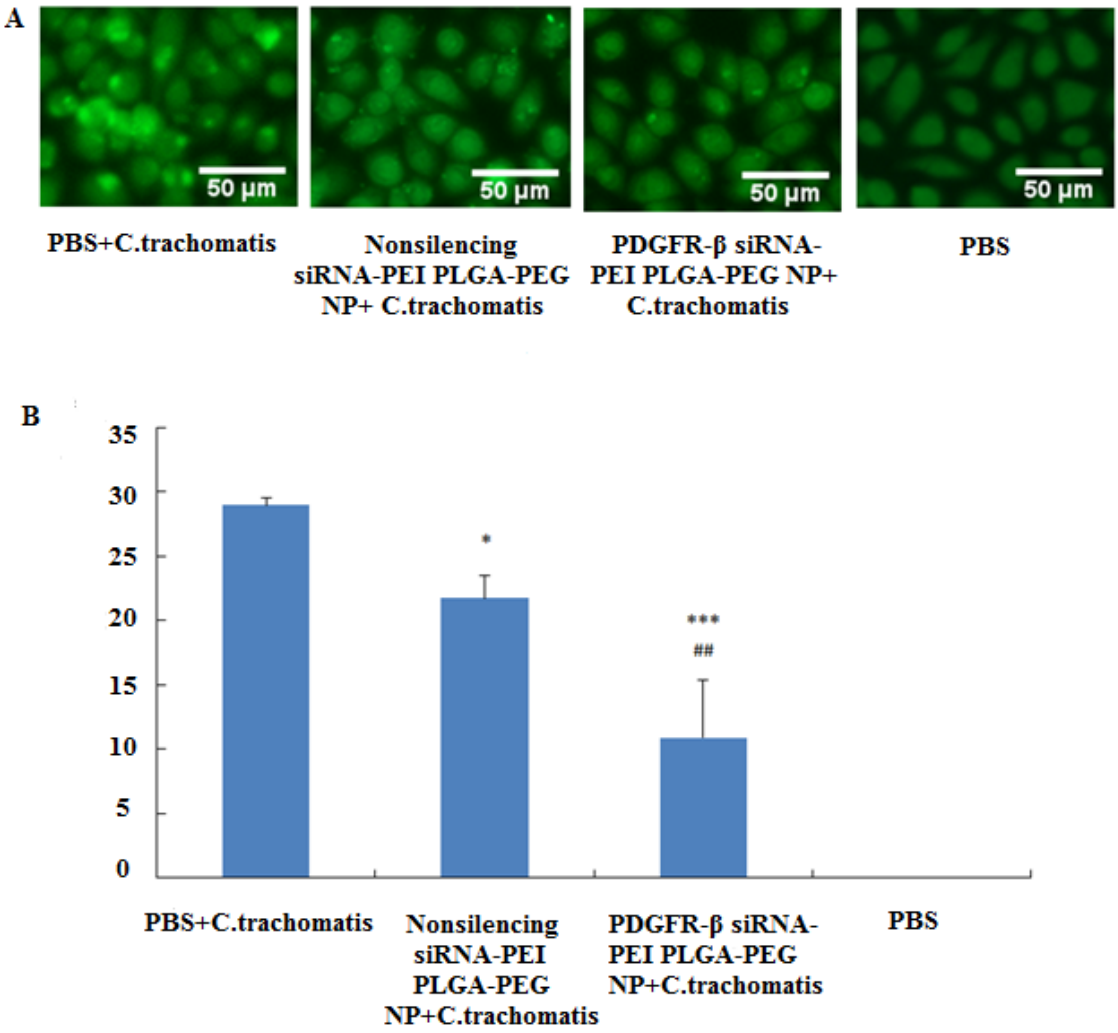

Figure 5.5: Intracellular production of C. trachomatis RBs in VK2/E6E7 cells. Cells were incubated with PBS, non-silencing siRNA-PEI-PLGA-PEG NP (1.334 mg/mL) or PDGFR-β siRNA-PEI-PLGA-PEG NP (1.334 mg/mL) for 48 hr and then infected with C. trachomatis. Images were taken 24 hr post C. trachomatis infection. (A) Intracellular C. trachomatis RB foci (green fluorescence foci inside of cells) were visualized using fluorescence microscopy. Experiments were conducted n=3 and a group of representative images were shown. (B) Semi-quantitative measurements of intracellular C. trachomatis RB foci were accomplished using Image J software. Values represent the mean±SD, n=3. *$p<0.05$, *** $p<0.001$ compared to PBS+ C. trachomatis, ##$p<0.01$ compared to nonsilencing siRNA-PEI-PLGA-PEG NP+C. trachomatis.

5.5 Discussion

Chlamydia infection is transmitted through unprotected sexual intercourse and can infect the vagina and cervix [304, 305]. Even though the organism is susceptible to antimicrobial agents, the occurrence of multi-drug resistant strains brings us big challenges in combating this pathogen. Considering the fact that an effective vaccine is still not available, we believe the use of a non-antibiotic based microbicide is an excellent alternative strategy to help prevent/reduce chlamydia infection in women in addition to regular screening of the pathogen in susceptible populations [28].

In the design of our microbicide, we combined two preventive strategies together, which includes the reduction of bacterial entry into host cells and augmentation of host defense against C. trachomatis. The strategies take advantage of the special characteristics of siRNA-PEI-PLGA-PEG NP, in which PEI plays an important role in promoting the autophagy in host cells as well as improving the encapsulation of siRNA into NP [260]. NP facilitate the delivery of siRNA for sufficient PDGFR-β gene knockdown and also helps reduce the cytotoxicity of PEI, thus making it possible to deliver adequate amounts of PEI into cells for inducing autophagy without causing cytotoxicity. Lin et al. have previously reported the protective role of branched PEI (25K) in inducing cell death in HeLa cervical cancer cells and mouse embryonic fibroblasts [306]. In their study, they found that PEI was capable of inducing autophagy, apoptosis and necrosis simultaneously. The induced autophagy assisted cell survival by providing nutrients that were recycled through autophagy, while apoptosis and necrosis contributed to cell death. Apoptosis may occur downstream of autophagy or independent of autophagy. This phenomenon is not only observed with PEI but potentially with all cationic polymers

[306]. Therefore, the potential role of using PEI-induced autophagy or cationic polymer-induced autophagy as a therapeutic therapy is largely limited by the cytotoxic effect on cells. Our findings are consistent with what has been reported whereby free PEI is highly toxic to cell lines e.g. in Chia-Wei's study, the cells can only tolerate 4 μg/mL of PEI for 4 hr and 1 μg/mL PEI for 48 hr. When encapsulated into NP, the toxicity of PEI was greatly minimized, based on the results of the MTS assay. VK2/E6E7 cells can tolerate up to 139.5 mg/mL of PEI (equivalent to 5 mg/mL siRNA-PEI-PLGA-PEG NP) for 48 hr without decreasing cell viability. More importantly, the NP can deliver sufficient amounts of PEI into cells to induce autophagy without causing inflammation, apoptosis or any decrease in cell viability. By using a NP formulation, we successfully resolved the problem associated with the cytotoxic effects of PEI but still retained the beneficial properties of PEI in inducing autophagy. We believe the key to decreasing the cytotoxicity of PEI is through encapsulation with NP which prevents the direct contact between the cationic polymer and membranes of cells and organelles, since it has been documented that the cytotoxicity of PEI is largely attributed to the permeabilization of plasma membranes [307], decrease of nuclear size, decrease of lysosomal mass/pH and the permeabilization of mitochondrial membrane [308].

Since autophagy is a dynamic process, the induction of autophagy was evaluated using three different methods. As mentioned in the introduction, intracellular LC3B correlates well with the number of autophagosomes, which would further indicate changes occurring during the initiation and degradation stages of autophagy since autophagosomes are formed during the initiation stage and degraded during the degradation stage. Generally, an increase in LC3B (equal increase in the amount of autophagosome) can

indicate: 1) an increased initiation stage followed by an unchanged degradation stage or 2) an unchanged initiation stage followed by a decreased degradation stage or 3) an increased initiation stage followed by a decreased degradation stage or 4) a predominant increased initiation stage followed by an increased degradation stage causing a combined effect of increased LC3B or 5) a decreased initiation stage followed by a predominant decreased degradation stage causing a combined effect of increased LC3B (Table 5.2). These conditions also correspond to different changes in autophagic flux, known as the autophagic degradation activity (Table 5.2). In the meanwhile, the indications of decreased LC3B level or an unchanged LC3B level were also listed in Table 5.2.

To summarize the results from all three studies, with respect to nonsilencing siRNA PLGA-PEG NP, there was an observed increase in the level of autophagic flux, an increase in the level of LC3B and an increase in the gene expression of VPS34 compared to naïve control. It appears that the results collected for the nonsilencing siRNA PLGA-PEG NP group possibly fit scenario No.4 in Table 5.2 except for a lack in the upregulation of the late-stage autophagy regulatory genes. This could be explained by the possibility that other autophagy regulatory genes/proteins may be involved, leading to the promotion of degradation stage of autophagy. Therefore, the nonsilencing siRNA PLGA-PEG NP augmented autophagic flux by potentially promoting the initiation and degradation stages simultaneously, but the degradation stage was not promoted as much as the initiation stage, putting a limit on the promotion of autophagic flux.

However, when PEI was encapsulated into NP, we found that compared to naïve control, nonsilencing siRNA-PEI-PLGA-PEG NP and PDGFR-β siRNA-PEI-PLGA-PEG NP did not change intracellular LC3B but significantly increased autophagic flux and upregulated

all four autophagy-related genes (scenario No.6, Table 5.2). This was because the increased initiation stage was followed by an equally increased degradation stage, causing the increased number of autophagosomes to be completely converted and degraded in the degradation stage. Therefore, the encapsulation of PEI into NP made a significant contribution to promoting the degradation stage of autophagy, therefore causing more increase in autophagic flux than NP without PEI.

Subsequently the comparisons were made between nonsilencing siRNA PLGA-PEG NP and nonsilencing siRNA-PEI PLGA-PEG NP. We found that in comparison to nonsilencing siRNA PLGA-PEG NP containing no PEI, the encapsulation of PEI into PLGA-PEG NP (regardless it is nonsilencing siRNA or siRNA PDGFR-β encapsulated) significantly decreased intracellular LC3B, increased autophagic flux, and augmented the expression of four autophagy-regulatory genes. Based on the analysis, the profiles of nonsilencing siRNA-PEI-PLGA-PEG NP and PDGFR-β siRNA-PEI-PLGA-PEG NP are likely to fit the criteria described in scenario No.11, Table 5.2. Even though we did not observe higher increase in the gene expression of TECPR-1 and UVRAG than Beclin-1 and VPS 34, scenario No.11 was the only one meeting all the other conditions. We thought there might be some other genes/proteins involved in the pathway of autophagy that were not measured in this study (like mentioned above) and all the participating factors led to the changes of LC3B and autophagic flux observed in this study. Therefore, based on the comparison, we believed that, on the basis of nonsilencing siRNA PLGA-PEG NP, PEI encapsulation could further promote the initiation stage and degradation stage simultaneously and more promotion could possibly occur in the degradation stage.

Previous literature has shown that free PEI can enhance the formation of autophagosomes and LC3B [306, 308] mainly during the early stages of autophagy. Whether or not the late stages of autophagy is affected (e.g., fusion of autophagosomes and lysosomes) is not clear. This made it difficult to conclude that the autophagic flux was augmented since as discussed earlier, blocking the late stage would halt the progression of autophagy, rendering the targets for degradation to accumulate in autophagosomes instead of being degraded in autolysosome. In our study, we have provided evidence showing that our nonsilencing siRNA-PEI-PLGA-PEG NP and PDGFR-β siRNA-PEI-PLGA-PEG NP can promote autophagic flux (degradative activity of autophagy) by promoting both the formation of autophagosomes (initiation stage) and the fusion of autophagosomes with lysosomes (degradation stage) simultaneously with more promotion made in the degradation stage, which has never been reported previously. And we found that the promotion of autophagic flux is related to the upregulation of four autophagy regulatory genes (Beclin-1, VPS34, TECPR-1 and UVRAG). We are not sure what other genes/protein are also involved in this process, therefore, further studies are required to discover the roles of other possible autophagy regulated genes/proteins to provide a complete explanation for the current findings.

Gao et al. have shown that free PEI was taken up by cells via clathrin-mediated endocytosis (CME) pathway and the CME pathway plays an important role in promoting the formation of autophagosomes [308]. Previous literature has also reported that PLGA-PEG NP (~300 nm, negatively charged) can be taken up by cells through both CME, and clathrin-/caveolae-independent pathways depending on the cell type [309]. Although the mechanism of entry into vaginal epithelial cells of our siRNA-PEI-PLGA-PEG NP has

not been investigated, it is possible that our siRNA-PEI-PLGA-PEG NP is also taken up by cells via the CME pathway due to the presence of PLGA-PEG which in turn promotes the formation of autophagosomes. Therefore, besides the upregulation of autophagy-regulatory genes, the cell uptake pathway of NP may also contribute to the promotion of initiation stage of autophagy.

Table 5.2: Changes in total LC3B with all possible changes in initiation stage & degradation stage of autophagy and autophagic flux.

No.	Total LC3B	Autophagy initiation stage (autophagosome formation, markers: Beclin-1 and VPS 34)	Autophagy degradation stage of autophagy (autophagosome degradation by forming autolysosome, the compartment for degradation markers: TECPR-1 and UVRAG)	Autophagic Flux
1	↑	↑	–	–
2	↑	–	↓	↓
3	↑	↑	↓	↓
4	↑	↑↑	↑	↑
5	↑	↓	↓↓	↓
6	–	↑↑	↑↑	↑↑
7	–	–	–	–
8	↓	↓	–	↓
9	↓	–	↑	↑
10	↓	↓	↑	↑ or – or ↓
11	↓	↑	↑↑	↑
12	↓	↓↓	↓	↓

Chapter 6

Conclusions and Future Directions

6.1 Conclusions

We have designed and developed a PLGA-based nanomedicine that can achieve active delivery of SQV to CD4+ immune cells. Our studies showed that the SQV-NP-CD4 had a particle size of about 280 nm, a zeta potential of approximately -10 mV and an EE% of 65%. Antibody can be efficiently conjugated to NP with an ACE% of 74% and an antibody loading of 35.7 ng/mg NP. The SQV-NP-CD4 was non-cytotoxic and could significantly increase SQV uptake by CD4+ cells in vitro. The nanomedicine could be further formulated into a vaginal gel without causing cytotoxicity. The 1% HEC gel loaded with SQV-NP-CD4 (5 mg NP/g gel) showed a similar viscosity as that of some commercially available products under the same condition, indicting its potential in improving vaginal retention of SQV-NP-CD4. However, the amount of SQV-NP-CD4 loading into the gel as well as the release of SQV-NP-CD4 from the gel need to be optimized in in vitro to achieve the expected efficacy and the viscosity of the gel has to be adjusted correspondingly into order to keep a balance between maintaining the vaginal retention of SQV-NP-CD4 and being able to release adequate amount of SQV-NP-CD4. Ritonavir, a CYP450 3A4 and 2D6 inhibitor can be considered to be co-encapsulated into NP with SQV (metabolized by CYP450 3A4) to slow down its metabolism in cells, or other antiretroviral drugs from different categories can be also co-encapsulated with SQV into NP to achieve a better efficacy.

Next, in order to improve the mucus penetration ability and stability of NP, we introduced PEG into the intravaginal NP system and developed a PLGA-PEG-based NP for delivering siRNA against CCR5 and siRNA against Nef simultaneously as a dual preventive strategy for vaginal transmission of HIV. The siRNA NP had a particle size of

256.0±7.2 nm and a zeta-potential of -15.62±1.64mV in PBS (pH 7.4) and a particle size of 271.6±1.8 nm and a zeta-potential of -8.66±2.43mV in VFS, pH 4.2). EE% was 75.6±0.9%. NPs showed a pH-dependent release profile, with sustained release of siRNA in PBS (pH 7.4) (~25% over 14 days) and <2% release of siRNA in VFS within 48 hr. Nef-CCR5 NP at a concentration of 1.334 mg/mL could efficiently knock down Nef and CCR5 in Nef-ER cells without reducing cell viability or causing increased production of pro-inflammatory cytokines. Knocking down Nef in vitro could also reactivate autophagy that was inhibited by Nef. The gene expression of autophagy regulatory genes VPS34, TECPR-1 and UVRAG was also improved when Nef was knocked down. Nef-CCR5 NP significantly reduced more than 60% production of HIV p24 in vitro within one week. After being formulated into a vaginal gel dosage form, the siRNA NP could readily release from gel, penetrated the vaginal epithelial layer, and got taken up into Nef-ER cells and knockdown Nef and CCR5. The knockdown efficiency was lower in the vaginal mucosal co-culture model compared to that in Nef-ER cell model when NP was dosed directly to Nef-ER cells, indicating the necessity of a multiple-dose regimen for future in vivo study. In order to improve in vivo delivery of siRNA into intravaginal CD4+ cells, anti-CD4 antibody was conjugated to siRNA NP. The siRNA-NP-CD4 showed a particle size of 295.6±9.2 nm and a zeta-potential of -9.51±0.30 mV in PBS (pH 7.4) and a particle size of 307.2±5.2 nm and a zeta-potential of -3.54±0.63 mV in VFS, pH 4.2). In vitro intracellular delivery of siRNA was improved by approximately 120% via antibody conjugation to siRNA NP. Multiple-dose regimen of the 0.5% HEC gel loaded with siRNA NP-CD4 significantly improved the delivery of siRNA to intravaginal cells in a mouse model and CCR5 gene expression was significantly decreased by approximately 40% in lower vagina and 25% in upper vagina and cervix with no significant gene

knockdown observed in the 0.5% HEC gel loaded with siRNA NP-IgG group. In the future, the dosing regimen could be further optimized to achieve maximum gene knockdown effect and an in vivo anti-HIV study could be potentially performed in a humanized mouse model to evaluate the efficacy of the formulation.

We further expanded the application of antibody-conjugated NP and used it as a vehicle to achieve the intravaginal delivery of anti-α4β7 monoclonal antibody. Our results have shown that anti-α4β7 monoclonal antibody-conjugated NP had a particle size of about 250 nm and a neutral zeta potential (0 mV) in NaH_2PO_4, pH 7.0 and a particle size of about 260 nm and a close-to-neutral zeta potential (2 mV) in vaginal fluid simulant, pH 4.2. A maximum antibody loading of 43.40±0.67 μg antibody/mg NP could be achieved. The anti-α4β7 monoclonal antibody-conjugated NP loaded in 1% HEC gel maintained the binding affinity of the antibody, and could block more than 75% of total α4β7 from ex vivo vaginal explants of RM within as rapidly as 1 hr. When intravaginally administered as a single dose in a RM model, the formulation penetrated the cervicovaginal mucus and preferentially bound to $\alpha4\beta7^{high}$ CD4+ T cells and $\alpha4\beta7^{high}$ CD3+ T cells and blocked approximately 50% of α4β7 in each cell population. However, the blocking effect was not significant in overall CD4+ T cells or T cells. Therefore, a multi-dosing regimen or a sustained release delivery system needs to be used in order to achieve maximum blocking efficacy in all T cell population and to improve the coverage in cervix. The advantage of this formulation is that its blocking effects are only restricted to vaginal tract without having any detected masking effects in blood, rectum and inguinal lymph nodes under current dosing regimen. Therefore, the antibody did not spread systemically. In the future, a multiple dose regimen could be evaluated in the same model to investigate the

maximum efficiency of the formulation and the in vivo safety profile of this formulation should be evaluated in the meanwhile.

In the last project, we took advantage of PEI encapsulated NP-induced autophagy and designed a siRNA-PEI encapsulated NP system that could decrease infection and inhibit intracellular growth of C. trachomatis by knocking down PDGFR-β and inducing autophagy simultaneously. Our results showed that PDGFR-β siRNA-PEI-PLGA-PEG NP significantly induced autophagy in human vaginal epithelial cells (VK2/E6E7) 48 hr post treatment by improving autophagic degradation activity without causing pro-inflammation, apoptosis or any decrease in cell viability. Beclin-1, VPS34 (markers for initiation stage of autophagy), UVRAG, TECPR-1 (markers for degradation stage of autophagy) were found to be significantly upregulated after the treatment of PDGFR-β siRNA-PEI-PLGA-PEG NP. Furthermore, PDGFR-β siRNA-PEI-PLGA-PEG NP decreased PDGFR-β mRNA expression by 50% and protein expression by 43% in VK2/E6E7 cells 48 hr post treatment. Treatment of cells with PDGFR-β siRNA-PEI-PLGA-PEG NP greatly decreased the size and amount of intracellular C. trachomatis inclusions and protected against C. trachomatis infection in vitro. In the future, studies evaluating the in vivo efficacy and safety profiles of this formulation could be potentially conducted in a mouse model and provide evidence for the development of non-antibiotics based anti-C. trachomatis strategies.

To summarize, these nanomedicines use small molecules, siRNAs or proteins as active ingredients to combat against HIV and chlamydia. NP and gel systems were successfully employed to deliver these active compounds to target cells. Physiochemical properties of these nanomedicines were characterized. Biological mechanism of the siRNA-based

nanomedicine was studied. And both cell and animal studies were conducted and demonstrated the therapeutic potential of these nanomedicines against HIV and chlamydia without causing any toxicity. In conclusion, our nanomedicine-based intravaginal drug delivery systems demonstrate potential utility as a platform for vaginal microbicide against vaginal transmission of HIV and C. trachomatis. This research provided a novel design of intravaginal drug delivery systems to promote drug delivery, a novel concept of using autophagy as a preventive mechanism against microorganism and novel preventative nanomicrobicide systems against vaginal transmission of HIV and chlamydia. Future research could be proposed and conducted based on the concepts, techniques and platforms presented in this research to further evaluate the therapeutic efficacy of these nanomedicines, to further study the therapeutic potential of autophagy, and to further promote the drug delivery systems for microbicides.

6.2 Significant contributions, limitations and future directions

We are the first one who developed an intravaginal nanoparticle formulation that could achieve targeted delivery of SQV to CD4+ cells, and this system is versatile to deliver both hydrophilic and hydrophobic drugs. However, at current stage, the evaluation of in vitro HIV inhibition effect and in vivo investigations of the formulation were beyond our current scope of research, and therefore, in the future, studies of these areas would provide better evidence with regards to the efficacy and safety of the system and provide more information on regimen of this formulation.

We developed a novel pH-responsive combination RNAi-based nanomicrobicide as a strategy to prevent/reduce vaginal transmission of HIV. Compared to previous work, first

we facilitated this system with a pH-responsive release profile that minimized the leakage of siRNA under acidic vaginal environment. Second, we proposed a novel dual preventative strategy of combating HIV by decreasing viral entry and improving autophagic degradation of invaded viruses simultaneously. Third, by employing antibody conjugation strategy, we developed a novel intravaginal drug delivery system that could achieve targeted siRNA-mediated gene knockdown in intravaginal CD4+ cells and this system provided a platform for future studies of targeted intravaginal gene knockdown. Based on current dosing regimen, the in vivo gene knockdown was approximately 40% and future studies could be conducted to further improve the gene knockdown efficiency and optimize the dosing regimen to maximize the efficacy of the formulation. And in the future, an in vivo anti-HIV study would be desired to provide more therapeutic evidence of this formulation. Currently, this system is designed to combat R5-tropic HIV infection (>90% vaginally transmitted HIV strains are R5-tropic) and the use of this nanomicrobicide against any X4-tropic HIV would not be desirable, so in the future, siRNAs targeting CXCR4 could be loaded in the system to address the gap. Unlike condoms, microbicides do not always provide 100% protection against vaginal transmission of HIV even if they are properly used, therefore, strategies for promoting the efficacy of RNAi-based gene therapy would be highly desired to promote the development of RNAi-based microbicides.

We successfully conjugated anti-α4β7 antibody to nanoparticles without compromising its binding affinity to create a novel intravaginal drug delivery system for delivering antibodies and using this system, we were able to block α4β7 ligands on intravaginal cells in RMs with only single dose. Based on current dosing regimen, we believe the efficacy

of the formulation could still be improved and future studies would be appreciated to evaluate the blocking efficacy with multiple doses in vivo to investigate the maximized therapeutic effect. The current RMs could not mimic the acidic vaginal environment of human, therefore, ex vivo study using human vaginal fluid would be useful to evaluate the stability of antibody in this formulation and provide more information on the stability of the formulation.

We took advantage of the abilities of PEI in promoting autophagy and improving siRNA loading into NP to develop a "two-in-one" nanomicrobicide against vaginal infection of C. trachomatis by knocking down C. trachomatis binding factor, PDGFR-β and promoting autophagic degradation activity in host cells. This study provided a novel strategy to combat intracellular bacteria and this system could be employed for combating any other intracellular bacteria if a good host target of siRNA could be found. This non-antibiotic based anti-C. trachomatis formulation would provide an extra option for physicians and patients for reducing vaginal infection of C. trachomatis. At current stage, we just provided a proof-of-concept design and the system needs to be further optimized in terms of efficacy and future in vivo studies would be required to fully evaluate the system.

References:

1. Habeshaw, J.A., et al., *How HIV-1 lentivirus causes immune deficiency disease.* Med Hypotheses, 1999. 52(1): p. 59-67.
2. Douek, D.C., et al., *HIV preferentially infects HIV-specific CD4+ T cells.* Nature, 2002. 417(6884): p. 95-8.
3. Wu, L. and V.N. KewalRamani, *Dendritic-cell interactions with HIV: infection and viral dissemination.* Nat Rev Immunol, 2006. 6(11): p. 859-68.
4. Koenig, S., et al., *Detection of AIDS virus in macrophages in brain tissue from AIDS patients with encephalopathy.* Science, 1986. 233(4768): p. 1089-93.
5. Eger, K.A. and D. Unutmaz, *The innate immune system and HIV pathogenesis.* Curr HIV/AIDS Rep, 2005. 2(1): p. 10-5.
6. Weiss, R., *How does HIV cause AIDS?* Science, 1993. 260(5112): p. 1273-1279.
7. Gonda, M.A., *Molecular genetics and structure of the human immunodeficiency virus.* J Electron Microsc Tech, 1988. 8(1): p. 17-40.
8. Gayle, H., *An overview of the global HIV/AIDS epidemic, with a focus on the United States.* Aids, 2000. 14: p. S8-S17.
9. UNAIDS, *FACT SHEET NOVEMBER 2016.* 2016.
10. UNAIDS, *2013 UNAIDS Report on the global AIDS epidemic.* 2013.
11. Canada, P.H.A.o., *Summary: Estimates of HIV incidence, prevalence and proportion undiagnosed in Canada, 2014.* 2014.
12. UNAIDS, *Global report: UNAIDS report on the global AIDS epidemic 2012.* 2012.
13. UNAIDS, *Women out load: how women living with HIV will help the world end AIDS.* 2013.
14. UNAIDS, *Women, girls, gender equality and HIV*. 2011.
15. Ribeiro, P.S., et al., *Priorities for women's health from the Global Burden of Disease study.* International Journal of Gynecology & Obstetrics, 2008. 102(1): p. 82-90.
16. Hladik, F. and M.J. McElrath, *Setting the stage: host invasion by HIV*. Nature Reviews Immunology, 2008. 8(6): p. 447-457.
17. Higgins, J.A., S. Hoffman, and S.L. Dworkin, *Rethinking gender, heterosexual men, and women's vulnerability to HIV/AIDS.* Am J Public Health, 2010. 100(3): p. 435-45.
18. Furuta, Y., et al., *Infection of vaginal and colonic epithelial cells by the human immunodeficiency virus type 1 is neutralized by antibodies raised against conserved epitopes in the envelope glycoprotein gp120.* Proc Natl Acad Sci U S A, 1994. 91(26): p. 12559-63.
19. Yeaman, G.R., et al., *Chemokine receptor expression in the human ectocervix: implications for infection by the human immunodeficiency virus-type I.* Immunology, 2004. 113(4): p. 524-33.
20. Bobardt, M.D., et al., *Cell-free human immunodeficiency virus type 1 transcytosis through primary genital epithelial cells.* J Virol, 2007. 81(1): p. 395-405.
21. Stoddard, E., et al., *gp340 expressed on human genital epithelia binds HIV-1 envelope protein and facilitates viral transmission.* J Immunol, 2007. 179(5): p. 3126-32.

22. Hladik, F., et al., *Initial events in establishing vaginal entry and infection by human immunodeficiency virus type-1.* Immunity, 2007. 26(2): p. 257-270.
23. Lederman, M.M., R.E. Offord, and O. Hartley, *Microbicides and other topical strategies to prevent vaginal transmission of HIV.* Nat Rev Immunol, 2006. 6(5): p. 371-82.
24. Bleul, C.C., et al., *The HIV coreceptors CXCR4 and CCR5 are differentially expressed and regulated on human T lymphocytes.* Proc Natl Acad Sci U S A, 1997. 94(5): p. 1925-30.
25. Lifson, J.D. and E.G. Engleman, *Role of CD4 in normal immunity and HIV infection.* Immunol Rev, 1989. 109: p. 93-117.
26. Oppermann, M., *Chemokine receptor CCR5: insights into structure, function, and regulation.* Cell Signal, 2004. 16(11): p. 1201-10.
27. Fatima Barmania, M.S.P., *C-C chemokine receptor type five (CCR5): An emerging target for the control of HIV infection.* Applied & Translational Genomics, 2013. 2: p. 3-16.
28. Malhotra, M., et al., *Genital Chlamydia trachomatis: an update.* Indian J Med Res, 2013. 138(3): p. 303-16.
29. Canda, P.H.A.o., *Canadian Guidelines on Sexually Transmitted Infections, Section 5 - Management and Treatment of Specific Infections, Chlamydia Infections.*
30. White, J.A., *Manifestations and management of lymphogranuloma venereum.* Curr Opin Infect Dis, 2009. 22(1): p. 57-66.
31. O'Farrell, N., et al., *Genital ulcers and concomitant complaints in men attending a sexually transmitted infections clinic: implications for sexually transmitted infections management.* Sex Transm Dis, 2008. 35(6): p. 545-9.
32. Prevention, C.f.D.C.a., *Chlamydia - CDC Fact Sheet.*
33. Totten S, M.R., Payne E, Severini A, *Chlamydia and lymphogranuloma venereum in Canada: 2003-2012 Summary Report.* Canada Communicable Disease Report, 2015. 41-01(1481-8531).
34. Patrick DM, W.T., Jordan R, *Sexually transmitted infections in Canada: recent resurgence threatens national goals.* Canadian Journal of Human Sexuality, 2000. 9: p. 149-165.
35. Elwell, C., K. Mirrashidi, and J. Engel, *Chlamydia cell biology and pathogenesis.* Nat Rev Microbiol, 2016. 14(6): p. 385-400.
36. Korenromp, E.L., et al., *What proportion of episodes of gonorrhoea and chlamydia becomes symptomatic?* Int J STD AIDS, 2002. 13(2): p. 91-101.
37. Sandoz, K.M. and D.D. Rockey, *Antibiotic resistance in Chlamydiae.* Future Microbiol, 2010. 5(9): p. 1427-42.
38. Louik, C., M.M. Werler, and A.A. Mitchell, *Erythromycin use during pregnancy in relation to pyloric stenosis.* American Journal of Obstetrics and Gynecology, 2002. 186(2): p. 288-290.
39. Bahat Dinur, A., et al., *Fetal safety of macrolides.* Antimicrob Agents Chemother, 2013. 57(7): p. 3307-11.
40. Cross, R., et al., *Revisiting doxycycline in pregnancy and early childhood--time to rebuild its reputation?* Expert Opin Drug Saf, 2016. 15(3): p. 367-82.
41. Periti, P., et al., *Adverse effects of macrolide antibacterials.* Drug Saf, 1993. 9(5): p. 346-64.

42. Sanchez, A.R., R.S. Rogers, 3rd, and P.J. Sheridan, *Tetracycline and other tetracycline-derivative staining of the teeth and oral cavity.* Int J Dermatol, 2004. 43(10): p. 709-15.
43. Taylor, B.D. and C.L. Haggerty, *Management of Chlamydia trachomatis genital tract infection: screening and treatment challenges.* Infect Drug Resist, 2011. 4: p. 19-29.
44. WHO, *Microbicides.*
45. Nutan and S.K. Gupta, *Microbicides: a new hope for HIV prevention.* Indian J Med Res, 2011. 134(6): p. 939-49.
46. Morrow, K.M. and C. Hendrix, *Clinical evaluation of microbicide formulations.* Antiviral Res, 2010. 88 Suppl 1: p. S40-6.
47. McGowan, I. and C. Dezzutti, *Rectal microbicide development.* Curr Top Microbiol Immunol, 2014. 383: p. 117-36.
48. Abdool Karim, S.S. and C. Baxter, *Overview of microbicides for the prevention of human immunodeficiency virus.* Best Pract Res Clin Obstet Gynaecol, 2012. 26(4): p. 427-39.
49. Ensign, L.M., et al., *Mucus-penetrating nanoparticles for vaginal drug delivery protect against herpes simplex virus.* Sci Transl Med, 2012. 4(138): p. 138ra79.
50. Kanazawa, T., et al., *Needle-free intravaginal DNA vaccination using a stearoyl oligopeptide carrier promotes local gene expression and immune responses.* Int J Pharm, 2013. 447(1-2): p. 70-4.
51. Woodrow, K.A., et al., *Intravaginal gene silencing using biodegradable polymer nanoparticles densely loaded with small-interfering RNA.* Nat Mater, 2009. 8(6): p. 526-33.
52. Morrow, R.J., et al., *Sustained release of proteins from a modified vaginal ring device.* Eur J Pharm Biopharm, 2011. 77(1): p. 3-10.
53. Acarturk, F., *Mucoadhesive vaginal drug delivery systems.* Recent Pat Drug Deliv Formul, 2009. 3(3): p. 193-205.
54. Nelson, A.L., *The Benefits of Vaginal Drug Administration—Communicating Effectively With Patients: The Vagina: New Options for the Administration of Medications.* Medscape, 2017.
55. Mahalingam, A., et al., *Vaginal microbicide gel for delivery of IQP-0528, a pyrimidinedione analog with a dual mechanism of action against HIV-1.* Antimicrob Agents Chemother, 2011. 55(4): p. 1650-60.
56. Wheeler, L.A., et al., *Inhibition of HIV transmission in human cervicovaginal explants and humanized mice using CD4 aptamer-siRNA chimeras.* J Clin Invest, 2011. 121(6): p. 2401-12.
57. Alexander, N.J., et al., *Why consider vaginal drug administration?* Fertil Steril, 2004. 82(1): p. 1-12.
58. Hickey, R.J., et al., *Understanding vaginal microbiome complexity from an ecological perspective.* Transl Res, 2012. 160(4): p. 267-82.
59. O'Hanlon, D.E., T.R. Moench, and R.A. Cone, *Vaginal pH and microbicidal lactic acid when lactobacilli dominate the microbiota.* PLoS One, 2013. 8(11): p. e80074.
60. Martin, R. and J.E. Suarez, *Biosynthesis and degradation of H2O2 by vaginal lactobacilli.* Appl Environ Microbiol, 2010. 76(2): p. 400-5.

61. Owen, D.H. and D.F. Katz, *A vaginal fluid simulant.* Contraception, 1999. 59(2): p. 91-5.
62. Spear, G.T., et al., *Effect of pH on Cleavage of Glycogen by Vaginal Enzymes.* PLoS One, 2015. 10(7): p. e0132646.
63. Acarturk, F., Z.I. Parlatan, and O.F. Saracoglu, *Comparison of vaginal aminopeptidase enzymatic activities in various animals and in humans.* J Pharm Pharmacol, 2001. 53(11): p. 1499-504.
64. Goldberg, D.M., D.M. Hart, and C. Watts, *Distribution of enzymes in human vaginal fluid . Relevance to the diagnosis of cervical cancer.* Cancer, 1968. 21(5): p. 964-73.
65. Dasari, S., W. Rajendra, and L. Valluru, *Evaluation of microbial enzymes in normal and abnormal cervicovaginal fluids of cervical dysplasia: a case control study.* Biomed Res Int, 2014. 2014: p. 716346.
66. Ensign, L.M., R. Cone, and J. Hanes, *Nanoparticle-based drug delivery to the vagina: a review.* J Control Release, 2014. 190: p. 500-14.
67. Charles R. B. Beckmann, W.H., Douglas Laube, Frank Ling, Roger Smith, *Obstetrics and Gynecology (7th edition).* Lippincott Williams & Wilkins, 2014: p. 260.
68. Katz, G.L.R.L.D.G.V., *Comprehensive Gynecology.* Elsevier, 2012: p. 532-533.
69. Lai, S.K., Y.Y. Wang, and J. Hanes, *Mucus-penetrating nanoparticles for drug and gene delivery to mucosal tissues.* Adv Drug Deliv Rev, 2009. 61(2): p. 158-71.
70. Kieweg, S.L., A.R. Geonnotti, and D.F. Katz, *Gravity-induced coating flows of vaginal gel formulations: in vitro experimental analysis.* J Pharm Sci, 2004. 93(12): p. 2941-52.
71. Kieweg, S.L. and D.F. Katz, *Squeezing flows of vaginal gel formulations relevant to microbicide drug delivery.* J Biomech Eng, 2006. 128(4): p. 540-53.
72. Wilson, M., *Book Bacteriology of Humans: An Ecological Perspective.* 2008: p. 197.
73. Sheehan, J.K. and I. Carlstedt, *Hydrodynamic properties of human cervical-mucus glycoproteins in 6M-guanidinium chloride.* Biochem J, 1984. 217(1): p. 93-101.
74. Thornton, D.J., et al., *Quantitation of mucus glycoproteins blotted onto nitrocellulose membranes.* Anal Biochem, 1989. 182(1): p. 160-4.
75. Dekker, J., et al., *The MUC family: an obituary.* Trends Biochem Sci, 2002. 27(3): p. 126-31.
76. Van Klinken, B.J., et al., *Mucin gene structure and expression: protection vs. adhesion.* Am J Physiol, 1995. 269(5 Pt 1): p. G613-27.
77. Ceric, F., D. Silva, and P. Vigil, *Ultrastructure of the human periovulatory cervical mucus.* J Electron Microsc (Tokyo), 2005. 54(5): p. 479-84.
78. Lai, S.K., et al., *Nanoparticles reveal that human cervicovaginal mucus is riddled with pores larger than viruses (vol 107, pg 598, 2010).* Proceedings of the National Academy of Sciences of the United States of America, 2011. 108(34): p. 14371-14371.
79. Sheehan, J.K., K. Oates, and I. Carlstedt, *Electron microscopy of cervical, gastric and bronchial mucus glycoproteins.* Biochem J, 1986. 239(1): p. 147-53.

80. das Neves, J., M. Amiji, and B. Sarmento, *Mucoadhesive nanosystems for vaginal microbicide development: friend or foe?* Wiley Interdiscip Rev Nanomed Nanobiotechnol, 2011. 3(4): p. 389-99.
81. das Neves, J., Sarmento, Bruno *Mucosal Delivery of Biopharmaceuticals: Biology, Challenges and Strategies.* Springer, 2014: p. 63.
82. Lai, S.K., et al., *Rapid transport of large polymeric nanoparticles in fresh undiluted human mucus.* Proc Natl Acad Sci U S A, 2007. 104(5): p. 1482-7.
83. Wang, Y.Y., et al., *Addressing the PEG mucoadhesivity paradox to engineer nanoparticles that "slip" through the human mucus barrier.* Angew Chem Int Ed Engl, 2008. 47(50): p. 9726-9.
84. Blaskewicz, C.D., J. Pudney, and D.J. Anderson, *Structure and function of intercellular junctions in human cervical and vaginal mucosal epithelia.* Biol Reprod, 2011. 85(1): p. 97-104.
85. Forbes, C.J., et al., *Modified silicone elastomer vaginal gels for sustained release of antiretroviral HIV microbicides.* J Pharm Sci, 2014. 103(5): p. 1422-32.
86. Chavoustie, S.E., et al., *Metronidazole vaginal gel 1.3% in the treatment of bacterial vaginosis: a dose-ranging study.* J Low Genit Tract Dis, 2015. 19(2): p. 129-34.
87. O'Brien, J.M., et al., *Progesterone vaginal gel for the reduction of recurrent preterm birth: primary results from a randomized, double-blind, placebo-controlled trial.* Ultrasound Obstet Gynecol, 2007. 30(5): p. 687-96.
88. Abdool Karim, Q., et al., *Effectiveness and safety of tenofovir gel, an antiretroviral microbicide, for the prevention of HIV infection in women.* Science, 2010. 329(5996): p. 1168-74.
89. Ning, M., et al., *Preparation, in vitro and in vivo evaluation of liposomal/niosomal gel delivery systems for clotrimazole.* Drug Dev Ind Pharm, 2005. 31(4-5): p. 375-83.
90. Zhang, Y., et al., *A Bioadhesive Nanoparticle-Hydrogel Hybrid System for Localized Antimicrobial Drug Delivery.* ACS Appl Mater Interfaces, 2016. 8(28): p. 18367-74.
91. Katz, D.F., A. Yuan, and Y. Gao, *Vaginal drug distribution modeling.* Adv Drug Deliv Rev, 2015. 92: p. 2-13.
92. Akil, A., et al., *Development and Characterization of a Vaginal Film Containing Dapivirine, a Non- nucleoside Reverse Transcriptase Inhibitor (NNRTI), for prevention of HIV-1 sexual transmission.* Drug Deliv Transl Res, 2011. 1(3): p. 209-222.
93. Ham, A.S., et al., *Vaginal film drug delivery of the pyrimidinedione IQP-0528 for the prevention of HIV infection.* Pharm Res, 2012. 29(7): p. 1897-907.
94. Zhang, W., et al., *Vaginal Microbicide Film Combinations of Two Reverse Transcriptase Inhibitors, EFdA and CSIC, for the Prevention of HIV-1 Sexual Transmission.* Pharm Res, 2015. 32(9): p. 2960-72.
95. Cunha-Reis, C., et al., *Nanoparticles-in-film for the combined vaginal delivery of anti-HIV microbicide drugs.* J Control Release, 2016. 243: p. 43-53.
96. Mishra, R., P. Joshi, and T. Mehta, *Formulation, development and characterization of mucoadhesive film for treatment of vaginal candidiasis.* Int J Pharm Investig, 2016. 6(1): p. 47-55.

97. Kumar, L., et al., *Preparation and characterisation of fluconazole vaginal films for the treatment of vaginal candidiasis.* Indian J Pharm Sci, 2013. 75(5): p. 585-90.
98. Moss, J.A., et al., *Pharmacokinetics of a multipurpose pod-intravaginal ring simultaneously delivering five drugs in an ovine model.* Antimicrob Agents Chemother, 2013. 57(8): p. 3994-7.
99. Villegas, G., et al., *A Novel Microbicide/Contraceptive Intravaginal Ring Protects Macaque Genital Mucosa against SHIV-RT Infection Ex Vivo.* PLoS One, 2016. 11(7): p. e0159332.
100. Gunawardana, M., et al., *An intravaginal ring for the sustained delivery of antibodies.* J Pharm Sci, 2014. 103(11): p. 3611-20.
101. Woolfson, A.D., R.K. Malcolm, and R.J. Gallagher, *Design of a silicone reservoir intravaginal ring for the delivery of oxybutynin.* J Control Release, 2003. 91(3): p. 465-76.
102. Roumen, F.J., *Review of the combined contraceptive vaginal ring, NuvaRing.* Ther Clin Risk Manag, 2008. 4(2): p. 441-51.
103. Bahadoran, P., F.K. Rokni, and F. Fahami, *Investigating the therapeutic effect of vaginal cream containing garlic and thyme compared to clotrimazole cream for the treatment of mycotic vaginitis.* Iran J Nurs Midwifery Res, 2010. 15(Suppl 1): p. 343-9.
104. Lebherz, T.B., et al., *A comparison of the efficacy of two vaginal creams for vulvovaginal candidiasis, and correlations with the presence of Candida species in the perianal area and oral contraceptive use.* Clin Ther, 1983. 5(4): p. 409-16.
105. Lindahl, S.H., *Reviewing the options for local estrogen treatment of vaginal atrophy.* Int J Womens Health, 2014. 6: p. 307-12.
106. Garcia Figueroa, R.G., et al., *[Effectiveness and safety of ciclopirox olamine 1% vaginal cream versus terconazole 0.8% vaginal cream in the treatment of genital candidiasis].* Ginecol Obstet Mex, 2000. 68: p. 154-9.
107. Larsson, P.G., et al., *Treatment with 2% clindamycin vaginal cream prior to first trimester surgical abortion to reduce signs of postoperative infection: a prospective, double-blinded, placebo-controlled, multicenter study.* Acta Obstet Gynecol Scand, 2000. 79(5): p. 390-6.
108. Scher, J., et al., *A Comparison between Vaginal Prostaglandin-E2 Suppositories and Intrauterine Extra-Amniotic Prostaglandins in the Management of Fetal Death Inutero.* American Journal of Obstetrics and Gynecology, 1980. 137(7): p. 769-772.
109. Gimes, G. and F. Peter, *[Clinical significance of betadine vaginal suppository treatment in pregnancy].* Acta Pharm Hung, 1997. 67(6): p. 249-53.
110. Anderson, M., S. Kutzner, and R.H. Kaufman, *Treatment of vulvovaginal lichen planus with vaginal hydrocortisone suppositories.* Obstet Gynecol, 2002. 100(2): p. 359-62.
111. Adamson, G.D., et al., *Three-day treatment with butoconazole vaginal suppositories for vulvovaginal candidiasis.* J Reprod Med, 1986. 31(2): p. 131-2.
112. Prutting, S.M. and J.D. Cerveny, *Boric acid vaginal suppositories: a brief review.* Infect Dis Obstet Gynecol, 1998. 6(4): p. 191-4.
113. Karasulu, H.Y., et al., *Efficacy of a new ketoconazole bioadhesive vaginal tablet on Candida albicans.* Farmaco, 2004. 59(2): p. 163-7.

114. Notelovitz, M., et al., *Estradiol absorption from vaginal tablets in postmenopausal women.* Obstet Gynecol, 2002. 99(4): p. 556-62.
115. Gupta, N.V., et al., *Bioadhesive vaginal tablets containing spray dried microspheres loaded with clotrimazole for treatment of vaginal candidiasis.* Acta Pharm, 2013. 63(3): p. 359-72.
116. Hassan, A.A., *A comparison of oral misoprostol tablets and vaginal prostaglandin E2 pessary in induction of labour at term.* J Coll Physicians Surg Pak, 2005. 15(5): p. 284-7.
117. McConville, C., et al., *Development of a multi-layered vaginal tablet containing dapivirine, levonorgestrel and acyclovir for use as a multipurpose prevention technology.* Eur J Pharm Biopharm, 2016. 104: p. 171-9.
118. Levy, T., et al., *Pharmacokinetics of natural progesterone administered in the form of a vaginal tablet.* Hum Reprod, 1999. 14(3): p. 606-10.
119. Cevrioglu, A.S., N. Akdemir, and G. Ilhan, *The comparison of hyaluronic acid vaginal tablets in the treatment of atrophic vaginitis.* Arch Gynecol Obstet, 2012. 286(1): p. 265.
120. Ham, A.S., et al., *Targeted Delivery of PSC-RANTES for HIV-1 Prevention using Biodegradable Nanoparticles.* Pharmaceutical Research, 2009. 26(3): p. 502-511.
121. Chaowanachan, T., et al., *Drug Synergy of Tenofovir and Nanoparticle-Based Antiretrovirals for HIV Prophylaxis.* Plos One, 2013. 8(4).
122. das Neves, J., et al., *Polymeric Nanoparticles Affect the Intracellular Delivery, Antiretroviral Activity and Cytotoxicity of the Microbicide Drug Candidate Dapivirine.* Pharmaceutical Research, 2012. 29(6): p. 1468-1484.
123. Date, A.A., et al., *Development and evaluation of a thermosensitive vaginal gel containing raltegravir plus efavirenz loaded nanoparticles for HIV prophylaxis.* Antiviral Research, 2012. 96(3): p. 430-436.
124. Peng, W.D., et al., *DNA nanotherapy for pre-neoplastic cervical lesions.* Gynecologic Oncology, 2013. 128(1): p. 101-106.
125. Blum, J.S., et al., *Prevention of K-Ras- and Pten-mediated intravaginal tumors by treatment with camptothecin-loaded PLGA nanoparticles.* Drug Delivery and Translational Research, 2011. 1(5): p. 383-394.
126. Yang, M., et al., *Vaginal Delivery of Paclitaxel via Nanoparticles with Non-Mucoadhesive Surfaces Suppresses Cervical Tumor Growth.* Advanced Healthcare Materials, 2014. 3(7): p. 1044-1052.
127. Steinbach, J.M., et al., *Polymer nanoparticles encapsulating siRNA for treatment of HSV-2 genital infection.* Journal of Controlled Release, 2012. 162(1): p. 102-110.
128. Woodrow, K.A., et al., *Intravaginal gene silencing using biodegradable polymer nanoparticles densely loaded with small-interfering RNA.* Nature Materials, 2009. 8(6): p. 526-533.
129. das Neves, J., et al., *Polymer-based nanocarriers for vaginal drug delivery.* Adv Drug Deliv Rev, 2015. 92: p. 53-70.
130. Jatzkewitz, H., *[Incorporation of physiologically-active substances into a colloidal blood plasma substitute. I. Incorporation of mescaline peptide into polyvinylpyrrolidone].* Hoppe Seylers Z Physiol Chem, 1954. 297(3-6): p. 149-56.

131. B.V.N. Nagavarma, H.Y., A. Ayaz, H. G. Shivakumar, *Different techniques for preparation of polymeric nanoparticles- A review.* Asian Journal of Pharmaceutical and Clinical Research, 2012. 5: p. 16-23.
132. Chen, Z.G., *Small-molecule delivery by nanoparticles for anticancer therapy.* Trends Mol Med, 2010. 16(12): p. 594-602.
133. Shu, S., et al., *Delivery of protein drugs using nanoparticles self-assembled from dextran sulfate and quaternized chitosan.* J Control Release, 2011. 152 Suppl 1: p. e170-2.
134. Munier, S., et al., *Cationic PLA nanoparticles for DNA delivery: comparison of three surface polycations for DNA binding, protection and transfection properties.* Colloids Surf B Biointerfaces, 2005. 43(3-4): p. 163-73.
135. Singh, R. and J.W. Lillard, Jr., *Nanoparticle-based targeted drug delivery.* Exp Mol Pathol, 2009. 86(3): p. 215-23.
136. Desai, M.P., et al., *The mechanism of uptake of biodegradable microparticles in Caco-2 cells is size dependent.* Pharm Res, 1997. 14(11): p. 1568-73.
137. Panyam, J. and V. Labhasetwar, *Biodegradable nanoparticles for drug and gene delivery to cells and tissue.* Adv Drug Deliv Rev, 2003. 55(3): p. 329-47.
138. Panyam, J., et al., *Fluorescence and electron microscopy probes for cellular and tissue uptake of poly(D,L-lactide-co-glycolide) nanoparticles.* Int J Pharm, 2003. 262(1-2): p. 1-11.
139. Choi, S., et al., *Single chain variable fragment CD7 antibody conjugated PLGA/HDAC inhibitor immuno-nanoparticles: developing human T cell-specific nano-technology for delivery of therapeutic drugs targeting latent HIV*. J Control Release, 2011. 152 Suppl 1: p. e9-10.
140. Sheng, Y., et al., *Long-circulating polymeric nanoparticles bearing a combinatorial coating of PEG and water-soluble chitosan.* Biomaterials, 2009. 30(12): p. 2340-8.
141. Shaikh, J., et al., *Nanoparticle encapsulation improves oral bioavailability of curcumin by at least 9-fold when compared to curcumin administered with piperine as absorption enhancer.* Eur J Pharm Sci, 2009. 37(3-4): p. 223-30.
142. Pongrac, I.M., et al., *Improved biocompatibility and efficient labeling of neural stem cells with poly(L-lysine)-coated maghemite nanoparticles.* Beilstein J Nanotechnol, 2016. 7: p. 926-36.
143. Campos, E.V., et al., *Polymeric and Solid Lipid Nanoparticles for Sustained Release of Carbendazim and Tebuconazole in Agricultural Applications.* Sci Rep, 2015. 5: p. 13809.
144. Lv, Y., et al., *Novel multifunctional pH-sensitive nanoparticles loaded into microbubbles as drug delivery vehicles for enhanced tumor targeting.* Sci Rep, 2016. 6: p. 29321.
145. Ballou, B., et al., *Nanoparticle transport from mouse vagina to adjacent lymph nodes.* PLoS One, 2012. 7(12): p. e51995.
146. Barua, S. and S. Mitragotri, *Challenges associated with Penetration of Nanoparticles across Cell and Tissue Barriers: A Review of Current Status and Future Prospects.* Nano Today, 2014. 9(2): p. 223-243.
147. Guo, S.T. and L. Huang, *Nanoparticles Escaping RES and Endosome: Challenges for siRNA Delivery for Cancer Therapy.* Journal of Nanomaterials, 2011.

148. Kumari, A., S.K. Yadav, and S.C. Yadav, *Biodegradable polymeric nanoparticles based drug delivery systems.* Colloids and Surfaces B-Biointerfaces, 2010. 75(1): p. 1-18.
149. Ensign, L.M., R. Cone, and J. Hanes, *Nanoparticle-based drug delivery to the vagina: A review.* Journal of Controlled Release, 2014. 190: p. 500-514.
150. G. F. Moore, S.M.S., *Advances in Biodegradable Polymers.* 1997.
151. Makadia, H.K. and S.J. Siegel, *Poly Lactic-co-Glycolic Acid (PLGA) as Biodegradable Controlled Drug Delivery Carrier.* Polymers (Basel), 2011. 3(3): p. 1377-1397.
152. Crotts, G. and T.G. Park, *Protein delivery from poly(lactic-co-glycolic acid) biodegradable microspheres: release kinetics and stability issues.* Journal of Microencapsulation, 1998. 15(6): p. 699-713.
153. Kranz, H., et al., *Physicomechanical properties of biodegradable poly(D,L-lactide) and poly(D,L-lactide-co-glycolide) films in the dry and wet states.* J Pharm Sci, 2000. 89(12): p. 1558-66.
154. Campolongo, M.J. and D. Luo, *Drug delivery: Old polymer learns new tracts.* Nature Materials, 2009. 8(6): p. 447-8.
155. Bicho, A., et al., *Anti-CD8 conjugated nanoparticles to target mammalian cells expressing CD8.* Int J Pharm, 2010. 399(1-2): p. 80-86.
156. Farokhzad, O.C., et al., *Targeted nanoparticle-aptamer bioconjugates for cancer chemotherapy in vivo.* Proceedings of the National Academy of Sciences of the United States of America, 2006. 103(16): p. 6315-6320.
157. Geldenhuys, W., et al., *Brain-targeted delivery of paclitaxel using glutathione-coated nanoparticles for brain cancers.* Journal of Drug Targeting, 2011. 19(9): p. 837-845.
158. Aaron C. Anselmo, S.M., *Nanoparticles in the clinic.* Bioengineering&Translational Medicine, 2016. 1(1): p. 10-29.
159. Vermani, K. and S. Garg, *The scope and potential of vaginal drug delivery.* Pharm Sci Technolo Today, 2000. 3(10): p. 359-364.
160. das Neves, J. and M.F. Bahia, *Gels as vaginal drug delivery systems.* International Journal of Pharmaceutics, 2006. 318(1-2): p. 1-14.
161. Sweet, R.L., *New approaches for the treatment of bacterial vaginosis.* Am J Obstet Gynecol, 1993. 169(2 Pt 2): p. 479-82.
162. Garg, S., et al., *Properties of a new acid-buffering bioadhesive vaginal formulation (ACIDFORM).* Contraception, 2001. 64(1): p. 67-75.
163. Kahraman, S., S.H. Karagozoglu, and G. Karlikaya, *The efficiency of progesterone vaginal gel versus intramuscular progesterone for luteal phase supplementation in gonadotropin-releasing hormone antagonist cycles: a prospective clinical trial.* Fertil Steril, 2010. 94(2): p. 761-3.
164. Carati, D., et al., *Safety, efficacy, and tolerability of differential treatment to prevent and treat vaginal dryness and vulvovaginitis in diabetic women.* Clin Exp Obstet Gynecol, 2016. 43(2): p. 198-202.
165. Michael E. Aulton, K.M.G.T., *Aulton's Pharmaceutics: The Design and Manufacture of Medicines (4th edition).* Elsevier, 2013: p. 743-746.
166. Forbes, C.J., et al., *Non-aqueous silicone elastomer gels as a vaginal microbicide delivery system for the HIV-1 entry inhibitor maraviroc.* Journal of Controlled Release, 2011. 156(2): p. 161-169.

167. Qiu, Y. and K. Park, *Environment-sensitive hydrogels for drug delivery.* Adv Drug Deliv Rev, 2001. 53(3): p. 321-39.
168. Chang, J.Y., et al., *Prolonged antifungal effects of clotrimazole-containing mucoadhesive thermosensitive gels on vaginitis.* J Control Release, 2002. 82(1): p. 39-50.
169. Gupta, K.M., et al., *Temperature and pH sensitive hydrogels: an approach towards smart semen-triggered vaginal microbicidal vehicles.* J Pharm Sci, 2007. 96(3): p. 670-81.
170. Chen, D., et al., *pH and temperature dual-sensitive liposome gel based on novel cleavable mPEG-Hz-CHEMS polymeric vaginal delivery system.* Int J Nanomedicine, 2012. 7: p. 2621-30.
171. Edith Mathiowitz, D.E.C.I., Claus-Michael Lehr, *Bioadhesive Drug Delivery Systems, Fundamentals, Novel Approaches, and Development.* 1999: p. 520-521.
172. Hoare, T.R. and D.S. Kohane, *Hydrogels in drug delivery: Progress and challenges.* Polymer, 2008. 49(8): p. 1993-2007.
173. Parker, R., *The global HIV/AIDS pandemic, structural inequalities, and the politics of international health.* Am J Public Health, 2002. 92(3): p. 343-6.
174. UNAIDS, *UNAIDS 2011 World AIDS Day Report.* 2011.
175. Smith, S.M., *Pre-exposure chemoprophylaxis for HIV: it is time.* Retrovirology, 2004. 1: p. 16.
176. Youle, M. and M.A. Wainberg, *Pre-exposure chemoprophylaxis (PREP) as an HIV prevention strategy.* J Int Assoc Physicians AIDS Care (Chic), 2003. 2(3): p. 102-5.
177. Garg, A.B., J. Nuttall, and J. Romano, *The future of HIV microbicides: challenges and opportunities.* Antivir Chem Chemother, 2009. 19(4): p. 143-50.
178. Vella, S. and M. Floridia, *Saquinavir. Clinical pharmacology and efficacy.* Clin Pharmacokinet, 1998. 34(3): p. 189-201.
179. *AIDSinfo Drug Database.* NIH.
180. Miller, C.J. and R.J. Shattock, *Target cells in vaginal HIV transmission.* Microbes Infect, 2003. 5(1): p. 59-67.
181. Govender, T., et al., *Polymeric Nanoparticles for Enhancing Antiretroviral Drug Therapy.* Drug delivery, 2008. 15(8): p. 493-501.
182. Mallipeddi, R. and L.C. Rohan, *Progress in antiretroviral drug delivery using nanotechnology.* International Journal of Nanomedicine, 2010. 5: p. 533-547.
183. Nowacek, A.S., et al., *Nanoformulated Antiretroviral Drug Combinations Extend Drug Release and Antiretroviral Responses in HIV-1-Infected Macrophages: Implications for NeuroAIDS Therapeutics.* Journal of Neuroimmune Pharmacology, 2010. 5(4): p. 592-601.
184. Peer, D., *Induction of therapeutic gene silencing in leukocyte-implicated diseases by targeted and stabilized nanoparticles: A mini-review.* Journal of Controlled Release, 2010. 148(1): p. 63-68.
185. Gandapu, U., et al., *Curcumin-loaded apotransferrin nanoparticles provide efficient cellular uptake and effectively inhibit HIV-1 replication in vitro.* Plos One, 2011. 6(8): p. e23388.
186. Dou, H., et al., *Development of a macrophage-based nanoparticle platform for antiretroviral drug delivery.* Blood, 2006. 108(8): p. 2827-35.

187. Reddy, S.T., et al., *In vivo targeting of dendritic cells in lymph nodes with poly(propylene sulfide) nanoparticles.* Journal of Controlled Release, 2006. 112(1): p. 26-34.
188. Date, A.A., et al., *Development and evaluation of a thermosensitive vaginal gel containing raltegravir+efavirenz loaded nanoparticles for HIV prophylaxis.* Antiviral Res, 2012. 96(3): p. 430-6.
189. Joag, S.V., et al., *Animal model of mucosally transmitted human immunodeficiency virus type 1 disease: Intravaginal and oral deposition of simian/human immunodeficiency virus in macaques results in systemic infection, elimination of CD4(+) T cells, and AIDS.* Journal of Virology, 1997. 71(5): p. 4016-4023.
190. Rao, J.P. and K.E. Geckeler, *Polymer nanoparticles: Preparation techniques and size-control parameters.* Progress in Polymer Science, 2011. 36(7): p. 887-913.
191. Farokhzad, O.C., et al., *Targeted nanoparticle-aptamer bioconjugates for cancer chemotherapy in vivo.* Proc Natl Acad Sci U S A, 2006. 103(16): p. 6315-20.
192. Hladik, F. and M.J. McElrath, *Setting the stage: host invasion by HIV.* Nat Rev Immunol, 2008. 8(6): p. 447-57.
193. Rohan, L.C., et al., *In Vitro and Ex Vivo Testing of Tenofovir Shows It Is Effective As an HIV-1 Microbicide.* Plos One, 2010. 5(2).
194. Karim, Q.A., *Effectiveness and safety of tenofovir gel, an antiretroviral microbicide, for the prevention of HIV infection in women (September, pg 1168, 2010).* Science, 2011. 333(6042): p. 524-524.
195. Merrill, D.P., et al., *Antagonism between human immunodeficiency virus type 1 protease inhibitors indinavir and saquinavir in vitro.* Journal of Infectious Diseases, 1997. 176(1): p. 265-268.
196. Mallipeddi, R. and L.C. Rohan, *Nanoparticle-based vaginal drug delivery systems for HIV prevention.* Expert Opin Drug Deliv, 2010. 7(1): p. 37-48.
197. Destache, C.J., et al., *Combination antiretroviral drugs in PLGA nanoparticle for HIV-1.* Bmc Infectious Diseases, 2009. 9.
198. Shah, L.K. and M.M. Amiji, *Intracellular delivery of saquinavir in biodegradable polymeric nanoparticles for HIV/AIDS.* Pharmaceutical Research, 2006. 23(11): p. 2638-2645.
199. Nowacek, A.S., et al., *Analyses of nanoformulated antiretroviral drug charge, size, shape and content for uptake, drug release and antiviral activities in human monocyte-derived macrophages.* Journal of Controlled Release, 2011. 150(2): p. 204-211.
200. Zhang, T., T.F. Sturgis, and B.B.C. Youan, *pH-responsive nanoparticles releasing tenofovir intended for the prevention of HIV transmission.* European Journal of Pharmaceutics and Biopharmaceutics, 2011. 79(3): p. 526-536.
201. das Neves, J., et al., *Polymeric nanoparticles affect the intracellular delivery, antiretroviral activity and cytotoxicity of the microbicide drug candidate dapivirine.* Pharmaceutical Research, 2012. 29(6): p. 1468-84.
202. Yang, J., et al., *Antibody conjugated magnetic PLGA nanoparticles for diagnosis and treatment of breast cancer.* Journal of Materials Chemistry, 2007. 17(26): p. 2695-2699.

203. Yang, L.L., et al., *Single Chain Epidermal Growth Factor Receptor Antibody Conjugated Nanoparticles for in vivo Tumor Targeting and Imaging.* Small, 2009. 5(2): p. 235-243.
204. Peer, D., et al., *Nanocarriers as an emerging platform for cancer therapy.* Nature Nanotechnology, 2007. 2(12): p. 751-760.
205. Bicho, A., et al., *Anti-CD8 conjugated nanoparticles to target mammalian cells expressing CD8.* International Journal of Pharmaceutics, 2010. 399(1-2): p. 80-86.
206. Dinauer, N., et al., *Selective targeting of antibody-conjugated nanoparticles to leukemic cells and primary T-lymphocytes.* Biomaterials, 2005. 26(29): p. 5898-5906.
207. Endsley, A.N. and R.J. Ho, *Enhanced anti-HIV efficacy of indinavir after inclusion in CD4-targeted lipid nanoparticles.* J Acquir Immune Defic Syndr, 2012. 61(4): p. 417-24.
208. das Neves, J., M. Amiji, and B. Sarmento, *Mucoadhesive nanosystems for vaginal microbicide development: friend or foe?* Wiley Interdisciplinary Reviews-Nanomedicine and Nanobiotechnology, 2011. 3(4): p. 389-399.
209. Musumeci, T., et al., *PLA/PLGA nanoparticles for sustained release of docetaxel.* Int J Pharm, 2006. 325(1-2): p. 172-179.
210. Kuo, Y.C. and H.H. Chen, *Entrapment and release of saquinavir using novel cationic solid lipid nanoparticles.* International Journal of Pharmaceutics, 2009. 365(1-2): p. 206-213.
211. Sharma, P. and S. Garg, *Pure drug and polymer based nanotechnologies for the improved solubility, stability, bioavailability and targeting of anti-HIV drugs.* Adv Drug Deliv Rev, 2010. 62(4-5): p. 491-502.
212. Sehgal, D. and I.K. Vijay, *A Method for the High-Efficiency of Water-Soluble Carbodiimide-Mediated Amidation.* Analytical Biochemistry, 1994. 218(1): p. 87-91.
213. Larsson, P.G. and J.J. Platz-Christensen, *The vaginal pH and leucocyte/epithelial cell ratio vary during normal menstrual cycles.* Eur J Obstet Gynecol Reprod Biol, 1991. 38(1): p. 39-41.
214. Mumper, R.J., et al., *Formulating a Sulfonated Antiviral Dendrimer in a Vaginal Microbicidal Gel Having Dual Mechanisms of Action.* Drug Development and Industrial Pharmacy, 2009. 35(5): p. 515-524.
215. Anderson, J.M. and M.S. Shive, *Biodegradation and biocompatibility of PLA and PLGA microspheres.* Adv Drug Deliv Rev, 1997. 28(1): p. 5-24.
216. Thiebaut, F., et al., *Cellular-Localization of the Multidrug-Resistance Gene-Product P-Glycoprotein in Normal Human-Tissues.* Proceedings of the National Academy of Sciences of the United States of America, 1987. 84(21): p. 7735-7738.
217. Cordoncardo, C., et al., *Multidrug-Resistance Gene (P-Glycoprotein) Is Expressed by Endothelial-Cells at Blood-Brain Barrier Sites.* Proceedings of the National Academy of Sciences of the United States of America, 1989. 86(2): p. 695-698.
218. Thiebaut, F., et al., *Immunohistochemical Localization in Normal-Tissues of Different Epitopes in the Multidrug Transport Protein P170 - Evidence for Localization in Brain Capillaries and Crossreactivity of One Antibody with a Muscle Protein.* Journal of Histochemistry & Cytochemistry, 1989. 37(2): p. 159-164.

219. Cordoncardo, C., et al., *Expression of the Multidrug Resistance Gene-Product (P-Glycoprotein) in Human Normal and Tumor-Tissues.* Journal of Histochemistry & Cytochemistry, 1990. 38(9): p. 1277-1287.
220. Flens, M.J., et al., *Tissue distribution of the multidrug resistance protein.* American Journal of Pathology, 1996. 148(4): p. 1237-1247.
221. Huisman, M.T., et al., *P-glycoprotein limits oral availability, brain, and fetal penetration of saquinavir even with high doses of ritonavir.* Molecular Pharmacology, 2001. 59(4): p. 806-813.
222. Alsenz, J., H. Steffen, and R. Alex, *Active apical secretory efflux of the HIV protease inhibitors saquinavir and ritonavir in Caco-2 cell monolayers. (vol 15, pg 423, 1998).* Pharm Res, 1998. 15(6): p. 958-958.
223. Valentin, A., et al., *Identification of a Potential Pharmacological Sanctuary for HIV Type 1 in a Fraction of CD4(+) Primary Cells.* Aids Research and Human Retroviruses, 2010. 26(1): p. 79-88.
224. Bining, N. and R.A. Miller, *Cytokine production by subsets of CD4 memory T cells differing in P-glycoprotein expression: Effects of aging.* Journals of Gerontology Series a-Biological Sciences and Medical Sciences, 1997. 52(3): p. B137-B145.
225. Eagling, V.A., et al., *CYP3A4-mediated hepatic metabolism of the HIV-1 protease inhibitor saquinavir in vitro.* Xenobiotica, 2002. 32(1): p. 1-17.
226. Karim, Q.A., et al., *Effectiveness and Safety of Tenofovir Gel, an Antiretroviral Microbicide, for the Prevention of HIV Infection in Women.* Science, 2010. 329(5996): p. 1168-1174.
227. Wang, Z., et al., *RNA interference and cancer therapy.* Pharm Res, 2011. 28(12): p. 2983-95.
228. Palliser, D., et al., *An siRNA-based microbicide protects mice from lethal herpes simplex virus 2 infection.* Nature, 2006. 439(7072): p. 89-94.
229. Jacque, J.M., K. Triques, and M. Stevenson, *Modulation of HIV-1 replication by RNA interference.* Nature, 2002. 418(6896): p. 435-438.
230. Hall, A.H. and K.A. Alexander, *RNA interference of human papillomavirus type 18 E6 and E7 induces senescence in HeLa cells.* Journal of Virology, 2003. 77(10): p. 6066-9.
231. Eszterhas, S.K., et al., *Nanoparticles containing siRNA to silence CD4 and CCR5 reduce expression of these receptors and inhibit HIV-1 infection in human female reproductive tract tissue explants.* Infect Dis Rep, 2011. 3(2): p. e11.
232. Wu, Y., et al., *Durable protection from Herpes Simplex Virus-2 transmission following intravaginal application of siRNAs targeting both a viral and host gene.* Cell Host Microbe, 2009. 5(1): p. 84-94.
233. Wu, Y.C., et al., *Durable Protection from Herpes Simplex Virus-2 Transmission Following Intravaginal Application of siRNAs Targeting Both a Viral and Host Gene.* Cell Host & Microbe, 2009. 5(1): p. 84-94.
234. Kumar, P., et al., *T cell-specific siRNA delivery suppresses HIV-1 infection in humanized mice.* Cell, 2008. 134(4): p. 577-586.
235. Xie, F.Y., M.C. Woodle, and P.Y. Lu, *Harnessing in vivo siRNA delivery for drug discovery and therapeutic development.* Drug Discovery Today, 2006. 11(1-2): p. 67-73.

236. Grivel, J.C., R.J. Shattock, and L.B. Margolis, *Selective transmission of R5 HIV-1 variants: where is the gatekeeper?* J Transl Med, 2011. 9 Suppl 1: p. S6.
237. Saba, E., et al., *HIV-1 sexual transmission: early events of HIV-1 infection of human cervico-vaginal tissue in an optimized ex vivo model.* Mucosal Immunol, 2010. 3(3): p. 280-90.
238. Hutter, G., et al., *Long-term control of HIV by CCR5 Delta32/Delta32 stem-cell transplantation.* N Engl J Med, 2009. 360(7): p. 692-8.
239. Kirchhoff, F., et al., *Brief Report - Absence of Intact Nef Sequences in a Long-Term Survivor with Nonprogressive Hiv-1 Infection.* New England Journal of Medicine, 1995. 332(4): p. 228-232.
240. Deacon, N.J., et al., *Genomic structure of an attenuated quasi species of HIV-1 from a blood transfusion donor and recipients.* Science, 1995. 270(5238): p. 988-91.
241. Casartelli, N., et al., *CD4 and major histocompatibility complex class I downregulation by the human immunodeficiency virus type 1 nef protein in pediatric AIDS progression.* J Virol, 2003. 77(21): p. 11536-45.
242. Collins, K.L., et al., *HIV-1 Nef protein protects infected primary cells against killing by cytotoxic T lymphocytes.* Nature, 1998. 391(6665): p. 397-401.
243. Yang, O.O., et al., *Nef-mediated resistance of human immunodeficiency virus type 1 to antiviral cytotoxic T lymphocytes.* J Virol, 2002. 76(4): p. 1626-31.
244. Lundquist, C.A., et al., *Nef-mediated downregulation of CD4 enhances human immunodeficiency virus type 1 replication in primary T lymphocytes.* J Virol, 2002. 76(9): p. 4625-33.
245. Aiken, C., et al., *Nef induces CD4 endocytosis: requirement for a critical dileucine motif in the membrane-proximal CD4 cytoplasmic domain.* Cell, 1994. 76(5): p. 853-64.
246. Lenassi, M., et al., *HIV Nef is secreted in exosomes and triggers apoptosis in bystander CD4+ T cells.* Traffic, 2010. 11(1): p. 110-22.
247. James, C.O., et al., *Extracellular Nef protein targets CD4+ T cells for apoptosis by interacting with CXCR4 surface receptors.* J Virol, 2004. 78(6): p. 3099-109.
248. Finkel, T.H., et al., *Apoptosis occurs predominantly in bystander cells and not in productively infected cells of HIV- and SIV-infected lymph nodes.* Nat Med, 1995. 1(2): p. 129-34.
249. Kyei, G.B., et al., *Autophagy pathway intersects with HIV-1 biosynthesis and regulates viral yields in macrophages.* J Cell Biol, 2009. 186(2): p. 255-68.
250. Glick, D., S. Barth, and K.F. Macleod, *Autophagy: cellular and molecular mechanisms.* J Pathol, 2010. 221(1): p. 3-12.
251. Yang, Z. and D.J. Klionsky, *Eaten alive: a history of macroautophagy.* Nat Cell Biol, 2010. 12(9): p. 814-22.
252. Xu, Y., et al., *Toll-like receptor 4 is a sensor for autophagy associated with innate immunity.* Immunity, 2007. 27(1): p. 135-44.
253. Travassos, L.H., et al., *Nod1 and Nod2 direct autophagy by recruiting ATG16L1 to the plasma membrane at the site of bacterial entry.* Nat Immunol, 2010. 11(1): p. 55-62.
254. Deretic, V., T. Saitoh, and S. Akira, *Autophagy in infection, inflammation and immunity.* Nat Rev Immunol, 2013. 13(10): p. 722-37.

255. Escoll, P., M. Rolando, and C. Buchrieser, *Modulation of Host Autophagy during Bacterial Infection: Sabotaging Host Munitions for Pathogen Nutrition.* Front Immunol, 2016. 7: p. 81.
256. Funderburk, S.F., Q.J. Wang, and Z. Yue, *The Beclin 1-VPS34 complex--at the crossroads of autophagy and beyond.* Trends Cell Biol, 2010. 20(6): p. 355-62.
257. Chen, D., et al., *A mammalian autophagosome maturation mechanism mediated by TECPR1 and the Atg12-Atg5 conjugate.* Mol Cell, 2012. 45(5): p. 629-41.
258. Jokerst, J.V., et al., *Nanoparticle PEGylation for imaging and therapy.* Nanomedicine (Lond), 2011. 6(4): p. 715-28.
259. Singha, K., R. Namgung, and W.J. Kim, *Polymers in Small-Interfering RNA Delivery.* Oligonucleotides, 2011.
260. Patil, Y. and J. Panyam, *Polymeric nanoparticles for siRNA delivery and gene silencing.* Int J Pharm, 2009. 367(1-2): p. 195-203.
261. Walk, S.F., et al., *Design and use of an inducibly activated human immunodeficiency virus type 1 Nef to study immune modulation.* Journal of Virology, 2001. 75(2): p. 834-843.
262. Gu, J.J., S.D. Yang, and E.A. Ho, *Biodegradable Film for the Targeted Delivery of siRNA-Loaded Nanoparticles to Vaginal Immune Cells.* Molecular Pharmaceutics, 2015. 12(8): p. 2889-2903.
263. Kyei, G.B., et al., *Autophagy pathway intersects with HIV-1 biosynthesis and regulates viral yields in macrophages.* Journal of Cell Biology, 2009. 186(2): p. 255-268.
264. Wang, Y.Y., et al., *Addressing the PEG Mucoadhesivity Paradox to Engineer Nanoparticles that "Slip" through the Human Mucus Barrier.* Angewandte Chemie-International Edition, 2008. 47(50): p. 9726-9729.
265. He, Z.L., et al., *Degradation behavior and biosafety studies of the mPEG-PLGA-PLL copolymer.* Physical Chemistry Chemical Physics, 2016. 18(17): p. 11986-11999.
266. Tang, C.H., C.J. Hsu, and Y.C. Fong, *The CCL5/CCR5 Axis Promotes Interleukin-6 Production in Human Synovial Fibroblasts.* Arthritis and Rheumatism, 2010. 62(12): p. 3615-3624.
267. Mizushima, N., T. Yoshimori, and B. Levine, *Methods in Mammalian Autophagy Research.* Cell, 2010. 140(3): p. 313-326.
268. Weber, N.D., et al., *PEGylated poly(ethylene imine) copolymer-delivered siRNA inhibits HIV replication in vitro.* Journal of Controlled Release, 2012. 157(1): p. 55-63.
269. Win, K.Y. and S.S. Feng, *Effects of particle size and surface coating on cellular uptake of polymeric nanoparticles for oral delivery of anticancer drugs.* Biomaterials, 2005. 26(15): p. 2713-2722.
270. Pretor, S., et al., *Cellular uptake of coumarin-6 under microfluidic conditions into HCE-T cells from nanoscale formulations.* Mol Pharm, 2015. 12(1): p. 34-45.
271. Rivolta, I., et al., *Cellular uptake of coumarin-6 as a model drug loaded in solid lipid nanoparticles.* J Physiol Pharmacol, 2011. 62(1): p. 45-53.
272. Yano, J. and P.L. Fidel, *Protocols for Vaginal Inoculation and Sample Collection in the Experimental Mouse Model of Candida vaginitis.* Jove-Journal of Visualized Experiments, 2011(58).

273. Blaskewicz, C.D., J. Pudney, and D.J. Anderson, *Structure and Function of Intercellular Junctions in Human Cervical and Vaginal Mucosal Epithelia.* Biology of Reproduction, 2011. 85(1): p. 97-104.
274. Damge, C., et al., *Nanocapsules as Carriers for Oral Peptide Delivery.* Journal of Controlled Release, 1990. 13(2-3): p. 233-239.
275. Ballou, B., et al., *Nanoparticle Transport from Mouse Vagina to Adjacent Lymph Nodes.* Plos One, 2012. 7(12).
276. Barczyk, M., S. Carracedo, and D. Gullberg, *Integrins.* Cell Tissue Res, 2010. 339(1): p. 269-80.
277. Petrovic, A., et al., *LPAM (alpha 4 beta 7 integrin) is an important homing integrin on alloreactive T cells in the development of intestinal graft-versus-host disease.* Blood, 2004. 103(4): p. 1542-7.
278. Berlin, C., et al., *alpha 4 integrins mediate lymphocyte attachment and rolling under physiologic flow.* Cell, 1995. 80(3): p. 413-22.
279. Butcher, E.C. and L.J. Picker, *Lymphocyte homing and homeostasis.* Science, 1996. 272(5258): p. 60-6.
280. Arthos, J., et al., *HIV-1 envelope protein binds to and signals through integrin alpha4beta7, the gut mucosal homing receptor for peripheral T cells.* Nat Immunol, 2008. 9(3): p. 301-9.
281. Cicala, C., et al., *The integrin alpha4beta7 forms a complex with cell-surface CD4 and defines a T-cell subset that is highly susceptible to infection by HIV-1.* Proc Natl Acad Sci U S A, 2009. 106(49): p. 20877-82.
282. Byrareddy, S.N., et al., *Targeting alpha4beta7 integrin reduces mucosal transmission of simian immunodeficiency virus and protects gut-associated lymphoid tissue from infection.* Nat Med, 2014. 20(12): p. 1397-400.
283. *Vedolizumab (Entyvio) for inflammatory bowel disease.* Med Lett Drugs Ther, 2014. 56(1451): p. 86-8.
284. *Vedolizumab (Anti-alpha4beta7) in Subjects With HIV Infection Undergoing Analytical Treatment Interruption.* 2016.
285. Singh, H., et al., *Vedolizumab: A novel anti-integrin drug for treatment of inflammatory bowel disease.* J Nat Sci Biol Med, 2016. 7(1): p. 4-9.
286. Fuss, I.J., et al., *Isolation of whole mononuclear cells from peripheral blood and cord blood.* Curr Protoc Immunol, 2009. Chapter 7: p. Unit7 1.
287. Larsson, P.G. and J.J. Platzchristensen, *The Vaginal Ph and Leukocyte Epithelial-Cell Ratio Vary during Normal Menstrual Cycles.* European Journal of Obstetrics Gynecology and Reproductive Biology, 1991. 38(1): p. 39-41.
288. Yang, S., et al., *Advancements in the field of intravaginal siRNA delivery.* J Control Release, 2013. 167(1): p. 29-39.
289. Bastidas, R.J., et al., *Chlamydial intracellular survival strategies.* Cold Spring Harb Perspect Med, 2013. 3(5): p. a010256.
290. Elwell, C.A., et al., *RNA interference screen identifies Abl kinase and PDGFR signaling in Chlamydia trachomatis entry.* PLoS Pathog, 2008. 4(3): p. e1000021.
291. French, W.J., E.E. Creemers, and M.D. Tallquist, *Platelet-derived growth factor receptors direct vascular development independent of vascular smooth muscle cell function.* Molecular and Cellular Biology, 2008. 28(18): p. 5646-5657.
292. Andrae, J., R. Gallini, and C. Betsholtz, *Role of platelet-derived growth factors in physiology and medicine.* Genes & Development, 2008. 22(10): p. 1276-1312.

293. Nakagawa, I., et al., *Autophagy defends cells against invading group A Streptococcus.* Science, 2004. 306(5698): p. 1037-40.
294. Gutierrez, M.G., et al., *Autophagy is a defense mechanism inhibiting BCG and Mycobacterium tuberculosis survival in infected macrophages.* Cell, 2004. 119(6): p. 753-66.
295. Py, B.F., M.M. Lipinski, and J. Yuan, *Autophagy limits Listeria monocytogenes intracellular growth in the early phase of primary infection.* Autophagy, 2007. 3(2): p. 117-25.
296. Al-Zeer, M.A., et al., *Autophagy restricts Chlamydia trachomatis growth in human macrophages via IFNG-inducible guanylate binding proteins.* Autophagy, 2013. 9(1): p. 50-62.
297. Gu, J., S. Yang, and E.A. Ho, *Biodegradable Film for the Targeted Delivery of siRNA-Loaded Nanoparticles to Vaginal Immune Cells.* Mol Pharm, 2015. 12(8): p. 2889-903.
298. Ho, E.A., et al., *Characterization of long-circulating cationic nanoparticle formulations consisting of a two-stage PEGylation step for the delivery of siRNA in a breast cancer tumor model.* J Pharm Sci, 2013. 102(1): p. 227-36.
299. Xie, Y.R., et al., *Targeted delivery of siRNA to activated T cells via transferrin-polyethylenimine (Tf-PEI) as a potential therapy of asthma.* Journal of Controlled Release, 2016. 229: p. 120-129.
300. Scidmore, M.A., *Cultivation and Laboratory Maintenance of Chlamydia trachomatis.* Curr Protoc Microbiol, 2005. Chapter 11: p. Unit 11A 1.
301. Yang, S., et al., *Novel intravaginal nanomedicine for the targeted delivery of saquinavir to CD4+ immune cells.* Int J Nanomedicine, 2013. 8: p. 2847-58.
302. Mizushima, N., T. Yoshimori, and B. Levine, *Methods in mammalian autophagy research.* Cell, 2010. 140(3): p. 313-26.
303. Mottet, D., et al., *Histone deacetylase 7 silencing alters endothelial cell migration, a key step in angiogenesis.* Circ Res, 2007. 101(12): p. 1237-46.
304. Prevention, C.f.D.C.a., *Chlamydia - CDC Fact Sheet.* 2016.
305. Svensson, L.O., et al., *Screening for Chlamydia trachomatis infection in women and aspects of the laboratory diagnostics.* Acta Obstet Gynecol Scand, 1991. 70(7-8): p. 587-90.
306. Lin, C.W., et al., *Protective role of autophagy in branched polyethylenimine (25K)- and poly(L-lysine) (30-70K)-induced cell death.* Eur J Pharm Sci, 2012. 47(5): p. 865-74.
307. Vaidyanathan, S., et al., *Quantitative Measurement of Cationic Polymer Vector and Polymer-pDNA Polyplex Intercalation into the Cell Plasma Membrane.* ACS Nano, 2015. 9(6): p. 6097-109.
308. Gao, X., et al., *The association of autophagy with polyethylenimine-induced cytotoxicity in nephritic and hepatic cell lines.* Biomaterials, 2011. 32(33): p. 8613-25.
309. Sahay, G., D.Y. Alakhova, and A.V. Kabanov, *Endocytosis of nanomedicines.* J Control Release, 2010. 145(3): p. 182-95.